Contributions à l'amélioration de la performance statique des réseaux T & D intégrés en présence des REDs

Thèse

Seyedmasoud Mohseni Bonab

Doctorat en génie électrique
Philosophiæ doctor (Ph. D.)

Québec, Canada

© Seyedmasoud Mohseni Bonab, 2020

Contributions à l'amélioration de la performance statique des réseaux T&D intégrés en présence des REDs

Thèse

Seyed Masoud Mohseni-Bonab

Sous la direction de:

Hoang Le-Huy, directeur de recherche
Inncoent Kamwa, codirecteur de recherche

Résumé

Avec la croissance des nouvelles technologies émergentes dans les réseaux de distribution, tels que les éoliennes, les panneaux solaires, les véhicules électriques et les sources de génération distribuées, la nécessité d'étudier simultanément les réseaux de transmission et de distribution (T&D) et leurs interactions bilatérales ne peut plus être négligée. Une forte pénétration des sources d'énergie renouvelable, naturellement stochastiques, peut inverser le flux d'énergie, ce qui ne rentre pas dans le paradigme d'un écoulement de puissance à flux descendant qui caractérise les systèmes d'alimentation conventionnels. Par conséquent, les méthodes d'étude de réseaux telles que le fux de puissance optimal (Optimal Power Flow), l'engagement des groupes de production (unit commitment) et l'analyse de la stabilité doivent être révisitées. Cette thèse propose l'application de systèmes de stockage d'énergie sur batterie (BESS) dans un cadre intégré de T&D minimisant les impacts négatifs des énergies renouvelables insérées dans le réseau de distribution ou chez le client. Les BESS peuvent être interprétés comme des équipements flexibles supplémentaires, contrôlés à distance et/ou localement, qui absorbent ou libèrent des puissances actives et réactives et améliorent l'efficacité globale du système T&D au complet du point de vue de la stabilité et de la performance dynamique.

Selon la pratique courante, les études des sytèmes T&D intégrés peuvent être classées en sous-groupes d'études dynamiques vs stationnaires ou en sous-groups d'études de co-optimisation vs co-simulation. Suivant la même approche, l'analyse à l'état d'équilibre est d'abord lancée par un nouvel outil d'allocation optimisée stochastique de BESS (VSC-SOBA) à contrainte de stabilité de tension. L'outil d'optimisation développé basé sur GAMS à deux niveaux prend en compte les BESS et des modèles détaillés de ressources énergétiques distribuées stochastiques tout en minimisant principalement les pertes de puissance active, mais les écarts de tension, les coûts de délestage, l'augmentation de la capacité de charge (chargeabilité ou « loadbility ») ainsi que la réduction de la vulnérabilité sont aussi des fonctions objectives qui ont été considérées. L'applicabilité de l'outil proposé a été confirmée

sur des cas d’utilisation basés sur des réseaux T&D benchmark de l’IEEE comportant des centaines de variables et contraintes.

Dans la partie suivante, l'architecture du framework de co-simulation, ainsi que les différents acteurs clés qui y participent seront examinés. Les objectifs de cette partie sont les suivants : développer, simuler et résoudre des équations algébriques de chaque niveau indépendamment, à l'aide de simulateurs bien connus, spécifiques à un domaine (c’est-à-dire, transport vs distribution), tout en assurant une interface externe pour l'échange de données. L'outil d'interface devrait établir une connexion de partage de données robuste, fiable et bilatérale entre deux niveaux de système. Les idées et les méthodologies proposées seront discutées.

Pour completer cette étude, La commutation optimale de réseaux de transport (Optimal Transmission Switching) en tant que nouvelle méthode de réduction des coûts d'exploitation est considérée d'un point de vue de la sécurité, en assument ou non la présensce des BESS. De toute évidence, l'OTS est un moyen efficace (tout comme la référence de tension ou le contrôle des références de puissances P-Q) qui s’avère nécessaire dans le cadre T&D intégré, tel que nous le démontrons à travers divers cas d'utilisation. Pour ce faire, afin de préserver la sécurité des systèmes de transport d'électricité contre les attaques ou les catastrophes naturelles telles que les ouragans et les pannes, un problème OTS stochastique orienté vulnérabilité (VO-SOTS) est également introduit dans cette thèse tout en considérant l'incertitude des charges via une approche par échantillonage de scénarios respectant la distribution statistique des incertitudes.

Abstract

With the growing trend of emerging new technologies in distribution networks, such as wind turbines, solar panels, electric vehicles, and distributed generations, the need for simultaneously studying Transmission & Distribution (T&D) networks and their bilateral interactions cannot be overlooked anymore. High penetration of naturally stochastic renewable energy sources may reverse the energy flow which does not fit in the top-down energy transfer paradigm of conventional power systems. Consequently, network study methods such as optimal power flow, unit commitment, and static stability analysis need to be revised. This thesis proposes application of battery energy storage systems (BESS) within integrated T&D framework minimizing the adverse impacts of renewable energy resources. The BESSs can be interpreted as additional flexible equipment, remotely and/or locally controlled, which absorb or release both active and reactive powers and improve the overall efficiency of the complete T&D system from both steady-state and dynamic viewpoints.

As a common practice, the integrated T&D framework studies are categorized into either dynamic and steady-state subcases or co-optimization framework and co-simulation framework. Following the same approach, the steady-state analysis is first initiated by a novel voltage stability constrained stochastic optimal BESS allocation (VSC-SOBA) tool. The developed bi-level GAMS-based optimization tool takes into account BESSs and detailed models of stochastic distributed energy resources while minimizing active power losses, voltage deviation, load shedding costs, increasing loadability, and vulnerability mitigation are objective functions. The applicability of proposed tool has been confirmed over large IEEE recognized T&D benchmarks with hundreds of variables and constraints.

In the next part, the architecture of co-simulation framework and different key players will be investigated. The objectives of this part are set as: developing, simulating, and solving differential and algebraic equations of each level independently, using existing well-known domain-specific simulators, while externally-interfaced for exchanging data. The interface

tool should stablish a robust, reliable, and bilateral data sharing connection between two levels of system. The ideas and proposed methodologies will be discussed.

To complete this study, optimal transmission switching (OTS) as a new method for reduction of operation costs is next considered from a security point of view. It is shown clearly that OTS is an effective mean (just like voltage reference or P-Q reference control), which is necessary in the integrated T&D framework to make it useful in dealing with various emerging use cases. To do so without impeding the security of power transmission systems against attacks or natural disasters such as hurricane and outages, a vulnerability oriented stochastic OTS (VO-SOTS) problem is also introduced in this thesis, while considering the loads uncertainty via a scenario-based approach.

Table des matières

Liste des figures

Liste des tableaux

Liste des abréviations

BESS	Battery Energy Storage Systems
BIP	Bus isolation probability
COP	Current operation point
CoTDS	Combined Transmission and Distribution Systems
CSA	Crow search algorithm
DER	Distributed energy resources
DG	Distributed Generations
DGPV	Distributed generation from solar photovoltaics
DN	Distribution networks
DR	Demand response
DVA	dynamic vulnerability assessment
ELM	Expected loading margin
EMS	Energy management systems
EPL	Expected power losses
EREC	Expected resilience enhancement cost
ETGC	Expected total generation cost
ETLS	Expected total load shedding
EVD	Expected voltage deviation
FDI	False data injection
FNCS	Framework for network co-simulation
GA	Genetic Algorithm
GPF	Global power flow
GSA	Gravitational Search Algorithm
HELICS	Hierarchical Engine for Large-scale Infrastructure Co-Simulation
HPC	High performance computing
ICA	Imperialist Competitive algorithm
IGMS	Integrated Grid Modeling System
LLP	Loadability limit point
LM	Loading margin
LOLP	loss of load probability
MILP	Mixed-integer linear programming

MINLP	Mixed integer nonlinear programming
MSS	Master–slave-splitting
NLP	non-linear programming
OPF	Optimal power flow
OTS	Optimal transmission switching
PCC	Point of Common Coupling
PCS	Power conversion system
PDF	Probability distribution functions
PF	Power flow
PFC	Parallel feeder chain
PL	Power losses
PMU	Phasor measurement unit
PNS	Power not supplied
PSO	Particle Swarm Optimization
RES	Renewable energy sources
VO-SOTS	Vulnerability-oriented stochastic optimal transmission switching
SOC	State of charge
SOTS	Stochastic optimal transmission switching ()
SSVA	Steady-state vulnerability assessment ()
T&D	Transmission & Distribution
TNs	Transmission networks
ULTC	Under-load tap changer
VCP	Voltage collapse point
VD	Voltage deviation
VSC-SOBA	Voltage security stochastic optimal BESS allocation
WAMS	Wide-area measurement system
WAN	Wide-area network
WT	Wind turbine

Je dédie ce travail:

À mes parents

Remerciements

Tout d'abord, je voudrais exprimer ma gratitude à mon directeur de recherche, le professeur Innocent Kamwa, pour m'avoir donné l'opportunité de travailler sur le projet PTDC et pour s’être assuré que j'aie le soutien scientifique et financier nécessaire pour m'investir pleinement dans mes travaux de recherche durant mes études à l'Université Laval. Merci de m'avoir fourni la liberté et les ressources nécessaires pour compléter ce travail de recherche. J'aimerai également exprimer ma sincère reconnaissance aux membres de mon comité de supervision, soit le docteur Ali Moeini et le professeur Hoang Le-Huy, pour leur soutien continu tout au long de mes travaux de recherche. Un gros merci au professeur Abbas Rabiee pour avoir effectué la pré-lecture de mes papiers.

Merci aux nombreux amis que je me suis faits pendant mon doctorat.

Mes travaux de recherche étaient financés dans le cadre du projet PTDC. Merci à l’Institut de recherche d'Hydro-Québec (IREQ) et au Conseil de recherches en sciences naturelles et en génie du Canada (CRSNG) pour leur soutien financier durant mes études.

Finalement, je remercie sincèrement mes chers parents, Mousa et Tahmineh, ma chère soeur, Mahsa, et ma chère amie Leila. Cette thèse est autant la vôtre que la mienne. Votre soutien tout au long de ma vie m'a donné la confiance nécessaire pour terminer ce que j'ai commencé.

Avant-Propos

En plus des chapitre introductifs, cette thèse contient sept articles qui sont publiés ou soumis pour publication dans des revues et conférences à comité de lecture. Le premier article a été présenté en juillet 2017 lors de la conférence «IEEE Electrical Power and Energy Conference (EPEC)» et il constitue le troisième chapitre de cette thèse. Le deuxième article a été présenté en 2018 lors de la conférence «IEEE/PES Transmission and Distribution Conference and Exposition (T&D)» et constitue le chapitre 4 de cette thèse. Le troisième article a été publié en Janvier 2019 dans les «IEEE Transactions on Sustainable Energy» et représente le chapitre 5 de cette thèse. Le quatrième article a été présenté en Octobre 2019 lors de la conférence «Innovative Smart Grid Technologies Europe (ISGT Europe)», c'est le chapitre 6 de cette thèse. Le cinquième article a été présenté en août 2020 lors de la conférence «IEEE PES General Meeting 2020» et apparaît au chapitre 7 de cette thèse. Le sixième article a été présenté en 2020 lors de la conférence «IEEE PES General Meeting 2020» et représente le chapitre 8 de cette thèse. Le septième article a été soumis à la revue «IEEE Transactions on Sustainable Energy» en août 2020 et est démontré comme le chapitre 9 de cette thèse. L'auteur de cette thèse, Seyed Masoud Mohseni-Bonab, est l'auteur principal de ces articles.

La contribution de l'auteur de cette thèse dans ces articles était d'effectuer tout le travail expérimental, la préparation et l'analyse des données, et d'écrire les premières versions en plus de contribuer significativemet à l'élaboration des concepts. Le format final de chaque article est un résultat direct de la collaboration avec les coauteurs listés. Le chapitre 2 était un effort de collaboration entre Seyed Masoud Mohseni-Bonab et les coauteurs Innocent Kamwa, Ali Moeini et Abbas Rabiee. Le chapitre 3 était un effort de collaboration entre Seyed Masoud Mohseni-Bonab et les coauteurs Innocent Kamwa, Abbas Rabiee et Ali Moeini. Le chapitre 4 était un effort de collaboration entre Seyed Masoud Mohseni-Bonab et les coauteurs Innocent Kamwa, Ali Moeini et Abbas Rabiee. Le chapitre 5 était un effort de collaboration entre Seyed Masoud Mohseni-Bonab et les coauteurs Innocent Kamwa et Ali Moeini. Le chapitre 6 était un effort de collaboration entre Seyed Masoud Mohseni-Bonab et les coauteurs Innocent Kamwa, Ali Moeini et Abbas Rabiee. Le chapitre 7 était un effort de

collaboration entre Seyed Masoud Mohseni-Bonab et les coauteurs Ali Hajebrahimi, Ali Moeini et Innocent Kamwa. Le chapitre 8 était un effort de collaboration entre Seyed Masoud Mohseni-Bonab et les coauteurs Innocent Kamwa, Abbas Rabiee et C. Y. Chung.

Introduction général

1.1 Contexte de la recherche - discussion générale

Avec la décarbonisation rapide de l'industrie de la production d'électricité et les normes de portefeuille des énergies renouvelables (RPS) instaurées dans la plupart des États nord-américains, le système d'alimentation électrique (système de transmission et de distribution) devrait se transformer rapidement dans un avenir proche. Ainsi, Hawaii vise à utiliser 100% d'énergie renouvelable d'ici 2045, la Californie vise 50% d'énergie propre d'ici 2030 tout comme plusieurs autres États dotés de normes de portefeuille des énergies renouvelables plus strictes (voir la figure 1.1) visant l'intégration progressive des ressources énergétiques distribuées (RED) principalement dans la distribution [1]. Plusieurs études exploratoires et démonstrations sur le terrain ont montré que les développements récents, y compris l'intégration des RED, des chargeurs de véhicules électriques et des unités de stockage d'énergie accentuent la contrainte exercée sur les systèmes de distribution d'énergie électrique [2, 3]. En outre, l'infrastructure de réseau électrique vieillissante et obsolète est inadéquate et doit faire face aux nouveaux défis liés à l'intégration attendue des RED [4]. Par conséquent, afin d'atteindre les cibles en matière d'énergie renouvelable, des innovations sont nécessaires pour intégrer de manière fiable les nouvelles ressources décentralisées de production d'énergie renouvelable dans le réseau existant.

Malgré le couplage physique des systèmes de transmission et distribution, ces systèmes sont gérés séparément par le gestionnaire de réseau de transport (GRT) et le gestionnaire de réseau de distribution (GRD) avec une coordination limitée. Le GRT fonctionne sans connaître les variations possibles du flux de puissance et les capacités de contrôle potentielles du GRD. Dans ce cas, le système de distribution est considéré comme une charge dont la valeur est mesurée au poste de distribution. De la même manière, le GRD considère généralement le côté transmission comme une source de tension, mesurée au poste de distribution. Ainsi, GRT et GRD sont presque « aveugles » aux conditions et aux commandes de leurs systèmes respectifs. En raison de la nature changeante des charges et de la forte pénétration de sources décentralisées d'énergie renouvelables naturellement stochastiques, le flux d'énergie peut changer ou même s'inverser à certains départs ou lignes de transmission, ce qui ne correspond

pas au concept de transfert d'énergie descendant des systèmes d'alimentation conventionnels. En conséquence, les méthodes d'étude du réseau telles que le « optimal power flow », le « unit commitment » et l'analyse de la stabilité doivent être révisitées. La modélisation intégrée de l'ensemble du système électrique est le seul moyen de capturer les effets des nouvelles sources d'énergie décentralisées à forte croissance et maximiser la participation des clients au modèle de marché du marché de l'énergie entre pairs (« peer-to-peer energy sharing »).

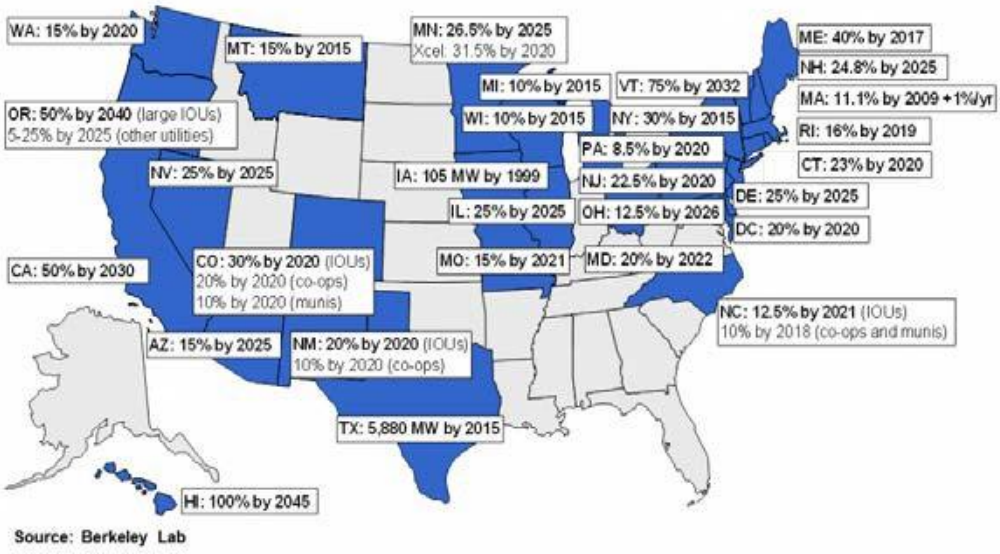

Figure 1. 1. Renewable Portfolio Standards

1.2 Problèmes de recherche, défis et signification

1.2.1 Problème général

L'impératif de transition énergétique pour décarboniser l'économie de demain se traduira par l'augmentation de la pénétration des énergies renouvelables distribuées, l'émergence des systèmes énergétiques incorporant l'électronique de puissance avancée (smart inverters), la e-mobilité et les villes intelligentes gravitant autour de réseaux de distribution actifs et communautaires. Le rôle pivot du réseau électrique dans cette transition rend nécessaire une nouvelle classe d'outils servant de base à la simulation et l'analyse de ces systèmes en évolution, tant au niveau du bouquet énergétique, de la forte granularité des équipements en jeu ainsi que des modèles d'affaires et de la nature des réponses attendues (ex : émissions de

GES d'une ville intelligente). La frontière traditionnelle entre transmission et distribution n'est plus bien définie, en particulier avec une augmentation de l'autoconsommation d'énergie de sources intermittentes, pouvant aller jusqu'à des clients net-zéro énergie qui ne contribuent pas aux coûts de fonctionnement du réseau selon le modèle tarifaire actuel.

La modélisation intégrée de l'ensemble du système électrique, en partant du fonctionnement du marché de gros jusqu'à la dynamique de la charge sans agrégation des composants dotés d'intelligence, est la seule capable de capter les effets des énergies décentralisées et des clients participatifs en illustrant les influences du système de transport sur la distribution et vice versa. Un tel simulateur d'un « système de systèmes », a pour but principal d'évaluer les impacts techniques et économiques de la transition énergétiques autant chez nous que dans les états voisins et de valider les nouveaux concepts de pilotage et flexibilité des réseaux intégrés.

1.2.2 Problèmes spécifiques - Manque d'une plate-forme formelle pour les systèmes intégrés de transport et de distribution

Considérant le problème général, le problème spécifique de cette recherche est présenté comme suit.

La plupart des études d'interconnexion RED existantes évaluent les défis d'intégration des RED à des taux de pénétration élevés, que ce soit au niveau de la distribution ou sur un système de transport et de distribution (T&D) découplé [5]. L'analyse du système T&D découplé suppose 1) un système de distribution en tant que charges forfaitaires ou 2) un système de transmission en tant que source d'alimentation constante. Les impacts potentiels sur le réseau de transport sont soit ignorés compte tenu du faible taux de pénétration des RED, soit non représentés en raison du modèle découplé T&D. Les projets de déploiement de RED à grande échelle, en cours et futurs, pourraient potentiellement affecter les opérations du réseau de transport régional [5, 6]. La situation s'aggrave dans les zones rurales lorsque le système de distribution est peu chargé et couvre une zone étendue avec une faible densité de charge. Dans la zone faiblement chargée, avec l'augmentation de la pénétration des REDs, la production décentralisée peut dépasser les besoins de consommation locaux, entraînant une inversion du flux de puissance des consommateurs individuels via les départs vers le poste

de distribution et éventuellement dans le système de transport [5]. Une inversion de flux de puissance peut nuire au bon fonctionnement des protections du réseau de transpor, entraînant des problèmes de régulation de la fréquence en raison d'un déséquilibre de puissance ou d'autres problèmes liés à la qualité de l'alimentation lorsqu'il est isolé. Afin d'atténuer les défis associés, de nouveaux outils capables de capturer les interactions entre les systèmes de T&D doivent être conçus.

1.3 Objectifs de la recherche

Sur la base de la revue de la littérature, les études de systèmes intégrés T&D portent soit sur des sous-cas dynamiques et stables, soit sur un cadre de co-optimisation et un cadre de co-simulation. La cooptimisation vise à construire un cadre ~~syndical~~, parfois sous forme de package, permettant d'étudier simultanément plusieurs niveaux de systèmes d'alimentation. Dans les études de co-simulation, différents logiciels dédiés, deux ou plus, sont utilisés simultanément pour étudier les effets de différents phénomènes dans les systèmes d'alimentation. Le but de cette thèse est de développer un cadre d'analyse des systèmes intégrés T&D afin de : 1) comprendre les impacts des RED connectés à la distribution (notamment les systèmes de stockage d'énergie par batterie (BESS)) sur le fonctionnement des systèmes de transmission et inversement, et 2) développer des méthodes d'utilisation des RED en tant que participant actif aux opérations du système d'alimentation électrique à grande échelle. Les objectifs spécifiques sont :

- Objectif 1) - Adressé au chapitre 2 - Élaborer des stratégies pour permettre aux consommateurs de participer à l’atténuation des problèmes liés aux réseaux de distribution en maximisant l’utilité du système BESS distribué.
- Objectif 2) - Adressé au chapitre 3 - Fournir un cadre de gestion pour l'intégration des RED (WT, BESS et PV) à un système intégré T&D, en tenant compte notamment de la nature stochastique de l'énergie éolienne et l'analyse de l'incertitude imposée via une approche basée sur des scénarios.
- Objectif 3) - Adressé au chapitre 4 - Planification optimale du BESS dans un système intégré T&D pour maximiser la marge de chargement (LM) du système en présence de vent ou d’énergie solaire, compte tenu de leur nature stochastique.

- Objectif 4) - Adressé au chapitre 5 - Utiliser GAMS pour la distribution et MATLAB/MATPOWER pour modéliser le réseau de transport afin de résoudre la répartition de puissance dans une système T&D intégré avec une méthode itérative.
- Objectif 5) - Adressé au chapitre 6 - Evaluation de la vulnérabilité dans les systèmes intégrés de T&D
- Objectif 6) - Adressé au chapitre 7 - Utiliser OpenDSS pour la distribution et MATLAB pour modéliser le réseau de transmission à travers une interface Python afin d'étudier de réalisation une co-optimisation du système T&D intégré pour satisfaire à la fois les intérêts des réseaux de distribution et transport en interactions bilatérales.
- Objectif 7) - Adressé au chapitre 8 - Fournir un cadre complet pour résoudre le problème OTS stochastique orienté résilience (VO-SOTS) en tenant compte du critère de contingence N-k des réseaux électriques.

1.4 Les contribution originale

En particulier, selon cette catégorisation de la thèse, ses principales contributions dans différents domaines (régime permanent, cadre de co-simulation) sont classées comme suit :

Au meilleur de notre connaissance, aucun travail dans la littérature n'inclut la gestion des ressources d'énergies renouvelables décentralisées et leurs incertitudes, en plus de l'allocation optimale de nombreux BESS dans un cadre de système intégré de T&D. En consultant la littérature, on peut déduire les remarques suivantes :

1- Les problèmes de dimensionnement (taille) et localisation des RED ont été examinés en tant que fonction objective dans la plupart des analyses de réseaux de distribution, mais un compromis entre réseaux de distribution et réseaux de transport a rarement été appliqué. Certaines recherches récentes ont uniquement porté sur ces deux réseaux en considérant uniquement la répartition de puissance conjointe T&D.

2- En augmentant le taux d'utilisation des sources d'énergie renouvelables dans les systèmes électriques pratiques, la nature incertaine et volatile de ces ressources devra être mieux gérée de manière à minimiser les problèmes de fonctionnement des systèmes électriques liés à

l’équilibrage de l’offre et de la demande sous contraintes de sécurité. Afin de gérer les incertitudes, le MCS est utilisé dans certaines publications, mais il s’agit d’une approche coûteuse en temps et en calculs.

3- Dans la plupart des références d'allocation BESS, les impacts des capacités de puissance réactive de BESS sont négligés. Il est vrai que le gain de puissance réactive est beaucoup plus faible que la puissance active des BESS, mais il peut être utile.

4- La dépendance croissante à l’égard du système de distribution d’électricité, associée au nombre croissant de catastrophes naturelles, a attiré l’attention des milieux de la recherche et de l’industrie sur le renforcement et la garantie de résilience. L'évaluation de la vulnérabilité dans les systèmes couplés T&D n'est pas examinée dans les travaux précédents et les impacts du BESS sur l'augmentation du niveau de vulnérabilité ne sont pas examinés dans les systèmes intégrés T&D (cet impact n'est pas étudié non plus au niveau de la transmission).

Les principales contributions de ce travail sont donc résumées comme suit :

1) Comparaison des impacts de l'allocation de BESS dans les modes distribué et agrégé sur le système intégré T&D. (Objectif 1)

2) Nouveau cadre de gestion pour l'intégration des RED (WT, BESS et PV) aux réseaux T&D et étude des impacts de l'intégration de BESS sur le T&D intégré. (Objectif 2)

3) Modélisation de la puissance réactive du BESS décentralisé pendant tout le processus d’allocation dans le réseau. (Objectif 2)

4) Planification optimale du BESS décentralisé dans un réseau T&D pour maximiser la capacité de chargement souhaitée du système en présence de puissances éoliennes et de leur nature stochastique. (Objectif 2)

5) Développement du modèle VSC-SOBA (objectif 2), puissant outil d'aide à la décision pour les opérateurs de système intégré T&D.

6) Prise en compte de « l’horizon temporel » et de la « nature stochastique des RED » dans l'analyse de vulnérabilité du système intégré a T&D afin de déterminer les meilleurs emplacements et les meilleurs moments où de multiples attaques intentionnelles ont eu lieu. Cette analyse peut être améliorée grâce à la structure de modélisation intégrée. (Objectif 2)

7) Mise en œuvre d'un cadre complet pour la planification optimale du BESS décentralisé dans le logiciel GAMS. (Objectif 2)

8) Développer, simuler et résoudre les équations de répartition de puissance de chaque niveau T ou D indépendamment, en utilisant des simulateurs bien connus spécifiques à un domaine T ou D, tout en assurant une interface externe pour l'échange de données inter-domaines. (Objectif 3)

9) Valider la convergence et la robustesse du flux de puissance T&D proposé au point de raccordement client en introduisant des erreurs dans les estimations initiales. (Objectif 3)

10) Proposer plusieurs idées systématiques dans « l’évaluation de la vulnérabilité des systèmes électriques » après avoir découvert les lacunes dans les connaissances actuelles à l’issue d’une revue critique de littérature. Les idées portent sur la conception d'un cadre modulaire avec des indices unifiés pour déterminer les zones vulnérables du système, l'évaluation intégrée de la vulnérabilité du système T&D et la vulnérabilité des systèmes informatiques aux cyber-attaques. (Objectif 3)

11) Optimisation des dispositifs contrôlables disponibles des systèmes de distribution (tels que le changeur de prise en charge (ULTC) et les batteries de condensateurs) dans les systèmes T&D intégrés. (Objectif 3)

12) Fournir un cadre complet pour résoudre le problème OTS stochastique orienté vulnérabilité (VO-SOTS) en tenant compte du critère de contingence N-k des réseaux électriques. Une procédure en trois étapes est proposée pour modéliser le problème VO-SOTS. Dans un premier temps, le problème OTS est résolu afin de minimiser les coûts de production. Étant donné que la commutation des lignes de transmission augmente la vulnérabilité du système, un autre problème d'optimisation est résolu pour déterminer la liste

des pertes de lignes les plus critiques entraînant le délestage de charge le plus important pour assurer la sécurité du réseau. Ensuite, le problème OTS est à nouveau résolu en excluant ces lignes, dans le but de minimiser les coûts de production. Dans le futur, cette approche sera appliquée aux réseaux T&D intégrés. (Objectif 4)

La Figure 1.2., montre le diagramme détaillé des activités constituant notre méthodologie de recherche.

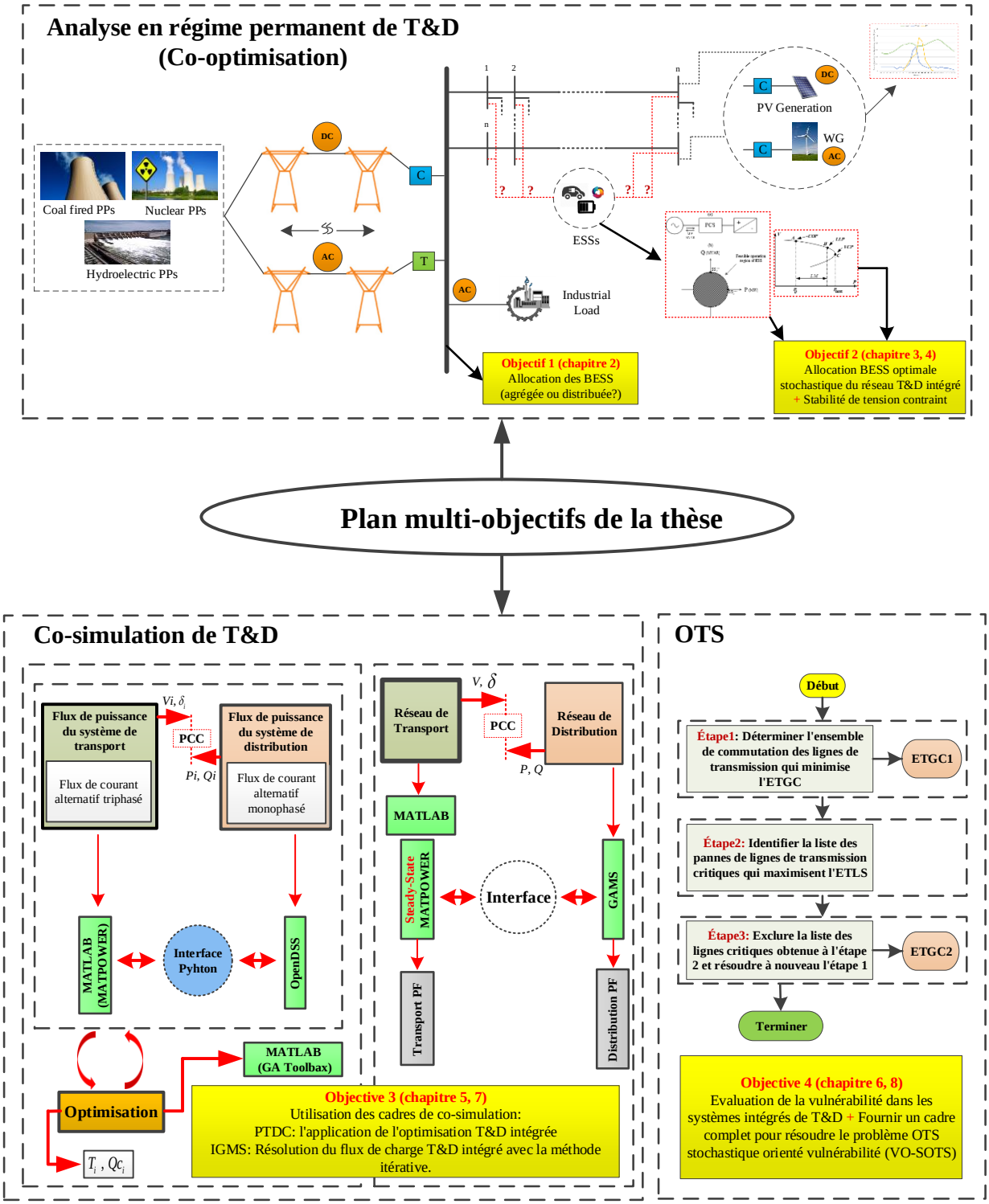

Figure 1. 2. Diagramme d'activités de la méthodologie de recherche

1.5 Organisation de la thèse

Cette dissertation est organisée comme suit. Le chapitre 1 élabore le contexte, les problèmes, les objectifs et présente un aperçu de la méthodologie proposée pour cette thèse. La vue d'ensemble des concepts, des défis et des problèmes relatifs à un réseau T&D intégré sera expliquée dans le deuxième chapitre. Ce chapitre présente une revue de la littérature des cadres de co-simulation/co-optimisation de systèmes T&D intégrés existants tout en proposant un nouveau cadre. Le chapitre 2, publié sous forme d'article dans la conférence " 2017 IEEE Electrical Power and Energy Conference (EPEC)", présente les stratégies permettant aux consommateurs de participer à l'atténuation des problèmes de réseau de distribution en maximisant l'utilité du système BESS distribué pour le réseau intégré. Le chapitre 3, publié en tant que document de conférence dans "2018 IEEE/PES Transmission and Distribution Conference and Exposition (T&D)", fournit un cadre de gestion pour l'intégration des RED (WT, BESS et PV) dans T&D. Ce chapitre inclut la nature stochastique de l'énergie éolienne et analyse l'incertitude imposée via une approche basée sur des scénarios.

Le chapitre 4, également publié sous la forme d'un article dans IEEE Transactions on Sustainable Energy, explique comment le BESS impose une règle particulière sur la maximisation de la marge de chargement (LM) d'un système intégré. Le chapitre 5, également présenté en tant qu'article dans la conférence ISGT Europe "2019 IEEE PES Innovative Smart Grid Technologies Europe (ISGT-Europe)", développe une plate-forme utilisant les outils GAMS et MATLAB (appelés IC-GAMA) pour résoudre la répartition de puissance des systèmes T&D intégrés. Le chapitre 6, accepté en tant qu'article de conférence dans "l'IEEE PES General Meeting 2020", examine la littérature récente sur l'évaluation de la vulnérabilité des systèmes électriques et propose plusieurs idées systématiques en guise de feuille de route pour les chercheurs. Le chapitre 7, également accepté en tant qu'article de conférence dans "l'IEEE PES General Meeting 2020", propose un nouveau cadre T&D pour optimiser les paramètres des RED contrôlables installés dans le réseau de distribution. Enfin, le chapitre 8, aussi soumis comme un article dans une revue scientifique (IEEE Transactions on Sustainable Energy), explique comment l'OTS, en tant que nouvelle méthode de réduction

des coûts d'exploitation du réseau de transport, peut être utilisée dans l'exploitation du système électrique. Un résumé, une conclusion et des perspectives de recherche sont fournis dans le dernier chapitre. Les articles publiés dans la thèse ont conservé leur contenu original.

Tel que mentionné, cette thèse est présentée sous la forme de plusieurs articles scientifiques issus de la recherche effectuée dans le cadre de ce projet de doctorat. De ce fait, certaines sections de la thèse peuvent contenir des informations redondantes et non évitables. Ceci a pour but de s’assurer que chaque article contient toutes les informations requises pour les lecteurs en tant que document de recherche indépendant.

2 Étude des avantages des systèmes BESS dans les systèmes de transmission et de distribution utilisant la cooptimisation intégrée du réseau électrique

2.1 Résumé

Cet article a pour objectif de développer un cadre permettant d'étudier et d'optimiser les avantages des systèmes de stockage d'énergie de batterie (BESS) à haute pénétration dans les systèmes de transmission et de distribution (T&D) intégrés. Un cadre d'analyse des systèmes T&D couplés est développé via une approche de co-optimisation. L'optimisation proposée prend en compte les fonctions objectives suivantes : 1) pertes de puissance réelle (PL), 2) déviation de tension (VD) au niveau des barres de charge, et 3) marge de chargement (LM) ou chargeabilité du système. Le cadre est utilisé pour étudier les impacts de fortes pénétrations de ressources énergétiques distribuées avec BESS intégré. Les simulations sont effectuées avec 100 et 50% de la capacité de charge du système BESS. Le cadre proposé est examiné sur le système de bus IEEE 118. Les résultats montrent que l'installation de BESS distribués du côté de la distribution diminue les PL et la VD et améliore également la chargeabilité totale du système.

Corps de l'article

Titre: Investigation of BESSs' Benefits in Transmission and Distribution Systems Operations using Integrated Power Grid Co-optimization

Seyed Masoud Mohseni-Bonab[1,2], Innocent Kamwa[2], Ali Moeini[2] and Abbas Rabiee[3]

[1] Electrical Engineering Department, Laval University, QC, Quebec, Canada (e-mail: s.m.mohsenibonab@ieee.org)

[2] Hydro-Québec/IREQ, Power System and Mathematics, Varennes QC J3X 1S1, Canada (e-mail: kamwa.innocent@ireq.ca, moeini.ali@ireq.ca)

[3] Electrical Engineering Department, University of Zanjan, Zanjan, Iran (e-mail: rabiee@znu.ac.ir)

Conférenc: 2017 IEEE Electrical Power and Energy Conference (EPEC)

2.2 Abstract

This paper aims to develop a framework to study and optimize the benefits high penetrations of battery energy storage systems (BESS) in the integrated transmission & distribution (T&D) systems. A coupled T&D systems analysis framework is developed through a co-optimization approach. The following objective functions are considered in the proposed optimization approach: 1) Real power losses (PL), 2) Voltage deviation (VD) at load buses, and 3) loading margin (LM) or loadability of system. The framework is utilized to investigate the impacts of high penetrations of distributed energy resources with embedded BESS. Simulations are performed with 100 and 50 percent of BESS charging capacity. The proposed framework is examined on the IEEE 118-bus system. The results show that the installation of distributed BESSs at the distribution side, decrease the PL and VD and also improve the system total LM.

Keywords: Integrated transmission and distribution (T&D) systems, battery energy storage systems (BESS), Real power losses (PL), Voltage deviation (VD), distributed energy resources (DER)

2.3 Nomenclature

N_B / N_j	Set of buses
N_L	Set of branches (transmission lines)
N_G	Set of generating units
N_D	Set of load buses
N_{BESS}	Set of candidate buses for BESS
i / j	Index of bus Number where $i = 1, 2, \ldots, N_B$
ℓ	Index of transmission lines
$y_\ell / g_\ell / b_\ell$	Admittance/conductance/ susceptance of ℓ *-th* line
$Y_{ij} = G_{ij} + jB_{ij}$	*ij-th* element of system Y_{bus} matrix
P_{Gi}	Active power production at bus *i*
$P_{G_i}^{\min} / P_{G_i}^{\max}$	Minimum/maximum value for active power
P_{D_i}	Real power of the *i-th* bus
$P_{D_{i,n}}$	Real power of the *i-th* bus when BESS is added
I_i^{BESS}	Optimal location of BESS (respect to objective functions)
Q_{D_i}	Reactive power of the *i-th* bus
$Q_{G_i}^{\min} / Q_{G_i}^{\max}$	Minimum/ Maximum value for reactive power of the *i-th* bus
$V_i^{\min} / V_i^{\max}$	Minimum/ Maximum value for voltage magnitude of the *i-th* bus
$S_\ell^{\max}$	Maximum value of power flow of ℓ *-th* transmission line
x	Vector of dependent variables (optimization variables)
u	Vector of control variables
V_i / V_j	Voltage magnitude of bus *i/j*
θ_i / θ_j	Voltage angle at bus *i/j*
S_ℓ	Power flow of ℓ *-th* transmission line
λ	Loading parameter of the system
K_{L_i}	Rate of load change at bus *i*
K_{G_i}	Rate of change in active power generation of unit *i*

PL /VD / LM Real Power Loss/ Voltage Deviation/ Loading Margin

2.4 Introduction

Beneficial integration of DERs into distribution grids and also of large-scale renewable power generation into transmission systems poses a considerable challenge to the existing power system planning and operation methods. Therefore, the integration of such volatile sources into electricity networks requires special considerations.

Previously, transmission and distribution networks were separately solved and simulated and also their characteristics were separately investigated as well. Currently, the interaction between transmission & distribution (T&D) is becoming more important due to an increased DERs penetration. In [7], a global power flow (GPF) method which considers T&D grids is proposed, combined with a master–slave-splitting (MSS) iterative method with convergence guarantee to alleviate boundary mismatches between the transmission and distribution grids [7]. A new method for T&D power flow (named as GTCA) is proposed in [8]. Next, Ref. [9] proposed a hybrid power flow formulation unifying three-phase and single-phase (positive sequence) models. A research team from NREL recently developed an Integrated Grid Modeling System (IGMS) simulator described in a project report [10] and relevant papers [11, 12]. According to these authors, IGMS is "a novel electric power system modeling platform for integrated transmission-distribution analysis that co-simulates off-the-shelf tools on high performance computing (HPC) platforms to offer unprecedented resolution from ISO markets down to appliances and other end uses". In contrast, either single-phase [13], [14] or three-phase [15] representation for T&D systems was used for dynamic simulations. In [16], the Multi-Area Thévenin Equivalent (MATE) approach is utilized for T&D integration. Moreover, power flow of T&D is solved using a three-sequence iterative method.

References [13-16] focused on dynamic analysis of T&D but this paper is more in line with steady-state analysis. Table 2.1 summarizes the findings of existing literatures and the main contributions of this paper.

To the best of our knowledge, no work in the literature (especially steady-state analysis papers [7-12]) is include transmission networks (TNs) and distribution networks (DN) together, while previous works use only power flow (PF) for DN (because of limitations in their utilized software such as GridLAB-D). Also, in previous works the impacts of BESSs' is not investigated.

Overall, the main contributions of this work are summarized as follows:

- Proposing a management framework for integrating DERs to T&D.
- Deriving strategies for enabling consumers' participation in alleviating distribution network challenges.
- Maximizing the utility of distributed BESS.
- Comparing impacts of BESS allocation in distributed and aggregate modes in different cases.

Table 2. 1. Summary of the existing literature and contributions of this work

	Study Network	T&D Analysis method	T&D PF or OPF solution?		DERs Impacts in T&D
	T&D (simultaneously)	Steady-State Analysis	PF	OPF	BESS
[7-9]	Y	Y	Y	N	N
[10]	Y	Y	Y	N	N
[11, 12]	Y	Y	Y	N	N
[13]	Y	N	N	N	N
[14]	Y	N	N	N	N
[15]	Y	N	Y	N	N
[16]	Y	N	Y	N	N
Pro.	Y	Y	Y	Y	Y

- Y/N denotes that the subject is/is not considered.

2.5 Problem Formulation

In this paper we want to study the impacts of DERs (especially BESS) on T&D system. We assume that the overall BESSs capacity in load buses are 30% of total feeder capacity (i.e. 2.4 MW). In all cases, BESS allocation is performed for 100% and 50% of BESS capacities.

2.5.1 Objective functions

In this paper the objectives are real power losses (PL), voltage deviation (VD) in load buses and loading margin (LM). In the aforementioned problem the vector of control/dependent variables can be formulated mathematically follows:

$$\begin{aligned} x^T &= \left[[V_i]^T, [\theta_i]^T, [Q_G]^T, [P_G]^T \right] \\ u^T &= \left[\left[P_{D_{i,n}} \right]^T, \left[I_i^{BESS} \right]^T \right] \qquad (\forall i \in N_{BESS}) \end{aligned} \tag{2-1}$$

2.5.1.1 Total active power losses

Minimization the total power losses in T&D system is important objective in power systems for improvement of the total energy efficiency and economic reasons. The active power losses can be mathematically expressed as follows:

$$PL(x,u) = \sum_{i=1}^{N_G} P_{G_i} - \sum_{i=1}^{N_B} P_{D_i} \tag{2-2}$$

2.5.1.2 Voltage deviation at load bus

The second objective of this paper is to maintain a proper voltage level at load buses. Electrical equipment is designed for optimum operation of nominal voltage. The deviation from the nominal voltage will decrease the efficiency and life of the electrical devices. Thus, the voltage profile of the system could be optimized by minimization of the sum voltage deviations from the corresponding rated values at load buses. This objective function is defined as follows:

$$VD(x,u) = \sum_{i=1}^{N_D} \left| V_i - V_i^{spc} \right| \tag{2-3}$$

2.5.1.3 Voltage deviation at load bus

One of the main factors for preserving a power system security is satisfying of specified desired loading margins (LMs). LM is defined as the amount of load increase not arousing voltage instability or violation of operational constraints [17]. In order to attain the LM, a continuation power flow is performed by increasing the loads and generations gradually. The

point where the operational constraints tend to be violated, is the loadability limit point. The distance in in MW or MVA from the current operating point and the loadability limit point is the LM.

Two basic interpretations of the load margin exist associated with the vector λ. A first one is based on a deterministic direction of load and generation increase K_{L_i} and K_{G_i} so λ is restricted to a single scalar. The following constraints for LM formulation are elaborated as:

$$P_{G_i} - P_{D_i}\left(1+\lambda K_{L_i}\right) = V_i \sum_{j=1}^{N_B} V_j \left[G_{ij}\cos\left(\theta_i - \theta_j\right) + B_{ij}\sin\left(\theta_i - \theta_j\right)\right] \tag{2-4}$$

$$Q_{G_i} - Q_{D_i}\left(1+\lambda K_{L_i}\right) = V_i \sum_{j=1}^{N_B} V_j \left[G_{ij}\sin\left(\theta_i - \theta_j\right) - B_{ij}\cos\left(\theta_i - \theta_j\right)\right] \tag{2-5}$$

$$\lambda > 0 \tag{2-6}$$

$$P_{G_i} = \min\left(P_{G_i}^{\max}, \left(1+\lambda K_{G_i}\right)P_{G_i}\right) \tag{2-7}$$

2.5.2 Equality Constraints/ Operational Limits

$$P_{G_i} - P_{D_i} = V_i \sum_{j=1}^{N_B} V_j \left[G_{ij}\cos\left(\theta_i - \theta_j\right) + B_{ij}\sin\left(\theta_i - \theta_j\right)\right] \tag{2-8}$$

$$Q_{G_i} - Q_{D_i} = V_i \sum_{j=1}^{N_B} V_j \left[G_{ij}\sin\left(\theta_i - \theta_j\right) - B_{ij}\cos\left(\theta_i - \theta_j\right)\right] \tag{2-9}$$

$$P_{G_i}^{\min} \le P_{G_i} \le P_{G_i}^{\max} \quad , \forall i \in N_G \tag{2-10}$$

$$Q_{G_i}^{\min} \le Q_{G_i} \le Q_{G_i}^{\max} \quad , \forall i \in N_G \tag{2-11}$$

$$V_i^{\min} \le V_i \le V_i^{\max} \quad , \forall i \in N_B \tag{2-12}$$

$$\left|S_\ell\right| \le S_\ell^{\max} \quad , \forall \ell \in N_L \tag{2-13}$$

2.5.3 BESS allocation

In this paper, BESS sources are modeled such as negative loads and installed in distribution network. It is assumed that the amount of BESS in each distribution load point is 30 percent of total feeder load. The problem is solved in two case: 1) with 100 percent charge of BESS. 2) With 50 Percent charge of BESS. This is expressed as the following formula.

$$P_{D_{i,n}} = P_{D_i} - 0.3P_{D_i} \quad , \forall i \in N_{BESS} \tag{2-14}$$

$$P_{D_{i,n}} = P_{D_i} - \left(0.3 \times 0.5 \times P_{D_i}\right) \quad , \forall i \in N_{BESS} \tag{2-15}$$

PL, VD and LM are calculated with installing BESS in all distribution buses. In addition, the number of parallel feeder chain (PFC) is defined as follows to synchronize the modified network with real IEEE-118 bus test system.

$$\begin{aligned} \text{NPFC} &= \textit{The Number of PFC in candidate buses} \\ &= \left\lfloor \frac{\text{Load amount at each of the candidate buses}}{\text{The sample feeder total load}} \right\rfloor \end{aligned} \tag{2-16}$$

For each combination of size and location of BESS the OPF problem is run to find the optimal dispatch (P_G, Q_G) to enable a converge state (V_i, θ_i) under steady-state network equations and operational constraints (Eq. 3-1).

2.6 Simulation Results

Simulations are carried out on the IEEE 118-bus test system. In order to show the effectiveness of the presented method, two cases are studied as follows:

(A) Case-I: BESS Allocation at candidate buses in PFCs

(B) Case-II: BESS Allocation in candidate load buses: From transmission network viewpoint

2.6.1 Case-I:

This system consists of 118 buses, where 54 buses are generator buses. Bus 69 is the slack bus. The network consists of 186 branches and 14 capacitor banks. In this paper, we choose 20 candidate buses for changing their loads to PFC. A simple 8-bus distribution feeder shown in Fig. 2.1 is used to build each distribution feeder. The total load on the feeder is 8 MW. The line codes and parameters are based on the IEEE 13-bus test feeder [16]. There are 7 equivalent loads, and their parameters are shown in Fig. 2.1. The power factor of all distribution loads is 0.95 lagging.

The single line diagram of this system is depicted in Fig. 2.2. The sample distribution system bus numbers are numbered by $1'$ to $7'$. For instance, bus number 1 is connected to $1'$, $2'$, $3'$, $4'$, $5'$, $6'$ and $7'$ and $11'$, $12'$, $13'$, $14'$, $15'$, $16'$ and $17'$ are constructed.

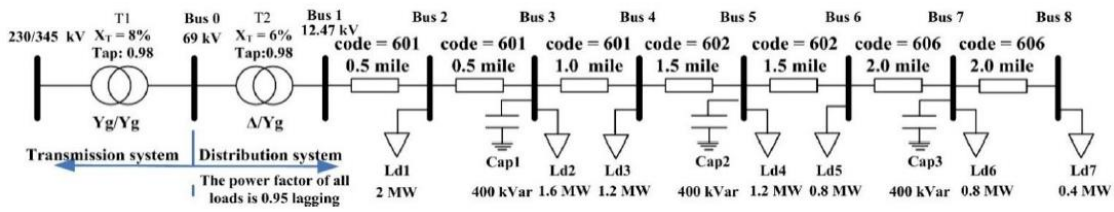

Figure 2. 1. A simple 8-bus distribution feeder

Figure 2.2 shows the modified system with respect to the considered PFCs. Table 2.2, reveals the number of each buses chain for modified version. For example, the actual load of bus 107 is 50 MW, but a simple feeder total loads is 8 MW. Hence, we considered 6 parallel feeders (i.e. totally 48 MW load) at bus 107, in order to balance the modified system generation and loads according to the original data of the system. In this case, we assume that BESSs are allocated in all of buses $1'$ to $7'$ of PFCs. For instance, according to the Table 2.2, in bus 116, we have 23 PFC and we assume that at first, BESSs are located in bus $1'$ of all PFCs in this bus. Then the BESSs are located in location $2'$ of PFCs. This process continues till the $7'$-th bus of PFCs of each bus. This process is shown in Fig. 2.2. It is observed from this figure that the green blocks reveals the process of BESS allocation in this case.

Besides, for this procedure, the BESSs capacities are calculated and shown in Table 2.2. After simulation, the amounts of considered objectives functions (PL, VD and LM) are depicted in figures 2.3-2.7. In addition, Table 2.3 compare the PL, VD and LM with and without the BESS in our T&D system. The completed results for each objective function, in each BESS scenario allocation, is available in the appendix [18].

In figures 2.3-2.6, there are 20 different colors, which each of these colors is represent the PL and VD in each of 20 candidate buses. In addition, in each branch there are 7 dots which represent the sample 8-bus distribution system buses.

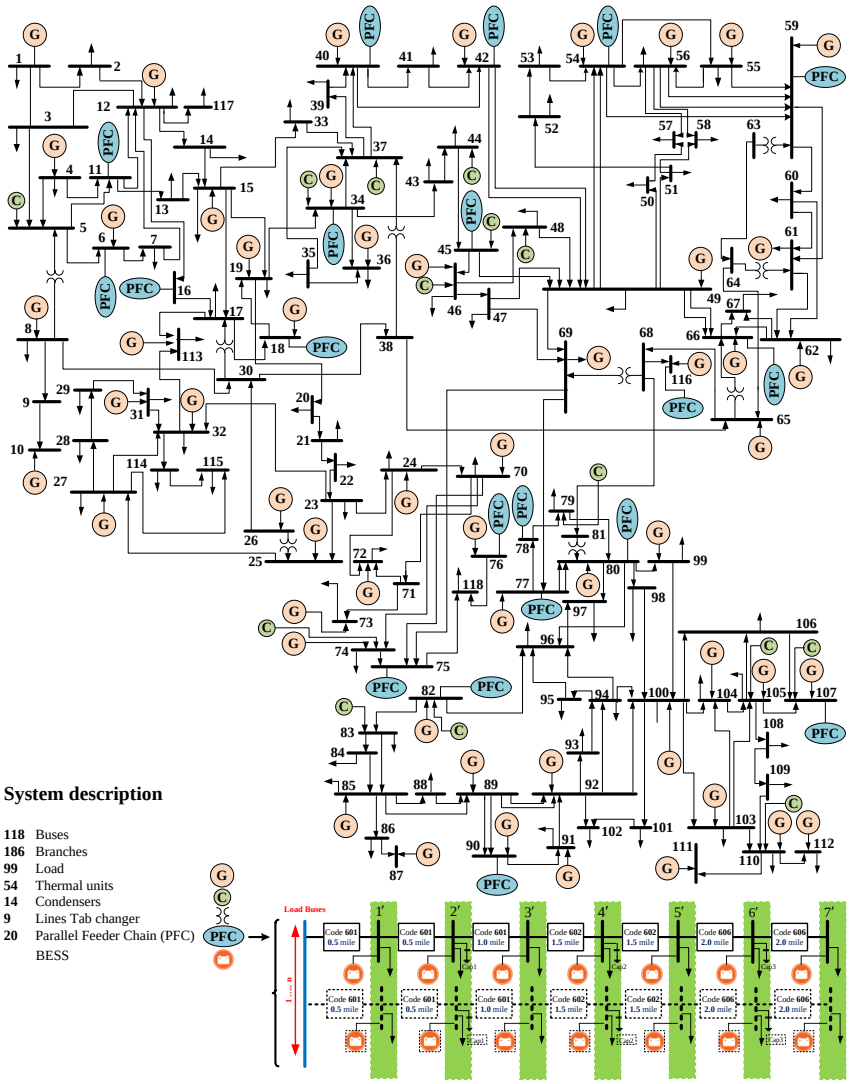

Figure 2. 2. Single line diagram of modified IEEE 118-bus test system integrated to PFCs (Case-I)

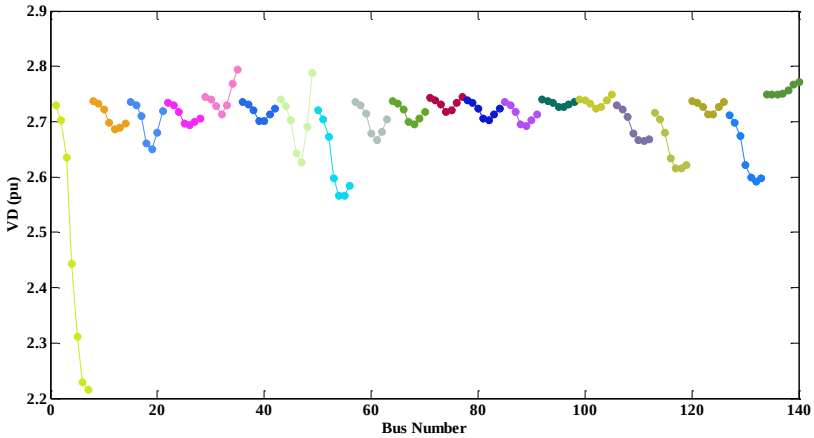

Figure 2. 3. Voltage deviation of system with 100 % charging of BESS (Case-I)

Table 2. 2. The loads and BESS capacities of candidate buses

Bus No.	Actual load (MW)	Number of considered PFCs of 8 MW	BESS Capacities (MW)	Approximated considered load (MW)
B116	184	23	23×2.4=55.2	184
B107	50	6	6×2.4=14.4	48
B90	163	20	20×2.4=48	160
B82	54	6	6×2.4=14.4	48
B80	130	16	16×2.4=38.4	128
B78	71	8	8×2.4=19.2	64
B59	277	34	34×2.4=81.6	272
B54	113	14	14×2.4=33.6	112
B42	96	12	12×2.4=28.8	96
B40	66	8	8×2.4=19.2	64
B34	59	7	7×2.4=16.8	56
B18	60	7	7×2.4=16.8	56
B11	70	8	8×2.4=19.2	64
B16	25	3	3×2.4=7.2	24
B6	52	6	6×2.4=14.4	48
B75	47	5	5×2.4=12	40
B76	68	8	8×2.4=19.2	64
B77	61	7	7×2.4=16.8	56
B45	53	6	6×2.4=14.4	48
B66	39	4	4×2.4=9.6	32

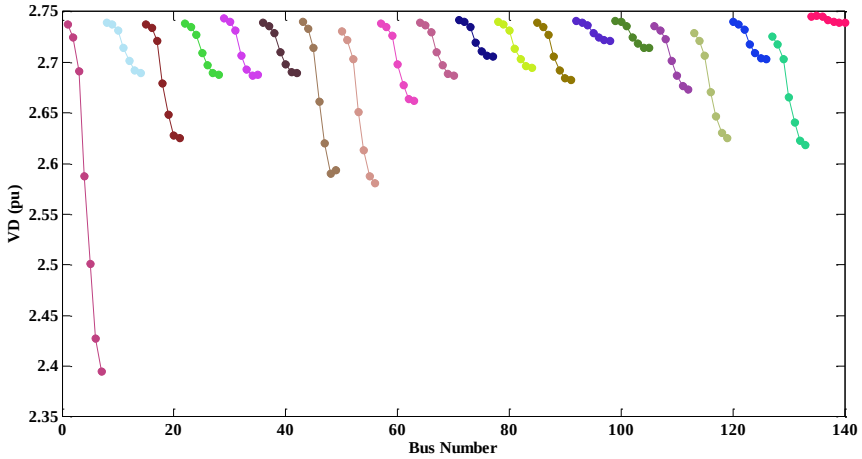

Figure 2. 4. Voltage deviation of system with 50 % charging of BESS (Case-I)

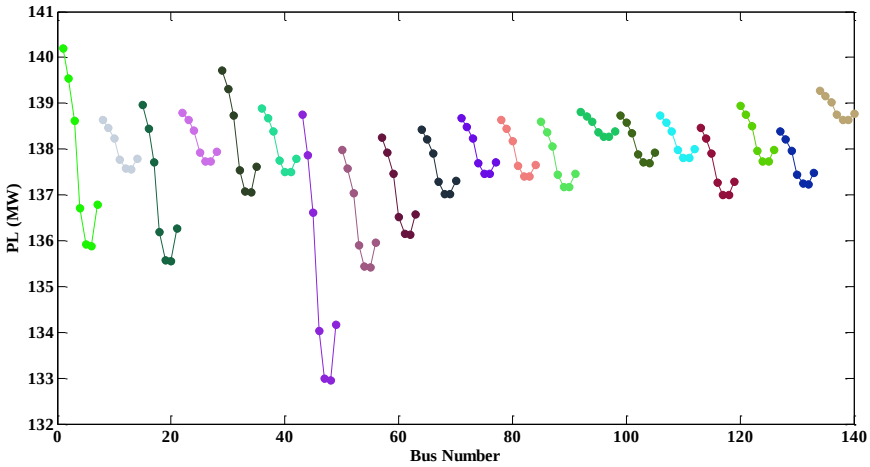

Figure 2. 5. Power loss of system with 100 % charging of BESS (Case-I)

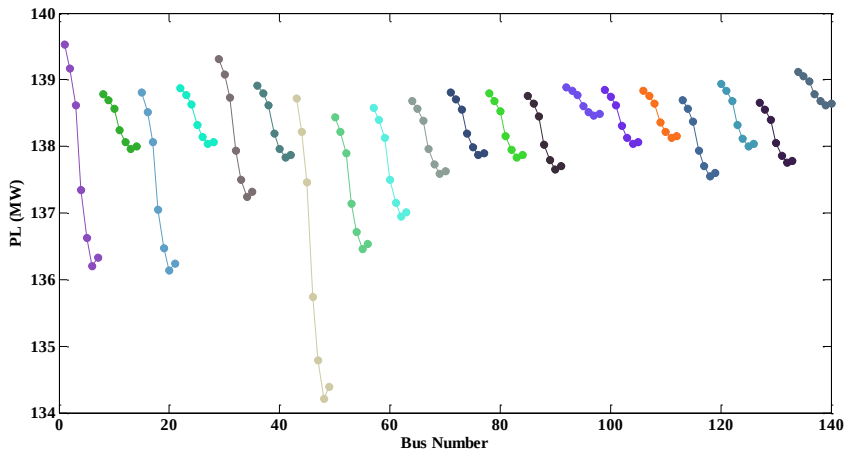

Figure 2. 6. Power loss of system with 50 % charging of BESS (Case-I)

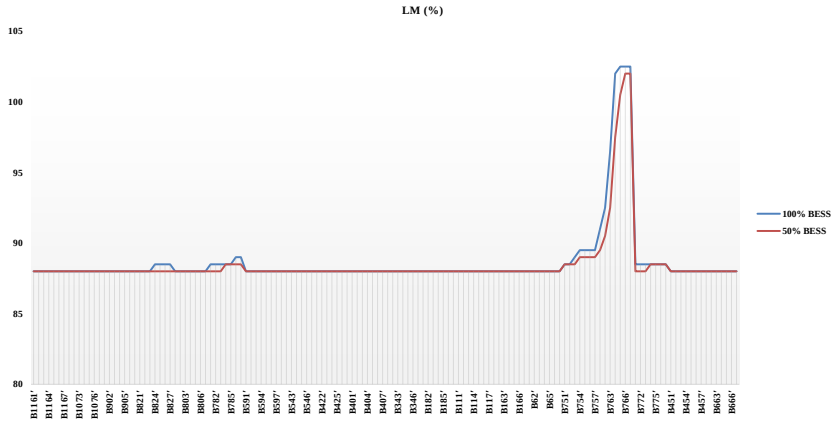

Figure 2. 7. Load margin of system with 100 and 50% charging of BESSs (Case-I)

Table 2. 3. Comparison between the primary objective functions (without BESS allocation) and minimum/maximum objective function values (with BESS allocation) for Case-I

	PL (MW) / Location	VD (pu) / Location	LM (%)
Primary IEEE-118 Bus	132.863		
Primary modified IEEE-118 Bus (Without BESS)	138.97	2.742	88
Maximum Value	140.2008 / B1161	2.7951 / B807′	102.5 / B765′
Minimum Value	132.9522 / B596′	2.2155 / B1167′	88
Improvement (%) for Minimum Value	4.33	19.2	16.47

2.6.2 Case-II:

The topology of this case test network is depicted in figure 2.8. In order to highlight the impact of BESS allocation in distribution side, in this case the BESSs are placed at the transmission side and in aggregated mode. The BESSs capacities are chosen according to Table 2.2. Hence, 20 scenarios produced for BESS allocation in our test system. The amounts of PL, VD and LM for 100% and 50% of BESS charge, are depicted in figures 2.9-2.13. The red boxes in these figures expressed the % improvement of objective functions, respect to the primary values (without BESS). In addition, Table 2.4 compares the PL, VD and LM with/without the BESSs and also expressed these objectives % improvements. According to these figures, in some cases this % is negative which means that with installing BESS in some buses in aggregate mode, the system status for losses and voltage deviation will deteriorate.

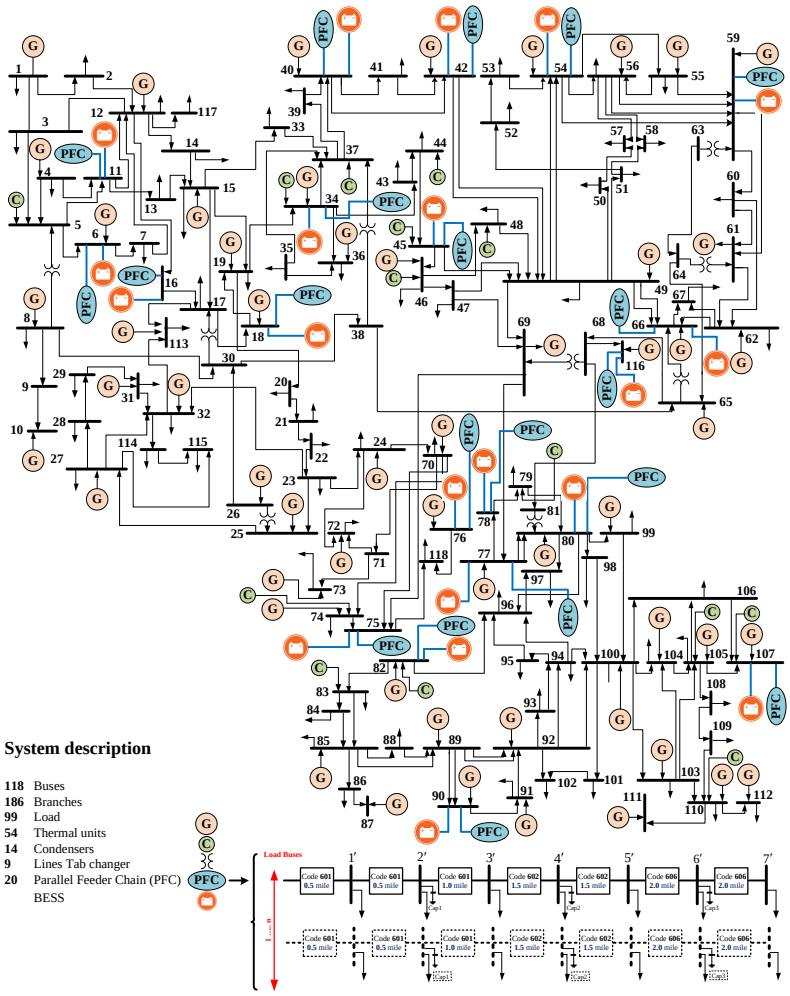

Figure 2. 8. Single line diagram of modified IEEE 118-bus test system integrated to parallel feeder chain – BESS allocation in respect to the TNs viewpoint (Case-II)

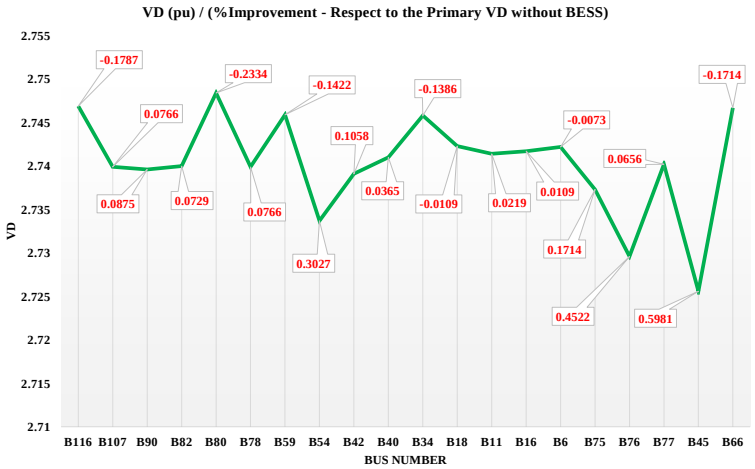

Figure 2. 9. Voltage deviation of system with 100 % charging of BESS (Case-II)

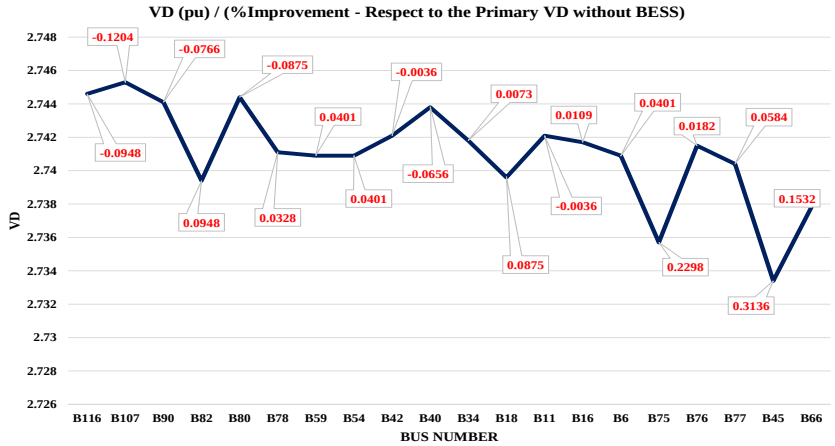

Figure 2. 10. Voltage deviation of system with 50 % charging of BESS (Case-II)

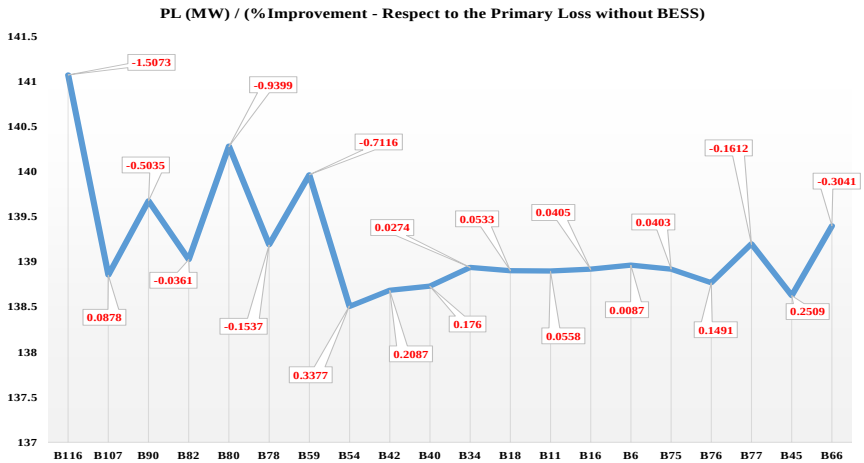

Figure 2. 11. Power loss of system with 100 % charging of BESS (Case-II)

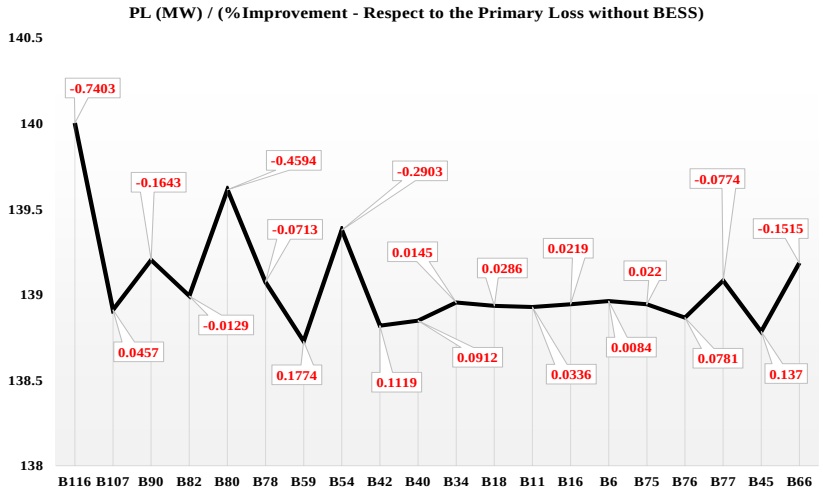

Figure 2. 12. Power loss of system with 50 % charging of BESS (Case-II)

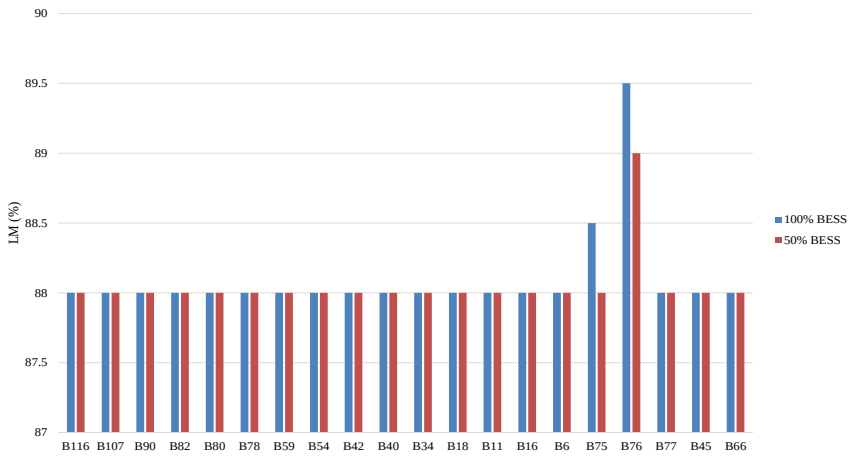

Figure 2. 13. Load margin of system with 100 % and 50% charging of BESSs (Case-II)

Table 2. 4. Comparison between the primary objective functions (without BESS allocation) and minimum/maximum objective function values (with BESS allocation) for case-II

	Location / PL (MW)	Location / VD (pu)	LM (%)
Primary IEEE-118 Bus	132.863		
Primary modified IEEE-118 Bus (Without BESS)	138.97	2.742	88
Maximum Value	B116 / 141.0687	B80 / 2.7484	B76 / 89.5
Minimum Value	B59 / 138.5046	B45 / 2.7256	88
Improvement (%) for Minimum Value	0.33	0.59	1.7

2.7 Discussion

In the cases I and II, the amount of BESSs capacities are chosen according Table 2.2. The results show that the best place for installing BESSs is bus B59 in both case-I and case-II for seeking to the minimum PL. The important point is, when system operator installs the 2.4 MW BESS in transmission network and in aggregate mode (case-II), the system PL is 138.5046 MW but when the similar battery installed in B596′, the PL is decreased to the 132.9522 MW (decrease 4%). Besides, the VD of system is decreased by 18% with this procedure. These points are depicted in figures 2.14 and 2.15. These figures are compared the minimum values of objective functions.

If the system operator want to compare the impact of BESS allocation in a specific bus, figures 2.16 and 2.17 can be the good references. In figure 2.16, power loss of system in B59 (case-II) is compared with B591′ - B597′ (Case-I). In addition, in figure 2.17, voltage deviation of system in B116 (case-II) is compared with B1161′ - B1167′ (Case-I). The results show that the PL and VD are decreased, when the BESS is allocated in distribution side.

It is worth to mention that LM value is increased by installing BESS in distributed type. This case has been investigated on the bus 76 and is shown in figure 2.18.

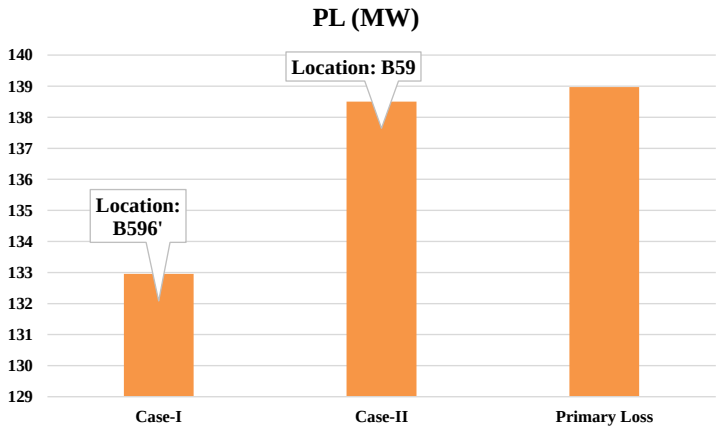

Figure 2. 14. Comparison between minimum PL of Case-I and Case-II

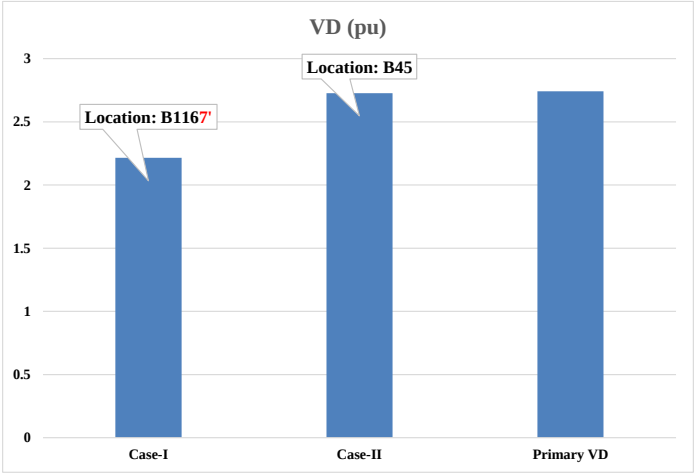

Figure 2. 15. Comparison between minimum VD of Case-I and Case-II

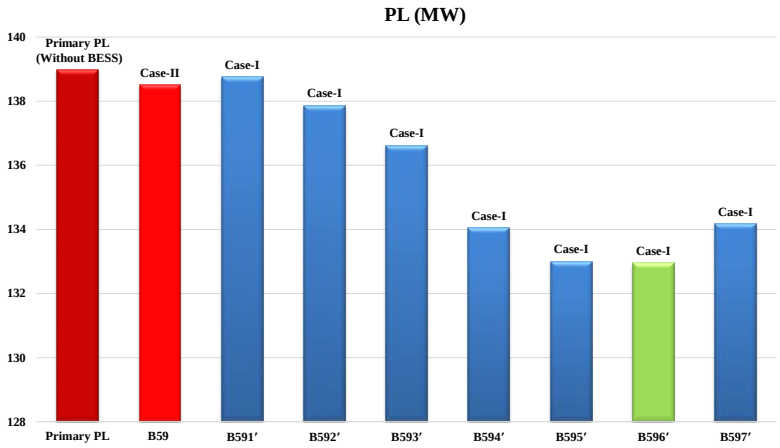

Figure 2. 16. Comparison between PL of case-I and case-II (in bus 59)

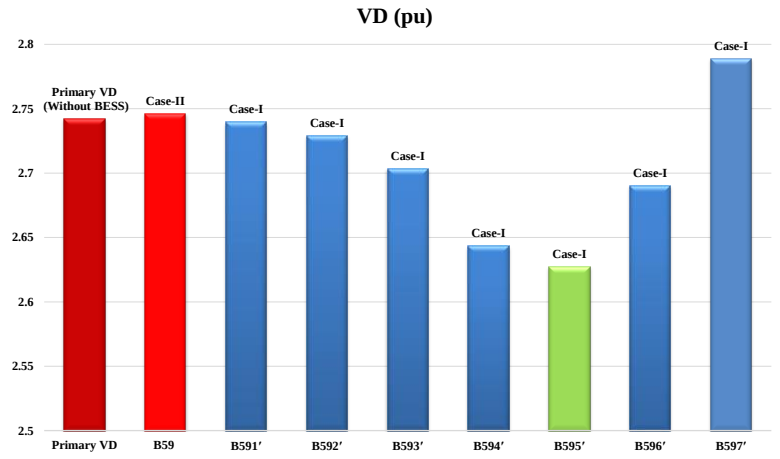

Figure 2. 17. Comparison between VD of case-I and case-II (in bus 59)

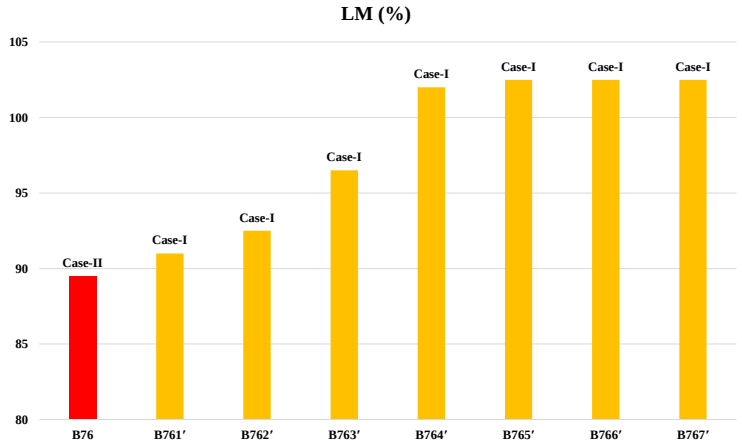

Figure 2. 18. Comparison between LM of case-I and case-II (in bus 76)

2.8 Conclusion

Optimal allocation of battery energy storage systems (BESSs) problem is studied in this paper at the integrated transmission and distribution (T&D) systems. The objective functions used in the proposed problem are real power losses (PL), voltage deviations (VD) and loading margin (LM). The proposed method which incorporated OPF solution with TN and DN combined equations is implemented and analyzed on IEEE-118 bus test case, and its effectiveness is verified using different simulations and comparisons. The main findings of this work are outlined as follow:

- With modeling BESS in distributed form (Case-I) the objectives functions are better than the aggregate form (Case-II) – (based on the results given in Figures 2.16-2.18).
- From the point of view of PL and LM, bus 59 and from the point of VD, bus 116, is the best locations for BESSs allocation (as shown in Figures 2.14-2.15)
- The LM value is improved in distributed mode in comparison with aggregate mode (Figure 2.18). The BESS place is important for the system (Appendix [18]).
- Considering figures 2.16 and 2.17, it is observed that the PL and VD values are decreased in distributed BESS allocation at first, but after that, it slightly increased, which means the necessity for optimal allocation of BESSs in the distribution system.

3 Allocation optimale à un jour d'avance des BESSs dans les systèmes T&D: approche basée sur la co-optimisation stochastique avec incertitudes de la production variable

3.1 Résumé

Compte tenu de la croissance des nouvelles technologies émergentes dans les réseaux de distribution, tels que l'énergie éolienne, l'énergie photovoltaïque ou les production décentralisée, il est extrêmement important d'examiner simultanément ces réseaux et les réseaux de transport. Dans cet article, un cadre efficace est proposé pour comprendre de manière transparente les interactions de transmission et de distribution (T&D) tout en incluant des modèles détaillés pour les ressources d'énergie distribuées (DER). L'éolien, le photovoltaïque et la demande sont étudiés en fonction de leur profil 24h. En outre, l'incertitude de l'énergie éolienne est prise en compte via la méthode du scénario. Enfin, les systèmes de stockage d'énergie par batterie (BESS) sont utilisés pour suivre la production probabiliste renouvelable et minimiser les pertes de puissance totales du système. Le système de test IEEE 9 barres modifié est sélectionné en tant que réseau de transmission et une simple artère radiale à 8 barres est sélectionnée en tant que réseau côté distribution. Le problème est formulé comme un problème d'optimisation par programmation non linéaire en nombres entiers (MINLP) et traité via le langage de programmation GAMS. Les résultats montrent que, compte tenu de la forte pénétration des sources d'énergie renouvelables au niveau de la distribution, la reprogrammation des principaux générateurs augmente l'efficacité énergétique du système. De plus, les BESS atténuent l'impact des sources renouvelables sur le transport et la distribution tout en réduisant les pertes d'énergie pendant les heures de pointe.

Corps de l'article

Titre: Stochastic Day-ahead Optimal BESSs' Allocation in T&D Systems: Co-optimization Based Approach with Uncertainties

Seyed Masoud Mohseni-Bonab[1,2], Innocent Kamwa[2], Abbas Rabiee[3] and Ali Moeini[2]

[1] Electrical Engineering Department, Laval University, QC, Quebec, Canada (e-mail: s.m.mohsenibonab@ieee.org)

[2] Hydro-Québec/IREQ, Power System and Mathematics, Varennes QC J3X 1S1, Canada (e-mail: kamwa.innocent@ireq.ca, moeini.ali@ireq.ca)

[3] Electrical Engineering Department, University of Zanjan, Zanjan, Iran (e-mail: rabiee@znu.ac.ir)

Conférence: 2018 IEEE/PES Transmission and Distribution Conference and Exposition (T&D)

3.2 Abstract

With the growth of emerging new technologies in distribution networks, such as wind power, photovoltaic or DGs, the need for simultaneously investigation of these networks alongside transmission networks is highly important. In this paper, an efficient framework is proposed to understand seamlessly transmission and distribution (T&D) interactions while including detailed models for distributed energy resources (DERs). Wind power, photovoltaic and demand are investigated according to their 24^h profile. Besides, wind power uncertainty is considered via the scenario-based method. Finally, Battery Energy Storage Systems (BESSs') are used to track probabilistic renewable generation and minimize the total system power losses. The modified IEEE 9-bus test system is selected as a transmission network and a simple 8-bus radial feeder is selected as a distribution side network. The problem modeled as a mixed integer nonlinear programming (MINLP) optimization problem and handled via GAMS programming language. The results show that with high penetration of renewable sources at distribution level, rescheduling main generators increases system energy efficiency. Moreover, the BESS can mitigate the impact of renewable sources on both transmission and distribution while reducing power losses during peak hours.

Keywords: Integrated transmission and distribution (T&D) systems, battery energy storage systems (BESS), wind power uncertainty, co-optimization, scenario-based approach.

3.3 Nomneclature

$\cos\left(\varphi_{lag,i}\right)$	Lag power factor limits of the wind farms located at node *i*.
E	Index of storage type.
$E_{BESS_i,s,t}$	Energy stored in BESS at node *i* in scenario *s* at time period *t*.
$E_{BESS_i}^{\min} / E_{BESS_i}^{\max}$	Maximum/minimum energy stored at node *i* (MWh).
i / j	Index of bus Number where $i = 1, 2, \ldots, N_B$.
$I_{E_i,s}$	Integer decision variable indicating the optimal number of BESS in scenario s.
ℓ	Index of transmission lines.
$L_{ESS_i,s,t}$	Power losses in ESS in scenario *s* at time *t* (MW).
N_B / N_j	Set of buses.
N_L	Set of branches (transmission lines).
N_G	Set of generating units.
N_D	Set of load buses.
N_{BESS}	Set of candidate buses for BESS.
N_W	Set of nodes containing wind turbines.
N_{PV}	Set of nodes containing PV.
$P_{G_i}^{\min} / P_{G_i}^{\max}$	Minimum/maximum value for active power of the *i-th* bus.
$P_{D_i,t}$	Real power of the *i-th* bus at time period *t*.
$P_{ch_i,s,t,E} / P_{dch_i,s,t,E}$	Charge/discharge power of BESS at node *i* in scenario *s* at time period *t* in storage type *E*.
$P_{ch_i}^{\min} / P_{ch_i}^{\max}$	Maximum/minimum power charge of BESS at node *i* (MW).
$P_{PV_i,s,t}$	Active power produced by PV at scenario *s* at time period *t*.
$P_{W_i}^{r}$	Wind farm rated capacity installed in bus *i*.
$P_{dch_i}^{\min} / P_{dch_i}^{\max}$	Maximum/minimum power discharge of BESS at node *i* (MW).
P_{BESS_i}	The available BESS types (E) capacity (MWh).
$PL_{s,t}\left(\bar{u}_{s,t}, \bar{x}_{s,t}\right)$	Real Power Loss in scenario s at time period *t*.
$P_{G_i,s,t} / Q_{G_i,s,t}$	Active/reactive power production at bus *i* in scenario *s* at time period *t*.
$P_{W_i,s,t} / Q_{W_i,s,t}$	Active/reactive power produced by wind turbine at scenario *s* at time period *t*.
$Q_{D_i,t}$	Reactive power of the *i-th* bus at time period *t*.
$Q_{G_i}^{\min} / Q_{G_i}^{\max}$	Minimum/ Maximum value for reactive power of the *i-th* bus.
s	Index of scenario numbers.
$S_{\ell}^{\max}$	Maximum value of power flow of ℓ *-th* transmission line.

$S_{\ell,s,t}$	Power flow of ℓ *-th* transmission line in scenario *s* at time period *t.*
t	Index for operation intervals.
$TP_{ch_i,s,t} / TP_{dch_i,s,t}$	Total charge/discharge power of all BESS types at node *i* in scenario *s* at time period *t.*
$\bar{u}_{s,t}$	Vector of control variables in scenario *s* at time period *t*.
$v_{in}^{c} / v_{out}^{c} / v_{rated}$	Cut-in/out/rated speed of wind turbine in m/s.
$V_i^{\min} / V_i^{\max}$	Minimum/Maximum value for voltage magnitude of the *i-th* bus.
$V_{i,s,t}$	Voltage magnitude of bus *i/j* in scenario *s* at time period *t.*
$\bar{x}_{s,t}$	Vector of dependent variables in scenario *s* at time period *t*.
$Y_{ij}\angle\gamma_{ij}$	Magnitude/angle of ij-th element of YBUS matrix (pu/radian).
$\theta_{i,s,t}$	Voltage angle at bus *i/j* in scenario *s* at time period *t.*
π_s	Probability of scenario s
η_{ch} / η_{dch}	Efficiency of charging and discharging of BESS (%).
$\zeta_{W_{i,s}}$	Percentage of wind power rated capacity realized at scenario *s* in bus *i*.

3.4 Introduction

Power distribution networks are faced with rampant integration of distributed renewable generation, electric vehicles, and energy storage units. Nowadays with increasing these technologies, the interaction between transmission & distribution (T&D) is becoming more important. The upward flowing inherently stochastic power impacts significantly transmission and production levels. In this context, the proposed research pioneers engineering innovations in the form of designs and algorithms targeting the distributed energy resources (DERs) characteristics in a management of distribution networks on transmission networks. Analyzing simultaneously T&D is categorized in two following forms:

- Dynamic analysis [15, 16]
- Steady-state analysis

In the area of steady-state, the researchers have focused on inventing ways to execute simultaneously power flow in T&D during recent years [7-9, 11]. In [7], a master-slave-splitting (MSS) iterative method is used for global power flow (GPF) in integrated T&D. Also, boundary mismatches between the T&D are alleviated with convergence guarantee of

GPF. A new global transmission contingency analysis (GTCA) based method is proposed in [8] for T&D PF.

As a common practice, transmission networks (TNs) are assumed as three-phase balanced systems. Distribution networks (DNs) are usually modeled in the form of single-phase (balanced or unbalanced [19]) or three phases [9]. Next, in [11] the IGMS concept is defined to simultaneously analyze T&D. An iterative approach is utilized in [20] for decomposing joint T&D optimal power flow to transmission OPF and distribution OPF. The residual demand curve integrated these two networks.

The impacts of BESS based DERs on distribution level has been highly reviewed in literatures. A mixed-integer linear programming (MILP) based method in [21] is utilized finding size and location of energy storage system (ESS) in a microgrid. The size and location is important when the discharged amount of ESSs are considered which has been investigated in [22]. In a recent study, the impact of BESS allocation on T&D, with emphasize on solving optimal PF (OPF) problem has also been investigated [23].

3.4.1 Contribution

To the best knowledge of the authors, there is no work addressing impact of renewable resources and their uncertainties plus BESS allocation on integrated T&D framework for loss minimization. Given the discussed context, the contributions of this paper are:

- Providing a management framework for integrating DERs (WTs, BESSs' and PVs) to T&D.
- Including stochastic nature of wind power and analyzing imposed uncertainty via scenario-based approach.
- Optimal scheduling of BESS in T&D for minimizing power losses and voltage deviation.
- Deriving strategies for enabling consumers' participation in alleviating distribution network challenges.

3.5 Uncertainty modeling

In this work wind speed uncertainty modeled by Weibull PDF as follows:

$$PDF(v) = \left(\frac{k}{\lambda}\right)\left(\frac{v}{\lambda}\right)^{k-1} \exp\left(-\frac{v}{\lambda}\right)^{k} \tag{3-1}$$

where k is the shape parameter and λ is the scale parameter attained from historical wind data. The procedure of scenario generation from (3-1) and the power curve of a wind turbine are adapted from [24]. Using this curve, the forecasted output power of the wind turbine for different wind speeds can be obtained using the following equation:

$$P_w^{avl} = \begin{cases} 0 & v_w \le v_w^{c,in} \ or \ v_w \ge v_w^{c,out} \\ \dfrac{v_w - v_w^{c,in}}{v_w^r - v_w^{c,in}} P_w^r & v_w^{c,in} \le v_w \le v_w^r \\ P_w^r & v_w^r \le v_w \le v_w^{c,out} \end{cases} \tag{3-2}$$

Based on (3-2), five scenarios are considered for wind power generation modeling, which are given in Table 3.1.

Table 3. 1. Wind power generation scenarios with the corresponding means and probabilities

Scenario	s_1	s_2	s_3	s_4	s_5
π_w	0.0689	0.2044	0.4048	0.1992	0.1227
P_w^{avl}	0	0.1287 P_w^r	0.4937 P_w^r	0.8683 P_w^r	P_w^r

3.6 Problem Formulation

3.6.1 Contribution Problem variables

The control/dependent variables of this paper for optimizing objective function can be categorized as follows.

$$\bar{u} = \begin{bmatrix} P_{G_i,s,t} & ,\forall i = N_G & ,\forall s,\forall t \\ Q_{G_i,s,t} & ,\forall i \in N_G & ,\forall s,\forall t \\ P_{ch_i,s,t} & ,\forall i \in N_{BESS} & ,\forall s,\forall t \\ P_{dch_i,s,t} & ,\forall i \in N_{BESS} & ,\forall s,\forall t \\ I_{E_i,s} & ,\forall i \in N_{BESS} & ,\forall s \end{bmatrix}, \bar{x} = \begin{bmatrix} P_{W_i,s,t} & ,\forall \ell \in N_W & ,\forall s,\forall t \\ Q_{W_i,s,t} & ,\forall \ell \in N_W & ,\forall s,\forall t \\ P_{PV_i,s,t} & ,\forall \ell \in N_W & ,\forall s,\forall t \\ \theta_{i,s,t} & ,\forall i \in N_B & ,\forall s,\forall t \\ S_{\ell,s,t} & ,\forall \ell \in N_L & ,\forall s,\forall t \end{bmatrix} \tag{3-3}$$

3.6.2 Objective functions

The power losses are increased by raising the energy consumption. Reduction of power losses is a critical aim for system operators. In the *s*-th scenario and *t*-th hour, the active power losses (PL) can be calculated as follows [25].

$$PL_{s,t}\left(\bar{u}_{s,t},\bar{x}_{s,t}\right)=\left(\sum_{i=1}^{N_G}P_{G_i,s,t}+\sum_{i=1}^{N_W}P_{W_i,s,t}+\sum_{i=1}^{N_{PV}}P_{PV_i,s,t}\right)-\sum_{i=1}^{N_B}P_{D_i,s}$$
$$\left(-\sum_{i=1}^{N_{BESS}}TP_{ch_i,s,t}+\sum_{i=1}^{N_{BESS}}TP_{dch_i,s,t}\right)+\sum_{i=1}^{N_{BESS}}L_{ESS_i,s,t} \tag{3-4}$$

$$\sum_{i=1}^{N_{BESS}}L_{ESS_i,s,t}=\left(1-\eta_{ch}\right)TP_{ch_i,s,t}+TP_{dch_i,s,t}\left(1/\eta_{dch}-1\right) \tag{3-5}$$

Since the $PL_{s,t}$ is scenario dependent, its expected value (i.e. expected power losses (EPL)) is regarded as the objective function, which is calculated as follows:

$$EPL=\sum_{t=1}^{t=24}\sum_{s=1}^{NS}\pi_s PL_{s,t} \tag{3-6}$$

In this work, five storage types are considered and charge/discharge power of BESS are calculated from (3-7) and (3-8). It is worth to note that the BESS are modeled as a multi-step source, i.e. a discrete variable is regarded for each BESS node as follows (Eq. 3-9). This variable determines the optimal steps of BESS injections. Also, as an important point, as is clear from Equation 3-9, this variable is independent of *t*.

$$TP_{ch_i,s,t}=\sum_{E=1}^{N_{BESS}}P_{ch_i,s,t,E} \tag{3-7}$$

$$TP_{dch_i,s,t}=\sum_{E=1}^{N_{BESS}}P_{dch_i,s,t,E} \tag{3-8}$$

$$E_{BESS_i,s,t}\le P_{BESS_i}\times I_{E_i,s}\ ,\ \forall i\in N_{BESS}\ ,\ \forall s \tag{3-9}$$

The objective function in (4-6) is subjected to the following constraints:

$$\begin{cases} P_{G_i,s,t} + P_{W_i,s,t} + P_{PV_i,s,t} - P_{D_i,t} - TP_{ch_i,s,t} + TP_{dch_i,s,t} = \\ \qquad V_{i,s,t}\sum_{j=1}^{N_B} V_{j,s,t} Y_{ij} \cos\left(\theta_{i,s,t} - \theta_{j,s,t} - \gamma_{ij}\right) \\ Q_{G_i,s,t} + Q_{W_i,s,t} - Q_{D_i,t} = \\ \qquad V_{i,s,t}\sum_{j=1}^{N_B} V_{j,s,t} Y_{ij} \sin\left(\theta_{i,s,t} - \theta_{j,s,t} - \gamma_{ij}\right) \end{cases} \tag{3-10}$$

$$P_{G_i}^{\min} \le P_{G_i,s,t} \le P_{G_i}^{\max} \quad , \forall i \in N_G \quad , \forall s , \forall t \tag{3-11}$$

$$Q_{G_i}^{\min} \le Q_{G_i,s,t} \le Q_{G_i}^{\max} \quad , \forall i \in N_G \quad , \forall s , \forall t \tag{3-12}$$

$$V_i^{\min} \le V_{i,s,t} \le V_i^{\max} \quad , \forall i \in N_B \quad , \forall s , \forall t \tag{3-13}$$

$$\left|S_{\ell,s,t}\right| \le S_\ell^{\max} \quad , \forall \ell \in N_L \quad , \forall s , \forall t \tag{3-14}$$

$$E_{BESS_i,s,t} = E_{BESS_i,s,t-1} + \left(\eta_{ch} P_{ch_i,s,t,E} - P_{dch_i,s,t,E} / \eta_{dch}\right)\Delta t \tag{3-15}$$

$$E_{BESS_i}^{\min} \le E_{BESS_i,s,t} \le E_{BESS_i}^{\max} \quad , \forall i \in N_{BESS} \quad , \forall s , \forall t \tag{3-16}$$

$$P_{ch_i}^{\min} \le P_{ch_i,s,t,E} \le P_{ch_i}^{\max} \quad , \forall i \in N_{BESS} \quad , \forall s , \forall t , \forall E \tag{3-17}$$

$$P_{dch_i}^{\min} \le P_{dch_i,s,t,E} \le P_{dch_i}^{\max} \quad , \forall i \in N_{BESS} \quad , \forall s , \forall t \ , \forall E \tag{3-18}$$

$$I_{E_i,s}^{\min} \le I_{E_i,s} \le I_{E_i,s}^{\max} \quad , \forall i \in N_{BESS} \quad , \forall s , \forall t \tag{3-19}$$

$$0 \le P_{W_i,s,t} \le \zeta_{W_{i,s,t}} \times P_{W_i}^r \quad , \forall i \in N_W \ , \forall s , \forall t \tag{3-20}$$

$$Q_{W_i,s,t} = tg\left(\varphi_{lag}\right) \times P_{W_i,s,t} \quad , \forall i \in N_W \ , \forall s , \forall t \tag{3-21}$$

Constraints (3-10)-(3-14) correspond to the operational limits, whereas (3-15)-(3-19) correspond to the BESS state of charge (SOC) limits. Moreover, (3-20) and (3-21) are available active/reactive power outputs of wind turbines. In this paper, the reactive power output of wind farms are limited to the corresponding active power output.

3.7 Simulation Results

3.7.1 Data and assumptions

The proposed method is modeled via GAMS. The MINLP part is handled by SBB solver, while CONOPT4 is utilized to solve the NLP part. Simulation is performed on a modified IEEE-9 bus system. A simple 8 MW distribution feeder replaces a portion of load connected to bus 7 (i.e. Case-I) or buses 7, 5 and 9 (i.e. Case-II). The remaining load is considered as industrial aggregated load. All distribution nodes are candidate for BESS installation. In addition, in Case-I, the wind turbine (WT) nodes are 12, 14 and 16 (rated as 1MW). Besides, the PVs, with 0.5 MW rated are added to nodes 13 and 15. In Case-II, it is assume that the WT nodes are B_{12}, B_{14}, B_{16}, B_{19}, B_{21}, B_{23}, B_{26}, B_{28} and B_{30} while B_{13}, B_{15}, B_{20}, B_{22}, B_{27} and B_{29} are selected as a PV nodes. The study system is shown in Fig. 3.1.

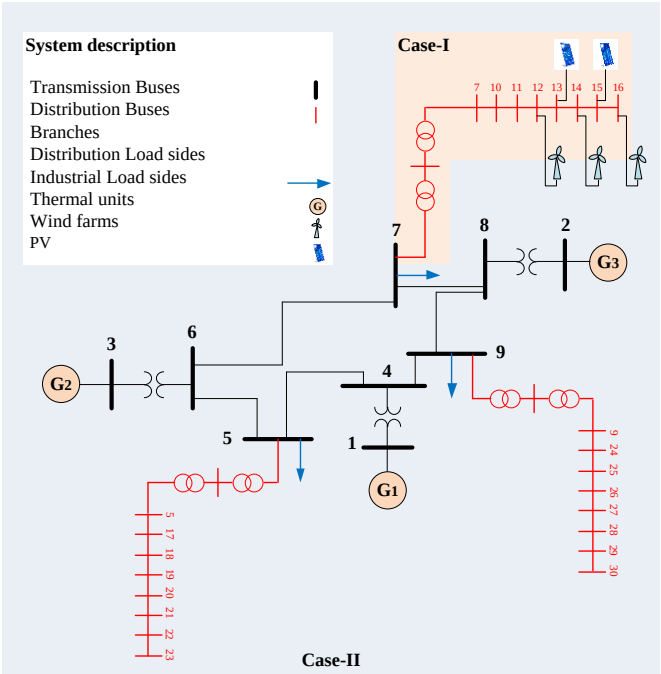

Figure 3. 1. Single line diagram of test system

In this paper, the simulations is performed according to the hourly variations in load, wind and PV, demand and generations. The daily load, wind and PV curve is shown in figure 3.2 [26]. The technical characteristics of the considered BESSs are described in Table 3.2.

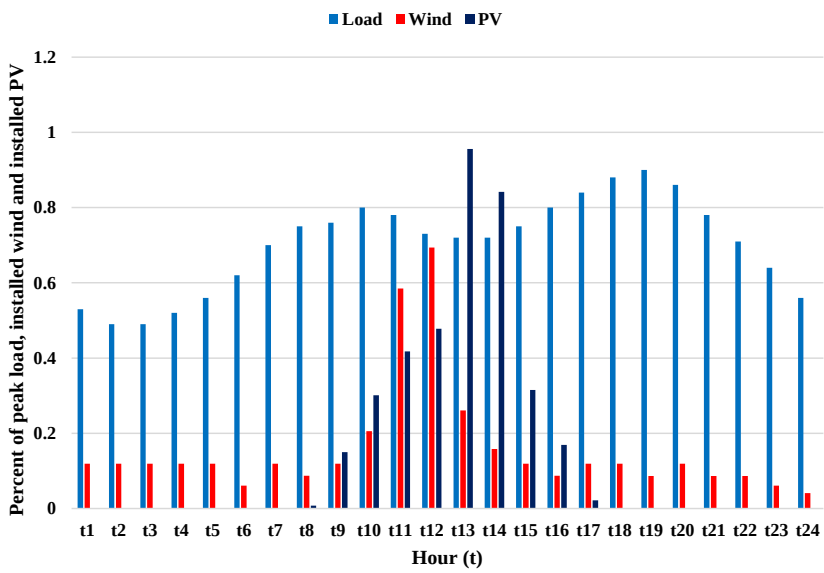

Figure 3. 2. Day-ahead load, wind and PV characteristics

Table 3. 2. Technical characteristics of BESS

Parameter	characteristic
P_{BESS_i}	E1=500KW, E2=400KW, E3=300KW, E4=200KW, E5=100KW
$I_{E_i,s}^{\min} / I_{E_i,s}^{\max}$	0 / 3
$E_{BESS_i}^{\min} / E_{BESS_i}^{\max}$	0 / $P_{BESS_i} \times I_{S_i,s}$
$P_{ch_i}^{\min} / P_{dch_i}^{\min}$	0
$P_{ch_i}^{\max} / P_{dch_i}^{\max}$	P_{BESS_i} (E1 – E5 capacities)
η_{ch} / η_{dch}	0.95

3.7.2 Case-I

Figure 3.3 shows the PL for different wind scenarios, with/without storage sources. It is clear that the BESS allocation reduces the PL. When BESS is charged the PL is increased but when the BESS discharged the PL is decreased. This is implied in fig 3.4. In this figure it is obvious that the maximum PL reduction is occurred at t=19. The expected value of PL % improvement, with/without BESS is depicted in fig 3.5.

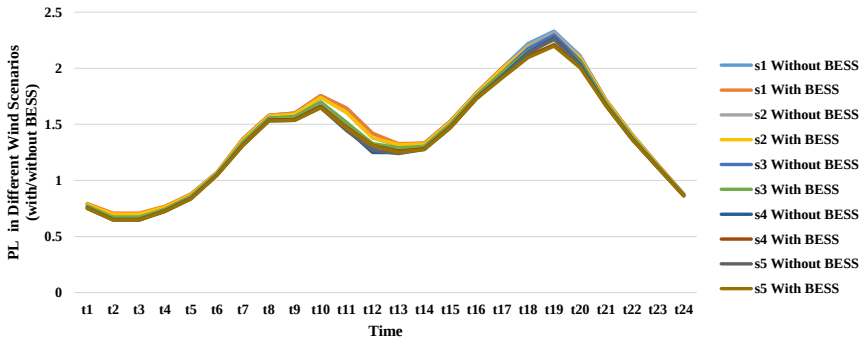

Figure 3. 3. PL with and without BESS in all scenarios

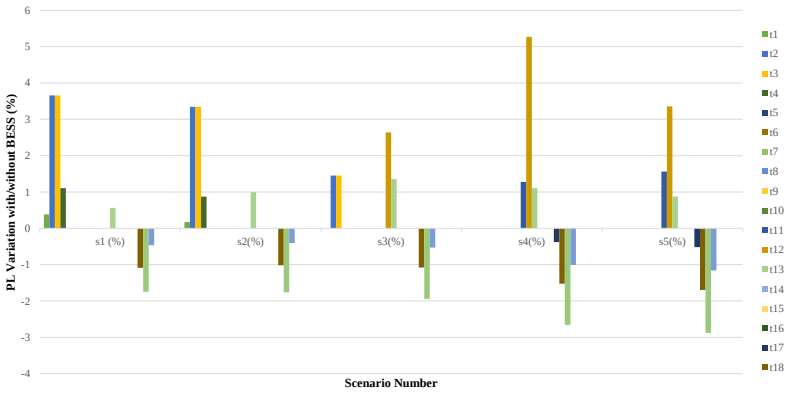

Figure 3. 4. PL variations in different scenarios and different hours (%)

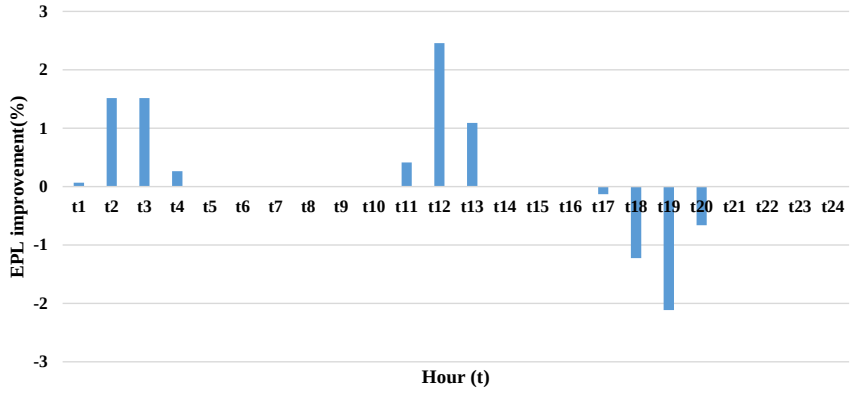

Figure 3. 5. EPL variations in different scenarios and different hours (%)

3.7.3 Control variables

According to the (4-3) for reaching the minimal power losses (figure 3.3, 3.4), the control variables must be adjusted. The optimal amount of BESS steps is given in figure 3.6. Given this figure, it is clear that the highest battery usage is in the scenarios 1. The total usage of BESS in different scenarios are: s_1=1.6 MW, s_2=0.6 MW, s_3=0.5 MW, s_4=0.9 MW, s_5=0.9 MW. For the sake of brevity the rest of the variables are reported only for s_5 but the completed results are available in appendix part. Figure 3.7 shows the SOC of BESS in different hours in scenario5. It is clear from the figure that the battery starts to charge at t=11, when the wind and PV produced powers are relatively high, and discharges at t=19. Besides, Fig. 3.8 depicts the active power generation at the generation buses for all 5 scenarios. According to SOC values, in s_5, the BESS is charged in t_{11}, t_{12} and t_{13}, and discharged in t_{17}, t_{18}, t_{19} and t_{20}. In other hours, the battery is idle. This is shown in Figure 3.9. The adjusted buses voltages for this optimization are given in Figure 3.10, as well.

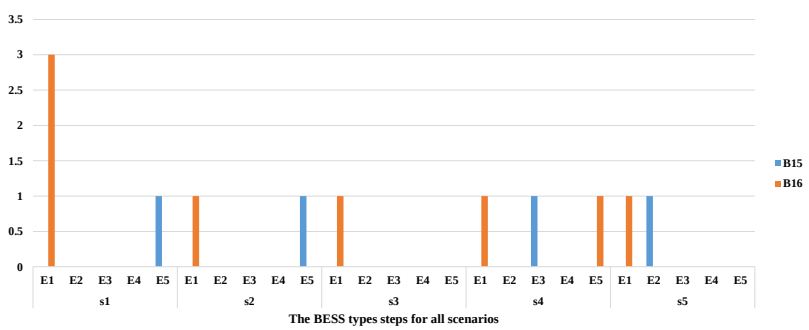

Figure 3. 6. The optimal amount of BESS types steps in all scenarios

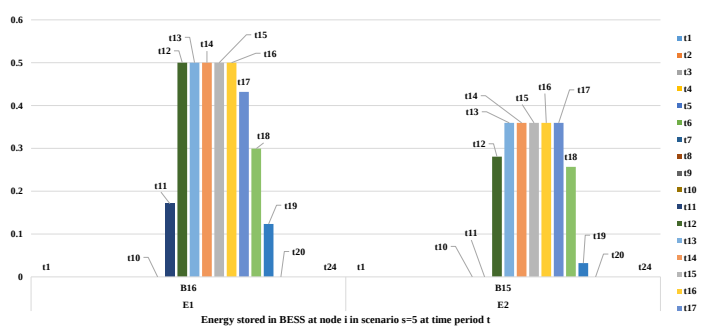

Figure 3. 7. Energy stored in BESS at node *i* in scenario *s*=5 at time *t* (MWh)

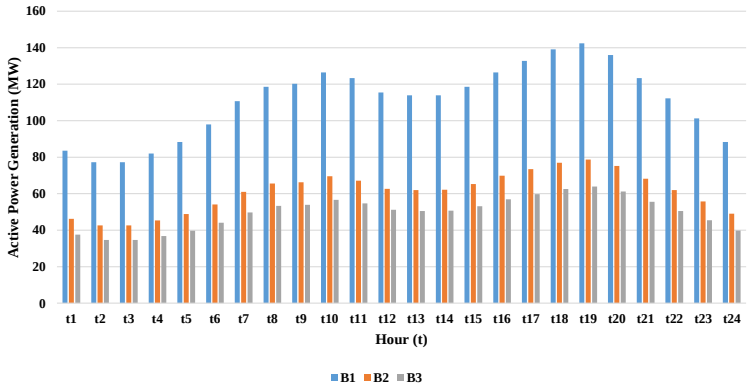

Figure 3. 8. Active power generations in scenario 5 at time period *t* (in MW)

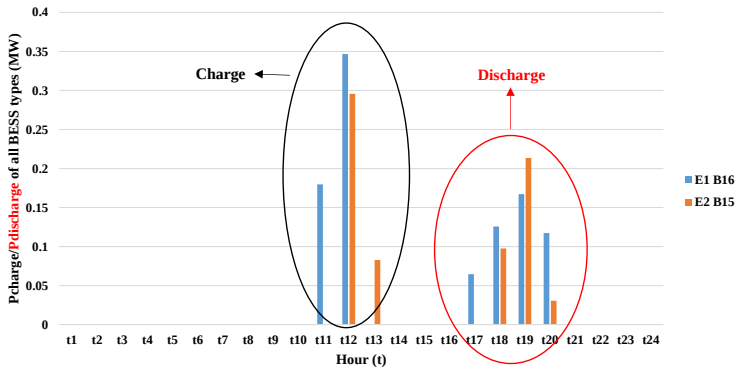

Figure 3. 9. Charge/discharge amount of BESS types in scenario 5 at time period *t* (in MW)

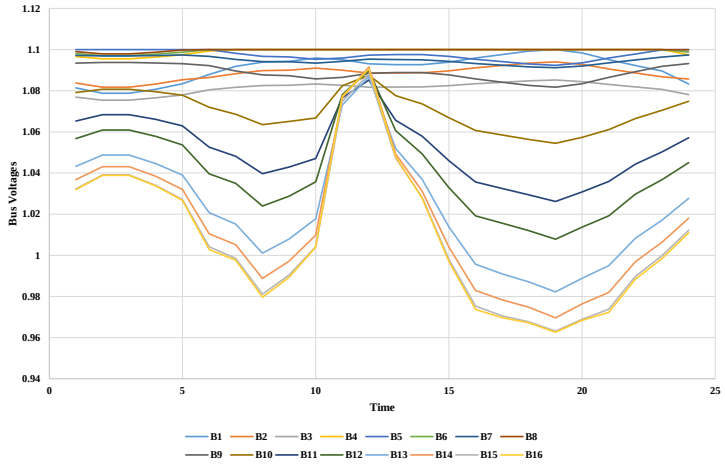

Figure 3. 10. The adjusted voltage of all buses in scenario 5 (pu)

3.8 Discussion

In this part the proposed methodology is investigated in a wide range. The following analysis is performed:

3.8.1 Analyzing the problem for a specific hour (t19):

According to the figure 3.4, t=19 have a minimum PL in different scenarios. The stored energy at different BESS types in this hour and one hour earlier are gathered in Table 3.3. According to this Table, it is clear that the algorithm discharges the BESS during the peak hour and reduces the power loss locally supplying a portion of load.

Table 3. 3. SOC of t_{19} and one hour before (MWh)

			t_{18}	t_{19}	t_{19}- t_{18}
s_1	E1	B_{16}	0.1658	0.0502	-0.1156
	E5	B_{15}	0.0854	0	-0.0854
s_2	E1	B_{16}	0.1626	0.0449	-0.1177
	E5	B_{15}	0.0888	0	-0.0888
s_3	E1	B_{16}	0.3012	0.0629	-0.2383
s_4	E1	B_{16}	0.2593	0.1305	-0.1288
	E3	B_{15}	0.1459	0	-0.1459
	E5	B_{16}	0.0833	0	-0.0833
s_5	E1	B_{16}	0.2996	0.1236	-0.176
	E2	B_{15}	0.2569	0.0322	-0.2247

3.8.2 Analyzing the problem for a specific scenario (s5):

Table 4.4, is shown the SOC of different BESS for all hours but in a specific scenario (s_5). According to the figure 3.2, in t_{12} and t_{13}, the wind power and PV generations are the maximum values, respectively and there is an opportunity for system operator to store the extra energy by charging the BESS. According to Table 3.3, from t_{16}, the BESSs starts to discharged slowly. Finally in t_{20} the BESSs energies are zero. Fig. 3.11 depicted the PL without/with BESSs along the total stored energy in BESSs, the system renewables production and the system loads in different hours.

Table 3. 4. SOC of BESS types in different times of scenario 5

	$E1 - B_{16}$	$E2 - B_{15}$
$t_1 - t_{10}$	**0**	**0**
t_{11}	0.1708	**0**
t_{12}	0.5	0.2809
$t_{13} - t_{16}$	0.5	0.3597
t_{17}	0.432	0.3597
t_{18}	0.2996	0.2569
t_{19}	0.1236	0.0322
$t_{20} - t_{24}$	**0**	**0**

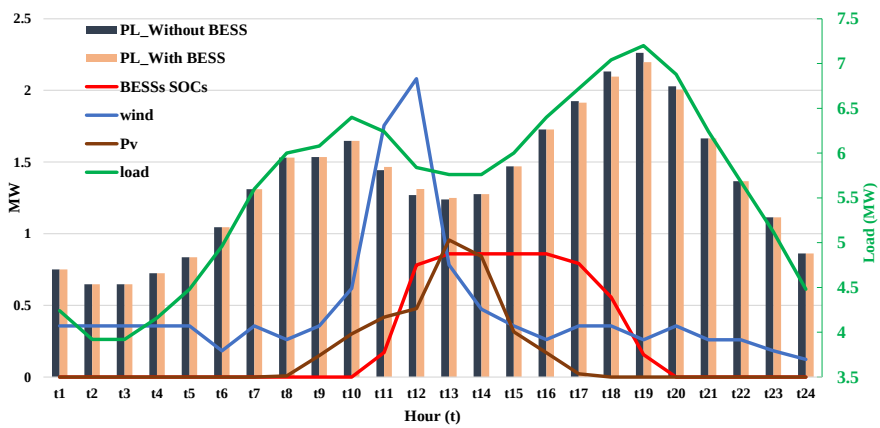

Figure 3. 11. Comparison between PL in different cases, SOCs, renewables production and system demand

3.8.3 Appling the proposed methodology on Case-II

In this case, the algorithm is applied on case-II. In this case, all load buses are replaced by the simple test feeder. Five different BESS types (E) are considered. The capacities of these BESS are as follows: E1=2 MW, E2=1.6 MW, E3=1.2 MW, E4=0.8 MW and E5=0.4 MW. It is assumed that $I_{E_i,s}^{\min}$ =0 and $I_{E_i,s}^{\max}$ =10. Similar to case I, as shown in Fig. 3.12, the system losses are reduced, as well. The completed results for this case is available in the appendix

[18]. It can be seen in fig. 3.12, with the optimal allocation of five different BESSs, the system losses in t_{19} can be reduced, up to the 7.6 %. Also, the expected PL for 'without BESS' and 'with BESS' cases are compared in Figure 3.13. The optimal BESSs amount for this case are shown in Table 3.5. The other control variables are given in the appendix.

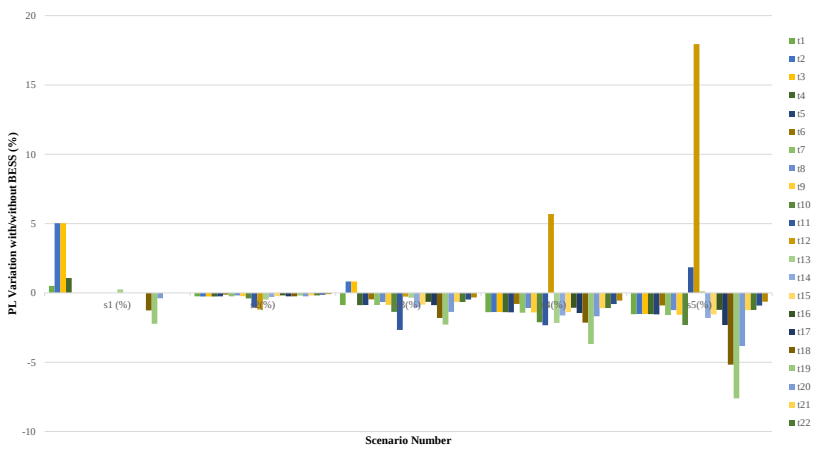

Figure 3. 12. PL variations in different scenarios and different hours (%) for case-II

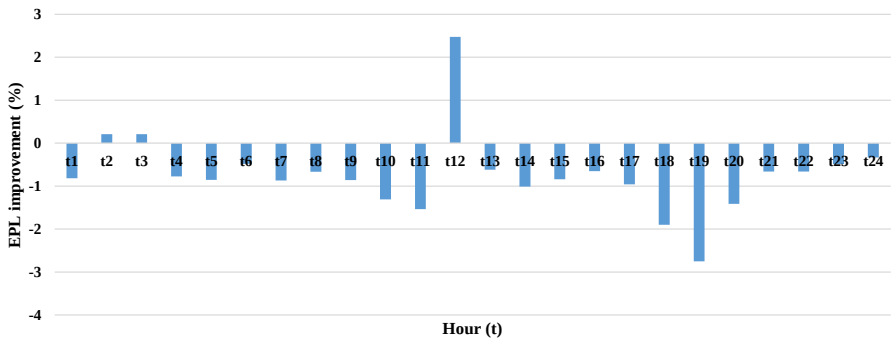

Figure 3. 13. EPL variations in different scenarios and hours (%) for case-II

Table 3. 5. The optimal amount of BESS types steps in all scenarios for case-II

Scenario	BESS type	Installed bus	$I_{E_i,s}$
s_1	E5	B_{14}	1
	E5	B_{23}	1
s_3	E4	B_{23}	1
s_4	E4	B_{14}	1
	E5	B_{20}	1
s_5	E5	B_{15}	2
	E2	B_{20}	1
	E5	B_{29}	1
	E5	B_{30}	2

3.9 Conclusion

In this paper, the optimal scheduling of BESS in T&D framework is investigated considering wind and PV sources. Also, wind power generation uncertainty is modeled with scenario-based approach. The results of different cases show that with BESS installation in T&D framework and balancing generators generation, the system operator can decrease the system power losses. The best answer is derived when all control parameters are set in their best values.

3.10 Appendix

For the sake of brevity, the proposed problem is solved for different cases. The results are categorized as follow [18].

Table 3. 6. The data of VAR Compensation devices

Appendixes	Modifications
Appendix 1	The completed results of case-I for all scenarios
Appendix 2	The completed results of case-II for all scenarios

4 Modèle de programmation stochastique sous contrainte de sécurité de tension pour la planification des BESS au jour le jour dans la co-optimisation des systèmes T&D

4.1 Résumé

L'éolien et le photovoltaïque sont désormais les sources d'énergie renouvelables (SER) qui connaissent la plus forte croissance dans le monde et l'atténuation de l'intermittence inhérente à de telles sources d'énergie grâce aux systèmes de stockage d'énergie par batterie (BESS) a attiré l'attention au cours des dernières années. Dans cet article, un nouveau problème d'allocation de BESS optimal (VSC-SOBA) optimal de sécurité de tension (VSC-SOBA) est proposé dans les systèmes intégrés de transmission et de distribution (T&D) tout en incluant des modèles réalistes de ressources énergétiques distribuées. Le problème de planification est étudié dans un cadre stochastique en considérant l'incertitude de l'énergie éolienne. En outre, les profils horaires de charge ainsi que les SER éoliens et photovoltaïques sont pris en compte. Maximiser la marge de chargement (LM) avec la meilleure allocation des différents types de BESS est l'objectif principal du document. De plus, l'impact de l'allocation sur l'écart de tension des bus de charge est étudié. Le modèle basé sur la programmation mixte non linéaire à nombres entiers (MINLP) est implémenté dans le logiciel GAMS en considérant P, Q et le contrôle simultané P+Q BESS. Les performances de la méthode proposée sont examinées sur des systèmes de test T&D à 16 bus, 62 bus, 286 bus et à grande échelle 1142 bus. Les résultats montrent que, dans le cas du VSC-SOBA, le LM souhaité est maximisé en présence de variables de contrôle BESS optimales.

Corps de l'article

Titre: Voltage Security Constrained Stochastic Programming Model for Day-Ahead BESS Schedule in co-optimization of T&D Systems

Seyed Masoud Mohseni-Bonab[1,2], Innocent Kamwa[2], Ali Moeini[2] and Abbas Rabiee[3]

[1] Electrical Engineering Department, Laval University, QC, Quebec, Canada (e-mail: s.m.mohsenibonab@ieee.org)

[2] Hydro-Québec/IREQ, Power System and Mathematics, Varennes QC J3X 1S1, Canada (e-mail: kamwa.innocent@ireq.ca, moeini.ali@ireq.ca)

[3] Electrical Engineering Department, University of Zanjan, Zanjan, Iran (e-mail: rabiee@znu.ac.ir)

Revue: IEEE Transaction on Sustainable Energy, vol. 11 (1), 2020, pp. 391-404.

4.2 Abstract

Wind and photovoltaic are now the fastest growing renewable energy sources (RES) around the world and mitigation of the inherent intermittency of such energy sources with Battery Energy Storage Systems (BESS) has gained attention in recent years. In this paper, a novel voltage security stochastic optimal BESS allocation (VSC-SOBA) problem is proposed in integrated transmission and distribution (T&D) systems while including realistic models of distributed energy resources. The scheduling problem is studied under stochastic framework by considering the wind power uncertainty. Besides, hourly profiles of load as well as wind and photovoltaic RESs are taken into account. Maximizing loading margin (LM) with the best allocation of different BESSs types is the main objective of the paper. Moreover, the allocation impact on voltage deviation of load buses is investigated. The mixed integer non-linear programming (MINLP)-based model is implemented in GAMS software considering P, Q, and simultaneous P+Q BESS control. The performance of proposed method is examined on T&D 16-bus, 62-bus, 286-bus and large scale 1142-bus test systems and the findings show that in the case of VSC-SOBA, the desired LM is maximized in the presence of optimal BESS control variables.

Keyword: Integrated transmission and distribution (T&D) systems, Battery Energy Storage Systems (BESS), voltage security constrained stochastic optimal BESS allocation (VSC-SOBA), co-optimization, loading margin, wind farms (WF).

4.3 Nomenclature

Sets:

Ω_B / Ω_L / Ω_G	Set of buses, branches and generating units.
Ω_W / Ω_{Ph}	Set of wind farms/ photovoltaic units.
Ω_S	Set of all possible scenarios.
Ω_t	Set of time periods.
Ω_{PQ} / Ω_{PV}	Set of PQ/PV buses.
Ω_{BESS}	Set of candidate buses for BESS.

Indices:

b / j	Index of bus numbers (*sl* is for slack bus).
s	Index of scenario.
w	Index of wind units.
ℓ	Index of transmission lines.
G	Index of generation units.
t	Index for operation intervals.
E	Index for BESS types.

Parameters:

π_s	The probability of scenario *s*.
$Y_{bj}\angle\gamma_{bj}$	Magnitude/angle of the jth element of Y_{BUS} matrix (pu/radian).
$P_b^{G,\min}$ / $P_b^{G,\max}$	Minimum/maximum of active power in the slack bus.
$Q_b^{G,\min}$ / $Q_b^{G,\max}$	Minimum/maximum value for reactive power of slack bus at bus *b*.
$P_{b,s,t}^D$ / $\tilde{P}_{b,s,t}^D$	Expected real power load of the bth bus in scenario *s* at time period *t* in normal mode/ loadability limit point.
$Q_{b,s,t}^D$ / $\tilde{Q}_{b,s,t}^D$	Expected reactive power load of the bth bus in scenario *s* at time period *t* in normal mode/ loadability limit point.
$V_b^{\min}$ / $V_b^{\max}$	Minimum/maximum values for voltage magnitude of the bth bus.
$S_\ell^{\max}$	Maximum transfer capacity of line ℓ .
P_w^{avl}	Available wind power generation.
$P_{b,s,t}^W$ / $Q_{b,s,t}^W$	Active/reactive powers produced by wind farm in scenario *s* at time period *t*.

$P_{b,s,t}^{ph}$	Active power produced by photovoltaic unit in scenario *s* at time period *t*.
$\cos\left(\varphi_{lag}\right)$	Lag power factor limits of the wind farms.
ζ_b^W	Percentage of wind power rated capacity realized in scenario *s* at bus *b* (%).
$\Lambda_b^W \ / \ \Lambda_b^{ph}$	Rated capacity of wind farm/photovoltaic.
$\Gamma_b^W \ / \Gamma_b^{ph} \ / \Gamma_b^D$	Percentage of wind power/photovoltaic/demand profile capacity realized at time period *t* (%).
$\mathrm{SS}_E^{\max}$	Maximum capacity of each BESS type (MW).
$\eta_{ch} \ / \ \eta_{dch}$	Efficiency of charging/discharging of BESS (%).
$ES_b^{\min} \ / \ ES_b^{\max}$	Maximum/minimum energy stored at node *b* (MWh).
$P_{\mathrm{b}}^{ch,\min} \ / \ P_{\mathrm{b}}^{ch,\max}$	Maximum/minimum charging powers of BESS (MW).
$P_{\mathrm{b}}^{dch,\min} \ / \ P_{\mathrm{b}}^{dch,\max}$	Maximum/minimum discharging powers of BESS (MW).
$I_E^{\min} \ / \ I_E^{\max}$	Minimum/maximum numbers of BESS from storage type *E*.
$k_b^D \ / \ k_b^G$	Rates of change in load/active power generation

Variables:

$c_{s,t} \ / \ d_{s,t}$	Vector of control/ dependent variables in scenario *s* at time period *t*.
$V_{b,s,t} \ / \tilde{V}_{b,s,t}$	Voltage magnitude of bus *b* in scenario *s* at time period *t* in normal mode/loadability limit point.
$\theta_{b,s,t} \ / \ \tilde{\theta}_{b,s,t}$	Voltage angle at bus *b* in scenario *s* at time period *t* in normal mode/loadability limit point.
$S_{\ell,s,t} \ / \ \tilde{S}_{\ell,s,t}$	Power flow of ℓ th branch in scenario *s* at time period *t* in normal mode/loadability limit point.
$P_{b,s,t}^G \ / \ \tilde{P}_{b,s,t}^G$	Active power production of slack bus in scenario *s* at time period *t* in normal mode/loadability limit point (MW).
$\lambda_{s,t}$	Loading margin index in scenario s at time period *t*.
$VD_{s,t}$	Voltage deviation of system in scenario *s* at time period *t*.
$Q_{b,s,t}^G \ / \ \tilde{Q}_{b,s,t}^G$	Reactive power production of slack bus in scenario *s* at time period *t* in normal mode/loadability limit point (MVar).
$I_{b,s,E}$	Integer decision variable indicating the optimal number of BESS in scenario *s* from storage type *E*.
$Q_{\mathrm{b},s,t,E}^{st}$	Reactive power of BESS at node *b* in scenario *s* at time period *t* from storage type *E* (MVar).
$P_{\mathrm{b},s,t,E}^{ch} \ / \ P_{\mathrm{b},s,t,E}^{ch}$	Charging/discharging powers of BESS at node *b* in scenario *s* at time period *t* from storage type *E* (MW).
$ES_{\mathrm{b},s,t,E}$	Energy stored in BESS at node *b* in scenario *s* at time period *t* from storage type *E* (MWh).

Functions:

$ELM \ / \ EVD \ / \ EPL$	Expected loading margin/voltage deviation/power losses of system at time period *t*. (%/pu/MW)

4.4 Introduction

4.4.1 Background and motivation

Conventional studies in distribution systems, such as power flow (PF), Optimal PF (OPF) and Distributed Generations (DGs) allocation, model transmission networks by an infinite bus [27]. Todays, with increasing integration of renewable energy sources (RES) such as wind power and solar photovoltaic to power grids, the need for modeling together these two networks is more important than before. Generally, distributed energy resources (DERs) in distribution networks are defined as power generation units and energy storage systems (ESSs), connected to an end-use customer. They supply a part of consumer's load, and they can even inject power to grid. The direction of power flow in modern power systems with considerable DERs is not always from the transmission level to the distribution level. A joint study conducted by Hawaiian Electric and the National Renewable Energy Laboratory states that many distribution feeders in Hawaii can send back energy into their substations during sunny days [28]. Ref [29] expresses the same concern that in Germany, PV capacity often exceeds the peak load on an actual LV distribution grid. The reverse power flow may lead to protection concerns, operating of reverse power relays of Substation Transformer, and malfunctioning of unidirectional voltage regulators [30]. According estimations made by Hydro-Quebec Distribution researchers, in less than five years, some rural distribution feeders in Quebec may experience reverse power flow in low-demand hours of summer. The reason is that installation of solar panels grows rapidly in rural areas, which have naturally low consumption during summer days.

Optimal allocation and scheduling strategies for maximizing technical and economic benefits of these limited and volatile sources is obligatory. In this paper, a massive parallel architecture that combines transmission and distribution analyzes, is proposed along with optimal scheduling of system operation point, considering different DERs and RESs, to improve system's efficiency from the loadability and voltage deviation point of view.

4.4.2 Literature review

The research body studied for this paper is divided into four categories:

B.1. Integrated T&D: Recent integrated T&D research works are focused on dynamic and steady-state analysis. In the area of steady-state analysis, researchers have focused on methods to simultaneously execute power flow in T&D [7-9, 11]. In [7], a master-slave-splitting (MSS) iterative method is used for global power flow (GPF) in integrated T&D. Also, boundary mismatches between the T&D are alleviated with convergence guarantee of GPF. A global transmission contingency analysis (GTCA)-based method is proposed in [8] for T&D power flow. As a common practice, transmission networks (TN) are assumed to be three-phase balanced systems and distribution networks (DN) are usually considered as single-phase (balanced or unbalanced [19]) or three-phase systems [9]. Next, in [11] the Integrated Grid Modeling System (IGMS) concept is defined to simultaneously analyze T&D.

B.2. ESS sizing and placement: the impact of BESS-based DERs on distribution level has been highly studied. A mixed-integer linear programming (MILP) based method is proposed in [21] to find the size and location of ESSs in a microgrid. The optimum size and location is important since the discharged energy of ESSs is limited [22].

B.3. Co-optimization: co-optimization term is a bit different from co-simulation term. The latter is used when different dedicated software (two or more) are used simultaneously to study the effects of different phenomena in power systems, such as failures among infrastructures. In co-simulation cases, the task of each software is different and an interface language connects them together (e.g. see Table 4.1). The intent of co-optimization is to construct a union framework (sometimes as a package) for studying several levels of power systems simultaneously. Generation and transmission expansion planning problem is co-optimized in electric power systems and the total system planning cost (comprising investment and operation costs) is minimized in one comprehensive co-optimized framework via CPLEX [31]. Transmission and distribution locational dynamic marginal price is defined and optimized in [32], simultaneously along with optimal scheduling of DERs. A co-optimization scheme for maximizing grid scale storage unit revenue in day-ahead energy and frequency regulation is also proposed in [33].

B.4. LM analysis: there are several subsidiary indices for static voltage stability assessment such as L-index [24], DSY [13], reactive power reserve, minimum eigenvalues of power flow Jacobian matrix, and etc. [34]. However, these indices depend on operational limits such as

reactive power generation limits, line flow limits, and voltage magnitude limits. When a limit is activated, these indices experience a sudden change or even discontinuity in the value, which is not desired, since the decision maker is not aware when a limit is activated. In addition, these indices do not linearly vary with respect to load increment. Therefore, employing such indices may not be proper for accurate characterization of the distance to voltage collapse point. A proper index for voltage stability evaluation is LM, since it describes directly the distance between the current operating point and the loadability limit point [35]. Hence, in this paper LM is used as the measure of voltage stability, as this index does not suffer from the above shortcomings.

4.4.3 Literature review

The following remarks can be inferred from the above literature survey:

1- DERs sizing and location problems have been considered as objective functions in most distribution network analysis literature. However, the actual bilateral connection between distribution and transmission networks has been rarely applied. Some recent researches have only investigated these two networks in PF aspects [7-9, 11].

2- Facing the increasing trends of DERs installation in power systems [21, 22], the uncertain and volatile nature of these energy resources should be properly handled in power system operation studies [27].

3- In most of the BESS allocation references, the impacts of reactive power capabilities of BESS are neglected [21, 22].

To the best of our knowledge, no work in the literature includes the RESs and their uncertainties along with BESS allocation on integrated T&D framework for LM maximization, while considering the voltage-constrained security analysis. Hence, this paper aims to fill the above gaps by developing a voltage security constrained stochastic optimal BESS allocation (VSC-SOBA) model. To do so, the Weibull probability distribution functions (PDF) used for modeling the wind uncertainty via a scenario-based approach. The desired expected LM (ELM) of the system is maximized as objective function, while expected voltage deviation (EVD) is investigated. The proposed VSC-SOBA problem is solved for three small and large-scale test systems. The main contributions of this work are

summarized as follows. Table 4.2 summarizes the findings of existing literatures and the main contributions of this paper.

1) Providing a management framework for integrating DERs (Wind generation, BESS and photovoltaic) to T&D and investigating the impact of BESS integration on integrated T&D.
2) Modeling reactive power of BESS during the whole allocation process.
3) Optimal scheduling of BESS in T&D for maximizing the LM of system in presence of wind or power, considering its stochastic nature.
4) Developing a VSC-SOBA model which is a powerful decision-making tool for system operators.

Table 4. 1. Summary of recent researches in terms of co-simulation framework

Ref.	Model name	Primary software (s)	Interface language (s)	Goal of simulator
[11]	IGMS	FESTIV, MATPOWER and GridLAB-D	C++	Analyzing high-penetration solar photovoltaic and price responsive load scenarios
[36]	OpenDSS (previously called: DSS)	Delphi programming, C++	Windows Component Object Model (COM)	Main: distribution feeders power flow
[37]	---	PSAT, MATLAB, NS2	Python, SimPy	Integration of heterogeneous systems with different dynamics and timescales
[6]	---	MATPOWER and GridLAB-D	FNCS	Hierarchical control framework that allows coordination between distributed energy resources and demand response
[38]	RunTS	OpenDSS, BaChMan	Python, Windows COM	Controls the application of state-changes
[39]	JADE	OMNeT++, PFSim	Java, transmission control protocol (TCP)	Java agent development framework is proposed for cyber-physical modeling of distributed and multi-agent systems
[40]	FNCS	GridPACK (transmission), GridLAB-D (distribution)	C++	Transient dynamics of the transmission and distribution systems
[41]	RT co-simulation	EMT part: Hypersim RT Simulator TSPart: Matlab/Simscape and ST600/RAMSES	Hypersim RT Simulator	Real-time simulation of large scale power-electronics rich networks with external network represented in stability simulation mode

Table 4. 2. Summary of the existing literature and contributions of this work

		[13-15]	[7-9]	[10-12]	[32]	Proposed
Study Network - T&D (simultaneously)		Y	Y	Y	Y	Y
T&D Analysis method	Steady-State Analysis	N	Y	Y	N	Y
	Dynamic Analysis	Y	N	N	Y	N
T&D PF or OPF solution?	PF	Y	Y	Y	Y	N
	OPF	N	N	N	N	Y
DERs Impacts in T&D		N	N	Y	Y	Y
Voltage security analysis of T&D		N	N	N	N	Y
P+Q BESS control		N	N	N	N	Y

- Y/N denotes that the subject is/is not considered.

4.4.4 Literature review Paper organization

This paper is organized as follows: in Section II, the LM concept is described. Section III reviews the technical approach for modeling wind power generation uncertainty via a stochastic approach. The proposed VSC-SOBA problem formulation is discussed in Section IV, followed by the simulation results in Section V. Finally, Section VI concludes the paper.

4.5 Voltage Stability Characterization Via Loading Margin

Voltage stability is defined as the capability of power system to maintain acceptable voltage magnitudes at all buses, not only under normal operation condition but also in transient condition [42]. It is a well-known fact that the main factors causing voltage collapse are increasing the system demand beyond certain limits, as well as the inability of power system to meet the demand of reactive power because of limitation in generation and transmission of reactive power. In this paper, LM is employed to characterize the voltage stability for a given operating point. The LM is defined as the amount of load increase not resulting in voltage instability or violation of operational constraints. This simply means that the power system is secure from voltage stability point of view when the LM between the current operation point (COP) and the loadability limit point (LLP) is sufficiently large. The LLP itself is defined as the point where at least one operational constraints such as voltage limits, generator reactive power limits and line/transformer flow limits begin to get violated, usually before the voltage collapse point (VCP). Figure 4.1, shows a typical P-V curve of an arbitrary load bus. Point A corresponds to the COP, whereas points B and C correspond to LLP and

VCP, respectively. Also, P_0 is the system demand at the COP. However, increasing the system demand at load buses will move the system operation point from the COP toward VCP. As mentioned before, the LLP is usually hold before VCP (in the case of limit-induced bifurcation). By definition, the LM represents the distance (in MW or MVA) between points A and B. In the case of saddle node bifurcation, the LLP coincides with VCP and the LM becomes the distance between A and C.

In order to have sufficient voltage stability margin, the LM should be greater than a certain threshold which is specified by the system operator. Also, it is necessary to consider power flow equations together for both COP and LLP (i.e. the points A and B in Fig. 5.1), simultaneously. Therefore, in this paper, a loading parameter (called λ) is considered to parameterize the power flow equations at LLP with respect to the corresponding power flow equations at the COP.

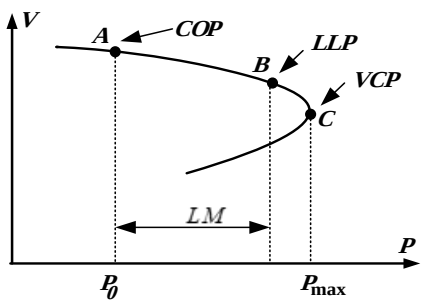

Figure 4. 1. The concept of LM on a typical P-V curve

4.6 RES Modeling

4.6.1 Wind power generation uncertainty modeling via scenario based approach

Generally, the wind speed uncertainty is modeled by Rayleigh or Weibull PDFs [43], the latter used in this paper for wind speed uncertainty characterization. Based on the characteristic curve of a wind turbine (which determines its output power), five different scenarios are created for wind power generation [44] as given in Table 4.3. The following values are considered for the PDF parameters [44]: k=2.5034 and λ =10.0434.

Table 4. 3. Wind power generation scenarios with the corresponding mean and probability

Scenario	s_1	s_2	s_3	s_4	s_5
π_s	0.0689	0.2044	0.4048	0.1992	0.1227
P_w^{avl}	0	$0.1287\,P_w^{rated}$	$0.4937\,P_w^{rated}$	$0.8683\,P_w^{rated}$	P_w^{rated}

The following equation describes the available active power outputs of wind farms:

$$P_{b,s,t}^{W} = \zeta_b^{W}\,\Lambda_b^{W}\,\Gamma_b^{W} \;\; ; \quad \forall b \in \Omega_W\,,\ \forall s \in \Omega_S\,,\ \forall t \in \Omega_t \tag{4-1}$$

The reactive power output of wind farm is modeled as:

$$Q_{b,s,t}^{W} = tg\left(\varphi_{lag}\right) \times P_{b,s,t}^{W} \;\; ; \quad \forall b \in \Omega_W\,,\ \forall s \in \Omega_S\,,\ \forall t \in \Omega_t \tag{4-2}$$

Therefore, in scenarios where the active power output of the wind farm decreases, the reactive power injection decreases accordingly.

4.6.2 PV modeling

The solar irradiation is also an uncertain parameter and a normal PDF is usually used to characterize it [26]. Thus, the power extracted from PV cells is expressed as follows:

$$P_{b,s,t}^{ph} = \Lambda_b^{ph}\Gamma_b^{ph} \;\; ; \quad \forall b \in \Omega_{ph}\,,\ \forall s \in \Omega_S\,,\ \forall t \in \Omega_t \tag{4-3}$$

4.7 VSC-SOBA Problem Formulation

4.7.1 Objective function

The ELM index is calculated as follows.

$$ELM\left(c_{s,t}, d_{s,t}\right) = \sum_{s=1}^{\Omega_S} \pi_s \lambda_{s,t} \tag{4-4}$$

where π_s is the probability of s-th wind power scenario.

4.7.2 Measurement of voltage deviation at load buses

Maintaining a proper voltage level at load buses is essential for power system operators. In this paper voltage deviation (VD) of system is calculated for different scenarios along maximization of LM.

$$EVD = \sum_{s=1}^{\Omega_S} \pi_s \left\{ \sum_{b=1}^{\Omega_B} \left| V_{b,s,t} - V_{b,s,t}^{spc} \right| \right\} \tag{4-5}$$

4.7.3 Modeling of BESS reactive power

The power conversion system (PCS) of a BESS is designed to control both active and reactive powers in compliance with the requirements of the connected system and to support wide variety of applications, e.g. voltage control, grid stabilization, and frequency reserve. In this work, PCSs are supposed to operate at four-quadrant areas as shown schematically in Fig. 4.2.

$$\left(P_{\mathrm{b},s,t,E}^{ch} - P_{\mathrm{b},s,t,E}^{dch}\right)^2 + \left(Q_{\mathrm{b},s,t,E}^{st}\right)^2 \le \left(\mathrm{SS}_E^{\max}\right)^2 ; \quad \forall b \in \Omega_{BESS}, \forall s \in \Omega_S, \forall t \in \Omega_t, \forall E \in \Omega_E \tag{4-6}$$

$$0 \le P_{\mathrm{b},s,t,E}^{ch} \le \mathrm{SS}_E^{\max} \quad ; \ \forall b \in \Omega_{BESS}, \forall s \in \Omega_S, \forall t \in \Omega_t, \forall E \in \Omega_E \tag{4-7}$$

$$0 \le P_{\mathrm{b},s,t,E}^{dch} \le \mathrm{SS}_E^{\max} \quad ; \ \forall b \in \Omega_{BESS}, \forall s \in \Omega_S, \forall t \in \Omega_t, \forall E \in \Omega_E \tag{4-8}$$

$$-\mathrm{SS}_E^{\max} \le Q_{\mathrm{b},s,t,E}^{st} \le \mathrm{SS}_E^{\max} \quad ; \ \forall b \in \Omega_{BESS}, \forall s \in \Omega_S, \forall t \in \Omega_t, \forall E \in \Omega_E \tag{4-9}$$

4.7.4 Constraints

D.1 BESS state of charge (SOC) constraints

The BESS technical operation constraints are:

$$ES_{\mathrm{b},s,t,E} = ES_{\mathrm{b},s,t-1,E} + \left(\eta_{ch} P_{\mathrm{b},s,t,E}^{ch} - P_{\mathrm{b},s,t,E}^{dch} / \eta_{dch}\right)\Delta t ; \quad \forall b \in \Omega_{BESS}, \forall s \in \Omega_S, \forall t \in \Omega_t, \forall E \in \Omega_E \tag{4-10}$$

$$ES_b^{\min} \le ES_{\mathrm{b},s,t,\mathrm{E}} \le ES_b^{\max} ; \forall b \in \Omega_{BESS}, \forall s \in \Omega_S, \forall t \in \Omega_t, \forall E \in \Omega_E \tag{4-11}$$

$$P_{\mathrm{b}}^{ch,\min} \le P_{\mathrm{b},s,t,E}^{ch} \le P_{\mathrm{b}}^{ch,\max} ; \forall b \in \Omega_{BESS}, \forall s \in \Omega_S, \forall t \in \Omega_t, \forall E \in \Omega_E \tag{4-12}$$

$$P_{\mathrm{b}}^{dch,\min} \le P_{\mathrm{b},s,t,E}^{dch} \le P_{\mathrm{b}}^{dch,\max} ; \ \forall b \in \Omega_{BESS}, \forall s \in \Omega_S, \forall t \in \Omega_t, \forall E \in \Omega_E \tag{4-13}$$

$$ES_{\mathrm{b},s,t,\mathrm{E}} \le \mathrm{SS}_E^{\max} \times I_{b,s,E} ; \forall b \in \Omega_{BESS}, \forall s \in \Omega_S, \forall t \in \Omega_t, \forall E \in \Omega_E \tag{4-14}$$

$$I_E^{\min} \le I_{b,s,E} \le I_E^{\max} ; \forall b \in \Omega_{BESS}, \forall s \in \Omega_S, \forall t \in \Omega_t, \forall E \in \Omega_E \tag{4-15}$$

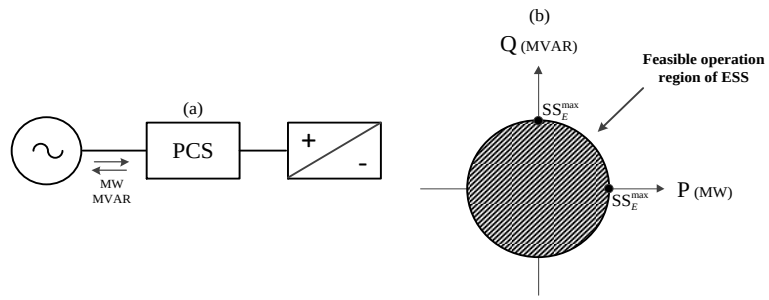

Figure 4. 2. (a) Scheme of PCS connections, (b) Covered working areas

Equation (4-10) shows how the stored energy of Eth BESS, installed at b^{th} bus, in scenario *s*, changes during time. The stored energy, charging and discharging limits of BESS are given in (4-11)-(4-13). It is worth to note that the BESSs are modeled as multi-size types, meaning that several energy storages with different sizes are constructed by multiplying a discrete variable to maximum capacity of storage types as given in (4-14). The discrete variable is restricted itself by (4-15).

D.2 AC power flow constraints at the COP

The AC power flow equality/inequality equations are expressed for current operation point (COP):

$$P_{b,s,t}^{G} + P_{b,s,t}^{W} + P_{b,s,t}^{ph} - \sum_{E=1}^{\Omega_{BESS}} P_{b,s,t,E}^{ch} + \sum_{E=1}^{\Omega_{BESS}} P_{b,s,t,E}^{dch} - P_{b,s,t}^{D}\Gamma_{b}^{D} = \sum_{j\in\Omega_B} V_{b,s,t}V_{j,s}Y_{bj}\cos\left(\theta_{b,s,t} - \theta_{j,s} - \gamma_{bj}\right) \quad ; \quad \forall b \in \Omega_B \ , \forall s \in \Omega_S , \forall t \in \Omega_t , \forall E \in \Omega_E \tag{4-16}$$

$$Q_{b,s,t}^{G} + Q_{b,s,t}^{W} + \sum_{E=1}^{\Omega_{BESS}} Q_{b,s,t,E}^{st} - Q_{b,s,t}^{D}\Gamma_{b}^{D} = \sum_{j\in\Omega_B} V_{b,s,t}V_{j,s}Y_{bj}\cos\left(\theta_{b,s,t} - \theta_{j,s} - \gamma_{bj}\right) \quad ; \quad \forall b \in \Omega_B \ , \forall s \in \Omega_S , \forall t \in \Omega_t , \forall E \in \Omega_E \tag{4-17}$$

The generator's active/reactive power outputs and buses/feeders voltages in normal mode should be kept within pre-specified limits, as follows.

$$P_b^{G,min} \le P_{b,s,t}^{G} \le P_b^{G,max} \ ; \ \forall b \in \Omega_{Sl} \ , \forall s \in \Omega_S , \forall t \in \Omega_t \tag{4-18}$$

$$Q_b^{G,min} \le Q_{b,s,t}^{G} \le Q_b^{G,max} \ ; \ \forall b \in \Omega_{Sl} \ , \forall s \in \Omega_S , \forall t \in \Omega_t \tag{4-19}$$

$$V_b^{\min} \le V_{b,s,t} \le V_b^{\max} \; ; \;\; \forall b \in \Omega_B \, , \, \forall s \in \Omega_S \, , \, \forall t \in \Omega_t \tag{4-20}$$

Besides, the line flow limits are as follows.

$$0 \le \left| S_{\ell,s,t} \right| \le S_\ell^{\max} \; ; \quad \forall \ell \in \Omega_L \, , \, \forall s \in \Omega_S \, , \, \forall t \in \Omega_t \tag{4-21}$$

D.3 AC power flow constraints at the LLP

The AC power flow equality/inequality equations at loadability limit point are expressed as follows.

$$\begin{aligned} &\tilde{P}_{b,s,t}^G + P_{b,s,t}^W + P_{b,s,t}^{pv} - \sum_{E=1}^{\Omega_{BESS}} P_{b,s,t,E}^{ch} + \sum_{E=1}^{\Omega_{BESS}} P_{b,s,t,E}^{dch} - \tilde{P}_{b,s,t}^D \Gamma_b^D = \\ &\qquad \sum_{j \in \Omega_B} \tilde{V}_{b,s,t} \tilde{V}_{j,s} Y_{bj} \cos\left(\tilde{\theta}_{b,s,t} - \tilde{\theta}_{j,s} - \gamma_{bj} \right) \quad ; \\ &\qquad \forall b \in \Omega_B \; , \, \forall s \in \Omega_S \, , \, \forall t \in \Omega_t \, , \, \forall E \in \Omega_E \end{aligned} \tag{4-22}$$

$$\begin{aligned} &\tilde{Q}_{b,s,t}^G + Q_{b,s}^W + \sum_{E=1}^{\Omega_{BESS}} Q_{b,s,t,E}^{st} - \tilde{Q}_{b,s,t}^D \Gamma_b^D = \\ &\qquad \sum_{j \in \Omega_B} \tilde{V}_{b,s,t} \tilde{V}_{j,s} Y_{bj} \cos\left(\tilde{\theta}_{b,s,t} - \tilde{\theta}_{j,s} - \gamma_{bj} \right) \quad ; \\ &\qquad \forall b \in \Omega_B \; , \, \forall s \in \Omega_S \, , \, \forall t \in \Omega_t \, , \, \forall E \in \Omega_E \end{aligned} \tag{4-23}$$

$$\tilde{P}_{b,s,t}^D = \left(1 + k_b^D \lambda_{s,t} \right) \times P_{b,s,t}^D \, ; \forall b \in \Omega_{PQ} \, , \forall s \in \Omega_S \, , \, \forall t \in \Omega_t \tag{4-24}$$

$$\tilde{Q}_{b,s,t}^D = \left(1 + k_b^D \lambda_{s,t} \right) \times Q_{b,s,t}^D \, ; \forall b \in \Omega_{PQ} \, , \, \forall s \in \Omega_S \, , \, \forall t \in \Omega_t \tag{4-25}$$

$$\begin{aligned} &\tilde{P}_{b,s,t}^G = \min\left(P_b^{G,\max} , \left(1 + k_b^G \lambda_{s,t} \right) \times P_{b,s,t}^G \right) \; ; \\ &\qquad \forall b \in \Omega_{PV} \, , \forall s \in \Omega_S \, , \, \forall t \in \Omega_t \end{aligned} \tag{4-26}$$

$$P_b^{G,min} \le \tilde{P}_{b,s,t}^G \le P_b^{G,max} \; ; \forall b \in \Omega_{Sl} \; , \, \forall s \in \Omega_S \, , \, \forall t \in \Omega_t \tag{4-27}$$

$$Q_b^{G,min} \le \tilde{Q}_{b,s,t}^G \le Q_b^{G,max} \; ; \;\; \forall b \in \Omega_{Sl} \; , \, \forall s \in \Omega_S \, , \, \forall t \in \Omega_t \tag{5-28}$$

$$V_b^{\min} \le \tilde{V}_{b,s,t} \le V_b^{\max} ; \forall b \in \Omega_B \, , \, \forall s \in \Omega_S \, , \, \forall t \in \Omega_t \tag{5-29}$$

$$0 \le \left| \tilde{S}_{\ell,s,t} \right| \le S_\ell^{\max} \quad ; \quad \forall \ell \in \Omega_L \, , \, \forall s \in \Omega_S \, , \, \forall t \in \Omega_t \tag{5-30}$$

Constraints (4-22)-(4-23) correspond to the power flow equations, whereas the constraints (4-24)-(4-25) correspond to the load increase pattern from current point to the loadability limit point. Moreover, (4-26) is the pattern of active power increase at loadability limit point. Besides, constraints (4-27)-(4-30) correspond to the operational limits at LLP.

D.4 Relationship between COP and LLP

The following constraints establish the relationship between the voltage of generator buses at the COP and LLP [45]. These equations ensure that if a generator reaches its reactive power limit (upper or lower limit), as result of load increment from COP toward LLP, its terminal voltage will not remain constant anymore. For example, if a specific generator reaches its upper reactive power limit subjected to the load increment, its terminal voltage will decrease as inferred from (5-31) and (5-32).

$$\tilde{V}_{b,s,t} = V_{b,s,t} + v^{up}_{b,s,t} - v^{dn}_{b,s,t} \; ; \forall b \in \Omega_G \, , \; \forall s \in \Omega_S \, , \; \forall t \in \Omega_t \tag{5-31}$$

$$\left(Q_b^{G,max} - \tilde{Q}^G_{b,s,t}\right) \times v^{up}_{b,s,t} \le 0 \quad ; \forall b \in \Omega_G \, , \; \forall s \in \Omega_S \, , \; \forall t \in \Omega_t \tag{5-32}$$

$$\left(\tilde{Q}^G_{b,s,t} - Q_b^{G,min}\right) \times v^{dn}_{b,s,t} \le 0 \quad ; \forall b \in \Omega_G \, , \; \forall s \in \Omega_S \, , \; \forall t \in \Omega_t \tag{5-33}$$

$$v^{dn}_{b,s,t}, v^{up}_{b,s,t} \ge 0 \tag{5-34}$$

D.5 Voltage security constraints

As it is aforementioned, in order to have sufficient voltage security margin, the LM should be greater than a predefined threshold (i.e. $\lambda^{des}_{s,t}$) in all time intervals and operational scenarios. This constraint is characterized by (5-35), as follows.

$$0 < \lambda^{des}_{s,t} \le \lambda_{s,t} \tag{5-35}$$

The term “security” in power systems is not ambiguous and it is intimately related to contingencies [46]. In practice, the system is operated to withstand a set of “credible” contingencies. This set includes the outage of any single component of the power system preceded or not by a fault (N-1 security criterion). In some cases, this set also includes the loss of double-circuit lines. Therefore, all procedures involving power system security should fulfill at least the N-1 security criterion.

On the other hand, there are ways to adapt the proposed procedure to take into account voltage security issues. For example:

1. By including in the OPF all post-contingency operating conditions related to N-1 security criterion. This is applied, for example, in [47]. In the case of the proposed scenario-based T&D operation procedure, this approach could be impractical, since the optimization model will be very large scale.
2. By performing an off-line contingency analysis to identify harmful (or severe) contingencies. Only the post-contingency operating conditions related to the harmful contingencies are included in the OPF. This approach is applied, for example, in [48].
3. An off-line contingency analysis can be performed, and the value of LM for system without contingency determined. This LM value should be enough to ensure the appropriate operation of the system in case that any of the contingencies pertaining to the N-1 security criterion occurs [49].

Occurrence of contingencies reduces the LM of the system. As mentioned in [50], in practical power systems, operators would be interested in operating the system with a given desired LM, so that contingencies do not make the system unstable. Hence, by directly incorporating the LM in the formulation of the scheduling model (the subject of our paper), it is possible to preserve the system security for further contingencies. In other words, in addition to the set of severe contingencies against which the system has been secured by performing SCUC or SC-OPF, the system is secured for further contingencies by satisfying the desired LM. This desired LM is determined off-line and by conducting extensive studied for different scenarios, system configurations and contingencies [51].

By performing an off-line contingency analysis, the desired LM value for the pre-contingency state of the system is determined. Next, the underlying operating points to be analysed are determined using the proposed VSC-SOBA in off-line mode for different values of desired LM. Then, by applying each contingency, and performing continuation power flow, the corresponding post-contingency state of the system is evaluated. Should the obtained post-contingency LM be less than 5% (based on the recommendation of [51]), the system is assumed to be insecure following that contingency; otherwise, the system is

considered to be secure. The resulting LM should be enough to ensure secure operation of the system in case that any of the credible contingencies occurs.

4.7.5 Decision variables

The control/dependent variables of this paper for maximizing LM can be categorized as follows.

$$c_{s,t} = \begin{bmatrix} V_{b,s,t} & ,\forall b = \Omega_B & ,\forall s, \forall t \\ P^G_{b,s,t} & ,\forall b = \Omega_{Sl} & ,\forall s, \forall t \\ Q^G_{b,s,t} & ,\forall b \in \Omega_{Sl} & ,\forall s, \forall t \\ P^{ch}_{b,s,t,E} & ,\forall b \in \Omega_{BESS} & ,\forall s, \forall t, \forall E \\ P^{dch}_{b,s,t,E} & ,\forall b \in \Omega_{BESS} & ,\forall s, \forall t, \forall E \\ Q^{st}_{b,s,t,E} & ,\forall b \in \Omega_{BESS} & ,\forall s, \forall t, \forall E \\ I_{b,s,E} & ,\forall b \in \Omega_{BESS} & ,\forall s, \forall E \\ ES_{b,s,t,E} & ,\forall b \in \Omega_{BESS} & ,\forall s, \forall t, \forall E \\ S_{\ell,s,t} & ,\forall \ell \in \Omega_L & ,\forall s, \forall t \end{bmatrix}, d_{s,t} = \begin{bmatrix} P_{W_i,s,t} & ,\forall \ell \in N_W & ,\forall s, \forall t \\ Q_{W_i,s,t} & ,\forall \ell \in N_W & ,\forall s, \forall t \\ P_{Ph_i,s,t} & ,\forall \ell \in N_W & ,\forall s, \forall t \end{bmatrix} \quad (5\text{-}36)$$

4.8 Simulation Results

The proposed VSC-SOBA is modeled as a mixed integer non-linear programing (MINLP) and implemented in GAMS environment [52]. The main MINLP model is handled by SBB solver [52], while CONOPT4 [52] is utilized to solve the NLP sub-problem. The SBB is a GAMS solver for MINLP models. It is based on a combination of the standard Branch and Bound (B&B) method known from Mixed Integer Linear Programming and some of the standard NLP solvers already supported by GAMS. SBB may perform better on models that have fewer discrete variables but more difficult nonlinearities [53]. Besides in this paper DICOPT, SNOPT and KNITRO solvers results are compared with the proposed methodology. In order to investigate the different aspects of proposed method, different cases are studied in four test systems here, as follows. For the sake of brevity, the detailed results are not presented for second, third and fourth test systems.

- *Case-I*: Integrated T&D without renewables
- *Case-II*: Integrated T&D with wind and photovoltaic renewables
- *Case-III*: Integrated T&D with wind and photovoltaic renewables and BESS
  Subcase A: Considering just P for BESS
  Subcase B: Considering just Q for BESS
  Subcase C: Considering P and Q for BESS

4.8.1 Assumptions

In this paper, the simulations are performed according to the hourly variation of load, wind, PV, and generation units [26]. The daily load, wind, and PV curves are shown in Fig. 4.3. The technical characteristics of the considered BESSs and their PCSs for different test systems are described in Table 4.4.

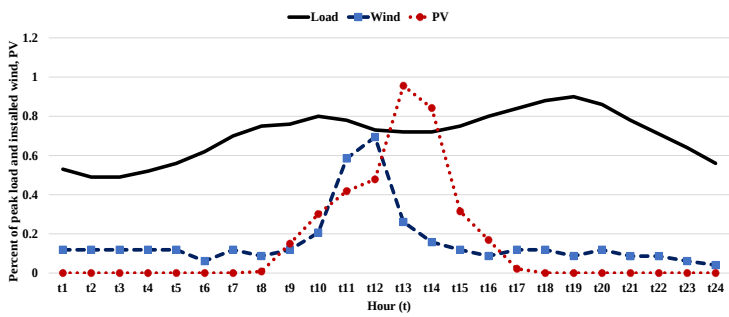

Figure 4. 3. Day-ahead load, wind, and PV characteristics

Table 4. 4. Technical characteristics of BESS/PCS in different test systems

Parameter	Test system 1	Test systems 2 and 3	Test system 4
SS_E^{max}	E_1=500KW, E_2=400KW, E_3=300KW, E_4=200KW, E_5=100KW	E_1=2.4MW, E_2=2MW, E_3=1.6MW, E_4=1.2MW, E_5=800KW	E_1=5MW, E_2=4MW, E_3=3MW, E_4=2MW, E_5=1MW
I_E^{min} / I_E^{max}	0 / 3	0 / 5	0 / 5
ES_b^{min} / ES_b^{max}	$0 / SS_E^{max} \times I_{b,s,E}$	$0 / SS_E^{max} \times I_{b,s,E}$	$0 / SS_E^{max} \times I_{b,s,E}$
$P_b^{ch,min}, P_b^{dch,min} / P_b^{ch,max}, P_b^{dch,max}$	$0 / SS_E^{max}$	$0 / SS_E^{max}$	$0 / SS_E^{max}$
η_{ch} / η_{dch}	0.95	0.95	0.95
PCS rating	1 p.u. (based on SS_E^{max}) for P and Q		

4.8.2 Studied benchmark systems

General characteristics of the four studied IEEE test systems are given in Table 4.5.

Table 4. 5. Studied benchmarks

Test system	#1	#2	#3	#4
Trans. buses	9	30	30	118
Dist. nodes	7	32	256	1024
T&D buses	16	62	286	1142
WT candidates	3	2	4	32
PV candidates	2	2	4	32
BESS candidates	All nodes	All nodes	All nodes	All nodes

4.8.3 Test system 1: T&D 16-bus

As a simple test system, the proposed algorithm is executed on a modified IEEE 9-bus system. A simple 8 MW distribution feeder replaces a portion of load connected to bus 7. The remaining load is considered as industrial aggregated load. All distribution nodes are set for BESS installation. In addition, in this test system, the wind turbines (WTs) are at nodes 12, 14 and 16 (rated as 1MW). Besides, the PVs, each 0.5 MW, are added to nodes 13 and 15. This test system is shown in Fig. 4.4.

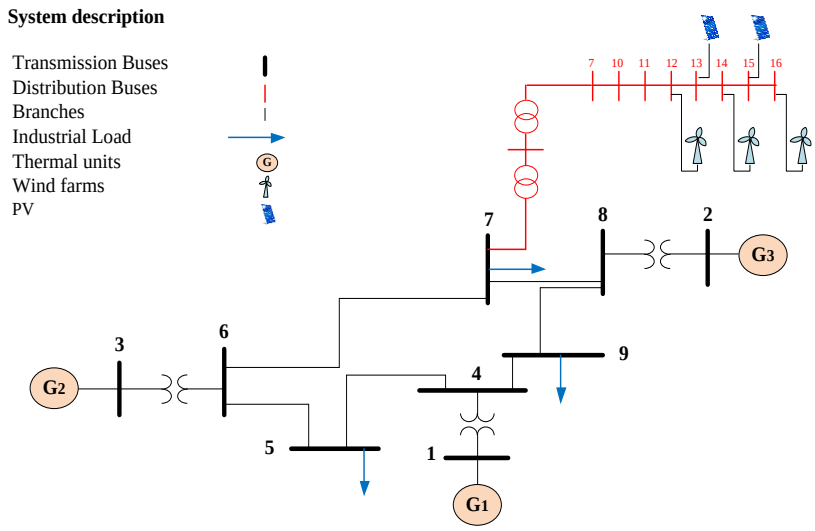

Figure 4. 4. Single line diagram of test system (test system 1)

C.1 LM & VD comparison

In this part the expected value of LM in different studied cases are summarized in Table 4.4. For example, at t_1 the Case I test system reaches the voltage collapse point when the base load is increased 43.429%. It is clear that using WTs and PVs yield better loadability. In addition, it is observed from Table 4.6 that the highest LM of system can be realized when both BESS active and reactive powers are optimized. Also, it can be seen that at 2nd, 3th, and 24th hours the system is stronger from voltage collapse point of view and Q-control result in higher LM increase than P-control.

In order to give an insight about the proposed method, the voltage deviation of different sub-cases of case-III are compared and reported in Fig. 4.5. The results show that with

simultaneously utilizing active and reactive powers of BESS (i.e. case III-C), the voltage deviation is minimized. Most of the benefit comes from P-control as expected, although at some time instants, Q-control adds to the gains.

C.2 Control variables of case-III

The control variables should be adjusted for the best LM. The obtained optimal control variables of (5-41) in case-III are reported in this part. For the sake of brevity, the variables are reported only for s_5 for E_1 type of BESSs but complete results are available in appendix [18]. Figs 4.6 and 4.7, show the SOC of BESS type E_1 in scenario s_5 for case-III-A and case-III-C, respectively.

Table 4. 6. LM variation in different hours and in different cases - (test system 1) (%)

Hour	*Case-I*:	*Case-II: ELM*	*Case-III-A: ELM*	*Case-III-B: ELM*	*Case-III-C: ELM*
t_1	43.429	48.848	62.212	60.75	110.383
t_2	69.077	76.977	113.366	101.795	136.118
t_3	52.667	58.69	113.495	101.801	130.096
t_4	50.124	56.239	92.262	86.84	96.2
t_5	42.671	48.386	64.086	55.185	88.162
t_6	33.219	35.899	42.313	38.557	78.09
t_7	22.424	26.99	38.553	32.79	70.258
t_8	16.357	19.442	25.482	21.734	65.23
t_9	14.616	20.017	27.007	23.491	65.153
t_{10}	11.814	21.558	29.056	25.738	60.271
t_{11}	14.147	38.435	48.537	43.288	68.456
t_{12}	18.844	48.735	52.151	50.345	76.512
t_{13}	22.102	45.25	51.677	47.012	76.232
t_{14}	21.611	38.746	46.079	42.179	74.102
t_{15}	16.247	23.801	32.21	27.173	7.81
t_{16}	11.269	15.629	27.56	19.572	64.855
t_{17}	8.937	12.961	28.614	24.488	58.79
t_{18}	7.109	11.484	28.185	24.188	58.672
t_{19}	5.467	8.637	28.035	24.407	57.092
t_{20}	8.646	12.992	28.365	25.54	60.376
t_{21}	12.552	15.206	32.342	28.757	65.908
t_{22}	22.667	26.165	39.956	30.726	74.828
t_{23}	30.973	33.623	49.841	38.771	104.533
t_{24}	42.99	44.981	82.303	76.591	126.201

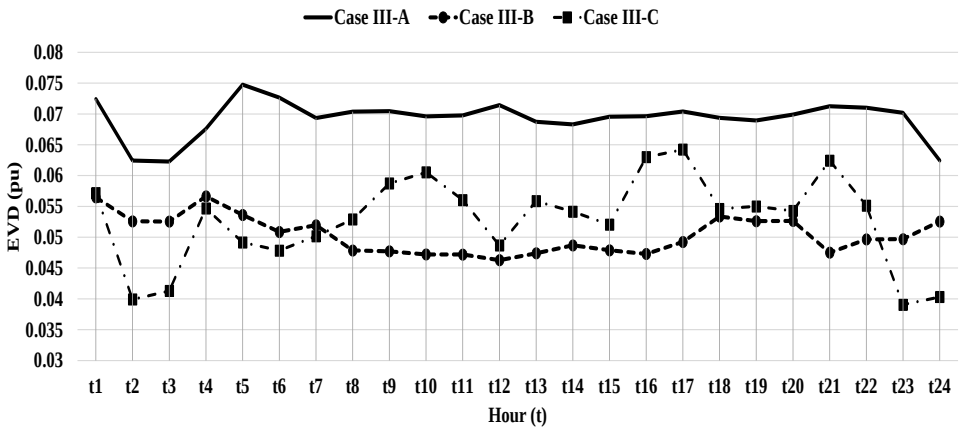

Figure 4. 5. EVD of system at load buses/nodes in test system 1, case-III

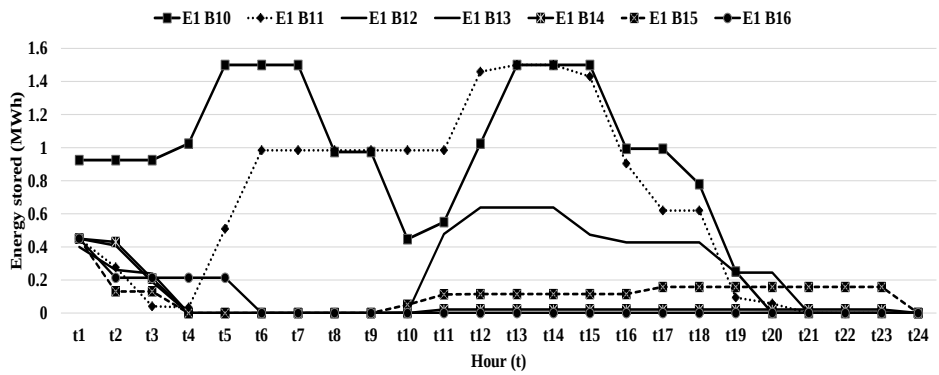

Figure 4. 6. Energy stored in BESS E1, at node b, in s5 at time t (MWh) (case-III-A)

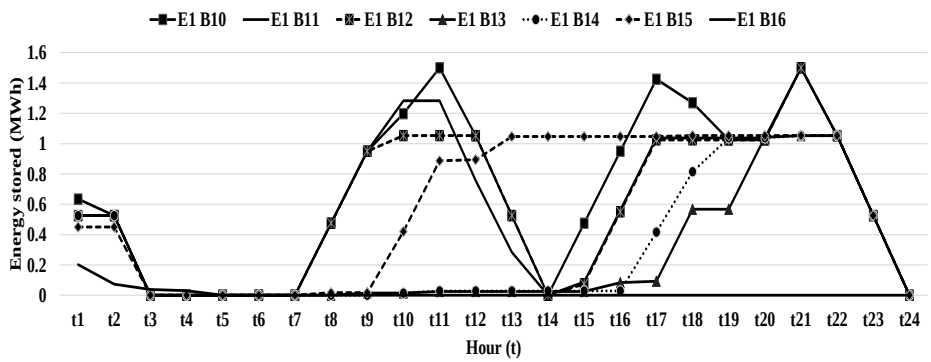

Figure 4. 7. Energy stored in BESS E1, at node b, in s5 at time t (MWh) (case-III-C)

These SOCs are obtained when the BESS type E_1 is charged or discharged according to the algorithm shown in Figs 4.8 and 4.9. As shown, the proposed method changes BESSs' operation modes to achieve maximum LM during each hour.

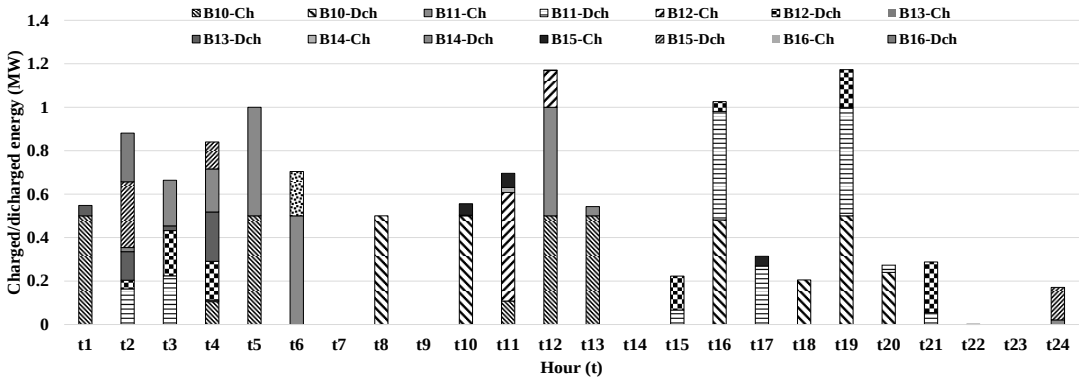

Figure 4. 8. Charged/discharged energy of BESS type E1, in s_5 at time period *t* (in MW) (case-III-A)

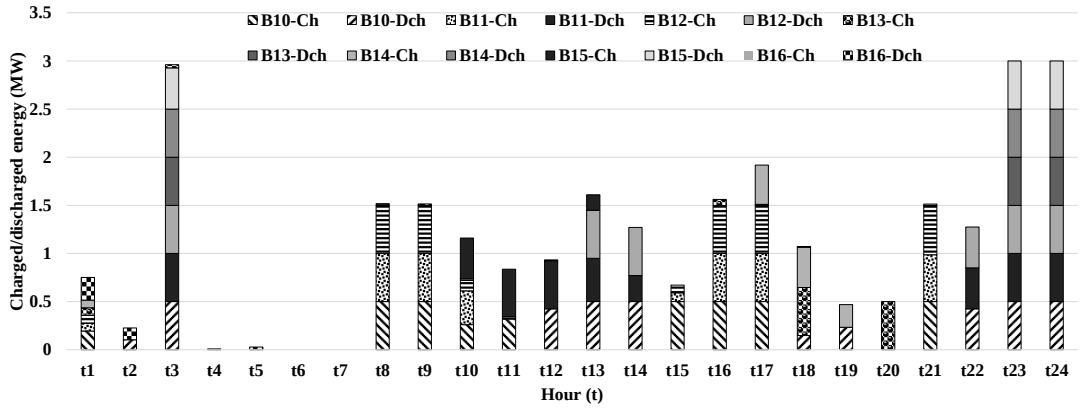

Figure 4. 9. Charged/discharged energy of BESS type E1, in s_5 at time period *t* (in MW) (case-III-C)

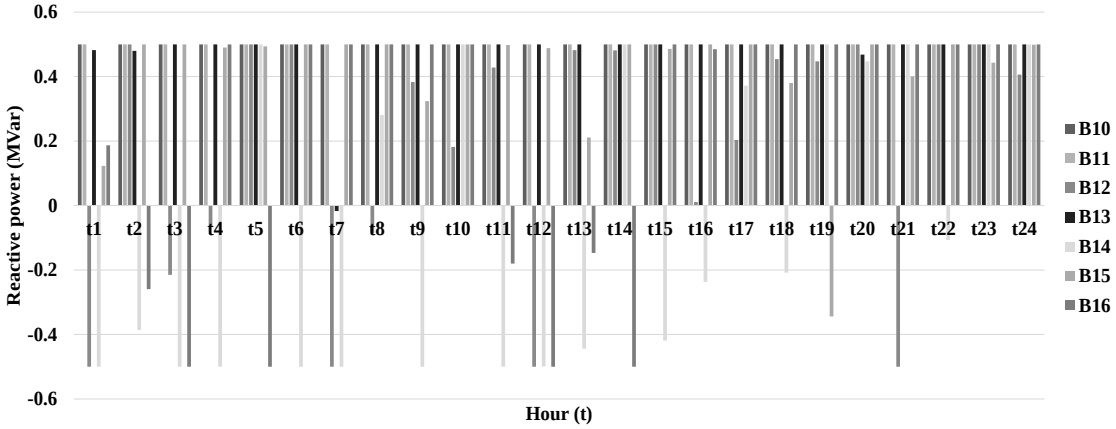

Figure 4. 10. Reactive power of BESS type E1, at node *b*, in s_5 at time *t* (MVar) (case-III-B)

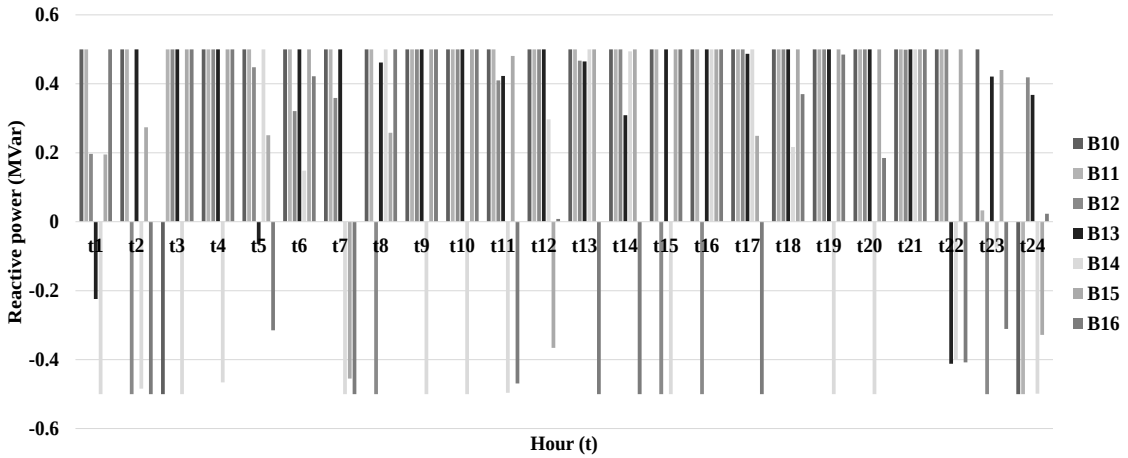

Figure 4. 11. Reactive power of BESS type E1, at node *b*, in s_5 at time *t* (MVar) (case-III-C)

In addition, BESS type E1 reactive power injection or absorptions in case-III-B and case-III-C are illustrated in Figs. 4.10 and 4.11. It is evident that in mode B, more reactive power is injected into the system to maximize LM. For case-III-C the optimal adjusted voltages at distribution nodes are given in Fig. 4.12. Also, Fig. 4.13 depicts the optimal value of slack bus generator's active power output in s_5.

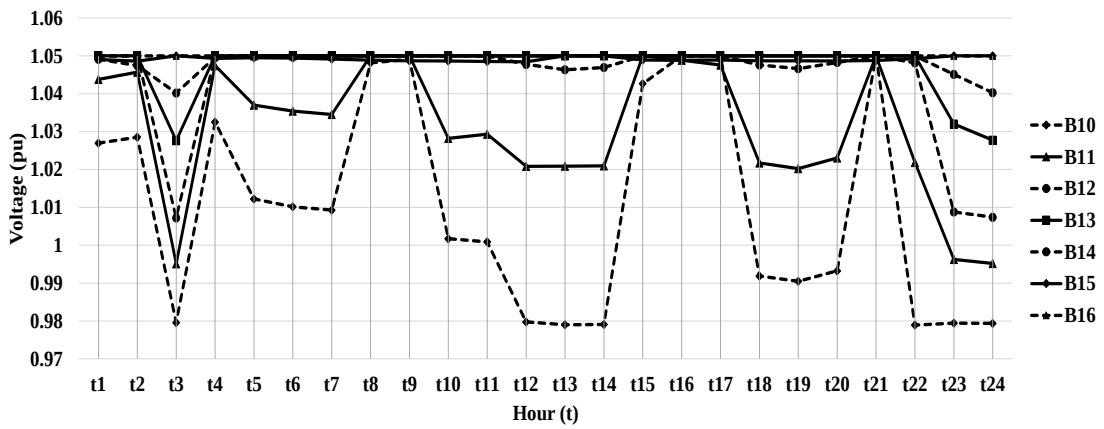

Figure 4. 12. The adjusted voltage of all distribution nodes in s_5 (pu) (case-III-C)

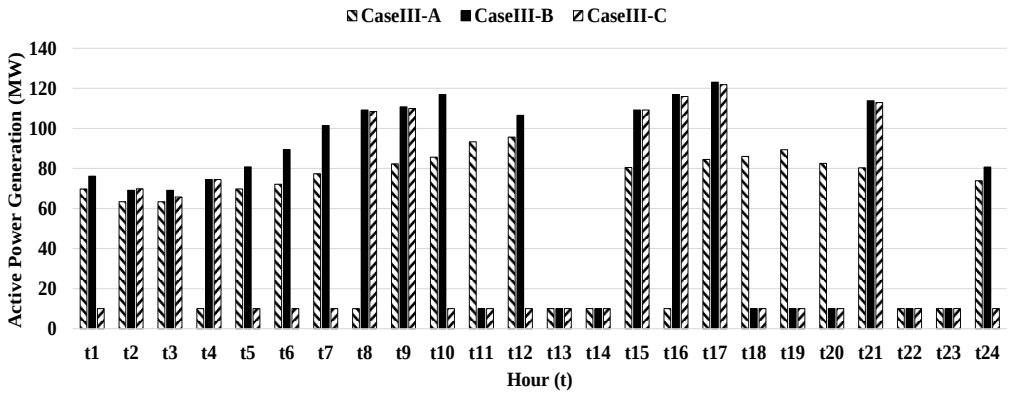

Figure 4. 13. Active power generations in s_5 at time period t (in MW)

C.3 Voltage limitation effects on distribution nodes

As an extra factor, we now consider that the range V_b^{min}/V_b^{max} of distribution nodes voltages are changed from 0.95/1.05 to 0.9/1.1. It is observed from Fig. 4.14 that with the new extended range of voltages, which means itself higher flexibility in optimal BESS scheduling, the LM also increases. Although results of case-III-C are the only reported, greater LM has been achieved for all subcases of case-III.

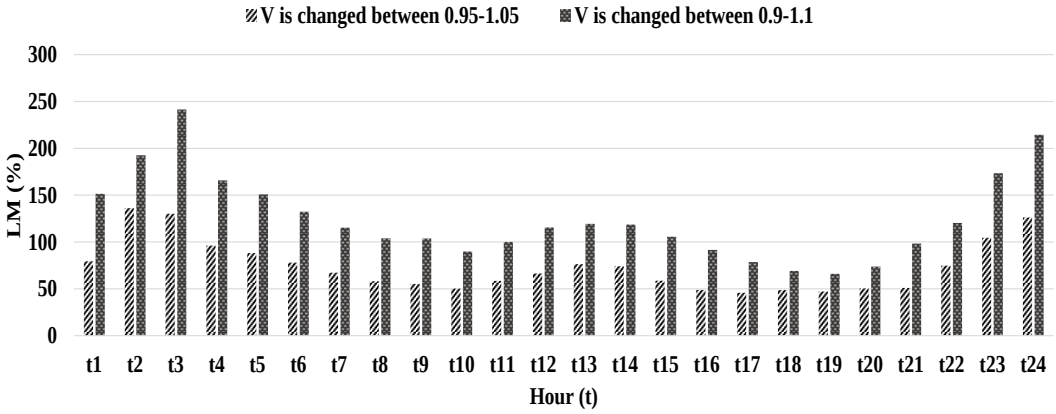

Figure 4. 14. Voltage change effect on the desired LM in case-III-C

4.8.4 Test system 2: T&D 62-bus

A well-known 12.66-kv IEEE 33-bus radial distribution system is studied here as a distribution part and IEEE 30-bus transmission network is selected as transmission side. In

this case, radial distribution feeder replaces total load connected to bus 26 of transmission side. It is also assumed that the distribution tie-line switches are in the off status (normal mode). Totally, new integrated network consists of 62 buses, which 6 of them are generator buses. Bus 1 is the slack buses, buses 2, 13, 22, 23 and 27 are taken as PV buses and the remaining 56 nodes are PQ buses. Thirty-two distribution nodes are the candidate nodes for installing BESSs. Also, the network has 78 branches. It is also assumed that the WT nodes are 47 and 54 (rated: 1MW) and PV nodes are 51 and 62 (rated: 0.5 MW). Figure 4.15 shows a simple schematic of created benchmark. The desired LM for different cases of this test system is shown in table 4.7. It can be observed from Table 4.7 that the impact of BESS active power is greater than reactive power (except during peak load hours). EVD values for different cases and optimal control variables values are available in appendix [18].

4.8.5 Test System 3: T&D 286-bus

This test system is quite similar to test system 2, except that, a distribution network replaces loads connected to buses 3, 10, 16, 18, 20, 23, 26 and 29. Totally, new integrated network consists of 286 buses which 256 of them selected as candidate nodes for BESS allocation. It is also assumed that the WT nodes are 62, 94, 126 and 158 (rated: 2MW) and PV nodes are 190, 222, 254, and 286 (rated: 1MW). These nodes are the last nodes of 8 installed distribution systems. LM variations in different case and subcases are depicted in Fig. 4.16. The control variables of this test system are available in appendix part [33].

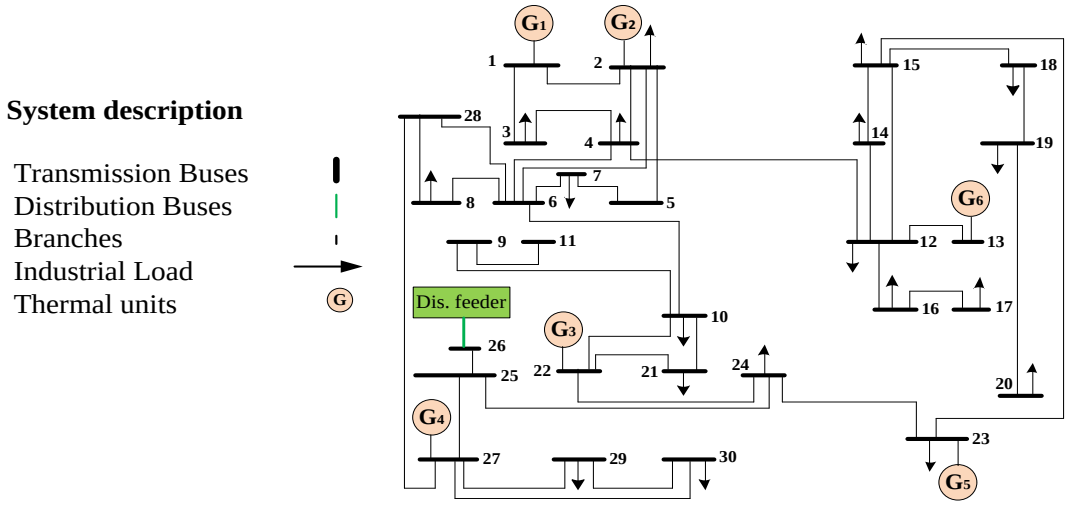

(a)

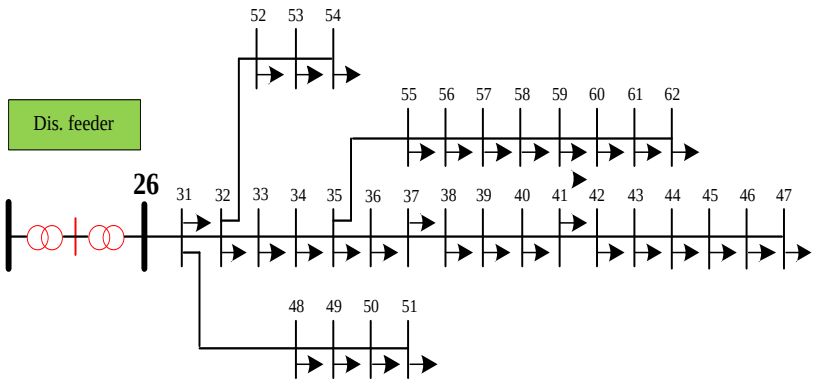

(b)

Figure 4. 15. (a) Single line diagram of modified IEEE 30-bus system, (b) Installed IEEE-33 bus distribution test system – (test system 2 and 3)

Table 4. 7. LM variation in different hours and in different cases - (test system 2) (%)

Hour	*Case-I*:	*Case-II: ELM*	*Case-III A: ELM*	*Case-III-B: ELM*	*Case-III-C: ELM*
t_1	141.067	150.841	239.794	226.579	245.851
t_2	160.746	167.766	271.295	253.341	275.76
t_3	155.533	167.724	270.533	253.341	275.208
t_4	145.703	155.786	239.259	230.731	253.214
t_5	128.231	137.496	217.246	209.196	224.653
t_6	101.953	110.881	185.071	178.856	188.123
t_7	82.585	89.698	150.964	147.37	155.047
t_8	70.354	73.247	133.621	130.352	136.586
t_9	68.113	78.449	130.445	127.967	133.253
t_{10}	59.707	75.773	118.286	116.413	121.105
t_{11}	63.782	92.783	123.95	122.505	126.821
t_{12}	75.022	107.06	140.015	137.942	142.954
t_{13}	77.513	111.029	144.119	141.206	146.908
t_{14}	77.452	102.587	144.127	141.096	147.286
t_{15}	70.412	82.271	133.436	131.004	136.587
t_{16}	59.761	68.369	118.425	116.556	120.355
t_{17}	52.154	57.414	104.873	101.161	108.774
t_{18}	45.238	48.796	93.771	90.372	95.785
t_{19}	42.01	46.945	88.376	85.377	90.16
t_{20}	38.312	54.679	99.82	95.262	102.312
t_{21}	63.802	69.565	124.296	121.536	126.411
t_{22}	80.013	84.242	147.546	143.855	149.713
t_{23}	99.634	105.089	179.64	169.904	183.846
t_{24}	105.518	132.724	223.944	209.1	230.738

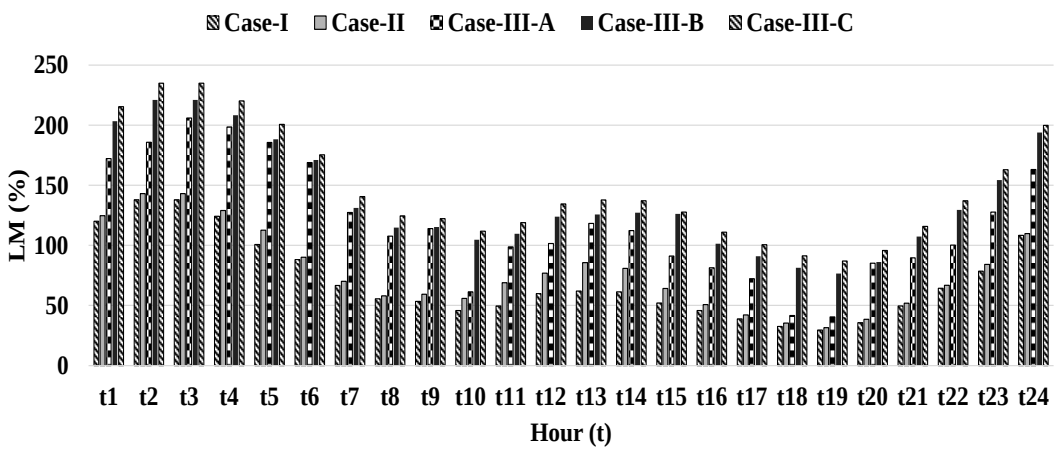

Figure 4. 16. LM variation in different cases (%)

4.8.6 Larger test system – T&D 1142-bus

IEEE 33-bus radial distribution system is considered in this part as a distribution side and IEEE 118-bus transmission network is selected as transmission side. In this case, radial distribution feeder replaces the whole load of a PQ bus, if its load is less than 20MW. The new integrated network consists of 1142 buses which 1024 of them selected as candidate nodes for BESS allocation. It is also assumed that the last nodes of each distribution systems are equipped with 5MW WTs and PVs. Figure 4.17 shows a simple schematic of created benchmark. The LM variations in different case and subcases are shown in Figure 4.18. It is concluded from Figure 4.18 that, except peak load hours, the impact of BESS active power is greater than reactive power. Such as test systems 2 and 3, the control variables of this test system are available in appendix part [33].

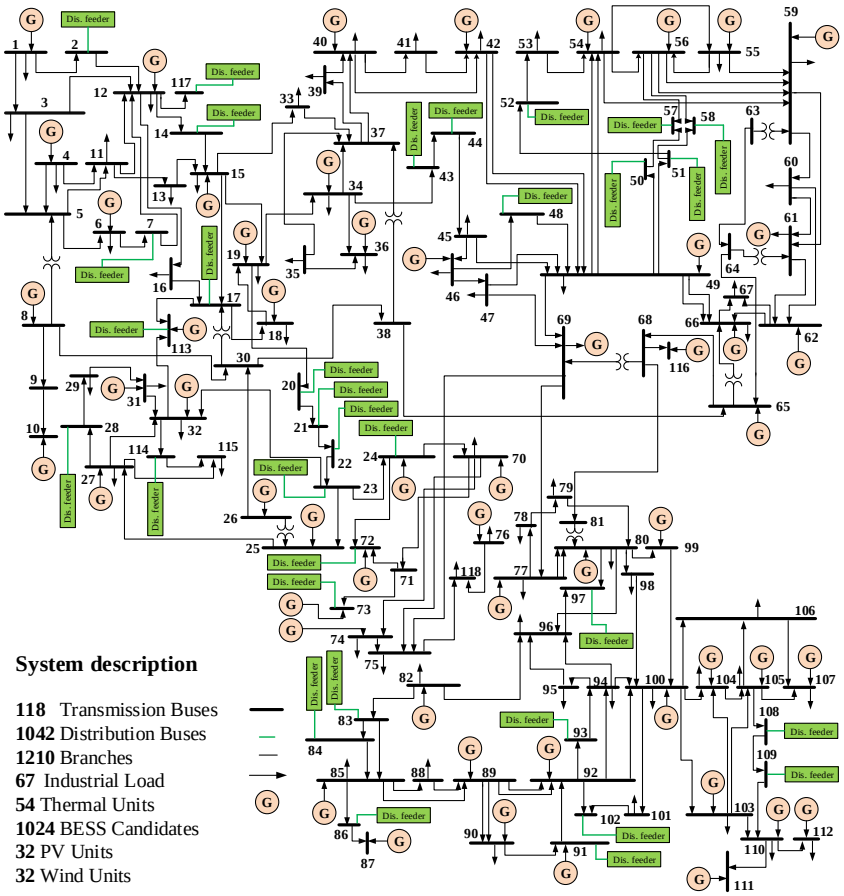

Figure 4. 17. Single line diagram of T&D 1142-bus system

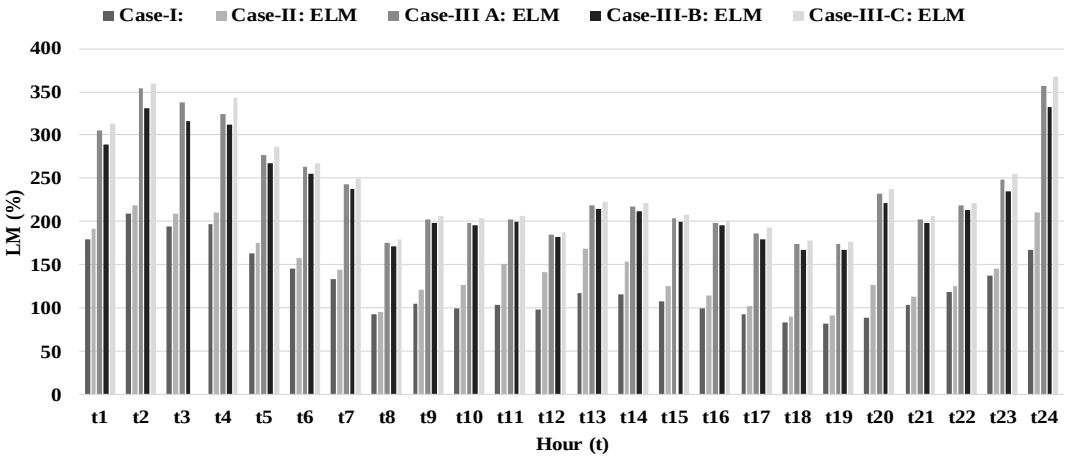

Figure 4. 18. LM variation in different hours and in different cases - (test system 4) (%)

In this part, a new objective function is also studied, namely the expected power losses (EPL). As a matter of fact, power losses are increased by raising energy consumption. Reduction of

power losses is a critical aim for system operators. In the s-*th* scenario and t-*th* hour, the active power losses (PL) can be calculated as follows [25].

$$PL_{s,t}\left(c_{s,t},d_{s,t}\right)=\left(P_{b,s,t}^{G}+P_{b,s,t}^{W}+P_{b,s,t}^{ph}\right)-P_{b,s,t}^{D}\Gamma_{b}^{D}\left(-\sum_{E=1}^{\Omega_{BESS}}P_{\mathrm{b},s,t,E}^{ch}+\sum_{E=1}^{\Omega_{BESS}}P_{\mathrm{b},s,t,E}^{dch}\right)+\sum_{E=1}^{\Omega_{BESS}}L_{ESS_{s,t,E}} \tag{5-37}$$

$$\sum_{E=1}^{\Omega_{BESS}}L_{ESS_{s,t,E}}=\left(1-\eta_{ch}\right)\times\sum_{E=1}^{\Omega_{BESS}}P_{\mathrm{b},s,t,E}^{ch}+\sum_{E=1}^{\Omega_{BESS}}P_{\mathrm{b},s,t,E}^{dch}\times\left(1/\eta_{dch}-1\right) \tag{5-38}$$

Since the $PL_{s,t}$ is scenario dependent, the EPL is regarded as the objective function to minimize, and calculated as follows:

$$EPL\left(c_{s,t},d_{s,t}\right)=\sum_{s=1}^{\Omega_{S}}\pi_{s}PL_{s,t} \tag{5-39}$$

The optimal (or minimum achievable) EPL for different cases of test system #4 is shown in Figure 4.19.

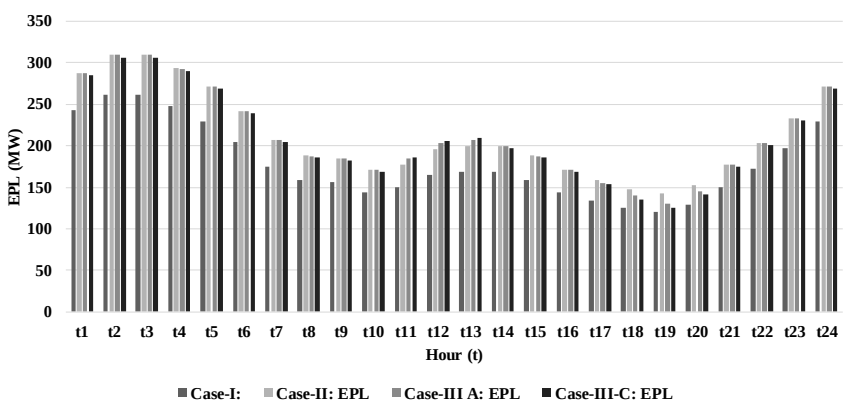

Figure 4. 19. EPL in different hours and cases - (test system 4) (MW)

According Figure 4.19 it is clear that although the EPL experiences an increment during BESS charging hours, the BESS, when discharging, is able to reduce the power loss. In addition, the optimal utilization of BESS reactive power, last columns, offers additional gain in the term of EPL. Table 4.8 shows the EPL of test system 4 at t_{10} (mid-day peak) for distribution, transmission and integrated system, separately.

Table 4. 8. EPL in transmission, distribution and integrated T&D - (test system 4) (MW) at t_{10}

Case	Transmission losses	Distribution losses	T&D Losses
Case-I:	84.702	59.59	144.3
Case-II:EPL	84.702	86.01	170.72
Case-III A:EPL	84.702	85.84	170.55
Case-III-C:EPL	84.702	84.14	168.84

4.8.7 Algorithm Performance

Considering non-convex nature of the studied problem, Table 4.9 compares performance of the proposed optimization method for different test systems and cases. Comparing case-I and case-II of test benchmark #1, the number of variables is increased by more than six time but the CPU time is just tripled. As shown for case-III-C, the proposed method is capable of generating optimal results for more than 1 million variables within 14 hours approximately. All the test cases were carried out on a laptop with Intel core i7 2.70 GHz CPU and 16 GB internal memory (RAM).

Table 4. 9. Comparison of proposed method performance in different test systems

System	CPU-time (second)	Number of variables	Number of iterations
Test S. #1, case-I	9.242	4393	153
Test S. #1, case-II	29.603	27721	181
Test S. #1, case-III-C	482.128	60896	1770
Test S. #2, case-III-C	9592.06	243081	8354
Test S. #3, case-III-C	51492.37	1160801	9937
Test S. #4, case-III-C	187951.08	4171720	19857

In addition, for comparing our results with the previous similar works, the proposed problem is solved without any objective function, OF=1, for studied benchmarks. It can be seen that the CPU time per bus for a complete successful load flow decreases as the number of buses increases. However, in IGMS framework [8] the ratio of CPU time over total T&D buses in IEEE-118 bus test system is 0.014. Similar metrics can be implied from Table 4.10.

Table 4. 10. CPU time per bus number in different test systems

	CPU time for power flow (sec)	CPU time per bus number
Benchmark 1	0.383	2.300E-02
Benchmark 2	0.397	6.400E-03
Benchmark 3	1.308	4.570E-03
Benchmark 4	4.576	4.007E-03

Giving the complexity of integer modeling and execution time of these kind of problems, the algorithm performance is compared with two different other solvers. KNITRO, DICOPT and SNOPT solvers are used for modeling MINLP and NLP parts. The comparative performances of these solvers given compared in Table 4.11, in terms of number of iterations and CPU-times. The obtained numerical results substantiate the effectiveness of the proposed model and its good performance. It can be seen that, after ESS installation and when the problem is converted to MINLP, based on the good performance of SBB solver, the result are better than with other solvers.

Table 4. 11. Comparison of proposed method performance with different algorithms

System	Proposed	DICOPT (MINLP), CONOPT4 (NLP)	DICOPT (MINLP), SNOPT (NLP)	SBB (MINLP), SNOPT (NLP)	SBB (MINLP), KNITRO (NLP)	KNITRO (MINLP), KNITRO (NLP)
	Number of iterations / CPU-time (second)	Number of iterations / CPU-time (second)	Number of iterations / CPU-time (second)	Number of iterations / CPU-time (second))	Number of iterations / CPU-time (second)	Number of iterations / CPU-time (second)
Test S. #1, case-I	153 / 9.242	153 / 10.862	63 / 11.524	63 / 11.22	7 / 8.730	7 / 8.701
Test S. #1, case-II	181 / 29.603	181 / 30.521	93 / 73.698	93 / 72.251	18 / 19.264	18 / 19.350
Test S. #1, case-III-C	4031 / 494.76	6002 / 743.33	NSR	NSR	NSR	NSR
Test S. #2, case-III-C	8354 / 9592.06	9578 / 14579.54	NSR	NSR	NSR	NSR
Test S. #3, case-III-C	9937 / 51492	NSR	NSR	NSR	NSR	NSR
Test S. #4, case-III-C	19857 / 187951	NSR	NSR	NSR	NSR	NSR

4.9 Conclusion

Due to the increasing utilization of RESs, a voltage security constrained stochastic optimal allocation of distributed BESS (VSC-SOBA) model is introduced in this paper while considering the interaction between the distribution and transmission networks. The VSC-SOBA framework takes into account the uncertainty of wind power generation through scenario-based approach. The goal of the proposed VSC-SOBA problem is to maximize the LM. According to different results, it is demonstrated that, with existing RESs, the proposed method can find an optimal schedule to maximize the LM. Moreover, PCS reactive power, if scheduled accurately, increases the LM, a gain which has not been addressed before during optimization process.

5 IC-GAMA: un nouveau cadre pour la co-simulation T&D intégrée

5.1 Résumé

Cet article propose une plate-forme intégrée de co-simulation de transmission et de distribution (T&D) utilisant les outils GAMS et MATLAB (appelés IC-GAMA). Le cadre proposé peut résoudre le flux de puissance des systèmes de distribution en co-simulation avec le réseau de transport, aussi bien dans des modèles détaillés que pour offrir une solution aux exploitants de systèmes indépendants et aux divisions de planification de systèmes d'énergie. Un cadre itératif est développé pour modéliser les interactions entre les systèmes de T&D. Les solutions du système de transmission, tension et angle PCC, et les solutions du système de distribution, puissances active et réactive du PCC, sont échangées entre les deux systèmes au point de couplage commun (PCC). Cinq stratégies sont proposées pour modéliser ces échanges et simulées sur des points de repère IEEE. Les résultats de la simulation montrent que, lorsque le processus itératif commence à partir d'un flux d'énergie total du côté de la distribution, le cadre T&D proposé présente une meilleure convergence et est plus robuste aux erreurs de suppositions initiales.

Corps de l'article

Titre: IC-GAMA: A Novel Framework for Integrated T&D Co-Simulation

Seyed Masoud Mohseni-Bonab[1,2], Innocent Kamwa[2] and Ali Moeini[2]

1. Electrical Engineering Department, Laval University, QC, Quebec, Canada (e-mail: s.m.mohsenibonab@ieee.org)

2. Hydro-Québec/IREQ, Power System and Mathematics, Varennes QC J3X 1S1, Canada (e-mail: kamwa.innocent@ireq.ca, moeini.ali@ireq.ca)

Conférenc: 2019 Innovative Smart Grid Technologies Europe (ISGT Europe)

5.2 Abstract

This paper proposes an integrated transmission and distribution (T&D) co-simulation platform utilizing GAMS and MATLAB tools (called IC-GAMA). The proposed framework can solve distribution systems power flow in co-simulation with transmission network both in detailed models to offering a solution for independent system operators and power system planification divisions. An iterative framework is developed to model the interactions between T&D systems. The solutions of the transmission system, PCC voltage and angle, and the solutions of the distribution system, PCC active and reactive powers, are exchanged between the two systems at the Point of Common Coupling (PCC). Five strategies are proposed for modeling these exchanges and simulated on IEEE benchmarks. The simulation results show that when the iterative process starts from full distribution-side power flow, the proposed T&D framework has better convergence and is more robust to errors in initial guesses.

Keyword: Power system simulation, integrated transmission and distribution (T&D) systems, co-simulation, iterative framework.

5.3 Introduction

Despite physical coupling of transmission and distribution systems, these systems are separately managed by the transmission system operator (TSO) and distribution operator

(DSO) with some limited coordination. The TSO operates without knowing potential power flow variations and possible controls from a DSO. In this case, the distribution system is considered as a load, the value of which is measured at the distribution substation. In the same way, the DSO operates the system while the transmission is modeled as a voltage source, the value of which is measured at the distribution substation. Thus, the current TSO and DSO are almost "blind" to each other's system conditions and controls.

With the growing trend of emerging new technologies in distribution networks, such as wind turbines, solar panels, electric vehicles, and distributed generations, the passive distribution systems may become "active," and thus the need for simultaneously studying Transmission & Distribution (T&D) networks, and corresponding bilateral interactions cannot be overlooked anymore. High penetration of naturally-stochastic renewable energy sources may reverse the energy flow which does not fit in the top-down energy transfer scope of conventional power systems. Consequently, network study methods such as optimal power flow, unit commitment, and stability analysis need to be revised.

Based on the literature review, the integrated T&D studies are into either dynamic and steady-state subcases or co-optimization framework and co-simulation framework. Co-optimization aims to construct a union framework, sometimes as a package, for studying several levels of power systems simultaneously. In co-simulation studies different dedicated software, two or more, are used simultaneously to study the effects of different phenomena in power systems, such as failures among infrastructures [54, 55], voltage stability assessment [56], power losses (with and without renewables) [57].

In this paper, the focus is on the co-simulation framework. In terms of dynamic co-simulated study, in [58] co-simulation of combined Transmission and Distribution Systems (CoTDS) is demonstrated using PSAT as the transmission system simulator and OpenDSS as the power flow tool for the distribution system.

In terms of steady-state co-simulated studies, In [59], a coordinated transmission and distribution AC optimal power flow (TDOPF) is proposed and solved with a mathematical master-slave structure. Similarly, an open-source co-simulation framework 'framework for network co-simulation' (FNCS), is proposed in [6, 40] to investigate the dynamic behaviors of both the transmission and distribution networks. To demonstrate the co-simulation through

FNCS framework, GridPACK™ and GridLAB-D™ are chosen as the simulators for transmission and distribution simulators, respectively. The Integrated Grid Modeling System (IGMS) [11, 12] is used as the platform to co-simulate (1) the transmission power flow using MATPOWER [60]; (2) distribution network using GridLAB-D [61]; and (3) wholesale market operations using FESTIV [11]. In [62], the impact of distributed generation from solar photovoltaics (DGPV) on the integrated T&D studied in IGMS framework. In [63], a new co-simulated framework called Hierarchical Engine for Large-scale Infrastructure Co-Simulation (HELICS) is proposed.

In this study, the architecture of the co-simulation framework and different key players are investigated. The objectives of this paper are set as (1) developing, simulating, and solving power flow equations of each level independently, using existing well-known domain-specific simulators, while externally-interfaced for exchanging data, (2) Validating the convergence and robustness of proposed T&D loaf-flow at PCC by introducing errors in initial guesses. The interface tool establishes a robust and bilateral data sharing a connection between two levels of a system.

This paper is organized in four sections including the introduction. In section two, the proposed IC-GAMA model is described. Some analysis using IC-GAMA is presented in section three. Finally, the conclusions are summarized in section four.

5.4 Model Description

The proposed framework is based on a co-simulation approach in which T&D networks are solved separately, and the interactions are captured by exchanging the solutions obtained for the two models. The schematic in Figure 5.1 shows how IC-GAMA operates in general. Different scenarios will be tested to find the best approach representing T&D interactions. One suggested approach is using an iterative framework.

An iterative framework is proposed by exchanging the solutions. The integrated model is solved when the solutions from the decoupled models converge. According to this approach, bus voltages and angles obtained from transmission network solver and active and reactive power flow obtained from distribution network solver are shared at the Point of Common

Coupling (PCC). The proposed framework is implemented using the following three modules:

Module 1: **Transmission system modeling and analysis:** The transmission system model includes a detailed network model with short-term load and generation forecast.

Module 2: **Distribution system modeling and analysis**: A detailed model for the distribution network is simulated while connected to the transmission side via an ideal power supply. An optimal power flow algorithm will be implemented for voltage regulation application.

Module 3: **T&D interaction framework**: Finally, the coupling between the two systems is achieved by interchanging power flow solutions. The solutions are updated iteratively until both flows converge.

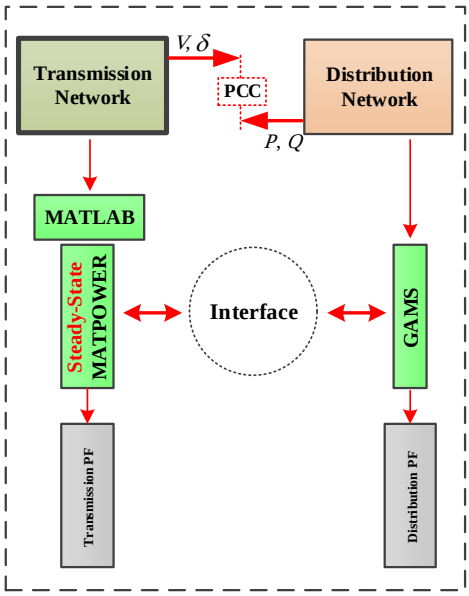

Figure 5. 1. Block diagram of the proposed approach to model T&D interactions (IC-GAMA)

5.5 Model Description

The proposed IC-GAMA is implemented in General Algebraic Modeling System (GAMS) software [52] and MATLAB environments. We will use MATLAB to model transmission network (MATPOWER package [60]) and to solve power flow. Distribution network power flow is programmed using GAMS. The GAMS CONOPT4 solver is utilized to solve the load

flow as non-linear programming (NLP) problem. The interface coupling the T&D models is implemented in MATLAB. All the test cases are carried out on a laptop with Intel Core i7 2.70 GHz CPU and 16 GB internal memory (RAM).

An overview of the proposed approach is shown in Figure 5.2, where bus voltages and angles (V, δ) obtained from transmission network load flow and active and reactive power flow (P, Q) obtained from distribution network flow are interchanged at the PCC. In this paper, five scenarios are proposed for modeling the interactions.

1- Scenario 1 (s_1): Starting from the transmission side, solve full power flow with initial guesses for P and Q of distribution side and transfer V and δ of PCC, solve distribution power flow with resulted V and δ, compute new P and Q, repeat this process until satisfying the threshold, finish.

2- Scenario 2 (s_2): Starting from distribution side, solve full power flow with given initial guesses for V and δ of the transmission side and transfer P and Q to the transmission side, solve transmission power flow with resulted P and Q, compute new V and δ, repeat until satisfying the threshold, finish.

3- Scenario 3 (s_3): Starting from the transmission side, solve power flow in one iteration with an initial guess for P and Q of distribution side and transfer V and δ of PCC, solve full distribution power flow with obtained V and δ, compute new P and Q, repeat until satisfying the threshold, finish.

4- Scenario 4 (s_4): Starting from distribution side, solve one iteration of power flow with initial guesses for V and δ of the transmission side and transfer P and Q of PCC, solve full transmission power flow with resulted P and Q, compute new V and δ, repeat until satisfying the threshold, finish.

5- Scenario 5 (s_5): Starting from the transmission side, solve one iteration of power flow with initial guesses for P and Q of distribution side and transfer V and δ of PCC, solve one iteration of distribution power flow with resulted given V and δ, compute new P and Q, repeat until satisfying the threshold, finish.

These scenarios are summarized in figure 5.3.

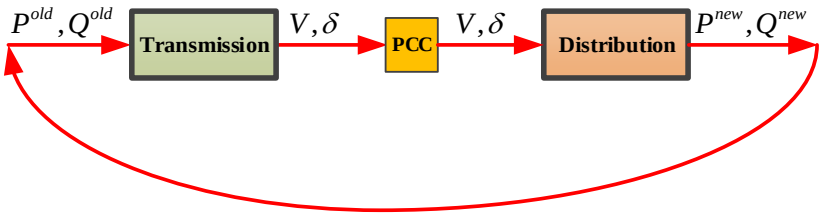

Figure 5. 2. Overview of the proposed approach to model T&D interactions

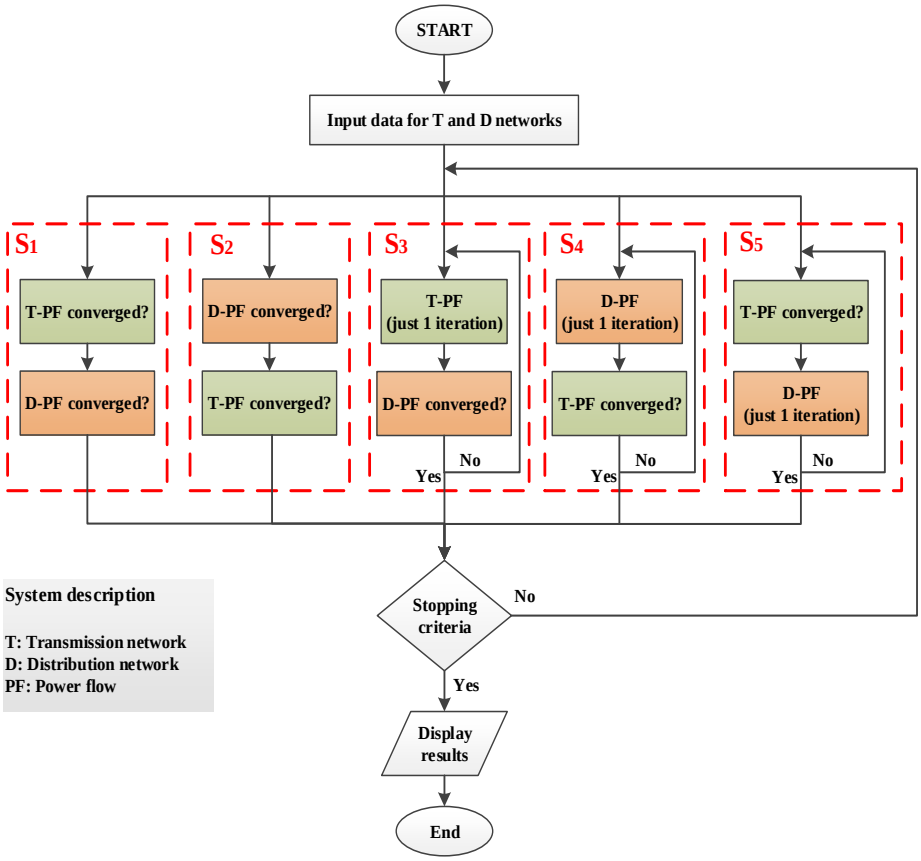

Figure 5. 3. Flowchart of the proposed scenarios

5.6 Analysis and Results

5.6.1 Test System

There are no integrated T&D datasets available for actual power systems, and hence, the authors developed a T&D test system that combines available transmission and distribution benchmarks. The well-known 12.66-kV IEEE 33-bus radial distribution system is studied

here as a distribution part, and the IEEE 30-bus transmission network is selected as the transmission side. In this case, radial distribution feeder replaces total load connected to the bus 26 of the transmission side. It is also assumed that the distribution tie-line switches are in the off status (normal mode).

5.6.2 Scenario 1

In this scenario, according to figure 5.2, the active and reactive powers of the PCC bus are selected as the inputs for IC-GAMA. Regarding $10e^{-8}$ as the threshold, after five iterations the power flow is converged. Figure 5.4 shows the P, Q, V and ∂ of this scenario.

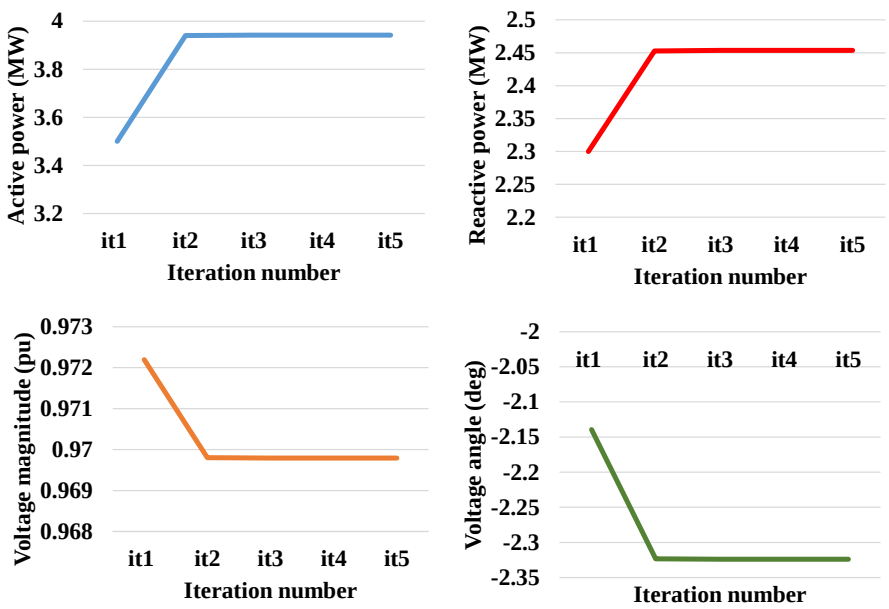

Figure 5. 4. Active power, reactive power, voltage magnitude and voltage angle of the PCC in scenario 1

5.6.3 Scenario 2

The input parameters of scenario 2 are PCC voltage magnitude and angle. Figure 5.5 shows the resulted P, Q, V and ∂. As shown, the results are similar to those of scenario 1.

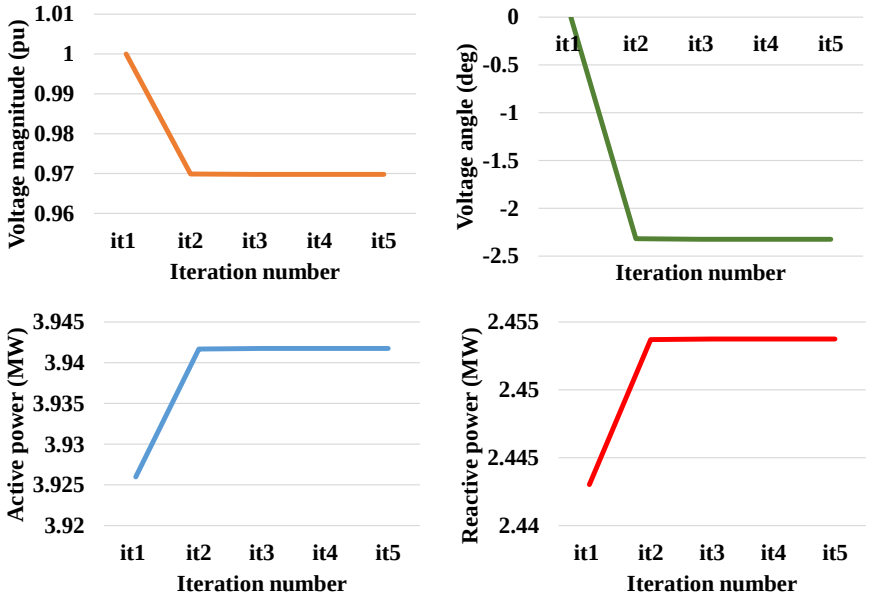

Figure 5. 5. Active power, reactive power, voltage magnitude and voltage angle of the PCC in scenario 2

5.6.4 Scenario 3

In this scenario, the power flow for the transmission network is executed for just one iteration, and then the achieved V and ∂ are transferred to the distribution side as the inputs. As mentioned before, the distribution load flow is not limited to one iteration. The results are plotted against scanario 1 in Figure 5.6. Although the power flow converges, the results of GAMS (V and ∂) are slightly different.

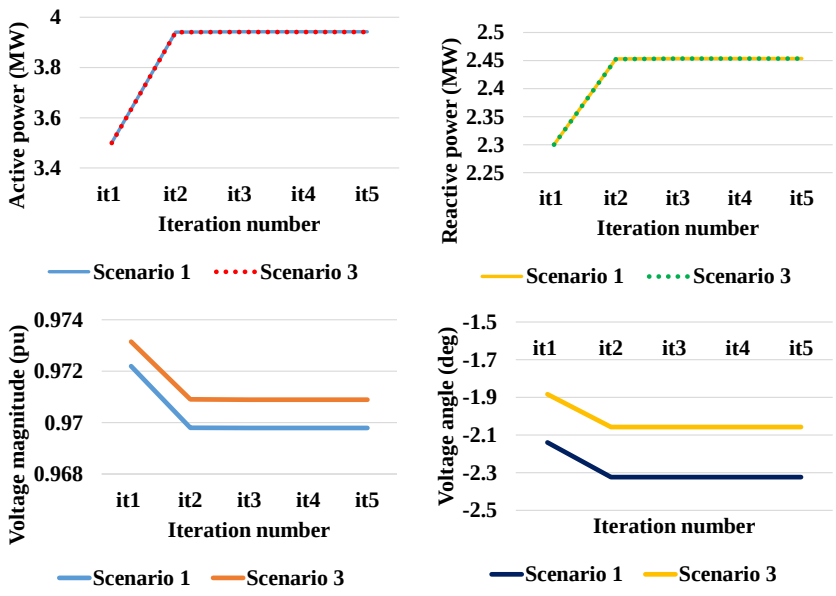

Figure 5. 6. Active power, reactive power, voltage magnitude and voltage angle of the PCC in scenario 3

5.6.5 Scenario 4

This scenario is the opposite of the previous scenario. The starting parameters are P and Q. The parameters of this scenario are given in figure 5.7. It is clear that the performance of this scenario is not as good as the previous ones because the parameters are not converged.

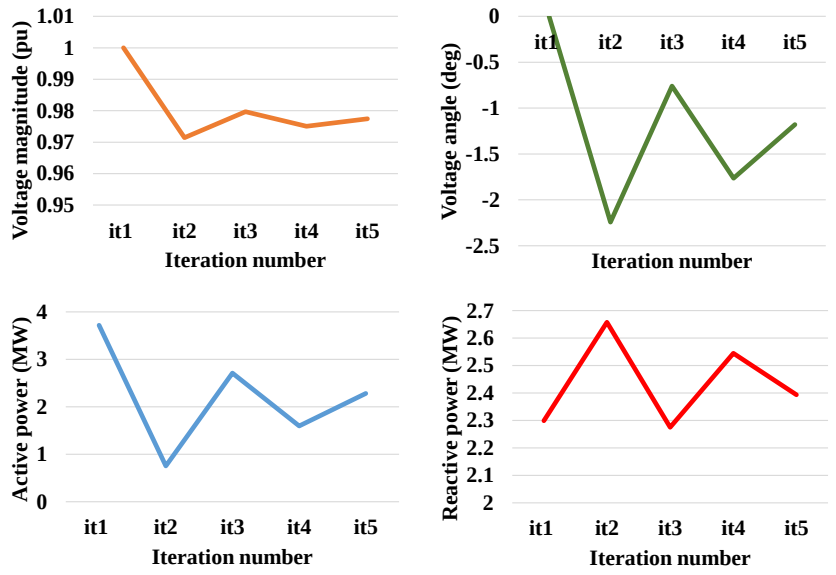

Figure 5. 7. Active power, reactive power, voltage magnitude and voltage angle of the PCC in scenario 4

5.6.6 Scenario 5

As the last scenario, the transmission and distribution power flows are executed with only one iteration and achieved results are exchanged. Figure 5.8 compares the results of this scenario with those of scenarios 1 and 3. It is evident that the performance of scenarios 1 and 3 are superior.

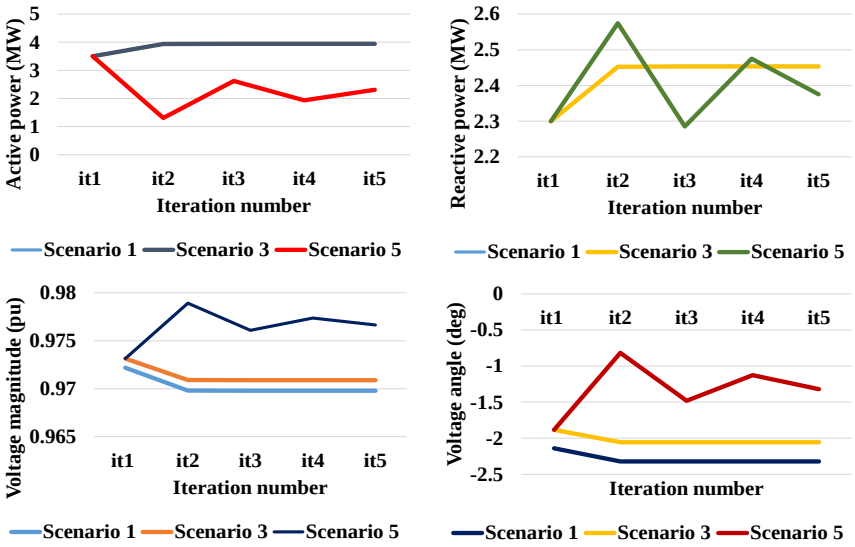

Figure 5. 8. Active power, reactive power, voltage magnitude and voltage angle of the PCC in scenario 5

5.6.7 Discussion

Table 5.1 compares the performance of the proposed IC-GAMA for different studied scenarios. Regarding scenarios 1 and scenario 2, it is evident that s_2 has a better performance in terms of CPU time and the number of iterations.

Table 5. 1. comparison of different schenarios performances

Scenario	CPU-time (second)			Number of iterations		
	T	D	Total	T	D	Total
#1	0.47	0.74	1.21	12	31	43
#2	0.424	0.492	0.916	12	29	41
#3	0.4	1.382	1.782	4	29	33
#4	0.452	0.395	0.847	12	4	16
#5	0.42	0.39	0.81	4	4	8

- T/D denotes the transmission/distribution networks.

Moreover, the robustness of the proposed tool is examined with +/- 10 and +/- 20 percent error in the initial guesses for scenarios 1 and 2. To do so, different cases are studied in two initial error setups, as follows:

Initial Error Setup1

Case-1: -10% error on active power
Case-2: -10% error on reactive power
Case-3: -10% error on active & reactive powers
Case-4: +10% error on active power
Case-5: +10% error on reactive power
Case-6: +10% error on active & reactive powers
Case-7: -20% error on active power
Case-8: -20% error on reactive power
Case-9: -20% error on active & reactive powers
Case-10: +20% error on active power
Case-11: +20% error on reactive power
Case-12: +20% error on active & reactive powers

Initial Error Setup2

Case-1: -10% error on voltage magnitude
Case-2: -10% error on voltage angle
Case-3: -10% error on voltage magnitude & angle
Case-4: +10% error on voltage magnitude
Case-5: +10% error on voltage angle
Case-6: +10% error on voltage magnitude & angle

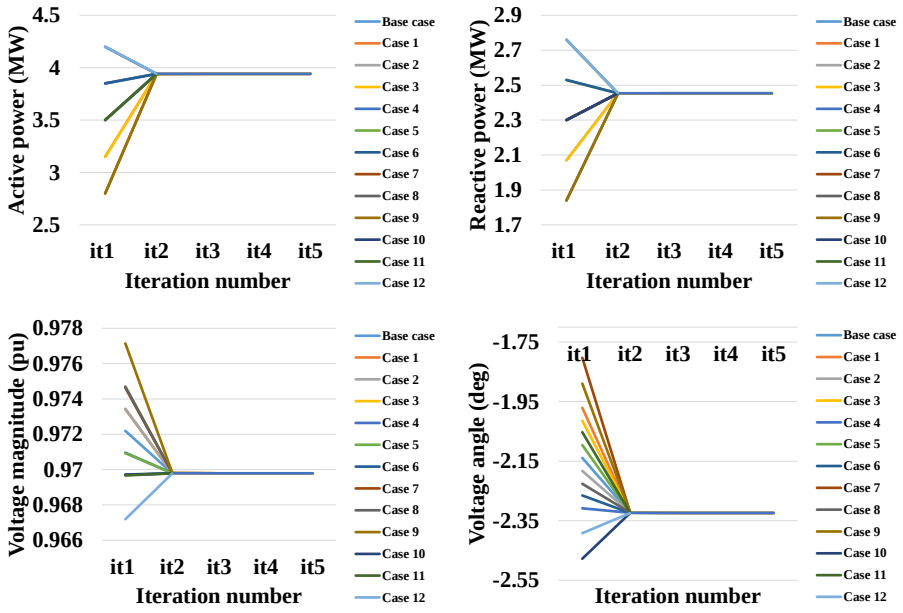

Figure 5. 9. Active power, reactive power, voltage magnitude and voltage angle of the PCC for scenario 1 with the Initial Error Setup1

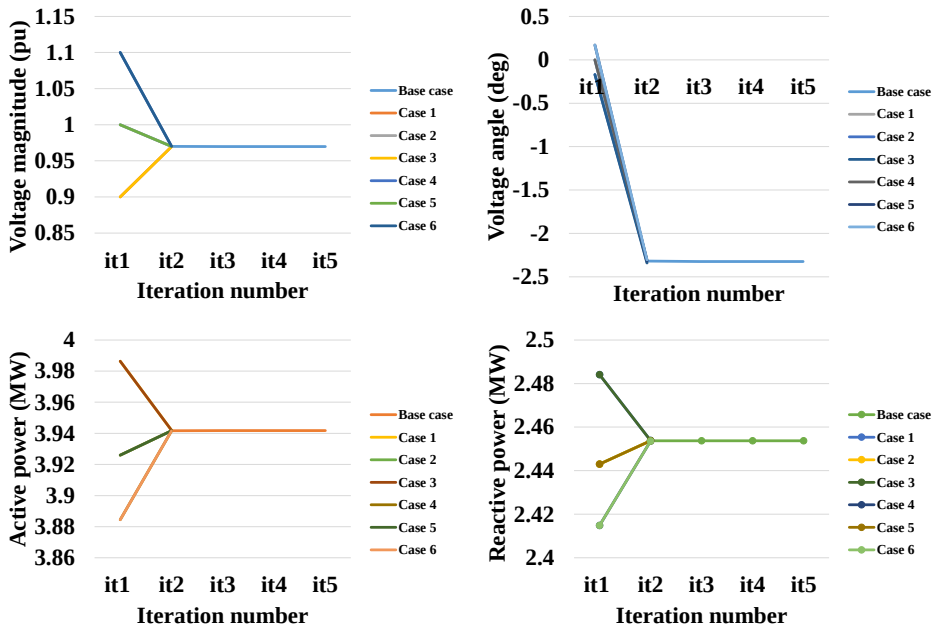

Figure 5. 10. Active power, reactive power, voltage magnitude and voltage angle of the PCC in scenario 2 with the Initial Error Setup2

Figures 5.9 and 5.10 depict the convergence performance of the IC-GAMA platform for scenarios 1 and 2. According to these figures, it can be concluded that, with 10 and 20 percent errors in initial guesses, the IC-GAMA is still capable of solving the T&D load flow problem.

5.7 Conclusion

A novel platform, IC-GAMA is proposed in this paper for simultaneously solving integrated transmission and distribution (T&D) power flows. IC-GAMA is a computationally efficient framework which takes into account the T&D interactions while including detailed models for both transmission and distribution systems. The developed package, based on MATLAB and GAMS, offers an iterative approach which enables the modeling of T&D systems and their interactions. The performance of the proposed framework was verified on IEEE test cases, and the results show that starting from full power flow of distribution system the IC-GAMA has better performance and is more robust to errors in initial guesses. In the future works, with the help of optimization tools of GAMS, the impact of renewable energy sources (RESs) and energy storage systems (ESSs) will be investigated using this new framework.

6 Évaluation de la vulnérabilité dans les systèmes électriques: examen et présentation de nouvelles perspectives

6.1 Résumé

En raison des impacts environnementaux et du coût élevé de l'extension du réseau de transport, les systèmes électriques sont chargés plus près de leurs limites, ce qui augmente leur vulnérabilité et les éventuelles coupures de courant. Dans cet article, la littérature récente sur l'évaluation de la vulnérabilité en état stable (SSVA) et l'évaluation dynamique de la vulnérabilité (DVA) est classée et passée en revue. Après avoir découvert les lacunes de la recherche découlant de la revue de la littérature actuelle, plusieurs idées systématiques sont présentées en termes de conception d'un cadre modulaire avec des indices unifiés pour déterminer les zones vulnérables du système, d'évaluation intégrée de la vulnérabilité du système T&D et de la vulnérabilité des PMUs aux cyberattaques.

Corps de l'article

Titre: Vulnerability Assessment in Power Systems: A Review and Representing Novel Perspectives

Seyed Masoud Mohseni-Bonab[1,2], Innocent Kamwa[2], Ali Moeini[2] and Abbas Rabiee[3]

[1] Electrical Engineering Department, Laval University, QC, Quebec, Canada (e-mail: s.m.mohsenibonab@ieee.org)

[2] Hydro-Québec/IREQ, Power System and Mathematics, Varennes QC J3X 1S1, Canada (e-mail: kamwa.innocent@ireq.ca, moeini.ali@ireq.ca)

[3] Electrical Engineering Department, University of Zanjan, Zanjan, Iran (e-mail: rabiee@znu.ac.ir)

Conférenc: IEEE PES General Meeting 2020

6.2 Abstract

Due to environmental impacts and high cost of transmission network expansion, power systems are loaded closer to their limits, which increases their vulnerability and possible blackouts. In this paper, the recent literature in the steady-state vulnerability assessment (SSVA) and dynamic vulnerability assessment (DVA) are classified and reviewed. After finding the research gaps arising from the current literature review, several systematic ideas are presented in terms of designing a modular framework with unified indices to determine the vulnerable areas of system, integrated T&D system vulnerability assessment, and vulnerability of PMUs to cyber-attacks.

Keyword: vulnerability assessment (VA), steady-state VA (SSVA), dynamic VA (DVA), ancillary service.

6.3 Introduction

Electricity utility, especially power system, is one of the nations' most crucial infrastructures and any failure to the system can severely affect the customers' safety and security. Multiple systems including healthcare, transportation, banking, etc. depend on the reliable and

continuous operation of power delivery systems. Unfortunately, the climate changes and an increased number of natural disasters may significantly increase the vulnerability of power systems, resulting in significant outages disrupting power supply to critical loads for days and sometimes for weeks [64]. During the years 2003 to 2012, severe weather-related events contributed to 58% outages in USA, which is estimated to have an average burden of 18–33 billion $/year to USA's economy [65].

The increasing dependency to power systems coupled with an increased number of natural disasters has drawn the attention of both research community and industry to enhance and ensure the system resilience [66-68].

6.4 Literature review

Generally, the previous researches in this area are divided into two groups including, a) steady-state vulnerability assessment (SSVA) and b) dynamic VA (DVA).

Based on the literature survey different indices are used for SSVA. In the most SSVA researches the main vulnerability indices are the expected load curtailment [69-72] and cost of finding the most vulnerable lines [69, 73], but in some cases, it would be the different. The difference is mainly in the following two cases. Firstly, in some cases the generation outages are also added to line outages in order to calculate the SSVA impact factors [74-78]. Secondly, in some researches the new indices are defined for analyzing SSVA, such as: bus isolation probability (BIP) [79], loss of load probability (LOLP) [79], expected power loss (EPL) [79, 80], probability of stability (POS) [79], integrated system vulnerability (ISV) [79], energy shortage [74], capacity shortage [74], power system failures [74], an index based on fault chains [81], a reliability based vulnerability assessment index [82], the centrality index [83], voltage deviation [71], an index based on electrical distance and line impedance [84], line temperature dynamics [80], vulnerability index of a generation unit (VIGS) and its sensitivity (SVIGS), hybrid flow betweenness (HFB), closeness centrality impact measure (CIc), network vulnerability index (NVI) [77], line outage impact on bus (LOIB) [78], generator outage impact on bus (GOIB) [78], an index based on the complex network theory

[85] and an index based on the system global efficiency which consists of each line's efficiency [86].

A recent research reveals that energy storage systems (ESSs) have a high potential to mitigate power system vulnerability. For instance, in [77] Battery Energy Storage Systems (BESS) is utilized for enhancing the level of vulnerability (i.e. disturbance-based vulnerability index (NVI)) or in [78] ESSs are used for power system vulnerability mitigation. This highly depends on the optimal location and size of installed the ESSs.

In [87, 88], in order to investigate the vulnerable features of branches in a fault propagation process, an adjacent graph is proposed from the overload mechanism of the electrical networks based on the proposed cascading faults graph.

For dynamic vulnerability assessment (DVA), a novel Fuzzy C-medoid algorithm (FCMdd) based approach is proposed in [89]. This approach is based on PMU allocation on wide-area measurement system (WAMS). In [90] the optimal phasor measurement unit (PMU) for dynamic vulnerability assessment is conducted. In this method, the buses which are sensitive to the changes in power system status, have to be equipped with PMUs to monitor the fragile areas of power systems.

In [91] both SSVA and DVA are analyzed to assess deterministic indices. In addition, load uncertainty is modeled and evaluated through Monte Carlo simulations. For SSVA index, the total amount of load curtailment under contingency scenarios is reduced by both generation redispatch and load shedding. For DVA part, the objective is to be able to estimate the energy margin (positive or negative) a few milliseconds after clearing the fault, either when the system reaches minimum kinetic energy (positive margin) or instability is detected (negative margin).

The vulnerability of the transmission network subject to the intentional attacks has also drawn the interest of researchers because of this problem assessment necessary precondition for monitoring and security control of power systems. Some recent researches study the cyber-to-physical bridge between the SCADA network and the power system, and reliability issues introduced by the cyber-attacks. For example, a number of quantitative methods for

vulnerability assessment are proposed for the SCADA/EMS system [92], for the wind integrated SCADA/EMS system [93], for wide-area network (WAN) [94], and for the integrated power, information and communication technology (ICT) systems.

Table 6.1 summarizes a complete review on the aforementioned researches carried out on the SSVA regarding security criterion (i.e. N-k criterion), indices, power flow (PF) methods, model types, simulators, deterministic or probabilistic approaches for uncertainty handling, and the renewables utilizations.

Table 6. 1. Summary of recent researches carried out on the SSVA/DVA problems

	N-k?	Outage type?	Stochastic? If yes (Method? And uncertain parameter?)	Index for vulnerability evaluation	Model/ Simulator	PF method	Renewable? (If yes, type?)
[69]	N-1	Lines	✓ Stochastic two-stage programming approach – Attackers attack plans	1. The expected load shed of the system 2. The expected cost of load shed of the system 3. The investment cost	MINLP / CPLEX	DCPF	×
[70]	N-2	Lines	×	Load shedding with/without line switching	Bi-level, MIP/ C++	DCPF	×
[71]	N-1	Lines	×	1. Load shedding with/without line switching 2. Voltage deviation	Bi-level, NLP / MATLAB , IPOPT	ACPF	×
[72]	N-1	Lines	×	Load shedding with/without line switching	Bi-level, BDLS, MINLP / GAMS	DCPF	×
[73]	N-1	Lines	×	The system operation and load shedding costs	Bi-level / MILP, GAMS	DCPF	×
[74]	N-1	Generat or, Line	×	1. Energy Shortage 2. Capacity Shortage 3. Power System Failures	NLP / EMPS	ACPF	×
[75]	N-1	Generat or, Line	×	Vulnerability index of a generation unit (VIGS) and its sensitivity (SVIGS)	NLP / MATLAB , PSAT	ACPF	×
[76]	N-3	Generat or, Line	×	A new closeness centrality impact measure (CIc)	NLP / MATLAB (simulatio ns), RTDS (real time	DCPF	×

					simulations)		
[77]	N-1	Generator, line, load	×	The disturbance-based vulnerability indices (network vulnerability index (NVI)) to enhance the level of vulnerability with minimum BES MWh installation.	NLP / NSGA-II	ACPF	BESS
[78]	N-2	Generator, Line	×	1. line outage impact on bus (LOIB) 2. generator outage impact on bus (GOIB)	NLP / Genetic algorithm, Borland C++	ACPF	ESSs
[79]	N-1	Lines	✓ Monte Carlo simulation – Initial faulted lines	1. Bus Isolation Probability (BIP) 2. Loss of Load Probability (LOLP) 3. Expected Power Loss (EPL) 4. Probability of Stability (POS) 5. Integrated System Vulnerability (ISV)	NLP / MATLAB	ACPF	×
[80]	N-1	Lines	×	Line loss formulation, Line temperature dynamics (with instanton formulation)	QCQP, GAMS	DCPF	Wind
[81]	N-1	Lines	×	A new index based on fault chains	NLP / C++	ACPF	×
[82]	N-1	Lines	×	A new reliability-based vulnerability assessment index	×	×	×
[83]	N-1	Lines	×	The centrality index	NLP /DigSilent PowerFactory	ACPF	×
[84]	N-3	Lines	×	A new index based on electrical distance and line impedance	LP / MATLAB, PowerWorld	DCPF	×
[85]	N-1	Lines	×	Analyzing the cascading faults graph (CFG) through indices based on the complex network theory	NLP / MATLAB	DCPF	×
[86]	N-1	Lines	✓ Monte Carlo simulation – Wind uncertainty	The composite vulnerability assessment index, derived from the	NLP / MATLAB	ACPF	Wind

				system global efficiency			
[87, 88]	N-1	Lines		Fault probability, load shedding, and topological structure based indices	LP / MATLAB	ACPF	×
[91]	N-2	Lines	✓ Monte Carlo simulation – Load uncertainty	SSVA: The total amount of load curtailment under contingency scenarios	NLP / ×	DCPF	×
[95]	N-1	Lines	×	finding the attack which maximizes the physical line flow on a target line after redispatch	NLP / MATLAB (CPLEX)	ACPF, DCPF	×
[96]	N-1	Lines	×	hybrid flow betweenness (HFB) with considering direction of power flow	NLP / MATLAB	ACPF	×

6.5 The research gaps arising from the review

methods for vulnerability assessment are proposed for the SCADA/EMS system [92], for the wind integrated SCADA/EMS system [93], for wide-area network (WAN) [94], and for the integrated power, information and communication technology (ICT) systems.

The following remarks inferred from the above literature survey:

1. Lack of a unified index: several methods and indices have been proposed in literatures for VA. Most of them offer ranking methods based on some performance indices which take into account information as well as bus voltages, active and reactive powers of generating units and transmission lines. Also, in some references, effective vulnerability mitigation approaches focused on ensuring resiliency and reliability of grid, are mandatory. To the best of our knowledge, there is a lack of unified index for both SSVA and DVA to give more precise information about how vulnerable an element is following a contingency while vulnerability assessment is done for all generating units, transmission lines, and buses. Any proposed unified index must cover wider range of operation to cover both dynamic and steady-state regimes.

2. Lack of distribution network impact: SSVA and DVA have been considered in most transmission network analysis literature. However, the actual bilateral connection between distribution and transmission networks (integrated T&D) is not considered. With the growing trend of emerging new technologies in distribution networks, such as wind turbines, solar panels, electric vehicles, and distributed generations, the passive distribution systems may become "active," and thus the need for simultaneously studying T&D networks, and corresponding bilateral interactions cannot be overlooked anymore.
3. Vulnerability of PMUs subject to cyber-attacks: In recent works such as [90, 95], the optimal PMU placement in DVA raised to minimise the number of PMUs and optimize their locations. However, it is crucial to evaluate the vulnerability of energy management systems (EMSs) and PMUs themselves to sophisticated cyber-attacks
4. The impact of ESS and demand response (DR) on the VA problem: To the best of the authors' knowledge no reference has investigated the ESS (while including detailed models) and DR impacts on SSVA. Basically, the SSVA problem find the most vulnerable lines by changing the system generators production. Here the idea is by changing the demand pattern, we need to know how we can minimize the possible damages.
5. The impact of distributed energy resources (DERs) uncertainties on the VA: Facing the increasing penetration of DERs in the emerging power systems, the uncertain and volatile nature of these energy resources should be properly handled in SSVA. Based on Table 7.1, it can be seen that most current references are neglected DERs and their volatile nature. Some recent references are focused on the status-vulnerability assessment when just wind power integration is considered [80, 86].

6.6 Potential works

1) Designing a modular framework for both SSVA and DVA with unified indices – A solution for the first gap

Although different indices are available to address the vulnerability of individual infrastructures, a comprehensive framework for evaluation of interdependency of these indices is needed. In this idea, we recommend a novel approach for system modeling by

decomposing the physical system layer into multiple component layers (see Fig. 6.1). Each component layer is modeled to include the interactions between electrical and other infrastructures. Any proposed framework should facilitates modeling the interactions of the power delivery component and interdependent layers, thus adding modularity to the analysis and potentially achieving scalability. The approach to develop the proposed modular framework is detailed as following. First, the components of the physical system layer are identified, and the component layer model is developed while including its interdependencies with multiple infrastructure systems. Next, the relationships between the components layers are obtained and coupling metrics are formulated. Finally, the detailed coupled framework is used to develop guidelines for resilient power system planning and operation.

2) Analyzing the integrated T&D system stability under uncertainty, and identifying risk threshold – A solution for second and fifth gap

The transient stability problem is one of the most important challenges for ensuring secure operation of power systems. In addition, the operations of distribution systems are becoming more complicated with the high penetration of distributed resources and energy storage systems. Therefore, the need for simultaneously studying Transmission & Distribution (T&D) networks and corresponding bilateral interactions cannot be overlooked anymore. Furthermore, as one typical cyber-physical system, the cyber component of the power system is subjected to various forms of uncertainties, such as faulty sensors or actuators, packet drops, and random delay in communication channels.

So, the second idea is to develop a comprehensive transient stability analysis tool for an integrated T&D system to identity a risk threshold-based data-centric risk assessment considering uncertainties. A critical set of generator and load buses that are most sensitive to uncertainties should also be identified.

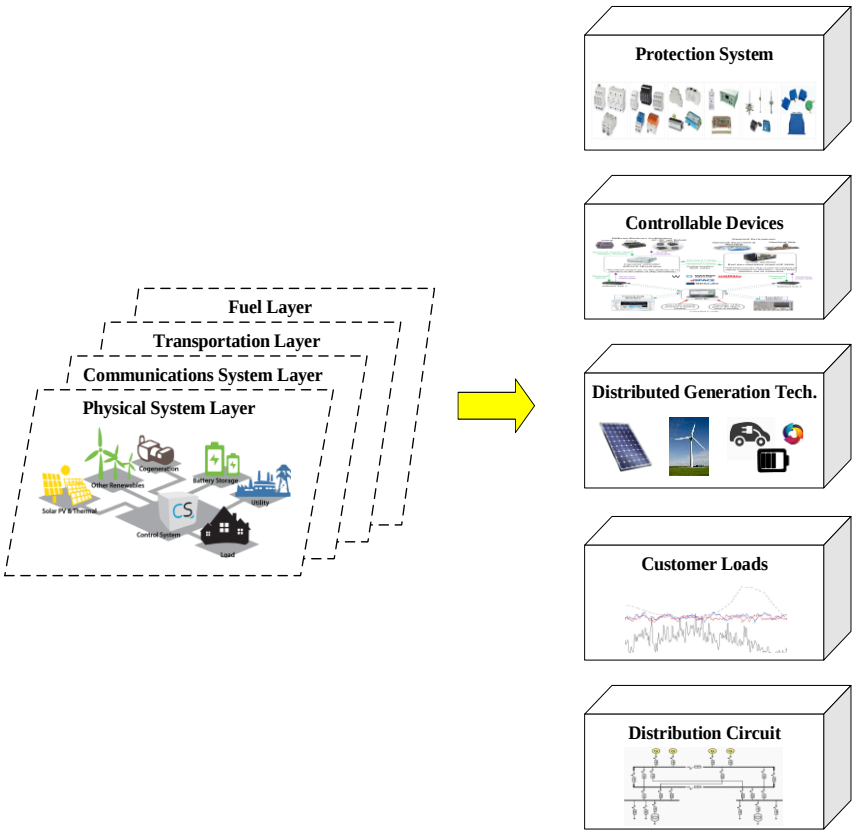

Figure 6. 1. Modern power delivery system

3) Vulnerability of PMUs to cyber-attacks – A solution for third gap

Even as PMU deployment in the transmission system is expanding, one can envision a situation in less than five years when highly affordable line-relay PMUs and even bus PMUs become the norm for telemetry data to monitor voltages, power and current flows. It is essential to understand the vulnerability of PMUs themselves to cyber-attacks. At its core, the future studies must seek to address if the GPS-time stamped PMU data can be changed by an attacker to spoof the system. Recent results suggest that for specific types of attackers that do not completely model the nature of PMU data (sparse at any instant in time and low-rank over an interval of time required to collect SCADA data), PMU data is indeed resilient to attacks [97]. However, it is naive to assume that the attacker cannot or will not model the temporal and spatial characteristics of PMU data. However, observations as indicated by recent researchers demonstrate that correlations between adjacent PMUs are crucial to

understand if realistic attacks are indeed possible on PMU data [98]. To this end, this sub-task has three questions that must be addressed:

- Can an attacker inject false data injection (FDI) attacks [95] to a small sub- network in an unobservable fashion that takes into account PMU data at faster time scales?
- Are networks with fewer PMUs more vulnerable to FDI attacks on PMU data?
- Can PMU and SCADA data be used cohesively to develop algorithms that can detect anomalous changes that a sophisticated attacker can induce (to either or both systems)?

4) **Stochastic time-based vulnerability assessment of power systems under optimal ESS scheduling – A solution for fourth gap**

To determine the most vulnerable lines of the system to intentional attacks, in this idea, a stochastic framework is recommended. A time-based stochastic vulnerability assessment problem considering optimal battery energy storage systems allocation (TSV-OBA) problem is proposed as a bi-level programming model and can be solved with GAMS software. In the upper level of the problem, an attacker is assumed to execute a attack plan, including the best locations and the best times over the time horizon. The system operator then minimizes the system operations and load shedding costs in the lower level. Utilizing linearization technique and duality theory, the optimization problem will be converted to a single level mixed integer linear programming problem. The problem can be solved in the integrated transmission and distribution (T&D) systems while including realistic models of distributed energy resources.

5) **Designing a risk model for vulnerability analysis and mitigation in power systems with high penetration of DERs**

The objective of this idea is to develop a risk model of medium voltage power systems to determine areas of vulnerability to faults. To reach this goal, a realistic representation of power systems including protective relays should be developed.

The proposed risk model must provide insights to vulnerable areas of power systems. The model can be used to mitigate such vulnerable areas strategically. The proposed equivalent model significantly should reduce the computation burden of simulation for large-scale systems as the downstream systems do not need to be modeled in details. The response of power systems with high penetration of DERs to faults will be better understood and possible miss-operations and shortcoming of the protection systems will be determined that can be used for improvement of protection systems.

6.7 Conclusion

A comparative study of different VA techniques for steady state VA (SSVA) and dynamic VA (DVA) was conducted in this paper. Firstly, the gaps arising from the literature review are shown. Then, five new directions are proposed.

7 Application d'optimisation dans les opérations de transport et de distribution intégrées: approche de co-simulation

7.1 Résumé

L’incrément de charge, conséquence de l’électrification de tout ce qui se trouve dans les réseaux de distribution modernes, impose d’analyser les interactions entre les systèmes de transmission et de distribution de l’énergie électrique (T&D). Une telle électrification massive peut détériorer les profils de tension et les échanges de puissance, ce qui entraîne par conséquent une efficacité moindre du réseau. En tant que solution économique et efficace, les dispositifs contrôlables installés pour la tension dans les réseaux de distribution, tels que le changeur de prise sous charge (ULTC) et les batteries de condensateurs, peuvent être optimisés pour relever les défis susmentionnés. Ce document propose une nouvelle plate-forme intégrée de co-simulation de transmission et de distribution dans laquelle les charges agrégées dans un simulateur de système de transmission (MATLAB) sont remplacées par un réseau de distribution modélisé dans un simulateur de système de distribution (OpenDSS) via une interface Python. L'efficacité globale du système T&D est ensuite optimisée tout en maximisant la marge de chargement (LM) et en minimisant les pertes de puissance totales du système, sont considérées comme deux fonctions objectives. L'approche proposée est appliquée à un réseau T&D construit avec 68 nœuds et les résultats démontrent que l'efficacité du réseau T&D peut être améliorée en définissant de manière optimale les variables de contrôle.

Corps de l'article

Titre: Optimization Application in Integrated Transmission and Distribution Operation: Co-Simulation Approach

Seyed Masoud Mohseni-Bonab[1,2], Ali Hajebrahimi[2], Ali Moeini[2] and Innocent Kamwa[2]

[1] Electrical Engineering Department, Laval University, QC, Quebec, Canada (e-mail: s.m.mohsenibonab@ieee.org, ali.hajebrahimi.1@ulaval.ca)

[2] Hydro-Québec/IREQ, Power System and Mathematics, Varennes QC J3X 1S1, Canada (e-mail: kamwa.innocent@ireq.ca, moeini.ali@ireq.ca)

Conférenc: IEEE PES General Meeting 2020

7.2 Abstract

The load increment as the consequence of electrification of everything in the modern distribution networks, makes it imperative to analyze the interactions between electric power transmission and distribution (T&D) systems. Such a massive electrification may deteriorate voltage profiles and power exchanges, which results consequently in lower grid efficiency. As a low-cost and effective solution, the installed controllable devices for voltage in distribution networks such as under-load tap changer (ULTC) and capacitor banks can be optimized to overcome the aforementioned challenges. This paper proposes a new integrated transmission and distribution co-simulation platform where the aggregated loads in transmission system simulator (i.e. MATLAB) are replaced by a distribution network modeled in distribution system simulator (OpenDSS) through a Python interface. The overall T&D system efficiency is then optimized while maximizing loading margin (LM) and minimizing the total system power losses are contemplated as two objective functions. The proposed approach is applied on a constructed T&D grid with 68K nodes and the results demonstrate that the efficiency of the T&D grid can be improved by optimal setting of the control variables.

Keyword: Integrated transmission and distribution (T&D) systems, Co-simulation, Optimization, Tap changer, Capacitor, loading margin.

7.3 Nomenclature

N_B / N_j	Set of buses.
N_L	Set of branches (transmission lines).
N_G	Set of generating units.
N_D	Set of load buses.
i / j	Index of bus Number where $i = 1, 2, \ldots, N_B$.
ℓ	Index of transmission lines.
$y_\ell / g_\ell / b_\ell$	Admittance/conductance/ susceptance of ℓth line.
$Y_{ij} = G_{ij} + jB_{ij}$	ij^{th} element of system Y_{bus} matrix.
P_{Gi}	Active power production at bus i .
$P_{G_i}^{\min} / P_{G_i}^{\max}$	Minimum/maximum values for active power.
P_{D_i}	Real power of the ith bus .
Q_{D_i}	Reactive power of the ith bus.
$Q_{G_i}^{\min} / Q_{G_i}^{\max}$	Minimum/ Maximum values for reactive power of the ith bus.
$V_i^{\min} / V_i^{\max}$	Minimum/ Maximum value for voltage magnitude of the ith bus.
$S_\ell^{\max}$	Maximum value of power flow of ℓth transmission line.
x	Vector of dependent variables (optimization variables).
V_i / V_j	Voltage magnitude of bus i/j .
θ_i / θ_j	Voltage angle at bus i/j .
Q_{C_i}	Reactive power compensation at bus i.
R_i	Voltage regulator at bus i.
S_ℓ	Power flow of ℓth transmission line.
λ	Loading parameter of the system.
K_{L_i}	Rate of load change at bus i.
K_{G_i}	Rate of change in active power generation of unit i.
PL / LM	Real power loss / loading margin.

7.4 Introduction

The integrated transmission and distribution (T&D) studies in power system can be broadly classified into two categories: A) co-simulation of integrated T&D and B) co-optimization of integrated T&D. Co-optimization aims to construct a union framework, sometimes as a package, for studying several levels of power systems simultaneously. In co-simulation studies different dedicated software, two or more, are used simultaneously to study the effects of different phenomena in power systems, such as failures among infrastructures [54, 99], voltage stability assessment [56], power losses (with and without renewables) [57]. In terms of steady-state co-simulated studies, in [59], a coordinated transmission and distribution AC optimal power flow (TDOPF) is proposed and solved with a mathematical master-slave structure. Similarly, an open-source co-simulation framework 'framework for network co-simulation' (FNCS), is proposed in [6, 40] to investigate the dynamic behaviors of both the transmission and distribution networks. To demonstrate the co-simulation through FNCS framework, GridPACK™ and GridLAB-D™ are chosen as the simulators for transmission and distribution simulators, respectively. The Integrated Grid Modeling System (IGMS) [11, 12] is used as the platform to co-simulate (1) the transmission power flow using MATPOWER [60]; (2) distribution network using GridLAB-D [61]; and (3) wholesale market operations using FESTIV [11]. In [62], the impact of distributed generation from solar photovoltaics (DGPV) on the integrated T&D is studied in IGMS framework. In [63], a new co-simulated framework called Hierarchical Engine for Large-scale Infrastructure Co-Simulation (HELICS) is proposed.

Table 7.1 summarizes the findings of existing literatures and the main contributions of this paper. This paper aims to optimize the status of ULTC and capacitor banks in an integrated grid with more than hundreds of transmission buses and hundreds to thousands of distribution nodes for improving the overall efficiency.

The rest is organized in five sections including the introduction. In section two, the proposed model characteristics are described. In section three, the proposed problem formulation is elaborated. Some analysis using the package is presented in section four. Finally, the conclusion remarks are provided in section five.

Table 7. 1. Summary of related literature and contributions of this paper

Ref	solver	U/B?	Scale			Optimization
			T	D	T&D	
[59]	OPF	B	57	126	183	N
[40]	PF	B	9	13×2	35	N
[6]	PF	U	118	123	241	N
[11, 12]	PF	U	250	1.3 M	1.3M	N
[62]	OPF	U	5	27k	27k	N
Pro.	**SCOPF /CPF**	**U**	**118**	**68k**	**68k**	**Y**

- Y/N denotes that the subject is/is not considered.
- PF/OPF/SCOPF/CPF denotes power flow/ optimal power flow/ security constraint optimal power flow/continuation power flow
- U/B denotes unbalanced 1-phase/balanced 3-phase distribution network.

7.5 Model description

7.5.1 Simulation tools

The proposed problem is implemented in OpenDSS software and MATLAB environments. We use MATLAB to model transmission network (MATPOWER package [60]) and to solve security constraint optimal power flow. Distribution network load flow is solved by OpenDSS. The interface coupling the transmission and distribution networks is implemented in Python. In addition, the optimization procedure is performed by Matlab optimization toolbox (Genetic algorithm). All the test cases are carried out on a laptop with Intel Core i7 2.70 GHz CPU and 16 GB internal memory (RAM). An overview of the proposed approach is shown in Fig. 7.1.

During the optimization, whenever, it is required to perform a T&D load flow, the proposed approach shown in Fig. 7.2 is executed where bus voltages and angles (V,δ) obtained from transmission network load flow and active and reactive power total demand (P,Q) of distribution network are interchanged at the Point of Common Coupling (PCC) [100].

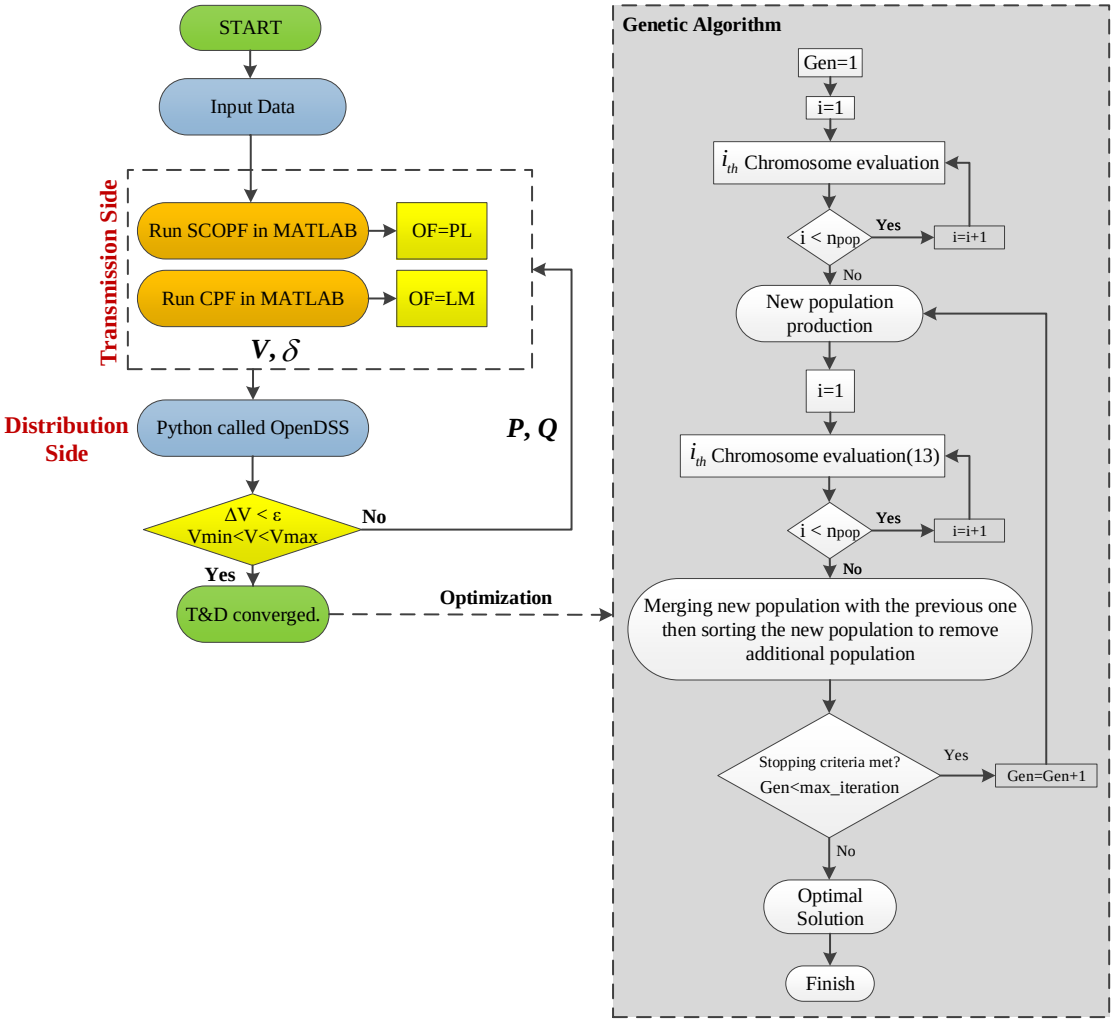

Figure 7. 1. Overview of the proposed approach to model T&D optimization.

7.5.2 Solution procedure

In the proposed co-simulation framework, T&D systems are solved independently, and the interactions are captured by interchanging the solutions obtained from the two simulators. The schematic in Fig. 7.2 shows how the proposed frameworks operates in general. Using [100], here the distribution side is the primary point for starting T&D full power flow.

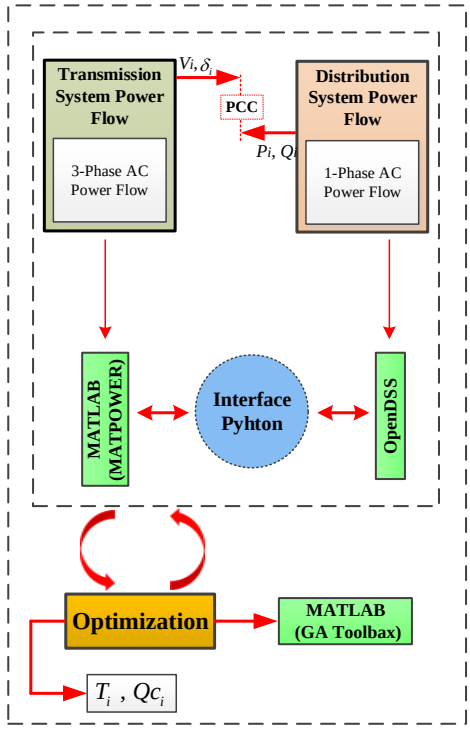

Figure 7. 2. Block diagram of the proposed approach to model T&D interactions.

An iterative framework is proposed by exchanging the solutions. The integrated model is solved when the solutions from the decoupled models converge. According to this approach, bus voltages and angles obtained from transmission network solver and active and reactive power flow obtained from distribution network solver are shared at the PCC.

7.6 Problem formulation

In this section, the studied objective function and problem constraints like load flow equations are described.

7.6.1 Objective functions

In this paper the objectives are real power losses (PL), and loading margin index (LM). In the aforementioned problem, the vector of control variables (optimization variables) can be mathematically formulated as follows:

$$x^T = \left[[V_i]^T, [\theta_i]^T, [Q_G]^T, [P_G]^T, \left[Q_{C_i}\right]^T, [T_i]^T \right] \tag{7-1}$$

7.6.1.1 Case-I: Total active power losses

Minimization of the total power losses in T&D system is important objective for improvement of the total energy efficiency and for economic reasons. The active power losses can be mathematically expressed as follows:

$$PL(x) = \sum_{i=1}^{N_G} P_{G_i} - \sum_{i=1}^{N_B} P_{D_i} \tag{7-2}$$

7.6.1.2 Loading margin

One of the main factors for preserving a power system security is to satisfy specified desired LMs. LM is defined as the amount of load increase not arousing voltage instability or violation of operational constraints [17]. In order to attain the LM, a continuation power flow is performed by increasing the loads and generations gradually. The point where the operational constraints tend to be violated, is the loadability limit point. The distance in MW or MVA from the current operating point and the loadability limit point is the LM. Simply, in other word, the power system is secure from voltage stability viewpoint while sufficient LM exists from the current operation point (COP) to the loadability limit point (LLP) as depicted in Fig. 7.3.

Two basic interpretations of the load margin exist associated with the vector λ. The first one is based on a deterministic direction of load and generation increase K_{L_i} and K_{G_i} so λ is restricted to a single scalar. The following constraints for LM formulation are elaborated as:

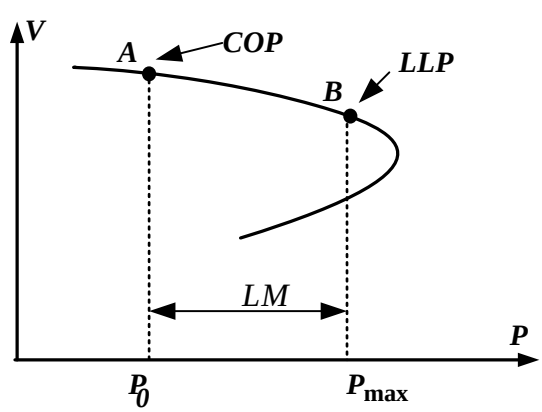

Figure 7. 3. The concept of LM on a typical P-V curve.

$$P_{G_i} - P_{D_i}\left(1+\lambda K_{L_i}\right) = V_i \sum_{j=1}^{N_B} V_j \left[G_{ij}\cos\left(\theta_i - \theta_j\right) + B_{ij}\sin\left(\theta_i - \theta_j\right)\right] \tag{7-3}$$

$$Q_{G_i} - Q_{D_i}\left(1+\lambda K_{L_i}\right) = V_i \sum_{j=1}^{N_B} V_j \left[G_{ij}\sin\left(\theta_i - \theta_j\right) - B_{ij}\cos\left(\theta_i - \theta_j\right)\right] \tag{7-4}$$

$$\lambda > 0 \tag{7-5}$$

$$P_{G_i} = \min\left(P_{G_i}^{\max}, \left(1+\lambda K_{G_i}\right)P_{G_i}\right) \tag{7-6}$$

7.6.2 Equality Constraints/ Operational Limits of SCOPF

$$P_{G_i} - P_{D_i} = V_i \sum_{j=1}^{N_B} V_j \left[G_{ij}\cos\left(\theta_i - \theta_j\right) + B_{ij}\sin\left(\theta_i - \theta_j\right)\right] \tag{7-7}$$

$$Q_{G_i} - Q_{D_i} = V_i \sum_{j=1}^{N_B} V_j \left[G_{ij}\sin\left(\theta_i - \theta_j\right) - B_{ij}\cos\left(\theta_i - \theta_j\right)\right] \tag{7-8}$$

$$P_{G_i}^{\min} \le P_{G_i} \le P_{G_i}^{\max} \quad , \forall i \in N_G \tag{7-9}$$

$$Q_{G_i}^{\min} \le Q_{G_i} \le Q_{G_i}^{\max} \quad , \forall i \in N_G \tag{7-10}$$

$$V_i^{\min} \le V_i \le V_i^{\max} \quad , \forall i \in N_B \tag{7-11}$$

$$Q_{C_i}^{\min} \le Q_{C_i} \le Q_{C_i}^{\max} \quad , \forall i \in N_C \tag{7-12}$$

$$T_i^{\min} \le T_i \le T_i^{\max} \quad , \forall i \in N_T \tag{7-13}$$

$$\left|S_\ell\right| \le S_\ell^{\max} \quad , \forall \ell \in N_L \tag{7-14}$$

Constraints (7-8)-(7-15) represent technical and operation limits on solving the proposed problem. Constraints (7-7)-(7-8) correspond to the equality constraints or AC power balance equations, whereas (7-9)-(7-15) correspond to the inequality constraints. Active/reactive power output of all the buses (including slack buses) and voltage buses limits are represented in (7-9)-(7-11). The reactive power output of VAR compensation devices and the steps of tap changers, which are the optimization variables, are also limited based on (7-12)-(7-13). The line flow limits are expressed by (7-14).

7.7 Results and discussion

7.7.1 Test System and assumptions

A well-known 4.16 kV IEEE 123-node unbalanced distribution system with a large scale IEEE 8500-node test feeder are studied here as distribution networks and IEEE 118-bus transmission network is selected as transmission side. IEEE 123-node radial distribution network replaces the loads connected to buses 23, 73 and 113 of transmission grid. Also, IEEE 8500-node distribution network replaces the loads connected to buses 29, 33, 53, 85, 86, 101, 103 and 115. These buses are selected based on IEEE 118-bus nominal loads capacities. The backbone diagram of the integrated system with 68,487 nodes is depicted in Fig. 7.4. In this paper, the load is assumed to follow the hourly load duration curve of the IEEE reliability test system (RTS) in [101]. Herein, three hours of a typical day are considered for the analysis: median hour (i.e. t_1 which load percentage=0.5782 pu), peak hour (i.e. t_2 which load percentage=1), and valley hour (i.e. t_3 which load percentage= 0.73 pu).

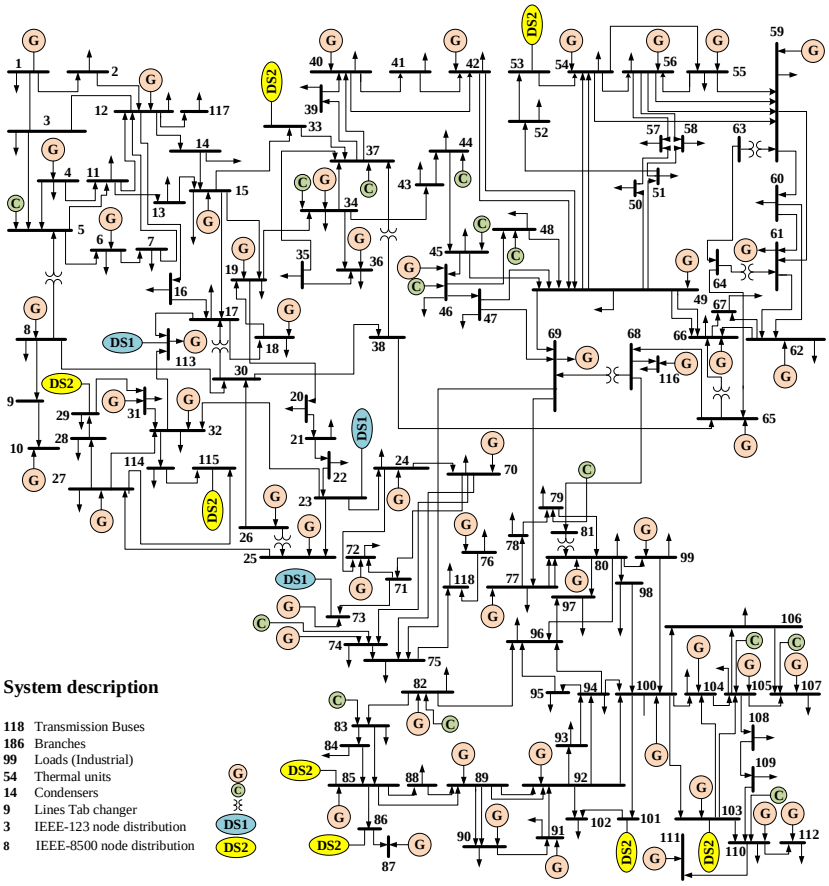

Figure 7. 4. Backbone of modified test system.

7.7.2 Case-I:

In this case, the objective function is to minimize PL of integrated T&D system. Fig. 7.5 shows the PL of base case (BC) before and after optimization. It is clear that the optimization of available control devices reduces the PL while this reduction is greater for t_2 (peak hour) where the PL improved with GA about 14% for distribution networks and 0.3% for transmission grid. The control variables such as optimal ULTC tap positioning in comparison with the base case are summarized in Table 7.2. Here for the sake of brevity only a few ULTC positions and capacitor sizes in three distribution networks are given.

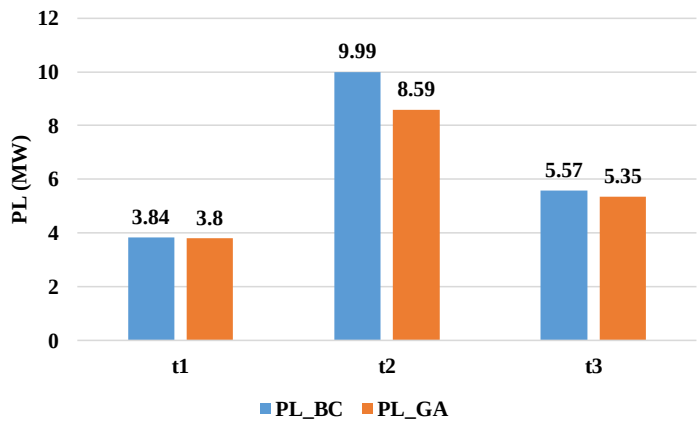

Figure 7. 5. PL in distribution networks with and without optimization in different scenarios

7.7.3 Case-II:

In this case, the optimization algorithm is applied on the second objective function (loadability maximization). To respect independent functionality of each sector in the co-simulation framework, the process of maximizing LM in the integrated T&D grid is performed using a heuristic approach described in the following steps:

- **Step 1:** Run CPF on the base case and identify voltage sensitivity index for each transmission bus as:

$$V_{si}^{i} = V_{iter}^{i} - V_{iter-1}^{i} \tag{7-15}$$

where *iter* stands for the last iteration of CPF.

Table 7. 2. Control variables for the base case and optimization case in both ieee 123-node and 8500-node test systems – (Case-I)

A typical IEEE 123-node			A typical IEEE 8500-node		
	BC	GA		BC	GA
DS1_23_T1	7	-3	DS2_101_T1	10	-9
DS1_23_T2	8	5	DS2_101_T2	6	-9
DS1_23_T3	1	9	DS2_101_T3	2	7
DS1_23_T4	5	-14	DS2_101_T4	16	-12
DS1_73_T1	7	-11	DS2_101_T5	10	-16
DS1_73_T2	8	-4	DS2_101_T6	1	7
DS1_73_T3	1	2	DS2_101_T7	12	6
DS1_73_T4	5	-9	DS2_101_T8	12	4
DS1_113_T1	7	-11	DS2_101_T9	5	-6
DS1_113_T2	8	-4	DS2_101_C1	22.22	21.43
DS1_113_T3	1	2	DS2_101_C2	24.37	10.66
DS1_113_T4	5	-9	DS2_101_C3	25.48	19.76

- DS1_23_T1 denotes the tap operation of UTLC when IEEE 123 is replaced the total load connected to bus 23.
- Capacitor sizes are based on KVAR.

- **Step 2:** Develop a weighted sum of normalized vector of load buses according to the voltage sensitivity index in Step 1.

$$LM = \sum_{i=1}^{N_B} V_{si}^{i} \times \frac{\tilde{P}_D^i}{P_D^i} \tag{7-16}$$

where $\tilde{P}_D^i$ indicates the updated value of P_D^i at each optimization iteration.

- **Step 3:** Minimize the defined function in Step 2 and obtained the optimal solution.
- **Step 4:** Apply the optimal solution to the base case and run CPF to calculate the new LM.

In this case only the results based on t_2 are represented. In a base case and without distribution systems impact, the IEEE 118-bus loading margin is equal to 1.458 pu which means that the system operator can increase the total load about 45% without instability or violation of operational constraints. The proposed approach increases this limit to 1.564 pu. In other hand with optimization, the LM increase about 12%. The control variables of this case for t_2 are shown in Table 7.3.

Finally, the results of PL and LM optimization approaches are compared in Fig. 7.6. To do so, the optimal set of parameters generated by first case is evaluated with CPF. In the same way, optimal results of Case-II are used to calculate the total power loss. As expected, the PL decreases more in Case-I, however, PL also decreases relatively in Case-II. The same situation is valid for the LM case. It is crystal clear that these two functions are not in contradict, nevertheless, the optimal configuration of the system is different according to the optimal value of each objective function.

Table 7. 3. Control variables for the base case and optimization case in both ieee 123-node and 8500-node test systems – (Case-II)

A typical IEEE 123-node			A typical IEEE 8500-node		
	BC	GA		BC	GA
DS1_23_T1	7	-15	DS2_101_T1	10	-13
DS1_23_T2	8	-6	DS2_101_T2	6	10
DS1_23_T3	1	-10	DS2_101_T3	2	-16
DS1_23_T4	5	11	DS2_101_T4	16	8
DS1_73_T1	7	13	DS2_101_T5	10	-12
DS1_73_T2	8	-2	DS2_101_T6	1	2
DS1_73_T3	1	9	DS2_101_T7	12	-9
DS1_73_T4	5	-1	DS2_101_T8	12	9
DS1_113_T1	7	-9	DS2_101_T9	5	0
DS1_113_T2	8	0	DS2_101_C1	22.22	13.42
DS1_113_T3	1	-1	DS2_101_C2	24.37	11.37
DS1_113_T4	5	9	DS2_101_C3	25.48	7.21

- DS1_23_T1 denotes the tap operation of UTLC when IEEE 123 is replaced the total load connected to bus 23.
- Capacitor amounts are based on KVAR.

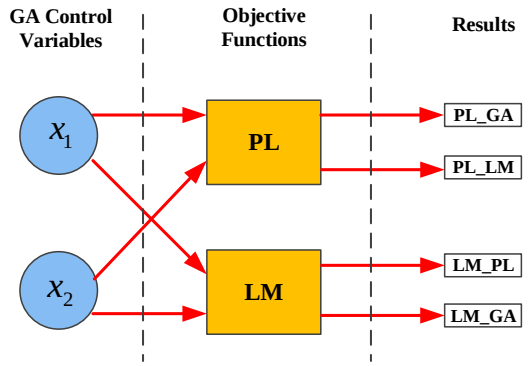

Figure 7. 6. Comparison of optimization results considering PL or LM as the objective function.

The PL in distribution networks are compared with the case in which the control variables are optimized for LM. It can be seen that the PL is decreased again but not such as the previous scenario. Also in this case T&D power losses in the BC is 77.5805 MW which decreased to 77.3843 MW (decreased about 0.3%). Also LM_PL in this case is 1.527 which shows that when the LM is the main objective the loadability is increased a bit more.

7.8 Conclusion

A novel platform is proposed in this paper for simultaneously solving integrated transmission and distribution (T&D) power flows. Also using this platform, the available controllable devices of distribution systems is optimized. The proposed framework is a computationally efficient framework which takes into account the T&D interactions while including detailed models for both transmission and distribution systems. The developed package, based on MATLAB and OpenDSS and Python, offers an iterative approach which enables the modeling of T&D systems and their interactions. The performance of the proposed framework was verified on IEEE large scale test cases. The results show that with balancing available control devices settings, the system operator can decrease the system power losses and also can increase the system loadability. The best answer is derived when all control parameters are set in their best values.

8 Commutation de transmission optimale: une approche stochastique en considérant la résilience du réseau

8.1 Résumé

Dans cet article, un problème de commutation de transmission optimale stochastique (SOTS) est développé sous l'incertitude de charge en tenant compte de la vulnérabilité du réseau. Une procédure en trois étapes, nommée SOTS orienté vulnérabilité (VO-SOTS), est proposée pour considérer l'ensemble des lignes de transport critiques, c'est-à-dire les lignes dont la panne impose la plus grande réduction de charge. Dans un premier temps, le problème SOTS est résolu dans le but de minimiser le coût total de production en supposant la possibilité de commutation pour toutes les lignes. Dans la deuxième étape, l'ensemble des lignes de transmission critiques est déterminé en résolvant un problème d'optimisation qui vise à maximiser la réduction de charge totale. Dans la troisième étape, le problème SOTS est à nouveau résolu mais en excluant cet ensemble de lignes critiques. Le modèle VO-SOTS proposé est formulé comme un problème d'optimisation de programmation non linéaire à nombres entiers mixtes et résolu à l'aide du logiciel GAMS. Les résultats optimaux obtenus par GAMS sont comparés à ceux de cinq algorithmes d'optimisation métaheuristique : génétique, optimisation de l'essaim de particules, compétition impérialiste, recherche gravitationnelle et recherche de corbeaux. De plus, le VO-SOTS proposé est comparé à l'approche des simulations déterministes et de Monte Carlo. Le modèle VO-SOTS proposé est appliqué aux systèmes de test standard bus IEEE 39, bus IEEE 118 et bus IEEE 2869 à grande échelle. Les résultats de la simulation pour ces cas montrent que la prise en compte de l'ensemble des lignes critiques permet au modèle VO-SOTS proposé de réduire les coûts de production tout en considérant efficacement la vulnérabilité du système. En outre, la suppression d’une ligne des systèmes électriques par le VO-SOTS proposé n’augmente pas l’exposition du réseau électrique à la vulnérabilité, contrairement à l’OTS conventionnel.

Corps de l'article

Titre: Decision Support System to Enhance Power Grid Secure Operation Margins Through Vulnerability Mitigation Under Uncertainties

Seyed Masoud Mohseni-Bonab[1,2], Innocent Kamwa[2], Abbas Rabiee[3], and C.Y. Chung[4]

[1] Electrical Engineering Department, Laval University, QC, Quebec, Canada (e-mail: s.m.mohsenibonab@ieee.org)

[2] Hydro-Québec/IREQ, Power System and Mathematics, Varennes QC J3X 1S1, Canada (e-mail: kamwa.innocent@ireq.ca)

[3] Electrical Engineering Department, University of Zanjan, Zanjan, Iran (e-mail: rabiee@znu.ac.ir)

[4] Electrical and Computer Engineering Department, University of Saskatchewan, Saskatoon, SK S7N5A9, Canada (e-mail: c.y.chung@usask.ca)

Revue: IEEE Transaction of Power Systems

8.2 Abstract

In this paper, a stochastic optimal transmission switching (SOTS) problem is developed under load uncertainty by considering grid vulnerability. A three-step procedure, named the vulnerability-oriented SOTS (VO-SOTS), is proposed to consider the set of critical transmission lines, i.e., lines whose outage imposes the largest load curtailment. In the first step, the SOTS problem is solved with the aim to minimize the total generation cost by assuming the possibility of switching for all lines. In the second step, the set of critical transmission lines is determined by solving an optimization problem that aims to maximize the total load curtailment. In the third step, the SOTS problem is solved again but excluding this set of critical lines. The proposed VO-SOTS model is formulated as a mixed integer non-linear programming optimization problem and solved using GAMS software. The optimal results obtained by GAMS are compared to those from five metaheuristic optimization algorithms: genetic, particle swarm optimization, imperialist competitive, gravitational search, and crow search. Moreover, the proposed VO-SOTS is compared with deterministic and Monte Carlo simulations approaches. The proposed VO-SOTS model is applied to the

IEEE 39-bus, IEEE 118-bus, and large-scale IEEE 2869-bus standard test systems. Simulation results for these cases show that considering the set of critical lines allows the proposed VO-SOTS model to reduce generation costs while effectively considering system vulnerability. In addition, removing a line from power systems by the proposed VO-SOTS does not increase the power grid's exposure to vulnerability, in contrast to conventional OTS.

Keyword: Stochastic optimal transmission switching (SOTS), resiliency, load curtailment, load uncertainty.

8.3 Nomenclature

Sets:

N_B	Set of buses.
N_i	Set of buses connected to bus *i*.
N_L	Set of branches.
N_G	Set of generating units.
N_s	Set of all possible scenarios.
N_L^{OTS}	Set of all candidate branches for OTS.

Indices:

i / j	Index of bus numbers.
s	Index of overall scenario numbers.
ℓ	Index of transmission lines.
G	Index of generation units.

Parameters:

π_s	The probability of scenario *s*.
$Y_{ij} = G_{ij} + jB_{ij}$	*ij*-th element of system Ybus matrix.
$P_i^{G,\min} / P_i^{G,\max}$	Minimum/maximum value for active power at bus *i*.
$Q_i^{G,\min} / Q_i^{G,\max}$	Minimum/maximum value for reactive power at bus *i*.
$P_{D_d}^{\min} / P_{D_d}^{\max}$	Minimum/maximum value of real power demand at *s*–th load scenario.
$P_{i,s}^D / Q_{i,s}^D$	Real/reactive power load of the *i*-th bus in scenario *s* (MW/MVAR).

$V_i^{\min} / V_i^{\max}$	Minimum/maximum value for voltage magnitude of the *b*-th bus.
$\theta_i^{\min} / \theta_i^{\max}$	Minimum/maximum level of voltage angle at bus *i*.
$S_\ell^{\max}$	Maximum transfer capacity of line ℓ .
R	Maximum number of open transmission lines.
Y_{ij}	Admittance of line between bus *i* and *j*.
λ_i^G	Operation cost of generation buses at bus *i* ($).

Variables:

$V_{i,s} / \theta_{i,s}$	Voltage magnitude/angle of bus *i* in scenario *s*.
$S_{\ell,s}$	Power flow of ℓ -th branch in scenario *s*.
$P_{i,s}^G / Q_{i,s}^G$	Active/reactive power production of generation buses at bus *i*.in scenario *s* (MW/MVAR).
u_ℓ	Binary variable which shows status (0:open, 1: close) of ℓ -th line.
$LS_{i,s}^P / LS_{i,s}^Q$	Active/reactive power production of fictitious generator at bus *i* (MW/MVAR).

Functions:

$TGC_s / ETGC$	Total generation cost in scenario *s*/expected *TGC* ($)
$TLS_s / ETLS$	Total load shedding in scenario *s*/expected *TLC* (MW)

8.4 Introduction

8.4.1 Background and motivation

Optimal transmission switching (OTS) [102, 103] aims to find an optimal generation dispatch and transmission network topology to meet goals such as minimum generation cost. The OTS problem is basically formulated as a mixed integer non-linear programming (MINLP) problem, taking into account the AC/DC power flow model of the system. In addition to decreasing operation costs, OTS has other advantages such as alleviation of over/under voltages, loss reduction, etc. [104].

However, by its very nature OTS more than often results in removing lines from the network to reduce operation costs, which intrinsically makes the system more vulnerable to security violations unless proper countermeasures are taken together with the line removal. These preventive control measures may include active and reactive power redispatch or

reconfiguration of secondary control reference settings. This perception of the OTS indirectly increasing power grid vulnerability in the sense of n-1 secure operation is supported by evidence to this effect; this remains the main barriers against its adoption in power systems operations. Therefore, the present paper aims to alleviate this pitfall by developing a vulnerability-oriented OTS that tries to balance the operation cost benefits of conventional OTS with the requirements of n-1 secure operations which can be alternatively be understood as operating the grid with reserve in generation capacity and transmission transfer capacity to always stay away from to vulnerable conditions, i.e., the edges of insecurity.

8.4.2 Literature review

Generally, OTS removes some transmission lines from service, or puts lines back into service, to optimize an objective such as generation cost reduction. To deal with this problem, both AC optimal power flow (ACOPF) and DC optimal power flow (DCOPF) models have been developed in the literature. ACOPF models [105] are not commonly used for OTS problems because they encounter some computational difficulties and therefore recent papers instead use less accurate DCOPF models [106-109]. However, in some case both models are combined [110, 111].

In some research, for the sake of efficiency the OTS problem is solved considering special constraints such as connectivity-ensuring constraints [112], or short-circuit current limitation constraints [113]. I The effects and efficiency of OTS have been investigated in some power system problems such as unit commitment (UC) [114], security-constrained UC [115], optimal PMU placement [116], energy clearing [117], vulnerability assessment [70] and expansion planning [118-120]. For instance, reference [114] indicates the co-optimization formulation of the generation unit commitment and transmission switching problem while ensuring N-1 reliability, and shows the optimal topology of the network can vary from hour to hour. The Dantzig-Wolfe decomposition-based method in [118-120] are used to solving stochastic integer programming-based transmission switching and line capacity expansion problems. In [116] at the first stage, PMUs are installed to achieve full observability of the power grid where in the second phase, to guarantee the $N-1$ observability of the power grid, additional PMUs are installed. In [117] for determining the optimal required energy and reserve values, OTS problem is solved with contingencies. Also. in this research for

minimizing the cost of supplying load, reliability expenses and avoidance of transient instability dynamic constraints are considered.

According to the above literature review, in the most OTS researches the main objective is the cost minimization but in some cases it is different. For instance, in [105] the total power loss of network was analyzed along the famous OTS functions like cost reduction and power not supplied (PNS) values. In [121] a dc optimal load shed recovery with transmission switching model is proposed.

Probabilistic OTS researches are increased in recent years. In [118], the problem is solved in large scale system with presence of wind generation unit and it can be deduce that OTS may reduce generation cost and increase the hosting capacity of network wind power. In [122] Monte Carlo simulation is used for modeling probabilistic nature of system component failures in optimal transmission switching problem in multi-objective framework.

Given the fact that the topology of the power grid will be changed if one or more transmission lines are disconnected, OTS can also be incorporated into the system operator's post-disruption decision for a better mitigation effect. Nevertheless, line-switching decisions are made with pre-defined, somewhat heuristic and system-dependent rules, which are not analytical and could be less effective under power flow patterns never seen before. As such, ref [70] concentrated on the idea of solving vulnerability constraints in the presence of line switching (e.g., resulting from malicious attacks) but operation costs were not part of the objective function. In most steady-state vulnerability assessment (VA) research [123], the main vulnerability indices are the expected load curtailment [69-72] and the cost of finding the most vulnerable lines [69, 73], but some cases would be different. In [70], a bi-level VA problem was reformulated as a single-level problem. For the sake of ease, only DC power flow was used to solve the mixed integer programming (MIP) problem. The authors also did not consider the impact of system uncertainties (e.g., load uncertainty, which is the key uncertainty factor [124]).

8.4.3 Contributions

From the above discussion, sufficient research work has evaluated the operations cost-based OTS in transmission networks taking into consideration various system constraints.

However, to the best of our knowledge, no work in the literature includes the systems vulnerability in the operations-cost based OTS problem. Also, no efficient method other than MCS has been developed for uncertainty handling in the SOTS up to now.

Therefore, the goal of this paper is to fill these gaps in the literature though an OTS implementation that encompasses uncertainty in a truly stochastic optimization framework while minimizing the vulnerability index [75] of post-OTS grid during n-1 security events. In fact, the resulting enhanced OTS solution will alleviate the main pitfall of conventional OTS, which is network exposure to increased risks of loss-of-load under n-1 events, by reducing the vulnerability index defined in [75] even below the base case without line switching, with the sacrifice being slightly higher operation costs that are still well below the operations cost without OTS.

To achieve this goal, which is actually a complicated multi-objective nonlinear optimization problem (i.e., minimizing both operation costs and vulnerability index [75]), we turn to a greedy three-stage optimization process where the final step aims to solve the OTS by removing lines whose outage results in maximum load shedding. By finding and eliminating these worst-case scenarios from the list of candidate lines to be switched off, the OTS problem solution displays a much-improved vulnerability index. In other word, the line maximizing load-shedding should never be switched off by the OTS process, which instead should turn to lines with lower adverse impact on system reliability, and therefore reduce the cost while avoiding an increase in the vulnerability index.

To find the lines maximizing load shedding, an artificial generator is added to all PQ buses in the system and the optimal power flow problem is solved for different outputs. The combination of the most vulnerable lines that cause the greatest load shedding is the solution to the proposed problem. Therefore, the main contributions of this work are summarized as follows:

1) Combating vulnerability induced by OTS, especially in N-k security assessment: this paper provides a comprehensive framework for solving a vulnerability-oriented SOTS (VO-SOTS) problem considering an N-k contingency criterion. A three-step procedure is proposed for modeling the VO-SOTS problem. First, the OTS problem is solved with the aim of minimizing generation costs. Because the transmission line switching increases the

vulnerability of the system, another optimization problem is solved in the second step to determine the list of the most critical line switching that leads to the largest load curtailment. In the third step the OTS problem is then solved again while excluding these lines, aiming to minimize generation costs.

2) Using a "fictitious generator" to smooth load flows in ill-conditioned networks: the concept of a fictitious generator to "measure" the criticality of the line is proposed in this paper. Finding the critical line is not easy if we must embed the impacts in the operation costs while ensuring the power flow constraints in each case. Satisfying the power flow constraints in n-k configurations and calculating operation costs is challenging without this concept. The fictitious generator concept is used in reactive power control (via synchronous condensers) to facilitate power flow convergence at Hydro-Quebec [125]. To determine the active power curtailment in the OTS problem with consideration of the N-k security criterion, the fictitious generator concept is useful and ensures the AC power flow feasibility.

3) It models the stochastic nature of loads in the proposed VO-SOTS model.

Table 8.1 summarizes the findings of the existing literature and the main contributions of this paper.

8.4.4 Paper organization

The rest of the paper is organized as follows. Section II introduces the modeling of load uncertainty using the scenario-based method and shows the objective functions and constraints of the proposed model. In Section III, the solution procedure is implemented on the proposed model with different heuristic and mathematical algorithms. Section IV presents the simulation results of the proposed model. Vulnerability assessment of system is performed in section V. Finally, conclusions are drawn in Section VI.

Table 8. 1. Summary of the existing literature and contributions of this work

Ref.	OTS is studied? Type?	Model type? Solver?	Objective function	OPF type	Uncertainties considered? Type? Modeling technique?
[105]	Single (N-1)	MINLP	Cost, Power Losses	ACOPF	N
[106]	Single (N-1)	MINLP	Cost	ACOPF+ DCOPF	N
[107]	Single (N-1)	MIP/Heuristics	Cost	DCOPF	N
[108]	Single (N-1)	MIP/Heuristics	Cost	DCOPF	N
[109]	Single (N-1)	MIP/CPLEX	Cost	DCOPF	N
[110]	Single (N-1)	MIP/Heuristics	Cost	ACOPF+ DCOPF	N
[111]	Single (N-1)	Decouple (MIP+ NLP)	Cost	ACOPF+ DCOPF	MCS
[112]	Single (N-1)	MILP	Cost	DCOPF	N
[113]	Single (N-1)	MIP	Cost	DCOPF	N
[114]	Single (N-1)	MIP	Cost, UC objectives	DCOPF	N
[115]	Single (N-1)	MIP	Cost, UC objectives	DCOPF	N
[116]	Single (N-1)	ILP	PMUs num. & loc.	DCOPF	N
[117]	Single (N-1)	MINLP	Cost, Dynamic OFs	ACOPF	N
[70]	Single (N-1)	MIP	Load shedding	DCOPF	N
[118]	Single (N-1)	MIP/ CPLEX	Cost	DCOPF	Demand and wind/Stochastic (Dantzig-Wolfe)
[119]	Single (N-1)	ILP	Cost	DCOPF	N
[120]	Single (N-1)	MIP	Cost	DCOPF	Demand and wind/Stochastic (Dantzig-Wolfe)
[121]	Double (N-2)	MIP/Heuristics	Load shedding	DCOPF	N
[122]	Single (N-1)	MIP/Heuristics	Cost	DCOPF	Loss of load probability (LOLP)/MCS
Pro.	Quintuple(N-5)	MINLP/Mathematical	Cost, Load shedding	ACOPF+ DCOPF	Demand /Stochastic (Scenario-based)

- N denotes that the subject is not considered.

8.5 Problem Formulation

This section provides the SOTS problem formulation. Because load demand is a key factor for determination of total generation cost, its uncertainty is considered in the formulation of the OTS problem. The load uncertainty is handled via scenarios and hence the stochastic OTS (SOTS) problem formulation will be established in this section. The set of critical transmission lines, i.e., the lines whose outage imposes the largest load curtailment, is then determined and the SOTS problem is solved again by considering the critical transmission lines.

8.5.1 Load uncertainty modeling

In order to model uncertainty of load, the PDF of the forecasted load is divided into some intervals with the width of one standard deviation [24]. A sample forecasted PDF of load which is divided into 5 intervals is depicted in Fig. 8.1. Each interval is corresponding to a specific scenario. Hence, two quantities should be calculated for each scenario, as follows.

1) The probability of each scenario, which is obtained by calculation of the area under the PDF in the corresponding interval.
2) The average value of each interval is considered as the load value in the corresponding scenario.

Table 8.2 summarizes the amount of average load and the corresponding probability for each scenario.

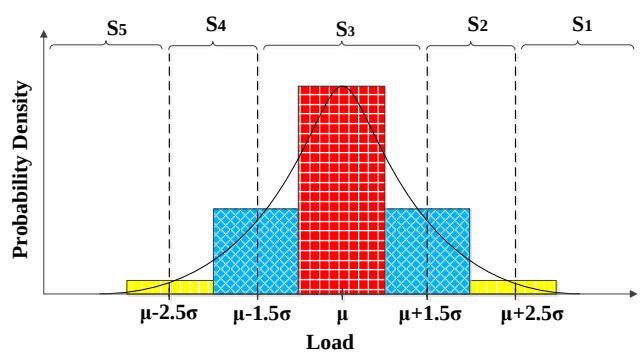

Figure 8. 1. A simple 8-bus distribution feeder

Table 8. 2. Summary of the existing literature and contributions of this work

Scenario Number	Load value in each scenario (P_{D_s})	Probability in each scenario (π_s)
s_1	$\mu - 2.5\sigma$	0.025
s_2	$\mu - 1.5\sigma$	0.135
s_3	μ	0.680
s_4	$\mu + 1.5\sigma$	0.135
s_5	$\mu + 2.5\sigma$	0.025

Each interval corresponds to a specific load scenario. In this paper, mean and standard deviation of the load PDF, i.e. μ and σ are assumed to be known, via load forecasting programs and historical data. Probability and the expected value of s-th load scenario are denoted by π_s and P_{D_s} respectively, which are calculated using Fig. 8.1, as follows.

$$\pi_s = \int_{P_{D_s}^{\min}}^{P_{D_s}^{\max}} \frac{1}{\sqrt{2\pi\sigma^2}} \exp\left[-\frac{\left(P_D - \mu\right)^2}{2\sigma^2} \right] dP_D \tag{8-1}$$

$$P_{D_s} = \frac{1}{\pi_s} \int_{P_{D_s}^{\min}}^{P_{D_s}^{\max}} \left(P_D \times \frac{1}{\sqrt{2\pi\sigma^2}} \exp\left[-\frac{\left(P_D - \mu\right)^2}{2\sigma^2} \right] \right) dP_D \tag{8-2}$$

8.5.2 SOTS problem formulation

The proposed SOTS model is formulated as a MINLP optimization problem. The following presents the objective functions considered along with the problem constraints. As mentioned above, the aim of the OTS problem is to minimize the total generation cost. But, when some transmission lines are switched off, the strength of the transmission system will be jeopardized and the load shedding in the system will increase subject to those switching actions. Hence, in this paper an VO-SOTS problem is formulated as a three-step optimization procedure. The following presents the formulation of the proposed VO-SOTS model.

The proposed VO-SOTS formulation is based on the ACOPF model. The main task of the ACOPF model is to minimize the generation cost while satisfying all technical constraints. In the s-th scenario, the total generation cost can be calculated as follows.

$$TGC_s = \sum_{i \in N_G} \lambda_i^G P_{i,s}^G \tag{8-3}$$

Because the TGC is scenario-dependent, its expected value (i.e., expected TGC (ETGC)) is regarded as one of the objective functions, which is calculated as follows.

$$ETGC = \sum_{s=1}^{N_S} \pi_s TGC_s \tag{8-4}$$

The *ETGC* is minimized subject to the following constraints.

$$P_{i,s}^G - P_{i,s}^D = V_{i,s} \sum_{j \in N_i} V_{j,s} \left[G_{ij} \cos\left(\theta_{i,s} - \theta_{j,s}\right) + B_{ij} \sin\left(\theta_{i,s} - \theta_{j,s}\right) \right] \tag{8-5}$$

$$Q_{i,s}^G - Q_{i,s}^D = V_{i,s} \sum_{j \in N_i} V_{j,s} \left[G_{ij} \sin\left(\theta_{i,s} - \theta_{j,s}\right) - B_{ij} \cos\left(\theta_{i,s} - \theta_{j,s}\right) \right] \tag{8-6}$$

$$P_i^{G,min} \le P_{i,s}^G \le P_i^{G,max} \;\; ; \;\; \forall i \in N_G \;\; , \forall s \in N_S \tag{8-7}$$

$$Q_i^{G,min} \le Q_{i,s}^G \le Q_i^{G,max} \;\; ; \;\; \forall i \in N_G \;\; , \forall s \in N_S \tag{8-8}$$

$$V_i^{\min} \le V_{i,s} \le V_i^{\max} \quad ; \quad \forall i \in N_B \,,\, \forall s \in N_S \tag{8-9}$$

$$\theta_i^{\min} \le \theta_{i,s} \le \theta_i^{\max} \quad ; \quad \forall i \in N_B \,,\, \forall s \in N_S \tag{8-10}$$

$$0 \le \left| S_{\ell,s} \right| \le S_\ell^{\max} \times u_\ell \quad , \forall \ell \in N_L \,,\, \forall s \in N_S \tag{8-11}$$

$$\sum_\ell (1-u_\ell) \le R \quad , \forall \ell \in N_L^{OTS} \tag{8-12}$$

$$Y_{ij} = G_{ij} + jB_{ij} = -u_\ell (g_{ij} + jb_{ij}) \quad \forall\, i \ne j,\, \ell : i \leftrightarrow j \tag{8-13}$$

$$Y_{ii} = G_{ii} + jB_{ii} = +\sum_j u_\ell (g_{ij} + jb_{ij}) \tag{8-14}$$

Constraints (8-5)-(8-14) represent technical and operation limits on solving the proposed problem. Constraints (8-5)-(8-6) correspond to the equality constraints or AC power balance equations, whereas (8-7)-(8-14) correspond to the inequality constraints. Active/reactive power output of all the buses (including slack buses) and specific limits of bus voltages is proposed in (8-7)-(8-10).

Also, cconstraint (8-11) shows power flow of an open line must be equal to zero. Constraint (8-12) represents the upper limit of the number of lines that can be opened in OTS problem (In this paper it is limited to five lines). It is worth to note that at the first stage of the proposed VO-SOTS model, all lines are candidate for switching, i.e. N_L^{OTS} in (8-12) is the same with N_L. But, at the second stage and by excluding the set of critical lines from the switching candidates, N_L^{OTS} will be a subset of N_L. Hence, u_ℓ will equal to 1 for the critical lines which means that these lines should not be considered as the candidate for switching at the second stage of VO-SOTS. Equations (8-13)-(8-14) are used for calculating the admittance of transmission lines in OTS problem.

8.5.3 Determination of Critical Lines Set

By considering *ETGC* as the objective of the SOTS problem, switching off some lines to minimize the *ETGC* weakens the transmission network, increases vulnerability index and hence increases the possibility of security violation and ultimately, load shedding. Load shedding is a common remedial action in emergency and extreme emergency conditions when the system is driven towards instability or even a blackout. In the contingency situation, if the controllers of the system cannot push the system to a normal state, load curtailment

must be applied as soon as possible. In this part, another objective function (i.e., TLS maximization) is presented for the SOTS problem to find the list of vulnerable (or critical) lines. If these critical lines are determined, the VO-SOTS problem can be solved by excluding these lines. In the s-th scenario of uncertainty, the total load shedding is expressed as follows.

$$TLS_s = \sum_{i \in N_i} LS_{i,s}^P \tag{8-15}$$

Because the value of *TLS* depends to the scenario number, its expected value is considered as the next objective function, which is calculated as follows.

$$ETLS = \sum_{s=1}^{NS} \pi_s TLS_s \tag{8-16}$$

The constraints should be considered for maximization of *ETLS* are almost the same, except that (9-5)-(9-6) should be replaced by (9-17)-(9-18), as follows.

$$P_{i,s}^G - \left(P_{i,s}^D - LS_{i,s}^P\right) = V_{i,s} \sum_{j \in N_i} V_{j,s} \left[G_{ij} \cos\left(\theta_{i,s} - \theta_{j,s}\right) + B_{ij} \sin\left(\theta_{i,s} - \theta_{j,s}\right)\right] \tag{8-17}$$

$$Q_{i,s}^G - \left(Q_{i,s}^D - LS_{i,s}^Q\right) = V_{i,s} \sum_{j \in N_i} V_{j,s} \left[G_{ij} \sin\left(\theta_{i,s} - \theta_{j,s}\right) - B_{ij} \cos\left(\theta_{i,s} - \theta_{j,s}\right)\right] \tag{8-18}$$

$$0 \le LS_{i,s}^P \le P_{i,s}^D \quad , \forall i \in N_i, \forall s \in N_S \tag{8-19}$$

$$0 \le LS_{i,s}^Q \le Q_{i,s}^D \quad , \forall i \in N_i, \forall s \in N_S \tag{8-20}$$

Active/reactive power limitation of production of fictitious generator expressed by (8-19)-(8-20). To model load shedding (i.e. $LS_{i,s}^P$ and $LS_{i,s}^Q$ in (8-19) and (8-20)) using heuristic algorithms, a procedure will be described in the next section based on the fictitious generator concept.

8.6 Solution procedure

8.6.1 VO-SOTS solution stages

As mentioned above, the aim of this work is to determine the set of transmission lines switching that minimizes the *ETGC*. On the other hand, the set of the most critical lines should be determined to consider the impact of line switching on reducing system security.

Hence, a three-step OTS model is described here. The flowchart of the proposed VO-SOTS model is shown in Fig. 8.2.

In the first step (i.e., *Step1*) the SOTS problem is solved considering all lines as candidates for switching purposes. The *ETGC* obtained in this step is denoted by *ETGC1*. However, it may weaken the system due to transmission line switching that results in inevitable load curtailment in some cases. Hence, it is necessary to identify the list of critical transmission lines, i.e., the lines whose switching leads to the largest amount of load curtailment (i.e., maximum *ETLS*), in *Step2*. Then, in *Step3* the SOTS problem is solved again to minimize the *ETGC* by excluding the list of critical lines to reduce the risk of load curtailment in the case of line switching. The *ETGC* obtained in this step is called *ETGC2*. The difference between the *ETGC* values obtained in *Step1* and *Step3* can be defined as the cost of considering grid resilience in the VO-SOTS. This cost is denoted by the expected resilience enhancement cost (*EREC*).

8.6.2 VO-SOTS solution algorithms

In order to examine the optimality of the obtained results by GAMS optimization software, the proposed MINLP optimization model is also solved by the following well-known heuristic algorithms.

8.6.2.1 Genetic Algorithm (GA) [126]

Genetic Algorithm is one of the evolutionary innovation approaches, which is developed by inspiration of Genetic science. In this algorithm, first, the several initial responses are produced to problem, which is called chromosome. Then, the new population is generated by using crossover and mutation functions. Finally, the previous population with new population is being integrated and the best chromosomes are passed into next generation. At the end, the chromosome, which has the high rate of merit, is reported as optimal solution. In this paper, the genes of each chromosome represent the number of lines which are disconnected from the network.

8.6.2.2 Particle Swarm Optimization Algorithm (PSO) [127]

One of the proposed methods in the field of optimization is Particle swarm optimization algorithm. Kennedy and Abrovhaut presents this method for the first time, in 1995. The inspiration source of this algorithm was the social behaviors of animals such as birds, and fishes. In PSO algorithm, each solution is called particle. The movement of particles depends on two factors in this algorithm: personal best and global best. All of the particles have special fitness value, which is obtained from the defined fitness function of different problems. In this paper, the situation of each particle shows that the number of disconnected lines.

8.6.2.3 Imperialist Algorithm (ICA) [128]

Imperialist Competitive algorithm is the method in the area of evolutionary calculation, which comes from mathematical modeling. The political-social evolution deals to find the different optimal solution. In ICA algorithm, the solutions are optimization problem are known as "country." These countries are divided to colony and Imperialist. Every Imperialist dominates some colonies according to its power and controls them. Assimilation, imperialistic competition, and revolution establish the fundamental basis of this algorithm. ICA algorithm is gradually improved the initial countries by using these functions and finally the response of optimal obtains. In this paper, each of components of culture shows the number of disconnected lines.

8.6.2.4 Gravitational Search Algorithm (GSA) [129]

Gravitational Search Algorithm (GSA) is based on the Newtonian laws of gravity and mass interaction. In this algorithm, agents are taken into consideration as objects and their performances are measured by their masses. Every object represents a solution or a part of a solution to the problem. All these objects attract each other by the gravity force, and this force causes a global movement of all objects towards the objects with heavier masses. In this paper, each of components of masses shows the number of disconnected lines.

8.6.2.5 Crow search algorithm (CSA) [130]

A new metaheuristic algorithm called the crow search algorithm (CSA) Recently was proposed. The CSA is similar to the PSO algorithm but is based on the intelligent behavior

of crows. The main concept behind the CSA is that crows store excess food in hiding places and retrieve it when needed. The primary advantage of the CSA is that it is, having just two parameters. In this paper, the situation of each crows reveals the number of disconnected lines. Rather than simplicity, due to the lower parameters (i.e. just two: flight length and awareness probability), it has higher fitness values and also it describes good optimal solution to the problem.

8.6.2.6 GAMS solver

The propose model is handled by KNITRO solver due to its good performance in large scale optimization problems [131]. The algorithms setting parameters are presented in Table 8.3. The proposed algorithms flowchart for solving the S-OTS problem is shown in Fig. 8.2.

Table 8. 3. Setting parameters of different algorithms

Algorithm	Parameters
GA	Max iteration=200, Number of population=200, Crossover=80%, Mutation =20%
PSO	Max iteration =200, Number of particles=200, Personal reasoning coefficient = 2, Global reasoning coefficient=2, Inertia weight= 0.7, Inertia weight camping rate=0.9
ICA	Max iteration =200, Number of initial country =200, Number of example=10, Revolution rate=0.1, Zeta=0.1
GSA	Max iteration =200, Number of population (mass)=120, Initial gravitational constant (G_0)=1,
CSA	Max iteration =200, Number of crows =120, Flight length *fl*=2, Awareness probability *AP*=0.1
All algorithms	Number of trial runs= 100
GAMS	MINLP formulation, KNITRO solver

8.6.3 Load curtailment modeling via heuristic algorithms

To model load shedding using the heuristic algorithms, the fictitious generator concept [132] is applied as follows:

1. A fictitious generator is added to all the buses with non-zero loads.
2. The amount of $P_i^{G,max} / Q_i^{G,max}$ for each fictitious generator is considered equal to the active/reactive power load which is connected to that bus ($P_{i,s}^D / Q_{i,s}^D$).
3. The amount of $P_i^{G,min} / Q_i^{G,min}$ for all fictitious generators is considered zero.
4. Large values for cost function coefficients are selected for fictitious generators so load shedding will be the last possible solution of *ETLS/ETGC*.

To calculate the amount of load shedding and generation cost for a particular combination (in any of the algorithms), an AC-OPF is first applied. If the problem does not converge, a DC-OPF is then applied.

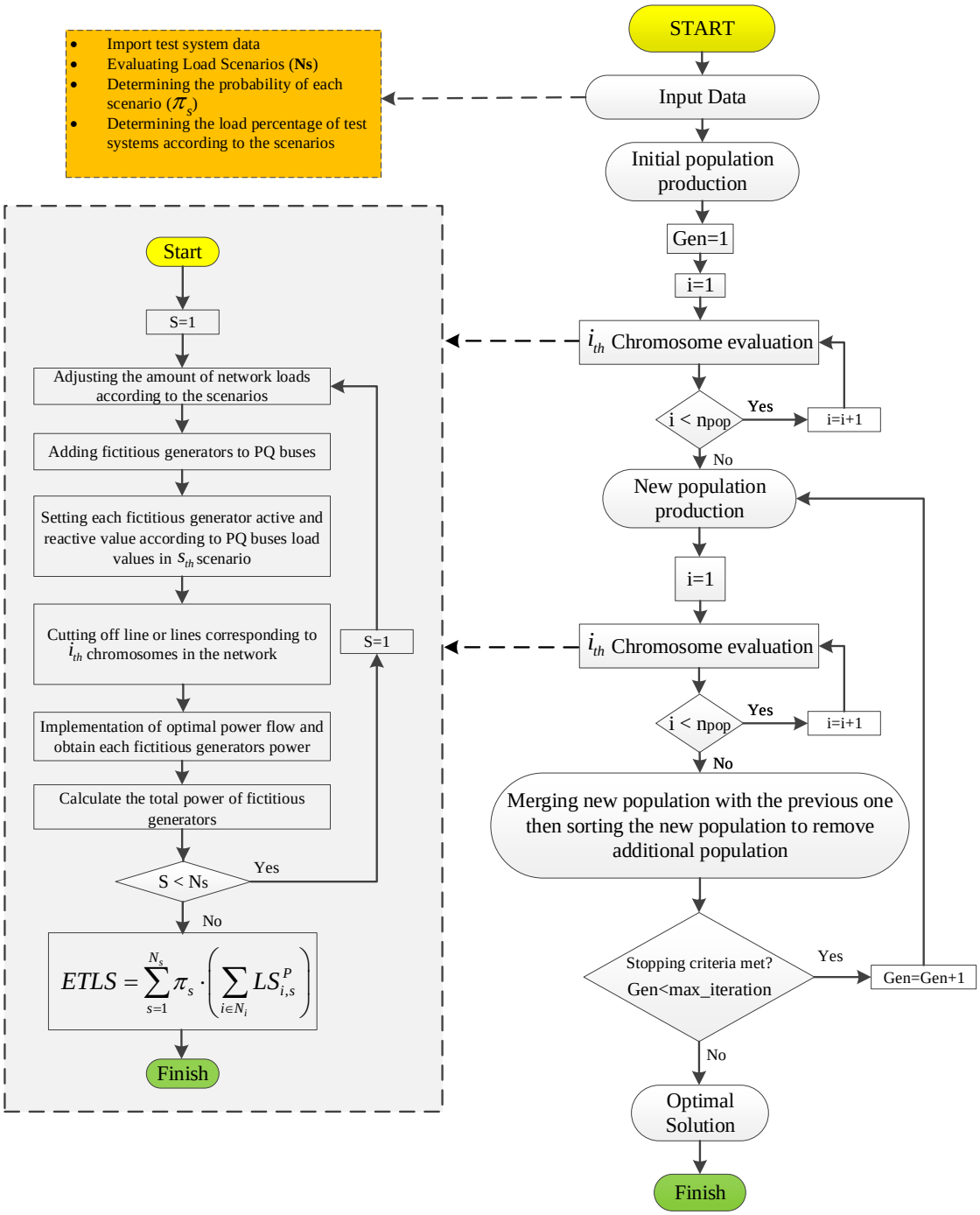

Figure 8. 2. Flowchart of the proposed algorithm

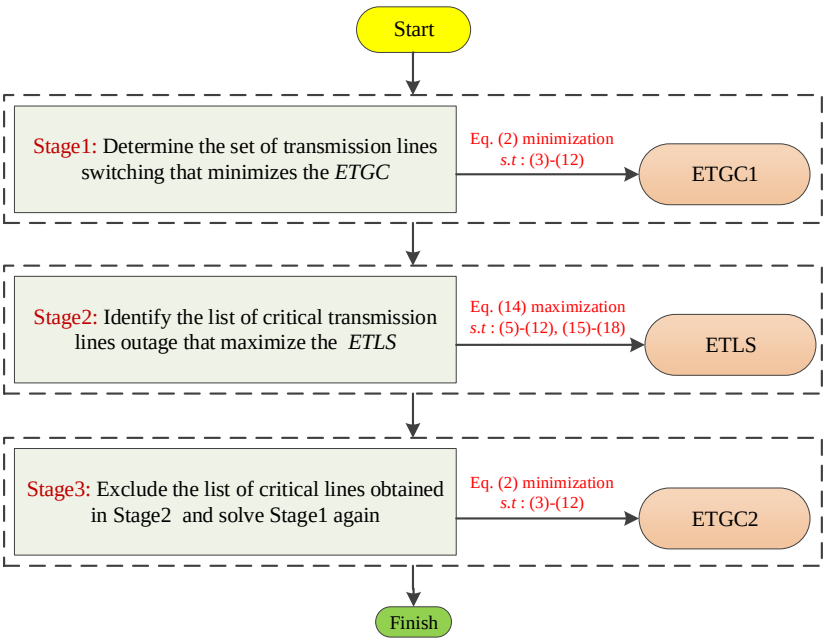

Figure 8. 3. The proposed three-stage VO-SOTS procedure

8.7 Case study and numerical results

8.7.1 Assumptions

Simulations are carried out on the standard IEEE 39-, IEEE 118-, and IEEE 2869-bus test systems, which are named Case I, Case II, and Case III, respectively. The proposed VO-SOTS model is implemented in MATLAB and GAMS environments and solved by heuristic algorithms and commercial solvers (as described in Section III), respectively. In each case, the proposed VO-SOTS problem is solved in five modes, namely VO-SOTS with 1, 2, 3, 4, and 5 lines switching.

8.7.2 Case-I: IEEE 39-bus system

In this section, the proposed VO-SOTS model is implemented on the IEEE 39-bus test system. The single-line diagram of this system is depicted in Fig. 8.4. First, to clearly illustrate the effectiveness of the proposed method, a comparison among the results of deterministic OTS (DOTS) optimization (ignoring the uncertainty in input parameter), SOTS, and MCS-based OTS is performed in Table 8.4. In the MCS method, 10,000 random iterations are performed to consider the stochastic behavior of loads. The results given in this

table show that, when the problem is solved considering load uncertainties, the total generation cost increased about 9%, but it is more realistic. Moreover, it is inferred from this table that the results obtained from the SOTS and MCS-OTS are very close. This means that the SOTS is an accurate method for dealing with such a probabilistic model. However, the number of runs and execution time of SOTS are much less than for MCS-OTS. Therefore, with a reasonable approximation for both objective function values, the performance of SOTS is desired in the probabilistic VO-SOTS problem.

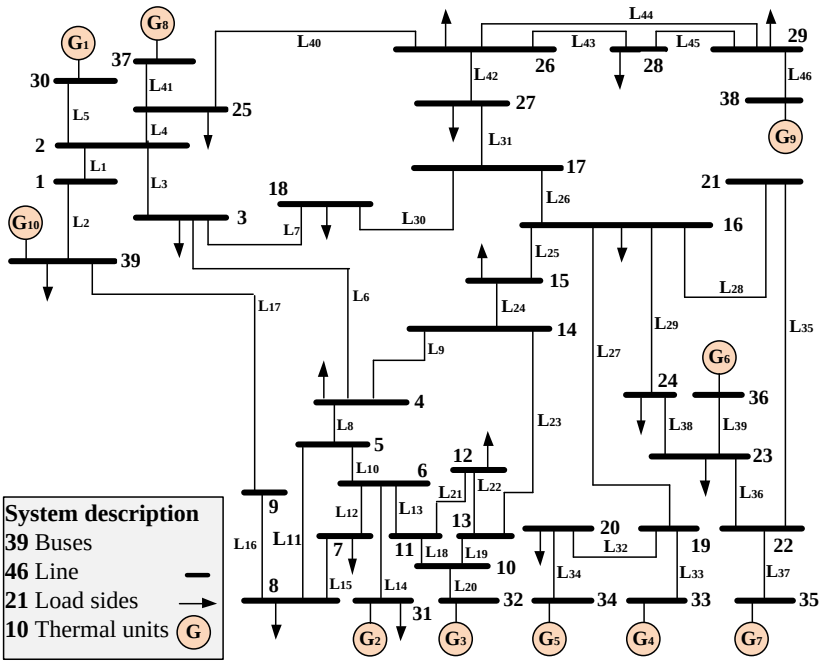

Figure 8. 4. Single-line diagram of IEEE 39-bus test system

Table 8. 4. Comparison between the results of VO-DOTS and VO-SOTS on the IEEE 39-bus system

		# of lines switching				
		#1	#2	#3	#4	#5
DOTS	*TGC* (k$)	33.23	31.06	29.85	28.02	27.05
SOTS	*ETGC* (k$)	36.85	34.45	33.11	31.07	30.01
MCS-OTS	*ETGC* (k$)	36.81	34.37	32.89	30.78	29.9

Table 8.5 gives the optimal results obtained by applying the first step (i.e., Step1) of the proposed SOTS model on this system. Without any switching, the *ETGC* equals k$41.86. According to Table 8.5, the KNITRO solver in GAMS clearly outperforms the heuristic algorithms in terms of the obtained *ETGC* when the number of permissible lines for switching increases. Among the heuristic algorithms, the CSA algorithm performs the best.

Based on the aforementioned procedure for VO-SOTS, the next step (i.e., *Step2*) is to determine the critical transmission lines. The outage of these lines will result in the maximum amount of *ETLS*. The list of these lines is given in Table 8.6 for this system. Tables 8.6 and 8.7 indicate some lines are common to both steps. This means it is necessary to exclude the critical lines that result in considerable *ETLS* to minimize the *ETGC*. Accordingly, minimization of the *ETGC* will be compromised.

Table 8. 5. VO-SOTS implementation on the IEEE 39-bus system (*ETGC minimization*)

#lines switching	Algorithm#	Removed line(s)	*ETGC* (k$)
1 line	All	L_{32}	36.85
2 lines	All	L_{24}, L_{26}	34.45
3 lines	GA, PSO and ICA	L_2, L_{17}, L_{32}	34.03
	GSA	L_7, L_{24}, L_{42}	33.76
	CSA	L_6, L_{17}, L_{26}	33.38
	GAMS	L_{16}, L_{24}, L_{26}	33.11
4 lines	GA, PSO and ICA	L_2, L_{11}, L_{12}, L_{44}	32.51
	GSA	L_{24}, L_{25}, L_{30}, L_{40}	32.51
	CSA	L_7, L_{24}, L_{25}, L_{40}	31.07
	GAMS	L_7, L_{24}, L_{33}, L_{40}	31.07
5 lines	GA, PSO, ICA and GSA	L_7, L_{24}, L_{25}, L_{38}, L_{40}	30.68
	CSA	L_7, L_{24}, L_{39}, L_{40}, L_{42}	30.68
	GAMS	L_1, L_{17}, L_{24}, L_{26}, L_{45}	30.01

Table 8.7 shows the results of *ETGC* minimization in two cases: without considering *ETLS* and excluding the removed lines in *ETLS* maximization (i.e., *Step3*). The *ETGC* is not reduced to its optimal value given in Table 8.5 and a new compromise solution is obtained. For example, in the case of four lines switching the *ETGC* increases from k$31.07 to k$33.36, which represents a 7.4% increase, but the new set of lines does not cause maximum load shedding. In Fig. 8.5, the *ETGC* is compared for different numbers of line outages, with and

without considering the impact of excluding the critical lines. As noted above, this difference in the *ETGC* values can be regarded as the cost of considering grid resilience in the proposed VO-SOTS problem, denoted *EREC* in Fig. 8.5. By increasing the number of lines switching, the *EREC* increases from k$0 for one line switching to k$2.58 for five lines switching, representing an increase of 8.6% in the *ETGC*.

Table 8. 6. Critical lines in IEEE 39-bus system

#lines outage	Algorithm#	Removed line(s)	*ETLS* (MW)
1 line	All	L_{27}	140.78
2 lines	All	L_{24}, L_{26}	431.82
3 lines	GA	L_7, L_{24}, L_{40}	645.32
	PSO	L_7, L_{24}, L_{40}	645.32
	ICA	L_7, L_{24}, L_{40}	645.32
	GSA	L_{24}, L_{30}, L_{40}	613.72
	CSA	L_7, L_{24}, L_{40}	645.32
	GAMS	L_7, L_{24}, L_{40}	645.32
4 lines	GA	L_7, L_{21}, L_{24}, L_{40}	645.32
	PSO	L_7, L_{21}, L_{24}, L_{40}	645.32
	ICA	L_7, L_{21}, L_{24}, L_{40}	645.32
	GSA	L_7, L_{21}, L_{24}, L_{40}	645.32
	CSA	L_{20}, L_{25}, L_{26}, L_{46}	661.18
	GAMS	L_{20}, L_{25}, L_{30}, L_{40}	730.3
5 lines	GA	L_6, L_{17}, L_{23}, L_{26}, L_{27}	773.58
	PSO	L_6, L_{17}, L_{23}, L_{26}, L_{27}	773.58
	ICA	L_6, L_{17}, L_{23}, L_{26}, L_{27}	773.58
	GSA	L_6, L_{17}, L_{23}, L_{26}, L_{27}	773.58
	CSA	L_3, L_{16}, L_{20}, L_{27}, L_{42}	871.42
	GAMS	L_6, L_{17}, L_{20}, L_{26}, L_{27}	871.44

Table 8. 7. ETGC with/without considering ETLS impact in IEEE39-bus system

#lines switching	Removed lines		*ETGC* (k$)	
	WO	W	WO	W
0 line	-	-	41.86	41.86
1 line	L_{32}	L_{32}	36.85	36.85
2 lines	L_{24}, L_{26}	L_1, L_{16}	34.45	35.11
3 lines	L_6, L_{17}, L_{26}	L_6, L_{17}, L_{26}	33.11	34.48
4 lines	L_7, L_{24}, L_{33}, L_{40}	L_2, L_{11}, L_{12}, L_{44}	31.07	33.36
5 lines	L_1, L_{17}, L_{24}, L_{26}, L_{45}	L_7, L_{24}, L_{39}, L_{40}, L_{42}	30.01	32.59

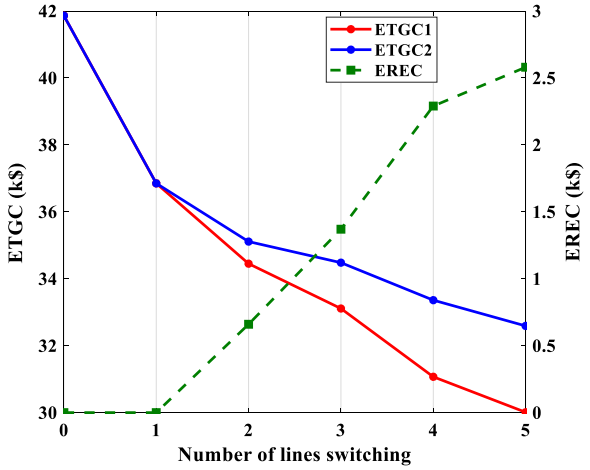

Figure 8. 5. ETGC with/without considering ETLS impact in IEEE39-bus (k$)

Also, it is inferred from this figure that in both cases (i.e., with and without considering critical lines) the *ETGC* decreases from its base value of *k$41.86*; this substantiates the capability of OTS for reducing system operation costs, even in the case when critical lines are excluded for *ETGC* minimization. The *ETGC1* and *ETLS* values in different scenarios are compared in Fig. 8.6 for the GAMS solution. It is observed from this figure that, for this system, by increasing demand, the *ETGC* and *ETLS* values both increase.

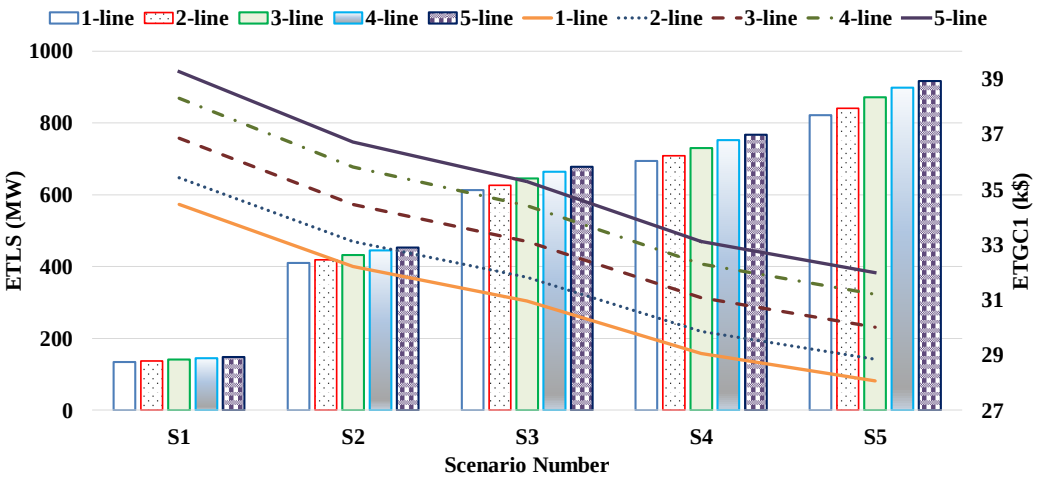

Figure 8. 6. Comparison between *ETGC1 and ETLS* values for each scenario using GAMS solutions

8.7.3 Case-II: IEEE 118-bus system

This part presents the VO-SOTS results for the IEEE 118-bus test system. The values of *ETGC* and *ETLS* for loss of each candidate line(s) are given in Tables 8.8 and 8.9. Also these amounts for different scnearios are depicted in Figure 8.7 and 8.8. These tables and figures demonstrate that switching some candidate lines presented in Tables 8.8 and 8.9 could jeopardize the security of the system. Similar to the IEEE-39 test system, the results obtained by GAMS are better than for the other algorithms. Similar to *Case I*, the optimal values for the *ETGC* with and without considering *ETLS* impact are given in Table 8.10.

Table 8. 8. SOTS implementation on the IEEE 118-bus system (ETGC minimization)

#lines switching	Algorithm#	Removed line(s) (from bus-to bus)	*ETGC* (k$)
1 line	All	(68-116)	122.73
2 lines	All	(68-116), (12-117)	122.43
3 lines	GA, PSO, ICA and GSA	(14-15), (12-16), (68-116)	122.733
	CSA	(19-34), (77-82), (68-116)	122.731
	GAMS	(62-67), (71-73), (68-116)	121.78
4 lines	GA, PSO, ICA, GSA and CSA	(81-80), (85-86), (92-94), (68-116)	122.01
	GAMS	(70-71), (85-88), (88-89), (68-116)	121.01
5 lines	GA	(16-17), (54-55), (82-96), (94-96), (68-116)	122.75
	PSO	(54-55), (51-58), (60-61), (24-70), (68-116)	122.79
	ICA	(11-13), (62-66), (85-86), (86-87), (68-116)	122.03
	GSA	(15-19), (65-66), (76-77), (68-116), (12-117)	121.97
	CSA	(19-20), (59-61), (65-66), (85-86), (68-116)	121.95
	GAMS	(23-32), (63-64), (110-112), (32-114), (68-116)	120.31

Table 8. 9. Critical lines in IEEE118-bus system

#lines outage	Algorithm#	Removed line(s) (from bus-to bus)	*ETLS* (MW)
1 line	All	(68-116)	184
2 lines	All	(110-112), (68-116)	252
3 lines	GA, PSO, ICA and GSA	(5-6), (7-12), (68-116)	255
	CSA and GAMS	(77-78), (79-80), (68-116)	294
4 lines	GA, PSO, ICA and GSA	(22-23), (85-86), (110-112), (68-116)	273
	CSA	(60-61), (77-78), (79-80), (68-116)	294
	GAMS	(77-78), (79-80), (110-112), (68-116)	362
5 lines	GA	(23-32), (55-56), (62-67), (110-112), (68-116)	252
	PSO, ICA	(30-17), (26-30), (77-78), (78-79), (68-116)	255
	GSA	(25-27), (30-38), (77-78), (79-80), (68-116)	294
	CSA	(11-13), (13-15), (85-86), (110-112), (68-116)	362
	GAMS	(77-78), (79-80), (83-85), (110-112), (68-116)	402

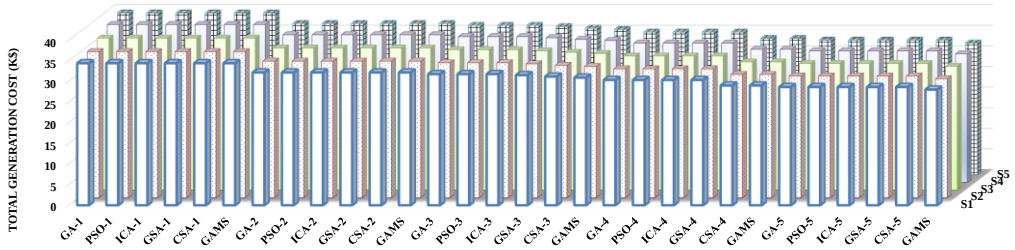

Figure 8. 7. Comparison between different algorithms ETGC in each scenario (k$)

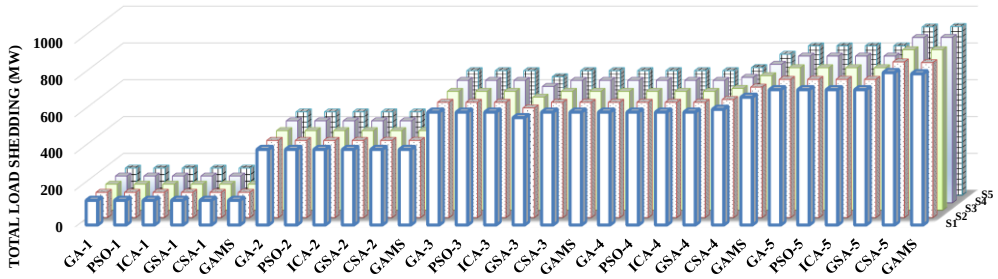

Figure 8. 8. Comparison between different algorithms ETLS in each scenario (MW)

Table 8. 10. ETGC with/without considering ETLS impact in IEEE118-bus system

#lines switching		*ETGC* (k$)	Removed line(s) (from bus-to bus)
0		129.66	
#1	wo	122.73	(68-116)
	w	123.85	(12-117)
#2	wo	122.43	(68-116), (12-117)
	w	123.11	(108-109), (110-112)
#3	wo	121.78	(62-67), (71-73), (68-116)
	w	122.89	(7-12), (35-36), (110-112)
#4	wo	121.01	(70-71), (85-88), (88-89), (68-116)
	w	122.49	(3-12), (34-43), (45-46), (71-73)
#5	wo	120.31	(23-32), (63-64), (110-112), (32-114), (68-116)
	w	121.63	(43-44), (45-46), (45-49), (62-67), (89-90)

wo/w: Without/with considering ETLS

By excluding the most critical lines, the *ETGC* increases. The *ETGC* value with and without considering *ETLS* is indicated in Fig. 8.9 along with the *EREC* for each permissible number of lines switching.

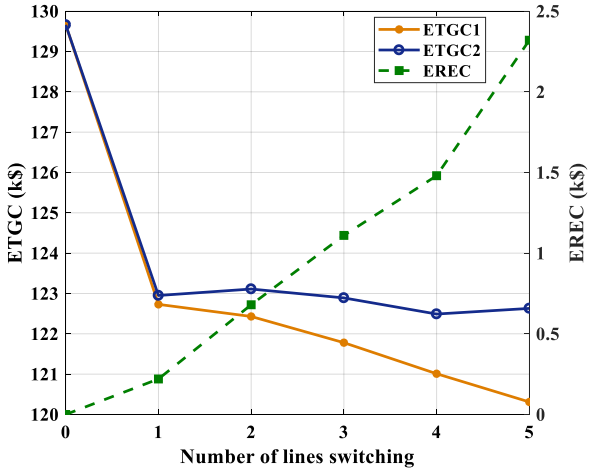

Figure 8. 9. ETGC with/without considering ETLS impact in IEEE118-bus

8.7.4 Case-III: IEEE 300-bus system

The ranking list of SOTS program for disconnecting of one to five lines in both *ETLS* and *ETGC* have been shown in Fig. 8.9 and Fig. 8.10. The most critical lines of this test system based on GAMS results which are better than others are: For *ETLS*: 1-line switching: L307, 2-lines switching: L307-L_{316}, 3-lines switching: L_{208}-L_{307}-L_{316}, 4-lines switching: L_{307}-L_{311}-L_{316}-L_{342}, 5-lines switching: L_{157}-L_{232}-L_{301}-L_{303}-L_{304}.

For *ETGC*: 1-line switching: L_{307}, 2-lines switching: L208-L_{307}, 3-lines switching: L_{79}-L_{303}-L_{310}.

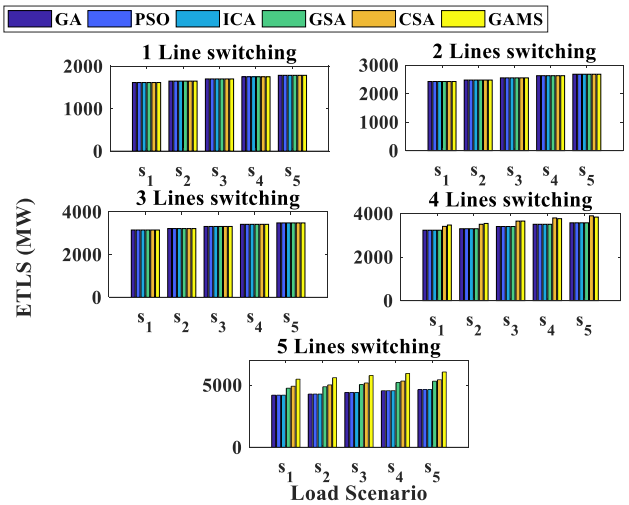

Figure 8. 10. Comparison between different algorithms *ETLS* in all scenarios (MW)

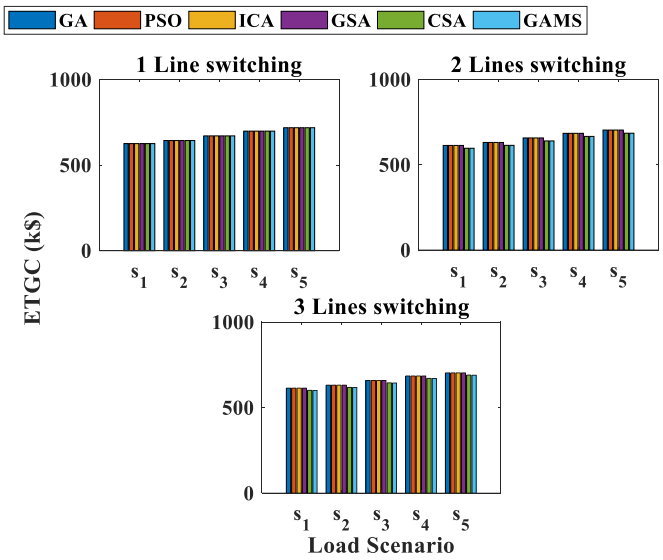

Figure 8. 11. Comparison between different algorithms *ETGC* in all scenarios (k$)

8.7.5 Case-III: IEEE 2869-bus system

For the sake of brevity, the problem is solved in this system (which is a portion of the European transmission system) for 1, 2, and 3 lines switching only. Fig. 8.12 shows the *ETGC1*, *ETGC2*, and corresponding *EREC* values for this system.

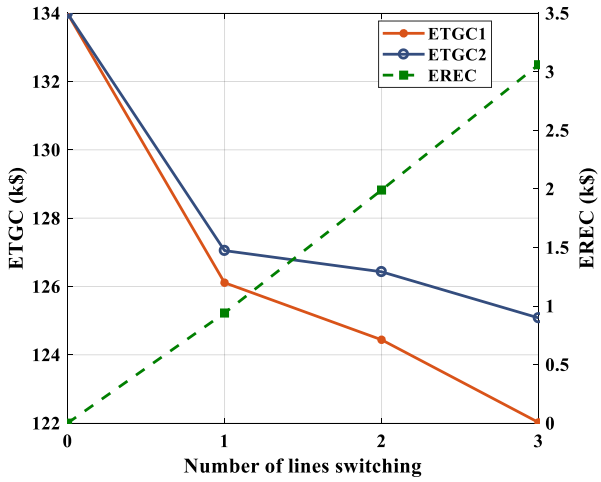

Figure 8. 12. ETGC with/without considering ETLS impact in IEEE2869-bus (k$)

8.7.6 Algorithms performance

Table 8.11 compares the performance of the proposed optimization methods for different test systems and cases (for all lines switching). In all cases, GAMS is faster than the other metaheuristic algorithms. As shown for Case III, the proposed method is capable of generating optimal results for the IEEE-2869 bus test system within approximately 28 hours. All test cases were carried out on a laptop with an Intel core i7 2.70 GHz CPU and 16 GB internal memory (RAM).

Table 8. 11. Comparison of proposed method performance in different cases

Case #			GA	PSO	ICA	GSA	CSA	GAMS
#1	*ETLS*	C_{pu}	232	259	249	250	221	165
		N	200×100					52
	ETGC	C_{pu}	224	267	254	261	234	184
		N	200×100					68
#2	*ETLS*	C_{pu}	452	487	478	480	442	210
		N	200×100					80
	ETGC	C_{pu}	446	480	470	475	433	220
		N	200×100					82
#3	*ETLS*	C_{pu}	1985	2010	2008	2213	1854	1542
		N	200×100					287
	ETGC	C_{pu}						1678
		N						298

Cpu: CPU-time (minute)
N: Number of iterations
200×100: 200 iteration of algorithm×100 trial runs

8.7.7 Value of Stochastic Solution

This section shows that it is necessary to consider a stochastic model for VO-SOTS, when severe uncertainties such as demand are mattered. To estimate the validity of stochastic formulation, value of stochastic solution (VSS) index [24] is evaluated here. VSS index is defined as follows:

$$VSS = EEV - SS \tag{8-21}$$

where EEV is the expected outcome of using the expected value [24]. For calculating the EEV, the uncertain parameters (i.e., load) are substituted with the corresponding expected values (mean values of different scenarios) and the resulting deterministic VO-SOTS problem is solved. The objective function value obtained in this case is named as the EVP solution. Then, stochastic variables are fixed with the corresponding value obtained from the

EVP solution. SS in (8-21) is the stochastic solution (SS), which is obtained by solving the original VO-SOTS problem considering all scenarios. The VSS for Case I (i.e., theIEEE-39 bus system) is calculated using the results given in Table 8.12. For example, in the case of one-line switching, the VSS for EPGC1 is 13.81 k$. The value obtained for the VSS indicates the extra cost using a purely deterministic model instead of the stochastic model. This substantiates the effectiveness of the stochastic framework for dealing with the VO-SOTS problem.

Table 8. 12. Values of EVP, SS and EEV for calculation of VSS, in Case I

# of lines switching	EVP (k$)	SS (k$)	EEV (k$)
1 line	36.85	36.85	50.66
2 line	34.45	34.45	46.71
3 line	33.11	33.11	45.11
4 line	31.07	31.07	41.89
5 line	30.01	30.01	41.08

8.8 Vulnerability Analysis

Based on the literature, different indices are used for static vulnerability assessment. In this paper, the Vulnerability Index (VI) [75] is used to specify the safety allowance factor of the whole power system under static conditions. The VI is defined as the inverse distance from the current operating point to security violation/boundary. It thus measures the lack of "head-room" (or reserve) in generation (from current generation to maximum) or transmission lines (from current loading to thermal rating). In this paper, the expected total VI (*ETVI*) is the sum of the aggregate generation and line VI. The larger the VI value, the more vulnerable the system. While (8-22) and (8-23) deal with individual units of equipment, the aggregate generation and line VI is given by (8-24):

$$VI_G = 1/2\left(P_{i,s}^{G} / P_{i,s}^{G,\max}\right)^2 \quad ;\forall i \in N_G \ , \ \forall s \in N_S \tag{8-22}$$

$$VI_\ell = 1/2\left(S_{\ell,s} / S_\ell^{\max}\right)^2 \ with \ S_{\ell,s}^2 = P_{\ell,s}^2 + Q_{\ell,s}^2 \ ; \ \forall \ell \in N_L, \ \forall s \in N_S \tag{8-23}$$

$$ETVI = ETVI_G + ETVI_\ell = \sum_{s=1}^{N_S} \pi_s \left(\sum_{i=1}^{N_G} VI_G + \sum_{i=1}^{N_L} VI_\ell \right) \tag{8-24}$$

Table 8.13 shows that the *ETVI* value for different cases increases with line switching but decreases considering the total load shedding impact.

Table 8. 13. Values of EVP, SS and EEV for calculation of VSS, in Case I

Case #		# of lines switching				
		1	2	3	4	5
Case I	A	12.23				
	B	12.43	12.51	12.55	12.6	12.68
	C	11.79	11.72	11.57	11.5	11.4
Case II	A	45.28				
	B	46.79	48.11	48.85	49.58	49.97
	C	41.34	40.75	40.09	39.78	38.98
Case III	A	141.22				
	B	142.57	143.94	145.4	146.32	147.06
	C	137.36	136.02	134.94	132.99	130.94

A: TVI value in base case
B: TVI value in Step1 (without ETLS impact)
C: TVI value in Step3 (with ETLS impact

For example, in the case of one line switching in Case I, the *ETVI* increases from 12.23 to 12.46 (with OTS dispatch) and decreases from 12.23 to 11.79 (with OTS dispatch + *TLS* consideration), which represents a 1.88% increase and 3.6% decrease, respectively. This shows that, with OTS, the lines and generators are more loaded; however, using *TLS* reduces the vulnerability of the system compared to basic OTS.

8.9 Conclusion

Optimal transmission switching (OTS) as a new method for reduction of operation costs is considered from a security point of view. To preserve the security of power transmission systems against attacks or natural disasters such as hurricanes and outages, a vulnerability-oriented SOTS (VO-SOTS) problem is introduced in this paper that considers load uncertainty via a scenario-based approach. The proposed three-step VO-SOTS minimizes the expected total generation costs (*ETGC*) while considering: 1) the possibility of switching for all lines and 2) excluding the set of critical transmission lines whose switching leads to the maximum load curtailment. The results obtained for different test systems substantiate the capability of the proposed VO-SOTS model for reduction of power generation costs, even when excluding critical lines for *ETGC* minimization. Contrary to the existing cost-oriented OTS approaches, the proposed VO-SOTS is also capable of reducing the risk of power system vulnerability.

Conclusions et travaux futures

Résumé

Cette thèse porte sur la modélisation des systèmes de transmission et de distribution intégrés (T&D) et leurs interactions, avec la possibilité d'incorporer des opérations de T&D avancées telles que le contrôle / la coordination de la tension, la répartition optimale des RED, ainsi que le fonctionnement et le contrôle en temps réel du système de distribution. Un logiciel prototype basé sur MATLAB, OpenDSS et GAMS a été développé. Dans les chapitres 1 à 8, nous présentons différents aspects de recherche couverts dans cette thèse. Dans les paragraphes suivants, un résumé de chaque chapitre est donné.

Dans le premier chapitre, nous avons présenté le contexte et les problèmes abordés par cette recherche. Nous avons expliqué que la plupart des études d'interconnexion RED existantes évaluent les défis d'intégration des pénétrations à taux élevé de RED, que ce soit au niveau de la distribution ou sur un système T&D découplé. Les impacts potentiels sur le réseau de transport sont soit ignorés compte tenu du faible taux de pénétration des RED, soit non représentatifs en raison du modèle découplé T&D. Les projets de déploiement de RED à grande échelle, en cours et futurs, pourraient potentiellement affecter les opérations du réseau de transport régional. Selon toutes ces limitations, le problème spécifique de cette thèse est présenté comme suit:

• Absence de plate-forme unifiée pour les systèmes intégrés de transport et de distribution.

Pour aborder le problème de la recherche et proposer et mettre en œuvre un cadre d'évaluation de l'accessibilité pour les systèmes de T&D intégrés prenant en compte différents facteurs, nous avons ciblé la réalisation des objectifs spécifiques suivants: 1) Élaborer des stratégies pour permettre aux consommateurs de participer à l’atténuation des problèmes liés aux réseaux de distribution en maximisant l’utilité du système BESS distribué, 2) Fournir un cadre de gestion pour l'intégration des RED (WT, BESS et PV) à T&D, y compris la nature stochastique de l'énergie éolienne et l'analyse de l'incertitude imposée via une approche basée sur des scénarios, 3) Planification optimale du BESS dans T&D pour maximiser la marge de chargement (LM) du système en présence de vent ou d’énergie, compte tenu de sa nature

stochastique, 4) Utiliser GAMS pour la distribution et MATLAB pour modéliser le réseau de transport afin de résoudre le flux de charge T&D intégré avec la méthode itérative, 5) Evaluation de la vulnérabilité dans les systèmes intégrés de T&D, 6) Utiliser OpenDSS pour la distribution et MATLAB pour modéliser le réseau de transmission à travers une interface Python afin d'étudier l'application de l'optimisation de la T&D intégrée, 7) Induire l'OTS d'un point de vue de vulnérabilité.

Dans le chapitre 1, nous avons fourni une revue de la littérature sur les sujets liés au contexte de cette thèse. Ce chapitre a permis de présenter les fondements théoriques en lien avec la recherche réalisée dans cette thèse. La revue de la littérature nous a aidé à identifier les problèmes de recherche et réviser les méthodes existantes. Cela nous a permis d'approfondir notre compréhension de ces méthodes et identifier les limites et les avantages de ces méthodes pour motiver notre recherche dans les chapitres subséquents.

Contribution de la thèse

Dans le chapitre 2, pour atteindre le premier objectif de la thèse, nous nous concentrons sur l'étude des impacts des fortes pénétrations de ressources énergétiques distribuées jumelées avec des BESS décentralisés. L'approche d'optimisation proposée prend en compte les fonctions objectives suivantes : 1) pertes de puissance réelles, 2) déviation de tension sur les bus de charge et 3) marge de chargement du système.

Au chapitre 3, un cadre efficace est proposé pour comprendre de manière transparente les interactions de transmission et de distribution (T&D) tout en incluant des modèles détaillés pour les ressources d'énergie distribuées (RED). L'éolien, le photovoltaïque et la demande sont étudiés en fonction de leur profil 24h. En outre, l'incertitude de l'éolien est prise en compte via la méthode du scénario. Enfin, les systèmes de stockage d'énergie par batterie (BESS) sont utilisés pour suivre la production probabiliste renouvelable et minimiser les pertes de puissance totales du système.

Au chapitre 4, un nouveau problème d'allocation optimale des BESS décentralisés pour améliorer la sécurité de tension est proposé dans les systèmes intégrés de transport et de distribution (T&D) tout en incluant des modèles réalistes de ressources énergétiques

distribuées. Le problème de planification est étudié dans un cadre stochastique en considérant l'incertitude de l'énergie éolienne. En outre, les profils horaires de charge ainsi que les SER éoliens et photovoltaïques sont pris en compte. Maximiser la marge de chargement avec la meilleure allocation des différents types de BESS est l'objectif principal du chapitre. De plus, l'impact de l'allocation sur l'écart de tension des bus de charge est étudié.

Au chapitre 5, on propose une plate-forme intégrée de co-simulation pour la transmission et la distribution (T&D) utilisant les outils GAMS et MATLAB (appelés IC-GAMA). Le cadre proposé peut résoudre la répartition de puissance des systèmes de distribution en co-simulation avec le réseau de transport, aussi bien dans des modèles détaillés que pour offrir une solution aux exploitants de systèmes indépendants et aux divisions de planification de systèmes d'énergie. Un cadre itératif est développé pour modéliser les interactions entre les systèmes de T&D. Les solutions du système de transmission, tension et angle PCC, et les solutions du système de distribution, puissances active et réactive du PCC, sont échangées entre les deux systèmes au PCC. Cinq stratégies sont proposées pour modéliser ces échanges et simulées sur des points de repère IEEE. Les résultats de la simulation montrent que, lorsque le processus itératif commence à partir d'un flux d'énergie total du côté de la distribution, le cadre T&D proposé présente une meilleure convergence et est plus robuste aux erreurs de suppositions initiales.

Au chapitre 6, la littérature récente sur l'évaluation de la vulnérabilité en régime permanent (SSVA) et l'évaluation dynamique de la vulnérabilité (DVA) est classée et passée en revue. Après avoir découvert les lacunes de la recherche découlant de la revue de la littérature actuelle, plusieurs idées systématiques sont présentées en termes de conception d'un cadre modulaire avec des indices unifiés pour déterminer les zones vulnérables du système, d'évaluation intégrée de la vulnérabilité du système T&D et de la vulnérabilité des PMU aux cyberattaques.

Au chapitre 7, nous avons proposé une nouvelle plate-forme intégrée de co-simulation de transmission et de distribution dans laquelle les charges agrégées dans le simulateur de système de transmission (MATLAB) sont remplacées par un réseau de distribution modélisé dans un simulateur de système de distribution (OpenDSS) via une interface Python.

L'efficacité globale du système T&D est ensuite optimisée tout en maximisant la marge de chargement (LM) et en minimisant les pertes de puissance totales du système, sont considérées comme deux fonctions objectives. L'approche proposée est appliquée à un réseau T&D construit avec 68 nœuds et les résultats démontrent que l'efficacité du réseau T&D peut être améliorée en définissant de manière optimale les variables de contrôle.

Dans le dernier chapitre, les auteurs ont introduit un problème OTS stochastique orienté sur de vulnérabilité (VO-SOTS). Le VO-SOTS en trois étapes proposé minimise les coûts totaux de production attendus (ETGC) tout en considérant : 1) la possibilité de commutation pour toutes les lignes, 2) à l'exclusion de l'ensemble des lignes de transmission critiques que leur commutation entraîne la réduction de la charge maximale. Ce travail fournit une voie utile pour l'adoption des STOS introduisant le système de pénalité de résilience d'origine. De plus, la validation des résultats sur les grands systèmes et avec 5 schémas d'optimisation méta-heuristiques, en plus d'une évaluation détaillée du temps CPU, a démontré un cadre complet pour l'analyse de SOTS.

Conclusions

Avec la tendance croissante des nouvelles technologies émergentes dans les réseaux de distribution, tels que les éoliennes, les panneaux solaires, les véhicules électriques et les générations distribuées, les systèmes de distribution passifs peuvent devenir « actifs » et donc la nécessité d'étudier simultanément le transport et la distribution intégrés (T&D).) et les interactions bilatérales correspondantes ne peuvent plus être négligés. En tant que solution, les chercheurs associent de plus en plus de simulateurs pour former un « nouveau travail de simulation parallèle pour les systèmes T&D intégrés ». Dans cette étude, l’objectif général était de développer une plate-forme T&D intégrée efficace pour répondre à plusieurs objectifs. Cela se fait en identifiant les modèles fondamentaux appropriés, en développant les algorithmes pertinents et en affinant les méthodologies requises pour concevoir un cadre robuste. Toutes les différentes phases de cette recherche ont permis d'atteindre l'objectif général de cette thèse, "concevoir un cadre unifié de recherche et de développement pour étudier les impacts du BESS décentralisé sur celui-ci". Enfin, l'OTS est censé remplacer les schémas de contrôle utilisés dans les études de réseaux T&D intégrés. Les objectifs

spécifiques de cette thèse ont également été atteints et la conclusion de ces objectifs est résumée comme suit.

1. Si le BESS est modélisé sous forme distribuée dans des systèmes T&D intégrés, les pertes de puissance réelles, les écarts de tension et la marge de charge sont meilleurs que dans le cas où le BESS est modélisé sous forme agrégée.

2- Avec l'installation BESS distribuée dans le réseau intégré T&D, l'opérateur du système peut réduire les pertes de puissance du système et augmenter également la capacité de chargement du système. La meilleure réponse est obtenue lorsque tous les paramètres de contrôle sont définis avec leurs valeurs optimisées.

3- Il est démontré que, avec les sources d'énergie renouvelables existantes, les méthodes proposées sont capables de trouver un programme optimal pour maximiser le LM. De plus, la puissance réactive du système de conversion de puissance (PCS), si elle est programmée avec précision, augmente le LM, un gain qui n’a pas été pris en compte auparavant au cours du processus d’optimisation.

4- Dans les systèmes T&D intégrés à partir de la répartitin de puissance complète du système de distribution, les structures de co-simulation offrent de meilleures performances et sont plus résistantes aux erreurs de suppositions initiales.

5- Les résultats obtenus pour différents systèmes IEEE de test de notre implémentation de l’OTS, justifient la capacité du modèle VO-SOTS proposé pour la réduction des coûts de production d'électricité, même dans le cas de l'exclusion des lignes critiques pour la minimisation ETGC.

Discussion et perspectives de la recherche

De nouvelles approches pour la modélisation des interactions T&D sont présentées dans cette thèse, mais il reste encore des lacunes de recherche et des défis d'application qui doivent être étudiés en tant que travaux futurs. Ici, en passant en revue les limites de cette thèse, nous discutons d'abord comment notre méthodologie proposée peut être étendue. Ensuite, nous

discutons des approches potentielles pour résoudre les défis restants et les lacunes de cette thèse.

1. Cette thèse vient d’examiner un cadre pour les réseaux de transport et de distribution et les impacts de la production et des clients n’ont même pas été pris en compte. Dans les travaux futurs, le cadre proposé pourra être étendu aux impacts des couches mentionnées. Les modèles clients peuvent être pris en compte par GridLab-D afin d’inclure tous les détails requis.

2. L'impact des véhicules électriques peut être pris en compte dans les études futures. Un modèle agrégé de véhicules électriques et de panneaux solaires de toit connectés directement aux bus de transmission est considéré pour le problème d'analyse de pénétration. Cependant, dans le monde actuel, les ressources en énergies renouvelables et les véhicules électriques échangent de l'énergie avec le réseau principal au niveau de la distribution et les centrales conventionnelles connectées au niveau du réseau de transport censé maintenir l'équilibre entre production et consommation.

3. L'OTS en tant que moyen de contrôle peut être ajouté à une étude d'allocation optimale de BESS décentralisé, selon une approche stochastique avec contrainte de sécurité de tension (VSC-SOBA) précédemment envisagée, afin de déterminer la "valeur" de l'OTS comme outil pour accroitre la capacité de charge et la sécurité de la tension dans le contexte du système T&D intégré et comparé les résultats avec le papier publié dans IEEE Transaction On Sustainable Energy.

4. Faire un lien entre l’OTS et les REDs augmenterait la cohérence de la thèse. Exemple : est-ce que l’OTS sera plus efficace en présence de REDs? Peut-on combiner l’OTS et le contrôle des REDs en régime permanent pour maximiser les avantages des REDs? Est-ce que l’intermittence du PV et de l’Éolien modifie les résultats concernant le concept proposé pour augmenter la « résilience » du réseau contrôler par l’OTS en présence de REDs?

Principaux codes GAMS mentionnés dans la thèse

```
***********Writtenr by SMMB-IEEE  TSTE-2018*****************************
*******************************Sets ************************************
sets
BusNo              Number of Buses                /B1*B16/
BusNoPQ(BusNo)           /B4*B16/
BusNoG(BusNo)            /B1*B3/
BusNoPV(BusNo)           /B2,B3/
L       Number of transmission lines   /L1*L16/
BusNoStorage(BusNo)              /B10*B16/
BusNoNoStorage(BusNo)             /B1*B9/
t              /t1*t24/
BusNoWnd(BusNo)    The Bus with installed Wind Power           /B12,B14,B16/
BusNoNotWnd(BusNo)   Buses with No Wind            /B1*B11,B13,B15/
S        index senario   /s1*s5/
BusNoPVV(BusNo)    The Bus with installed Wind Power           /B13,B15/
BusNoNotPVV(BusNo)   Buses with No Wind            /B1*B12, B14,B16/
;
*************************************************************************
alias(BusNo,j)
**********************************Tables-Data***************************
table Hin(L,BusNo)     Hin
    B1   B2   B3   B4   B5   B6   B7   B8   B9   B10  B11  B12  B13  B14  B15  B16
L1   1    0    0    0    0    0    0    0    0    0    0    0    0    0    0    0
L2   0    0    0    1    0    0    0    0    0    0    0    0    0    0    0    0
L3   0    0    0    0    1    0    0    0    0    0    0    0    0    0    0    0
L4   0    0    1    0    0    0    0    0    0    0    0    0    0    0    0    0
L5   0    0    0    0    0    1    0    0    0    0    0    0    0    0    0    0
L6   0    0    0    0    0    0    1    0    0    0    0    0    0    0    0    0
L7   0    0    0    0    0    0    0    1    0    0    0    0    0    0    0    0
L8   0    0    0    0    0    0    0    1    0    0    0    0    0    0    0    0
L9   0    0    0    0    0    0    0    0    1    0    0    0    0    0    0    0
L10  0    0    0    0    0    0    1    0    0    0    0    0    0    0    0    0
L11  0    0    0    0    0    0    0    0    0    1    0    0    0    0    0    0
L12  0    0    0    0    0    0    0    0    0    0    1    0    0    0    0    0
L13  0    0    0    0    0    0    0    0    0    0    0    1    0    0    0    0
L14  0    0    0    0    0    0    0    0    0    0    0    0    1    0    0    0
L15  0    0    0    0    0    0    0    0    0    0    0    0    0    1    0    0
L16  0    0    0    0    0    0    0    0    0    0    0    0    0    0    1    0
;
table Hout(L,BusNo)     Hout
    B1   B2   B3   B4   B5   B6   B7   B8   B9   B10  B11  B12  B13  B14  B15  B16
L1   0    0    0    1    0    0    0    0    0    0    0    0    0    0    0    0
L2   0    0    0    0    1    0    0    0    0    0    0    0    0    0    0    0
L3   0    0    0    0    0    1    0    0    0    0    0    0    0    0    0    0
```

```
L4   0   0   0   0   0   1   0   0   0   0   0   0   0   0   0   0
L5   0   0   0   0   0   0   1   0   0   0   0   0   0   0   0   0
L6   0   0   0   0   0   0   0   1   0   0   0   0   0   0   0   0
L7   0   1   0   0   0   0   0   0   0   0   0   0   0   0   0   0
L8   0   0   0   0   0   0   0   0   1   0   0   0   0   0   0   0
L9   0   0   0   1   0   0   0   0   0   0   0   0   0   0   0   0
L10  0   0   0   0   0   0   0   0   0   1   0   0   0   0   0   0
L11  0   0   0   0   0   0   0   0   0   0   1   0   0   0   0   0
L12  0   0   0   0   0   0   0   0   0   0   0   1   0   0   0   0
L13  0   0   0   0   0   0   0   0   0   0   0   0   1   0   0   0
L14  0   0   0   0   0   0   0   0   0   0   0   0   0   1   0   0
L15  0   0   0   0   0   0   0   0   0   0   0   0   0   0   1   0
L16  0   0   0   0   0   0   0   0   0   0   0   0   0   0   0   1
;
table BY(BusNo,j)     imaginary part of Ybus
    B1              B2   B3              B4              B5              B6              B7              B8
B9              B10              B11              B12              B13              B14              B15
B16
B1   -17.3611111111111 0     0                17.3611111111111 0                0                0
0             0             0             0             0             0             0             0             0
B2   0             -16  0             0             0             0             0             16            0
0             0             0             0             0             0             0
B3   0                0    -17.0648464163823 0                0                17.0648464163823 0
0             0             0             0             0             0             0             0             0
B4   17.3611111111111  0    0              -39.47588873     10.5106820518679  0             0
0             11.6040955631399  0             0             0             0             0             0
0
B5   0             0    0              10.5106820518679 -16.09892701      5.58824496236153 0
0             0             0             0             0             0             0             0             0
B6   0                0    17.0648464163823  0                5.58824496236153  -32.43736181
9.78427042636317  0             0             0             0             0             0             0
0             0
B7   0             0    0              0             0              9.78427042636317  -24.36264624
13.6979785969084 0              0.880397220280055  0             0             0             0
0             0
B8   0             16   0             0             0             0             13.6979785969084  -
35.67311313      5.97513453330859  0             0             0             0             0
0             0
B9   0                0    0                11.6040955631399 0                0                0
5.97513453330859 -17.5792301       0             0             0             0             0
0             0
B10  0             0    0              0             0             0             0.880397220280055 0
0             -1.76079444056011  0.880397220280055 0             0             0             0
0
B11  0             0    0              0             0             0             0             0             0
0.880397220280055  -1.76079444056011 0.880397220280055 0             0             0
0
```

B12 0 0 0 0 0 0 0 0 0
0 0.880397220280055 -1.48250330111725 0.602106080837191 0 0
0
B13 0 0 0 0 0 0 0 0 0
0 0 0.602106080837191 -1.20421216167438 0.602106080837191 0
0
B14 0 0 0 0 0 0 0 0 0
0 0 0 0.602106080837191 -1.13576182849433 0.533655747657143
0
B15 0 0 0 0 0 0 0 0 0
0 0 0 0 0.533655747657143 -1.06731149531429
0.533655747657143
B16 0 0 0 0 0 0 0 0 0
0 0 0 0 0 0.533655747657143 -
0.533655747657143
;
table GY(BusNo,j) real part of Ybus
B1 B2 B3 B4 B5 B6 B7 B8 B9
B10 B11 B12 B13 B14 B15 B16
B1 0 0 0 0 0 0 0 0 0 0
0 0 0 0 0 0
B2 0 0 0 0 0 0 0 0 0 0
0 0 0 0 0 0
B3 0 0 0 0 0 0 0 0 0 0
0 0 0 0 0 0
B4 0 0 0 3.30737896202531 -1.94219124871473 0 0 0 -
1.36518771331058 0 0 0 0 0 0 0
B5 0 0 0 -1.94219124871473 3.22420038713884 -1.28200913842411 0 0
0 0 0 0 0 0 0 0 0
B6 0 0 0 0 -1.28200913842411 2.43709661931421 -1.1550874808901 0
0 0 0 0 0 0 0 0 0
B7 0 0 0 0 0 -1.1550874808901 3.071903084 -1.61712247324614
0 -0.299693129803555 0 0 0 0 0
0
B8 0 0 0 0 0 0 -1.61712247324614 2.80472685253728
-1.18760437929115 0 0 0 0 0 0
0
B9 0 0 0 -1.36518771331058 0 0 0 -1.18760437929115
2.55279209260173 0 0 0 0 0 0
0
B10 0 0 0 0 0 0 -0.299693129803555 0 0
0.599386259607111 -0.299693129803555 0 0 0 0 0
B11 0 0 0 0 0 0 0 0 0 -
0.299693129803555 0.599386259607111 -0.299693129803555 0 0 0
0
B12 0 0 0 0 0 0 0 0 0 0
-0.299693129803555 0.683259268654131 -0.383566138850575 0 0 0

```
B13  0    0    0    0              0              0              0              0              0              0
0              -0.383566138850575 0.767132277701151  -0.383566138850575 0              0
B14  0    0    0    0              0              0              0              0              0              0
0              0              -0.383566138850575 1.33800041574937   -0.954434276898794 0
B15  0    0    0    0              0              0              0              0              0              0
0                  0                  0                  -0.954434276898794 1.90886855379759    -
0.954434276898794
B16  0    0    0    0              0              0              0              0              0              0
0              0              0              0              -0.954434276898794 0.954434276898794
;
table LineData(L,*)    Transmission lines data
    BL              GL              B0     G0   Smax
L1   -17.3611111111111  0              0      0    2.5
L2   -10.5106820518679  1.94219124871473  0.079  0    2.5
L3   -5.58824496236153  1.28200913842411  0.179  0    1.5
L4   -17.0648464163823  0              0      0    3
L5   -9.78427042636317  1.1550874808901   0.1045 0    1.5
L6   -13.6979785969084  1.61712247324614  0.0745 0    2.5
L7   -16              0              0      0    2.5
L8   -5.97513453330859  1.18760437929115  0.153  0    2.5
L9   -11.6040955631399  1.36518771331058  0.088  0    2.5
L10  -0.880397220280055 0.299693129803555 0      0    0
L11  -0.880397220280055 0.299693129803555 0      0    0
L12  -0.880397220280055 0.299693129803555 0      0    0
L13  -0.602106080837191 0.383566138850575 0      0    0
L14  -0.602106080837191 0.383566138850575 0      0    0
L15  -0.533655747657143 0.954434276898794 0      0    0
L16  -0.533655747657143 0.954434276898794 0      0    0
;
table BusData(BusNo,*)
    Vmin Vmax Pload Qload
B1   0.9  1.1  0     0
B2   0.9  1.1  0     0
B3   0.9  1.1  0     0
B4   0.9  1.1  0     0
B5   0.9  1.1  0.9   0.3
B6   0.9  1.1  0     0
B7   0.9  1.1  0.92  0.338
B8   0.9  1.1  0     0
B9   0.9  1.1  1.25  0.5
B10  0.9  1.1  0.02  0
B11  0.9  1.1  0.016 0.004
B12  0.9  1.1  0.012 0
B13  0.9  1.1  0.012 0.004
B14  0.9  1.1  0.008 0
B15  0.9  1.1  0.008 0.004
B16  0.9  1.1  0.004 0
```

```
;
table GenData(BusNoG,*)
    Pmin Pmax Qmin  Qmax
B1   0.1  2.5  -3    3
B2   0.1  3    -3    3
B3   0.1  2.7  -3    3
;
$ontext
table GenData(BusNoG,*)
    Pmin  Pmax  Qmin  Qmax
B1   0.1   2.5   -3    3
B2   1.63  1.63  -3    3
B3   0.85  0.85  -3    3
;
$offtext
table InitPoint(BusNoPV,*)
    Qg0                Pg0                Vg0
*B1   0.365644334421315  -0.146055027973465 1
B2   0.0323894634217163 1.63               1
B3   -0.133777803528998 0.85               1
;
****************************Scenario*************************************
table Prof(t,*)
    load wind   Pv
t1   0.53 0.119  0
t2   0.49 0.119  0
t3   0.49 0.119  0
t4   0.52 0.119  0
t5   0.56 0.119  0
t6   0.62 0.061  0
t7   0.7  0.119  0
t8   0.75 0.087  0.008
t9   0.76 0.119  0.15
t10  0.8  0.206  0.301
t11  0.78 0.585  0.418
t12  0.73 0.694  0.478
t13  0.72 0.261  0.956
t14  0.72 0.158  0.842
t15  0.75 0.119  0.315
t16  0.8  0.087  0.169
t17  0.84 0.119  0.022
t18  0.88 0.119  0
t19  0.9  0.0868 0
t20  0.86 0.119  0
t21  0.78 0.0867 0
t22  0.71 0.0867 0
t23  0.64 0.061  0
```

```
t24  0.56 0.041  0
;
table scen(s,*)
        Pw_avl       Prob
s1       0           0.0689
s2       0.1287       0.2044
s3       0.4937       0.4048
s4       0.8683       0.1992
s5       1            0.1227
;
*******************************Wind*************************************
parameter Wind_Cap(BusNoWnd)
/
B12    0.01
B14    0.01
B16    0.01
/;
*******************************PV***********************************
parameter PV_Cap(BusNoPVV)
/
B13   0.005
B15   0.005
/;
parameters w1, w2
;
parameters LM_min ,LM_max ;
*******************************Variables*********************************
variable
   Pw(s,BusNo,t)         Active Power of wind in scenario s
   Qw(s,BusNo,t)         Rective Power of wind in scenario s
   Ppv(s,BusNo,t)        Rective Power of wind in scenario s
   V(s,BusNo,t)          Magnitude of Voltage at Bus i
   Pg(s,BusNo,t)         Generation of Active Power From Bus i
   Qg(s,BusNo,t)         Generation of Rective Power From Bus i
   OF
   th(s,BusNo,t)         Angle of Voltage at Bus i
   Plij(s,L,t)           Active Power flow of line L in time T (direction: i to j)
   Qlij(s,L,t)           Reactive Power flow of line L in time T (direction: i to j)
   Sij(s,L,t)
*Total_Ploss
*Total_VD
Total_LM
*-----------------------------
*GY(BusNo,j)
*BY(BusNo,j)
*-----------------------------
;
```

```
*************************************************************************
   V.up(s,BusNo,t)=BusData(BusNo,'Vmax');
   V.lo(s,BusNo,t)=BusData(BusNo,'Vmin');
   Pg.up(s,BusNoG,t)=GenData(BusNoG,'Pmax');
   Pg.lo(s,BusNoG,t)=GenData(BusNoG,'Pmin');
   Qg.up(s,BusNoG,t)=GenData(BusNoG,'Qmax');
   Qg.lo(s,BusNoG,t)=GenData(BusNoG,'Qmin');
   Pg.fx(s,BusNoPQ,t)=0;
   Qg.fx(s,BusNoPQ,t)=0;
   th.fx(s,'B1',t)=0;
*   Pw.lo(s,BusNoWnd,t)=0;
   Pw.fx(s,BusNoWnd,t)= scen(s,'Pw_avl') * Prof(t,'wind') * Wind_Cap(BusNoWnd);
   Pw.fx(s,BusNoNotWnd,t)=0 ;
   Qw.fx(s,BusNoNotWnd,t)=0;
   Qw.fx(s,BusNoWnd,t)= 0.75 * Pw.l(s,BusNoWnd,t) ;
*   Ppv.lo(s,BusNoPVV,t)=0;
   Ppv.fx(s,BusNoPVV,t)= Prof(t,'PV') * PV_Cap(BusNoPVV);
   Ppv.fx(s,BusNoNotPVV,t)=0 ;
*   Qw.fx(s,BusNoNotWnd,t)=0;
*   Sij.up(L)=sqr(LineData(L,'Smax'));
*   Sij.lo(L)=0;
******************************Storage ************************************
set
StorageType            /ss1*ss5/
integer Variable  SS(s,BusNo, StorageType);
*S(BusNoStorage)=power(S(BusNoStorage),2);
SS.up(s,BusNo, StorageType)=3  ;
SS.lo(s,BusNo, StorageType)=0  ;
parameter CStorage(StorageType)
/
ss1   0.005
ss2   0.004
ss3   0.003
ss4   0.005
ss5   0.001
/
;
Parameter
Sm(StorageType);
Sm(StorageType)=CStorage(StorageType) ;
********************************Variables**********************************
Variable
  Estorage(StorageType,s,BusNo,t)
  Pch (StorageType,s,BusNo,t)
  Pdch (StorageType,s,BusNo,t)
  tPch
  tPdch
```

```
   Qs(StorageType,s,BusNo,t)
   Pg_STA(s,BusNo,t)          Total Active Power Generation in bus BusNo and time T
   Qg_STA(s,BusNo,t)          Total Reactive Power Generation in bus BusNo and time T
   Teta_STA(s,BusNo,t)        Angle of Buses' voltages in Radian
   V_STA(s,BusNo,t)           Voltage magnitude of Buses
*------------
;
    Estorage.lo(StorageType,s,BusNo,t)=0;
    Estorage.fx(StorageType,s,BusNoNoStorage,t)=0;
*    Pstorage.fx(s,BusNoNoStorage,t)=0;
*    Qs.fx(s,BusNoNoStorage,t)=0;
   Pch.lo(StorageType,s,BusNo,t)=0  ;
   Pdch.lo(StorageType,s,BusNo,t)=0  ;
   Pch.up(StorageType,s,BusNoStorage,t)=CStorage(StorageType) ;
   Pdch.up(StorageType,s,BusNoStorage,t)=CStorage(StorageType)  ;
   Pch.fx(StorageType,s,BusNoNoStorage,t)=0;
   Pdch.fx(StorageType,s,BusNoNoStorage,t)=0;
   V_STA.lo(s,BusNo,t)=0.98*BusData(BusNo,'Vmin');
   V_STA.up(s,BusNo,t)=BusData(BusNo,'Vmax');
   Pg_STA.lo(s,BusNoG,t)=GenData(BusNoG,'Pmin');
   Pg_STA.up(s,BusNoG,t)=GenData(BusNoG,'Pmax');
   Qg_STA.lo(s,BusNoG,t)=GenData(BusNoG,'Qmin');
   Qg_STA.up(s,BusNoG,t)=GenData(BusNoG,'Qmax');
   Pg_STA.fx(s,BusNoPQ,t)=0;
   Qg_STA.fx(s,BusNoPQ,t)=0;
          Qs.up(StorageType,s,BusNo,t)=Sm(StorageType);
   Qs.lo(StorageType,s,BusNo,t)=-Sm(StorageType);
   Qs.fx(StorageType,s,BusNoNoStorage,t)=0;
positive variables
               LM(s,t),  Vup(s,BusNoG,t), Vdn(s,BusNoG,t) ;
;
Vup.up(s,BusNoG,t)=0.4*(BusData(BusNoG,'Vmax')-BusData(BusNoG,'Vmin'));
Vdn.up(s,BusNoG,t)=0.4*(BusData(BusNoG,'Vmax')-BusData(BusNoG,'Vmin'));
*******************************Equations*********************************
equation
*Q_wind1(s,BusNoWnd,t)
*Q_wind2(s,BusNoWnd,t)
P_Bus(s,BusNo,t)
Q_Bus(s,BusNo,t)
*Ploss_Calc (s,t)
*VoltDev_Calc_1
*VoltDev_Calc_2
*VoltDev_Calc_3
*loss_const
*Epsilon_const_LM
*-----------------------------
P_Line_ij(s,L,t)
```

```
Q_line_ij(s,L,t)
S_line_ij(s,L,t)
*-----------------------------
*Storage1 (s,BusNo,t)
*Storage2
*Storage3
Storage5
Storage6
Storage7
*-----------------------------
Q_Storage1
*Q_Storage2(s,BusNo,t)
*-----------------------------
*Ploss_Calc1
LM_calc1
*-----------------------------
ENG1
ENG2
ENG3
*-----------------------------
P_STA_PV
V_STA_G
V_G_Limup
V_G_Limdn

P_Bus_STA
Q_Bus_STA
*-----------------------------
;
parameter eta, E0,epsilon;
epsilon = inf;
*L_Epsilon= inf;
eta = 0.95;
E0=0.0000001
;

Parameters Pld(s,BusNo,t), Qld(s,BusNo,t);
Pld(s,BusNo,t)= Prof(t,'load') * BusData(BusNo,'Pload');
Qld(s,BusNo,t)= 0.8*Prof(t,'load')* BusData(BusNo,'Qload');

V.l(s,j,t)=1;
th.l(s,j,t)=0;
V_STA.l(s,j,t)=1;
Teta_STA.l(s,BusNo,t)=0;

Parameter ES0(StorageType);
ES0(StorageType)=0.3*CStorage(StorageType);
```

```
*-------------------------------------------------------------------------------

*loss_const ..  Total_VD =l= epsilon;
*Epsilon_const_LM ..  Total_LM =L= L_Epsilon;
P_Bus(s,BusNo,t)  ..  Pg(s,BusNo,t)+Pw(s,BusNo,t)+Ppv(s,BusNo,t)-  sum(StorageType,
Pch(StorageType,s,BusNo,t)  )+  sum(StorageType,  Pdch(StorageType,s,BusNo,t)  )-
Pld(s,BusNo,t)      =e=      sum(j,V(s,BusNo,t)*V(s,j,t)*(GY(BusNo,j)*cos(th(s,BusNo,t)-
th(s,j,t))+ BY(BusNo,j)*sin( th(s,BusNo,t) -th(s,j,t) ) ) );
Q_Bus(s,BusNo,t)                  ..                  Qg(s,BusNo,t)+Qw(s,BusNo,t)+
sum(StorageType,Qs(StorageType,s,BusNo,t))-          Qld(s,BusNo,t)          =e=
sum(j,V(s,BusNo,t)*V(s,j,t)*(GY(BusNo,j)*sin(th(s,BusNo,t)-th(s,j,t))                -
BY(BusNo,j)*cos(th(s,BusNo,t)-th(s,j,t) ) ) );
*Ploss_Calc(s,t)          ..          Ploss(s,t)          =e=          sum(BusNo,
Pg(s,BusNo,t)+Pw(s,BusNo,t)+Ppv(s,BusNo,t)-  tPch(s,BusNo,t)+  tPdch(s,BusNo,t)-
Pld(s,BusNo,t) )  + sum(BusNo,( (1-eta)*tPch(s,BusNo,t)+ tPdch(s,BusNo,t)*((1/eta)-1) ))  ;
*VoltDev_Calc_1(BusNo,s,t) .. Voltdev_POS(BusNo, s,t)- Voltdev_NEG(BusNo, s,t) =e=
V(s,BusNo,t)-1;
*VoltDev_Calc_2(BusNo,s,t) .. Voltdev_POS(BusNo, s,t)+ Voltdev_NEG(BusNo, s,t) =e=
abs_Voltdev(BusNo,s,t);
*VoltDev_Calc_3  ..  Total_VD  =e=  sum((BusNo,s,t),  scen(s,"Prob")*
abs_Voltdev(BusNo,s,t) );

*
*----------***************   LM    ********-------------------
*+dv(s,BusNoG,t)

LM_calc1 .. Total_LM =e= sum((t,s), scen(s,"Prob")*LM(s,t) ) ;
P_STA_PV(s,BusNoPV,t).. Pg_STA(s,BusNoPV,t)=l=Pg(s,BusNoPV,t)*(1+LM(s,t));
V_STA_G(s,BusNoG,t)..  V_STA(s,BusNoG,t)  =e=  V(s,BusNoG,t)+  Vup(s,BusNoG,t)-
Vdn(s,BusNoG,t);
V_G_Limup(s,BusNoG,t)..  (  GenData(BusNoG,'Qmax')  -  Qg_STA(s,BusNoG,t)  )*
Vup(s,BusNoG,t) =l= 0;
V_G_Limdn(s,BusNoG,t)..  (  Qg_STA(s,BusNoG,t)  -  GenData(BusNoG,'Qmin')  )  *
Vdn(s,BusNoG,t) =l= 0;
P_Bus_STA(s,BusNo,t)..                Pg_STA(s,BusNo,t)+Pw(s,BusNo,t)+Ppv(s,BusNo,t)-
sum(StorageType,          Pch(StorageType,s,BusNo,t)        )+        sum(StorageType,
Pdch(StorageType,s,BusNo,t)                                  )                    -
Pld(s,BusNo,t)*(1+LM(s,t))=e=V_STA(s,BusNo,t)*sum(j,V_STA(s,j,t)*(GY(BusNo,j)*co
s(Teta_STA(s,BusNo,t)-Teta_STA(s,j,t))+BY(BusNo,j)*sin(Teta_STA(s,BusNo,t)-
Teta_STA(s,j,t))));
Q_Bus_STA(s,BusNo,t)..                          Qg_STA(s,BusNo,t)+Qw(s,BusNo,t)+
sum(StorageType,Qs(StorageType,s,BusNo,t))-
Qld(s,BusNo,t)*(1+LM(s,t))=e=V_STA(s,BusNo,t)*sum(j,V_STA(s,j,t)*(GY(BusNo,j)*si
n(Teta_STA(s,BusNo,t)-Teta_STA(s,j,t))-BY(BusNo,j)*cos(Teta_STA(s,BusNo,t)-
Teta_STA(s,j,t))));
*----------***************   SOC   ********-------------------
```

```
ENG1(StorageType,s,BusNoStorage,t) $( ord(t)>1) ..
Estorage(StorageType,s,BusNoStorage,t) =e= Estorage(StorageType,s,BusNoStorage,t-1) +
Pch(StorageType,s,BusNoStorage,t)*eta - Pdch(StorageType,s,BusNoStorage,t)/eta ;
ENG2(StorageType,s,BusNoStorage,t) .. Estorage(StorageType,s,BusNoStorage,t)=l=
CStorage(StorageType)* SS(s,BusNoStorage, StorageType);
ENG3(StorageType,s,BusNoStorage,'t1') .. Estorage(StorageType,s,BusNoStorage,'t1')=e=
ES0(StorageType)* SS(s,BusNoStorage, StorageType) +
Pch(StorageType,s,BusNoStorage,'t1')*eta-Pdch(StorageType,s,BusNoStorage,'t1')/eta;

*Storage3(s,BusNoStorage,t) .. sum(StorageType, SS(s,BusNoStorage, StorageType)) =l=
5;
*Storage7(StorageType,s,BusNoStorage,t) .. Pch(StorageType,s,BusNoStorage,t)*
Pdch(StorageType,s,BusNoStorage,t)=L=0;
*----------***************  PQS  ********-------------------
P_Line_ij(s,L,t).. Plij(s,L,t) =e= (LineData(L,'GL')+LineData(L,'G0'))*sum(BusNo
$Hout(L,BusNo) ,Hout(L,BusNo)*sqr(V(s,BusNo,t))) - sum(BusNo $Hout(L,BusNo)
,Hout(L,BusNo)*V(s,BusNo,t))*sum(BusNo $Hin(L,BusNo)
,Hin(L,BusNo)*V(s,BusNo,t))*(LineData(L,'BL')*sin(sum(BusNo $Hout(L,BusNo)
,Hout(L,BusNo)*th(s,BusNo,t))-sum(BusNo $Hin(L,BusNo) ,
Hin(L,BusNo)*th(s,BusNo,t)))+LineData(L,'GL')*cos(sum(BusNo $Hout(L,BusNo)
,Hout(L,BusNo)*th(s,BusNo,t))-sum(BusNo $Hin(L,BusNo) ,
Hin(L,BusNo)*th(s,BusNo,t))));
Q_line_ij(s,L,t).. Qlij(s,L,t) =e= -(LineData(L,'BL')+LineData(L,'B0'))*sum(BusNo
$Hout(L,BusNo),Hout(L,BusNo)*sqr(V(s,BusNo,t))) + sum(BusNo $Hout(L,BusNo)
,Hout(L,BusNo)*V(s,BusNo,t))*sum(BusNo $Hin(L,BusNo)
,Hin(L,BusNo)*V(s,BusNo,t))*(LineData(L,'BL')*cos(sum(BusNo $Hout(L,BusNo)
,Hout(L,BusNo)*th(s,BusNo,t))-sum(BusNo $Hin(L,BusNo) ,
Hin(L,BusNo)*th(s,BusNo,t)))-LineData(L,'GL')*sin(sum(BusNo $Hout(L,BusNo)
,Hout(L,BusNo)*th(s,BusNo,t))-sum(BusNo $Hin(L,BusNo) ,
Hin(L,BusNo)*th(s,BusNo,t))));
S_line_ij(s,L,t).. Sij(s,L,t) =e= sqr(Plij(s,L,t))+ sqr(Qlij(s,L,t));
*----------,-------------------
*
*Ploss_Calc1 .. Total_Ploss=e= sum(t,sum(s,scen(s,"Prob")*sum(BusNo,
Pg(s,BusNo,t)+Pw(s,BusNo,t)+Ppv(s,BusNo,t)- tPch(s,BusNo,t)+ tPdch(s,BusNo,t)-
Pld(s,BusNo,t) ) + sum(BusNo,( (1-eta)*tPch(s,BusNo,t)+ tPdch(s,BusNo,t)*((1/eta)-1) )) )
) ;

*1*sum(BusNo,Pg(s,BusNo,t)+ Pstorage(BusNo,t)-Pld(BusNO,t)));
*VoltDev_Calc1 .. Total_VD =e=sum(t,1 );
*----------***************  Q  ********-------------------
Q_Storage1(StorageType,s,BusNoStorage,t) .. power(Pch(StorageType,s,BusNoStorage,t)-
Pdch(StorageType,s,BusNoStorage,t),2)+power( Qs(StorageType,s,BusNoStorage,t) ,2) =l=
power(Sm(StorageType) ,2);

*Q_Storage2(s,BusNo,t) .. Qs(s,BusNo,t) =l= 1 * Pstorage(s,BusNo,t);
*Q_wind1(s,BusNoWnd,t) .. Qw(s,BusNoWnd,t) =g= - 0.30 * Pw(s,BusNoWnd,t);
```

```
*Q_wind2(s,BusNoWnd,t) .. Qw(s,BusNoWnd,t) =l=  0.75 * Pw(s,BusNoWnd,t);
*-----------------------------
$ontext
model LM_mAXimize /P_Bus, Q_Bus,
            LM_calc1, V_STA_G, P_STA_PV, V_G_Limup, V_G_Limdn,
            P_Line_ij, Q_Line_ij, S_Line_ij,
            P_Bus_STA, Q_Bus_STA,
            Storage3, Storage7,
            ENG1, ENG2, ENG3/;
$offtext

*$ontext
model LM_mAXimize /P_Bus, Q_Bus,
            LM_calc1, V_STA_G, P_STA_PV, V_G_Limup, V_G_Limdn,
            P_Line_ij, Q_Line_ij, S_Line_ij,
            P_Bus_STA, Q_Bus_STA,
                Q_Storage1,
            ENG1, ENG2, ENG3/;
*$offtext

option MINLP=sbb;
Option NLP = conopt4;

LM_mAXimize.iterlim=1000000;
LM_mAXimize.reslim=1000000;
LM_mAXimize.workfactor=6;

Parameter
dataout(s,*,t)
*dataout2(BusNo,s,*,t)
ss1(s,BusNo, StorageType,t)
*Ttap(wset,TapSet)
VV(s,BusNo,t)
PGG(s,BusNo,t)
QGG(s,BusNo,t)
*QCC(wset,BusNo)
VVoltdev(s,t)
*OFF(s,t)
ESS(StorageType,s,BusNo,t)
QSS(StorageType,s,BusNo,t)
PWW(s,BusNo,t)
QWW(s,BusNo,t)
PPpv(s,BusNo,t)
PPch(StorageType,s,BusNo,t)
PPdch(StorageType,s,BusNo,t)
*tPPch(s,BusNo,t)
*tPPdch(s,BusNo,t)
```

```
PPld(s,BusNo,t)
QQld(s,BusNo,t)
PPlij(s,L,t)
QQlij(s,L,t)
SSlij(s,L,t)
;

solve LM_mAXimize using MINLP maximizing Total_LM ;
LM_max = Total_LM.l;
*******************************Output*********************************
*parameters  tPch(s,BusNo,t), tPdch(s,BusNo,t);
*tPch(s,BusNo,t)= sum(StorageType,  Pch.l(StorageType,s,BusNo,t) );
*tPdch(s,BusNo,t)= sum(StorageType, Pdch.l(StorageType,s,BusNo,t) )
*Voltdev_Min= Total_VD.l ;


*w11(wset)=w1;
*w22(wset)=w2;
ss1(s,BusNo,StorageType,t)=ss.l(s,BusNo, StorageType);
VV(s,BusNo,t)=V.l(s,BusNo,t);
*Ttap(wset,TapSet)=tap.l(TapSet) ;
*VVoltdev(s,wset,t)=Voltdev.L(s,t);
PGG(s,BusNo,t)=Pg.l(s,BusNo,t)*100;
QGG(s,BusNo,t)=Qg.l(s,BusNo,t)*100;
PPpv(s,BusNo,t)= Ppv.l(s,BusNo,t);
ESS(StorageType,s,BusNo,t)=Estorage.l(StorageType,s,BusNo,t);
PPch(StorageType,s,BusNo,t)=Pch.l (StorageType,s,BusNo,t);
PPdch(StorageType,s,BusNo,t)=Pdch.l (StorageType,s,BusNo,t);
*tPPch(s,BusNo,t)=tPch.l(s,BusNo,t);
*tPPdch(s,BusNo,t)=tPdch.l(s,BusNo,t);
PWW(s,BusNo,t)=Pw.l(s,BusNo,t);
QWW(s,BusNo,t)=Qw.l(s,BusNo,t);
QSS(StorageType,s,BusNo,t)=Qs.l(StorageType,s,BusNo,t);
dataout(s,'LM',t)=100*LM.L(s,t);
*dataout2(BusNo,s,'Vdev',t)=abs_Voltdev.l(BusNo,s,t);
*OFF(s,t)=-OF.l;
PPld(s,BusNo,t) = Pld(s,BusNo,t);
QQld(s,BusNo,t) = Qld(s,BusNo,t);

PPlij(s,L,t)  =    Plij.l(s,L,t);
QQlij(s,L,t)  =    Qlij.l(s,L,t);
SSlij(s,L,t)  =    Sij.l(s,L,t);
*Parameter
*mean_OFF(wset)
*variance_OFF(wset)
*SD_OFF(wset)
*;
```

```
*mean_OFF(wset)=sum(it,OFF(it,wset))/card(it);
*variance_OFF(wset)=sum(it,(sqr( OFF(it,wset)-mean_OFF(wset) ) / card(it) ) );
*SD_OFF(wset)=sqrt(variance_OFF(wset));


Parameters
*abs_Voltdev(BusNo,s,t)
*Voltdev_POS(BusNo, s,t)
*Total_VD
*Voltdev_NEG(BusNo, s,t)
Voltdev(s,t)
ELM (t)
EVD (t)
;

Voltdev(s,t)=sum(BusNo,power((V.l(s,BusNo,t)-1),2))  ;
ELM (t)=sum(s,scen(s,"Prob")*dataout(s,'LM',t));
EVD (t)=sum(s,scen(s,"Prob")*Voltdev(s,t));
*abs_Voltdev(BusNo,s,t)=Voltdev_POS(BusNo, s,t)+ Voltdev_NEG(BusNo, s,t) ;
*Total_VD = sum((BusNo,s,t), scen(s,"Prob")* abs_Voltdev(BusNo,s,t) );
*Voltdev_POS(BusNo, s,t)- Voltdev_NEG(BusNo, s,t) = V(s,BusNo,t)-1;
* = ;

Display
QSS,ELM,ss1,ESS,PPch,PPdch,Voltdev,ESS,PPpv,PPch,PPdch,PWW,QWW,ss1,ESS,PG
G,VV,dataout;

*******************************Excel*************************************
execute_unload "results_T1-Case3-C.gdx" dataout
execute 'gdxxrw.exe results_T1-Case3-C.gdx par=dataout  rng=sheet1!a1'

execute_unload "results_T1-Case3-C.gdx" PGG
execute 'gdxxrw.exe results_T1-Case3-C.gdx par=PGG  rng=sheet2!a1'

execute_unload "results_T1-Case3-C.gdx" QGG
execute 'gdxxrw.exe results_T1-Case3-C.gdx par=QGG  rng=sheet3!a1'

execute_unload "results_T1-Case3-C.gdx" PPld
execute 'gdxxrw.exe results_T1-Case3-C.gdx par=PPld  rng=sheet4!a1'

execute_unload "results_T1-Case3-C.gdx" QQld
execute 'gdxxrw.exe results_T1-Case3-C.gdx par=QQld  rng=sheet5!a1'

execute_unload "results_T1-Case3-C.gdx" VV
execute 'gdxxrw.exe results_T1-Case3-C.gdx par=VV  rng=sheet6!a1'
```

```
execute_unload "results_T1-Case3-C.gdx" PPlij
execute 'gdxxrw.exe results_T1-Case3-C.gdx par=PPlij  rng=sheet7!a1'

execute_unload "results_T1-Case3-C.gdx" QQlij
execute 'gdxxrw.exe results_T1-Case3-C.gdx par=QQlij  rng=sheet8!a1'

execute_unload "results_T1-Case3-C.gdx" SSlij
execute 'gdxxrw.exe results_T1-Case3-C.gdx par=SSlij  rng=sheet9!a1'

execute_unload "results_T1-Case3-C.gdx" PWW
execute 'gdxxrw.exe results_T1-Case3-C.gdx par=PWW  rng=sheet10!a1'

execute_unload "results_T1-Case3-C.gdx" QWW
execute 'gdxxrw.exe results_T1-Case3-C.gdx par=QWW  rng=sheet11!a1'

execute_unload "results_T1-Case3-C.gdx" PPpv
execute 'gdxxrw.exe results_T1-Case3-C.gdx par=PPpv rng=sheet12!a1'

execute_unload "results_T1-Case3-C.gdx" ELM
execute 'gdxxrw.exe results_T1-Case3-C.gdx par=ELM rng=sheet13!a1'

execute_unload "results_T1-Case3-C.gdx" ESS
execute 'gdxxrw.exe results_T1-Case3-C.gdx par=ESS  rng=sheet14!a1'

execute_unload "results_T1-Case3-C.gdx" PPch
execute 'gdxxrw.exe results_T1-Case3-C.gdx par=PPch  rng=sheet15!a1'

execute_unload "results_T1-Case3-C.gdx" PPdch
execute 'gdxxrw.exe results_T1-Case3-C.gdx par=PPdch  rng=sheet16!a1'

execute_unload "results_T1-Case3-C.gdx" ss1
execute 'gdxxrw.exe results_T1-Case3-C.gdx par=ss1  rng=sheet17!a1'

execute_unload "results_T1-Case3-C.gdx" QSS
execute 'gdxxrw.exe results_T1-Case3-C.gdx par=QSS  rng=sheet18!a1'

execute_unload "results_T1-Case3-C.gdx" Voltdev
execute 'gdxxrw.exe results_T1-Case3-C.gdx par=Voltdev rng=sheet19!a1'

execute_unload "results_T1-Case3-C.gdx" EVD
execute 'gdxxrw.exe results_T1-Case3-C.gdx par=EVD rng=sheet20!a1'
*$offtext
```

Bibliographies

[1] [Online]. Available:"https://emp.lbl.gov/projects/renewables-portfolio."

[2] K. Eber and D. Corbus, *Hawaii solar integration study: executive summary*. National Renewable Energy Laboratory, 2013.

[3] J. Smith, "Stochastic analysis to determine feeder hosting capacity for distributed solar PV," *Electric Power Research Inst., Palo Alto, CA, Tech. Rep,* vol. 1026640, 2012.

[4] A. Dubey and S. Santoso, "Electric vehicle charging on residential distribution systems: Impacts and mitigations," *IEEE Access,* vol. 3, pp. 1871-1893, 2015.

[5] P. Evans, "Regional transmission and distribution network impacts assessment for wholesale photovoltaic generation," *California Energy Commission, CEC-200-2014-004,* 2014.

[6] J. Hansen, T. Edgar, J. Daily, and D. Wu, "Evaluating transactive controls of integrated transmission and distribution systems using the framework for network co-simulation," in *American Control Conference (ACC), 2017*, 2017, pp. 4010-4017: IEEE.

[7] H. Sun, Q. Guo, B. Zhang, Y. Guo, Z. Li, and J. Wang, "Master–slave-splitting based distributed global power flow method for integrated transmission and distribution analysis," *IEEE Transactions on Smart Grid,* vol. 6, no. 3, pp. 1484-1492, 2015.

[8] Z. Li, J. Wang, H. Sun, and Q. Guo, "Transmission contingency analysis based on integrated transmission and distribution power flow in smart grid," *IEEE Transactions on Power Systems,* vol. 30, no. 6, pp. 3356-3367, 2015.

[9] J. M. T. Marinho and G. N. Taranto, "A hybrid three-phase single-phase power flow formulation," *IEEE Transactions on Power Systems,* vol. 23, no. 3, pp. 1063-1070, 2008.

[10] B. Palmintier *et al.*, "Integrated Distribution-Transmission Analysis for Very High Penetration Solar PV (Final Technical Report)," *National Renewable Energy Laboratory, Golden, CO, NREL/TP-5D00-65550,* 2016.

[11] B. Palmintier *et al.*, "IGMS: An Integrated ISO-to-Appliance Scale Grid Modeling System," *IEEE Transactions on Smart Grid,* 2016.

[12] B. Palmintier, E. Hale, B.-M. Hodge, K. Baker, and T. M. Hansen, "Experiences integrating transmission and distribution simulations for DERs with the Integrated Grid Modeling System (IGMS)," in *Power Systems Computation Conference (PSCC), 2016*, 2016, pp. 1-7: IEEE.

[13] P. Aristidou and T. Van Cutsem, "A parallel processing approach to dynamic simulations of combined transmission and distribution systems," *International Journal of Electrical Power & Energy Systems,* vol. 72, pp. 58-65, 2015.

[14] Y. Zhang, A. Allen, and B.-M. Hodge, "Impact of distribution-connected large-scale wind turbines on transmission system stability during large disturbances," in *PES General Meeting| Conference & Exposition, 2014 IEEE*, 2014, pp. 1-5: IEEE.

[15] H. Jain, A. Parchure, R. P. Broadwater, M. Dilek, and J. Woyak, "Three-Phase Dynamic Simulation of Power Systems Using Combined Transmission and Distribution System Models," *IEEE Transactions on Power Systems,* vol. 31, no. 6, pp. 4517-4524, 2016.

[16] Q. Huang and V. Vittal, "Integrated Transmission and Distribution System Power Flow and Dynamic Simulation Using Mixed Three-Sequence/Three-Phase Modeling," *IEEE Transactions on Power Systems*, vol. 32, no. 5, pp. 3704-3714, 2017.

[17] A. Rabiee, M. Parvania, M. Vanouni, M. Parniani, and M. Fotuhi-Firuzabad, "Comprehensive control framework for ensuring loading margin of power systems considering demand-side participation," *IET Generation, Transmission & Distribution*, vol. 6, no. 12, pp. 1189-1201, 2012.

[18] [Online]. Available: https://sites.google.com/site/mohsenibonab/download."

[19] H. P. Schmidt, J. C. Guaraldo, M. da Mota Lopes, and J. A. Jardini, "Interchangeable Balanced and Unbalanced Network Models for Integrated Analysis of Transmission and Distribution Systems," *IEEE Transactions on Power Systems*, vol. 30, no. 5, pp. 2747-2754, 2015.

[20] N. G. Singhal and K. W. Hedman, "An integrated transmission and distribution systems model with distribution-based LMP (DLMP) pricing," in *North American Power Symposium (NAPS), 2013*, 2013, pp. 1-6: IEEE.

[21] I. Alsaidan, A. Khodaei, and W. Gao, "Distributed energy storage sizing for microgrid applications," in *Transmission and Distribution Conference and Exposition (T&D), 2016 IEEE/PES*, 2016, pp. 1-5: IEEE.

[22] I. Alsaidan, A. Khodaei, and W. Gao, "Determination of optimal size and depth of discharge for battery energy storage in standalone microgrids," in *North American Power Symposium (NAPS), 2016*, 2016, pp. 1-6: IEEE.

[23] S. M. Mohseni-Bonab, I. Kamwa, and A. R. Moeini, Abbas;, "Investigation of BESSs' Benefits in Transmission and Distribution Systems Operations Using Integrated Power Grid Co-optimization," 2017.

[24] S. M. Mohseni-Bonab and A. Rabiee, "Optimal Reactive Power Dispatch: A Review, and a New Stochastic Voltage Stability Constrained Multi-Objective Model at the Presence of Uncertain Wind Power Generation," *IET Generation Transmission & Distribution*, in *2017 IEEE Electrical Power and Energy Conference (EPEC), 2017*, 2017: IEEE, pp. 1-6.

[25] A. Soroudi, P. Siano, and A. Keane, "Optimal DR and ESS scheduling for distribution losses payments minimization under electricity price uncertainty," *IEEE Transactions on Smart Grid*, vol. 7, no. 1, pp. 261-272, 2016.

[26] S. Mohammadi, S. Soleymani, and B. Mozafari, "Scenario-based stochastic operation management of microgrid including wind, photovoltaic, micro-turbine, fuel cell and energy storage devices," *International Journal of Electrical Power & Energy Systems*, vol. 54, pp. 525-535, 2014.

[27] A. Rabiee and S. M. Mohseni-Bonab, "Maximizing Hosting Capacity of Renewable Energy Sources in Distribution Networks: A Multi-objective and Scenario-based Approach," *Energy*, vol. 120, pp. 417-430, 2017.

[28] A. Hoke *et al.*, "Setting the Smart Solar Standard: Collaborations Between Hawaiian Electric and the National Renewable Energy Laboratory," *IEEE Power and Energy Magazine*, vol. 16, no. 6, pp. 18-29, 2018.

[29] J. Von Appen, M. Braun, T. Stetz, K. Diwold, and D. Geibel, "Time in the sun: the challenge of high PV penetration in the German electric grid," *IEEE Power and Energy magazine*, vol. 11, no. 2, pp. 55-64, 2013.

[30] R. Seguin, J. Woyak, D. Costyk, J. Hambrick, and B. Mather, "High-penetration PV integration handbook for distribution engineers," *National Renewable Energy Laboratory, Golden, CO NREL/TP-5D00-63114*, 2016.

[31] A. Khodaei and M. Shahidehpour, "Microgrid-based co-optimization of generation and transmission planning in power systems," *IEEE transactions on power systems*, vol. 28, no. 2, pp. 1582-1590, 2013.

[32] M. Caramanis, E. Ntakou, W. W. Hogan, A. Chakrabortty, and J. Schoene, "Co-optimization of power and reserves in dynamic T&D power markets with nondispatchable renewable generation and distributed energy resources," *Proceedings of the IEEE*, vol. 104, no. 4, pp. 807-836, 2016.

[33] A. Arabali, B. Asghari, and R. Sharma, "A new co-optimization model for grid scale storage units in energy and frequency regulation markets," in *Transmission and Distribution Conference and Exposition (T&D), 2016 IEEE/PES*, 2016, pp. 1-5: IEEE.

[34] C. A. Canizares, "Voltage stability assessment: concepts, practices and tools," *Power System Stability Subcommittee Special Publication IEEE/PES, Final Document (thunderbox. uwaterloo. ca/~ claudio/claudio. html# VSWG)*, 2002.

[35] A. Rabiee, S. Nikkhah, A. Soroudi, and E. Hooshmand, "Information gap decision theory for voltage stability constrained OPF considering the uncertainty of multiple wind farms," *IET Renewable Power Generation*, vol. 11, no. 5, pp. 585-592, 2016.

[36] R. C. Dugan and T. E. McDermott, "An open source platform for collaborating on smart grid research," in *Power and Energy Society General Meeting, 2011 IEEE*, 2011, pp. 1-7: IEEE.

[37] R. Caire, J. Sanchez, and N. Hadjsaid, "Vulnerability Analysis of Coupled Heterogeneous Critical Infrastructures: a Co-simulation approach with a testbed validation," in *Innovative Smart Grid Technologies Europe (ISGT EUROPE), 2013 4th IEEE/PES*, 2013, pp. 1-5: IEEE.

[38] S. Broderick, A. Cruden, S. Sharkh, and N. Bessant, "A Technique to Interconnect and Control Co-Simulation Systems," *IET Generation, Transmission & Distribution*, vol. 11, no. 12, pp. 3115-3124, 2017.

[39] Y. Duan, L. Luo, Y. Li, Y. Cao, C. Rehtanz, and M. Küch, "Co-simulation of distributed control system based on JADE for smart distribution networks with distributed generations," *IET Generation, Transmission & Distribution, IET Generation, Transmission & Distribution*, vol. 11, no. 12, pp. 3097-3105, 2017.

[40] R. Huang, R. Fan, J. Daily, A. Fisher, and J. Fuller, "Open-source framework for power system transmission and distribution dynamics co-simulation," *IET Generation, Transmission & Distribution*, vol. 11, no. 12, pp. 3152-3162, 2017.

[41] P. Le-Huy, G. Sybille, P. Giroux, L. Loud, J. Huang, and I. Kamwa, "Real-time electromagnetic transient and transient stability co-simulation based on hybrid line modelling," *IET Generation, Transmission & Distribution*, vol. 11, no. 12, pp. 2983-2990, 2017.

[42] P. Kundur, N. J. Balu, and M. G. Lauby, *Power system stability and control*. McGraw-hill New York, 1994.

[43] A. Soroudi, B. Mohammadi-Ivatloo, and A. Rabiee, "Energy Hub Management with Intermittent Wind Power," in *Large Scale Renewable Power Generation*(Green Energy and Technology: Springer Singapore, 2014, pp. 413-438.

[44] S. Wen, H. Lan, Q. Fu, D. Yu, and L. Zhang, "Economic Allocation for Energy Storage System Considering Wind Power Distribution." *IEEE Transactions on Power Systems,* vol. 30, no. 2, pp. 644-652, 2015.

[45] R. J. Avalos, C. A. Cañizares, F. Milano, and A. J. Conejo, "Equivalency of continuation and optimization methods to determine saddle-node and limit-induced bifurcations in power systems," *IEEE Transactions on Circuits and Systems I: Regular Papers,* vol. 56, no. 1, pp. 210-223, 2009.

[46] P. Kundur *et al.*, "Definition and classification of power system stability," *IEEE transactions on Power Systems,* vol. 19, no. 2, pp. 1387-1401, 2004.

[47] J. Condren, T. W. Gedra, and P. Damrongkulkamjorn, "Optimal power flow with expected security costs," *IEEE Transactions on Power Systems,* vol. 21, no. 2, pp. 541-547, 2006.

[48] R. Zárate-Miñano, F. Milano, and A. J. Conejo, "An OPF methodology to ensure small-signal stability," *IEEE Transactions on Power Systems,* vol. 26, no. 3, pp. 1050-1061, 2011.

[49] A. Rabiee and M. Parniani, "Voltage security constrained multi-period optimal reactive power flow using benders and optimality condition decompositions," *Power Systems, IEEE Transactions on,* vol. 28, no. 2, pp. 696-708, 2013.

[50] W. D. Rosehart, C. A. Canizares, and V. H. Quintana, "Multiobjective optimal power flows to evaluate voltage security costs in power networks," *IEEE Transactions on power systems,* vol. 18, no. 2, pp. 578-587, 2003.

[51] W. E. C. Council, "Voltage stability criteria, undervoltage load shedding strategy, and reactive power reserve monitoring methodology," *Final Report, available at: http://www. wecc. biz/main. html, accessed April*, 2007.

[52] A. Brooke, D. Kendrick, and A. Meeraus, *GAMS Release 2.25: A user's guide*. GAMS Development Corporation Washington, DC, 1996.

[53] [Online]. Available: https://www.gams.com/latest/docs/S_SBB.html."

[54] Q. Huang and V. Vittal, "Advanced EMT and Phasor-Domain Hybrid Simulation with Simulation Mode Switching Capability for Transmission and Distribution Systems," *IEEE Transactions on Power Systems,* 2018.

[55] D. M. Gonzalez, L. Robitzky, S. Liemann, U. Häger, J. Myrzik, and C. Rehtanz, "Distribution network control scheme for power flow regulation at the interconnection point between transmission and distribution system," in *Innovative Smart Grid Technologies-Asia (ISGT-Asia), 2016 IEEE*, 2016, pp. 23-28: IEEE.

[56] A. Singhal and V. Ajjarapu, "Long-term voltage stability assessment of an integrated transmission distribution system," in *Power Symposium (NAPS), 2017 North American*, 2017, pp. 1-6: IEEE.

[57] S. M. Mohseni-Bonab, I. Kamwa, A. Moeini, and A. Rabiee, "Investigation of BESSs' Benefits in Transmission and Distribution Systems Operations Using Integrated Power Grid Co-optimization," in *2017 IEEE Electrical Power and Energy Conference (EPEC), 2017*, 2017: IEEE, pp. 1-6.

[58] R. Venkatraman, S. K. Khaitan, and V. Ajjarapu, "Dynamic Co-Simulation Methods for Combined Transmission-Distribution System and Integration Time Step Impact on Convergence," *arXiv preprint arXiv:1801.01185,* 2018.

[59] Z. Li, Q. Guo, H. Sun, and J. Wang, "Coordinated transmission and distribution AC optimal power flow," *IEEE Transactions on Smart Grid,* vol. 9, no. 2, pp. 1228-1240, 2018.

[60] R. D. Zimmerman, C. E. Murillo-Sánchez, and R. J. Thomas, "MATPOWER: Steady-state operations, planning, and analysis tools for power systems research and education," *Power Systems, IEEE Transactions on*, vol. 26, no. 1, pp. 12-19, 2011.

[61] D. P. Chassin, J. C. Fuller, and N. Djilali, "GridLAB-D: An agent-based simulation framework for smart grids," *Journal of Applied Mathematics*, vol. 2014, 2014.

[62] H. Jain, B. Palmintier, I. Krad, and D. Krishnamurthy, "Studying the Impact of Distributed Solar PV on Power Systems Using Integrated Transmission and Distribution Models," in *2018 IEEE/PES Transmission and Distribution Conference and Exposition (T&D)*, 2018, pp. 1-5: IEEE.

[63] B. Palmintier, D. Krishnamurthy, P. Top, S. Smith, J. Daily, and J. Fuller, "Design of the HELICS high-performance transmission-distribution-communication-market co-simulation framework," in *Proc. 2017 Workshop on Modeling and Simulation of Cyber-Physical Energy Systems, Pittsburgh, PA*, 2017.

[64] Y. Wang, C. Chen, J. Wang, and R. Baldick, "Research on resilience of power systems under natural disasters—A review," *IEEE Transactions on Power Systems*, vol. 31, no. 2, pp. 1604-1613, 2016.

[65] W. House, "Economic benefits of increasing electric grid resilience to weather outages," *Washington, DC: Executive Office of the President*, 2013.

[66] M. Panteli and P. Mancarella, "Influence of extreme weather and climate change on the resilience of power systems: Impacts and possible mitigation strategies," *Electric Power Systems Research*, vol. 127, pp. 259-270, 2015.

[67] C. Chen, J. Wang, F. Qiu, and D. Zhao, "Resilient distribution system by microgrids formation after natural disasters," *IEEE Transactions on smart grid*, vol. 7, no. 2, pp. 958-966, 2016.

[68] H. Gao, Y. Chen, Y. Xu, and C.-C. Liu, "Resilience-oriented critical load restoration using microgrids in distribution systems," *IEEE Transactions on Smart Grid*, vol. 7, no. 6, pp. 2837-2848, 2016.

[69] M. Carrión, J. M. Arroyo, and N. Alguacil, "Vulnerability-constrained transmission expansion planning: A stochastic programming approach," *IEEE Transactions on Power Systems*, vol. 22, no. 4, pp. 1436-1445, 2007.

[70] L. Zhao and B. Zeng, "Vulnerability analysis of power grids with line switching," *IEEE Transactions on Power Systems*, vol. 28, no. 3, pp. 2727-2736, 2013.

[71] T. Kim, S. J. Wright, D. Bienstock, and S. Harnett, "Analyzing vulnerability of power systems with continuous optimization formulations," *IEEE Transactions on Network Science and Engineering*, vol. 3, no. 3, pp. 132-146, 2016.

[72] A. Delgadillo, J. M. Arroyo, and N. Alguacil, "Analysis of electric grid interdiction with line switching," *IEEE Transactions on Power Systems*, vol. 25, no. 2, pp. 633-641, 2010.

[73] S. Sayyadipour, G. R. Yousefi, and M. A. Latify, "Mid-term vulnerability analysis of power systems under intentional attacks," *IET Generation, Transmission & Distribution*, vol. 10, no. 15, pp. 3745-3755, 2016.

[74] G. L. Doorman, K. Uhlen, G. Kjolle, and E. S. Huse, "Vulnerability analysis of the Nordic power system," *IEEE Transactions on Power Systems*, vol. 21, no. 1, pp. 402-410, 2006.

[75] L. Lenoir, I. Kamwa, and L.-A. Dessaint, "Overload alleviation with preventive-corrective static security using fuzzy logic," *IEEE Transactions on Power Systems*, vol. 24, no. 1, pp. 134-145, 2009.

[76] A. Srivastava, T. Morris, T. Ernster, C. Vellaithurai, S. Pan, and U. Adhikari, "Modeling cyber-physical vulnerability of the smart grid with incomplete information," *IEEE Transactions on Smart Grid,* vol. 4, no. 1, pp. 235-244, 2013.

[77] A. Moeini, I. Kamwa, M. de Montigny, and L. Lenoir, "Application of Battery Energy Storage for network vulnerability mitigation," in *Transmission and Distribution Conference and Exposition (T&D), 2016 IEEE/PES*, 2016, pp. 1-5: IEEE.

[78] J.-H. Teng, C.-Y. Chen, and I. C. Martinez, "Utilising energy storage systems to mitigate power system vulnerability," *IET Generation, Transmission & Distribution,* vol. 7, no. 7, pp. 790-798, 2013.

[79] X. Yu and C. Singh, "A practical approach for integrated power system vulnerability analysis with protection failures," *IEEE Transactions on Power Systems,* vol. 19, no. 4, pp. 1811-1820, 2004.

[80] J. Kersulis, I. Hiskens, M. Chertkov, S. Backhaus, and D. Bienstock, "Temperature-based instanton analysis: Identifying vulnerability in transmission networks," in *PowerTech, 2015 IEEE Eindhoven*, 2015, pp. 1-6: IEEE.

[81] A. Wang, Y. Luo, G. Tu, and P. Liu, "Vulnerability assessment scheme for power system transmission networks based on the fault chain theory," *IEEE Transactions on power systems,* vol. 26, no. 1, pp. 442-450, 2011.

[82] C. J. Wallnerstrom and P. Hilber, "Vulnerability analysis of power distribution systems for cost-effective resource allocation," *IEEE Transactions on power systems,* vol. 27, no. 1, pp. 224-232, 2012.

[83] J. Fang, C. Su, Z. Chen, and P. Lund, "Power system structural vulnerability assessment based on an improved maximum flow approach," *IEEE Transactions on Smart Grid,* vol. 9, no. 2, pp. 777-785, 2018.

[84] S. Poudel, Z. Ni, and W. Sun, "Electrical distance approach for searching vulnerable branches during contingencies," *IEEE Transactions on Smart Grid,* vol. 9, no. 4, pp. 3373-3382, 2018.

[85] X. Wei, J. Zhao, T. Huang, and E. Bompard, "A novel cascading faults graph based transmission network vulnerability assessment method," *IEEE Transactions on Power Systems,* vol. 33, no. 3, pp. 2995-3000, 2017.

[86] H. Han, C. Wu, S. Gao, and G. Zu, "An Assessment Approach of the Power System Vulnerability Considering the Uncertainties of Wind Power Integration," in *2018 China International Conference on Electricity Distribution (CICED)*, 2018, pp. 741-745: IEEE.

[87] T. Zang, S. Gao, T. Huang, X. Wei, and T. Wang, "Complex Network-Based Transmission Network Vulnerability Assessment Using Adjacent Graphs," *IEEE Systems Journal, Early Access,* 2019.

[88] T. Zang *et al.*, "Adjacent Graph Based Vulnerability Assessment for Electrical Networks Considering Fault Adjacent Relationships Among Branches," *IEEE Access,* vol. 7, pp. 88927-88936, 2019.

[89] I. Kamwa, A. K. Pradhan, G. Joos, and S. Samantaray, "Fuzzy partitioning of a real power system for dynamic vulnerability assessment," *IEEE Transactions on Power Systems,* vol. 24, no. 3, pp. 1356-1365, 2009.

[90] C. Lu, Z. Wang, and Y. Yu, "Optimal PMU placement for pessimistic dynamic vulnerability assessment," *IET Generation, Transmission & Distribution,* vol. 12, no. 10, pp. 2231-2237, 2017.

[91] A. M. L. da Silva, J. L. Jardim, L. R. de Lima, and Z. S. Machado, "A method for ranking critical nodes in power networks including load uncertainties," *IEEE Transactions on Power Systems,* vol. 31, no. 2, pp. 1341-1349, 2015.

[92] Y. Zhang, L. Wang, Y. Xiang, and C.-W. Ten, "Inclusion of SCADA cyber vulnerability in power system reliability assessment considering optimal resources allocation," *IEEE Transactions on Power Systems,* vol. 31, no. 6, pp. 4379-4394, 2016.

[93] Y. Zhang, Y. Xiang, and L. Wang, "Power system reliability assessment incorporating cyber attacks against wind farm energy management systems," *IEEE transactions on smart grid,* vol. 8, no. 5, pp. 2343-2357, 2016.

[94] Q. Wang, M. Pipattanasomporn, M. Kuzlu, Y. Tang, Y. Li, and S. Rahman, "Framework for vulnerability assessment of communication systems for electric power grids," *IET Generation, Transmission & Distribution,* vol. 10, no. 2, pp. 477-486, 2016.

[95] J. Liang, L. Sankar, and O. Kosut, "Vulnerability analysis and consequences of false data injection attack on power system state estimation," *IEEE Transactions on Power Systems,* vol. 31, no. 5, pp. 3864-3872, 2016.

[96] H. Bai and S. Miao, "Hybrid flow betweenness approach for identification of vulnerable line in power system," *IET Generation, Transmission & Distribution,* vol. 9, no. 12, pp. 1324-1331, 2015.

[97] J. Zhang and L. Sankar, "Physical system consequences of unobservable state-and-topology cyber-physical attacks," *IEEE Transactions on Smart Grid,* vol. 7, no. 4, 2016.

[98] S. Mousavian, J. Valenzuela, and J. Wang, "A probabilistic risk mitigation model for cyber-attacks to PMU networks," *IEEE Transactions on Power Systems,* vol. 30, no. 1, pp. 156-165, 2014.

[99] S. M. Mohseni-Bonab, I. Kamwa, A. Moeini, and A. Rabiee, "Voltage Security Constrained Stochastic Programming Model for Day-Ahead BESS Schedule in co-optimization of T&D Systems," *IEEE Transactions on Sustainable Energy,* vol. 11, no. 1, pp. 391-404, 2020.

[100] S. M. Mohseni-Bonab, I. Kamwa, A. Moeini, and A. Rabiee, "IC-GAMA: A Novel Framework for Integrated T&D Co-Simulation," in *ISGT Europe,* 2019, pp. 1-6.

[101] C. Grigg *et al.,* "The IEEE reliability test system-1996. A report prepared by the reliability test system task force of the application of probability methods subcommittee," *IEEE Transactions on power systems,* vol. 14, no. 3, pp. 1010-1020, 1999.

[102] C. Barrows and S. Blumsack, "Transmission switching in the RTS-96 test system," *IEEE Transactions on Power Systems,* vol. 27, no. 2, pp. 1134-1135, 2012.

[103] E. B. Fisher, R. P. O'Neill, and M. C. Ferris, "Optimal transmission switching," *IEEE Transactions on Power Systems,* vol. 23, no. 3, pp. 1346-1355, 2008.

[104] Z. Boshi, H. Zechun, Z. Qian, H. Zhang, and S. Yonghua, "Optimal transmission switching to eliminate voltage violations during light-load periods using decomposition approach," *Journal of Modern Power Systems and Clean Energy,* vol. 7, no. 2, pp. 297-308, 2019.

[105] M. T. Hagh, M. Z. Gargari, and M. J. V. Pakdel, "A sequential analysis of optimal transmission switching with contingency assessment," *IET Generation, Transmission & Distribution,* vol. 12, no. 6, pp. 1390-1396, 2018.

[106] M. Khanabadi, H. Ghasemi, and M. Doostizadeh, "Optimal transmission switching considering voltage security and N-1 contingency analysis," *IEEE Transactions on Power Systems,* vol. 28, no. 1, pp. 542-550, 2013.
[107] K. W. Hedman, R. P. O'Neill, E. B. Fisher, and S. S. Oren, "Optimal transmission switching with contingency analysis," *IEEE Transactions on Power Systems,* vol. 24, no. 3, pp. 1577-1586, 2009.
[108] J. D. Fuller, R. Ramasra, and A. Cha, "Fast heuristics for transmission-line switching," *IEEE Transactions on Power Systems,* vol. 27, no. 3, pp. 1377-1386, 2012.
[109] M. Jabarnejad, "Approximate optimal transmission switching," *Electric Power Systems Research,* vol. 161, pp. 1-7, 2018.
[110] M. Soroush and J. D. Fuller, "Accuracies of optimal transmission switching heuristics based on DCOPF and ACOPF," *IEEE Transactions on Power Systems,* vol. 29, no. 2, pp. 924-932, 2014.
[111] P. Henneaux and D. S. Kirschen, "Probabilistic security analysis of optimal transmission switching," *IEEE Transactions on Power Systems,* vol. 31, no. 1, pp. 508-517, 2016.
[112] J. Ostrowski, J. Wang, and C. Liu, "Transmission switching with connectivity-ensuring constraints," *IEEE Transactions on Power Systems,* vol. 29, no. 6, pp. 2621-2627, 2014.
[113] Z. Yang, H. Zhong, Q. Xia, and C. Kang, "Optimal transmission switching with short-circuit current limitation constraints," *IEEE Transactions on Power Systems,* vol. 31, no. 2, pp. 1278-1288, 2016.
[114] K. W. Hedman, M. C. Ferris, R. P. O'Neill, E. B. Fisher, and S. S. Oren, "Co-optimization of generation unit commitment and transmission switching with N-1 reliability," *IEEE Transactions on Power Systems,* vol. 25, no. 2, pp. 1052-1063, 2010.
[115] A. Khodaei and M. Shahidehpour, "Transmission switching in security-constrained unit commitment," *IEEE Transactions on Power Systems,* vol. 25, no. 4, pp. 1937-1945, 2010.
[116] S. Mousavian, J. Valenzuela, and J. Wang, "A two-phase investment model for optimal allocation of phasor measurement units considering transmission switching," *Electric Power Systems Research,* vol. 119, pp. 492-498, 2015.
[117] R. Aazami, M. R. Haghifam, F. Soltanian, and M. Moradkhani, "A comprehensive strategy for transmission switching action in simultaneous clearing of energy and spinning reserve markets," *International Journal of Electrical Power & Energy Systems,* vol. 64, pp. 408-418, 2015.
[118] J. C. Villumsen, G. Bronmo, and A. B. Philpott, "Line capacity expansion and transmission switching in power systems with large-scale wind power," *IEEE Transactions on Power Systems,* vol. 28, no. 2, pp. 731-739, 2013.
[119] A. Khodaei, M. Shahidehpour, and S. Kamalinia, "Transmission switching in expansion planning," *IEEE Transactions on Power Systems,* vol. 25, no. 3, pp. 1722-1733, 2010.
[120] J. C. Villumsen and A. B. Philpott, "Investment in electricity networks with transmission switching," *European Journal of Operational Research,* vol. 222, no. 2, pp. 377-385, 2012.

[121] A. R. Escobedo, E. Moreno-Centeno, and K. W. Hedman, "Topology control for load shed recovery," *IEEE Transactions on Power Systems,* vol. 29, no. 2, pp. 908-916, 2014.
[122] C. Zhang and J. Wang, "Optimal transmission switching considering probabilistic reliability," *IEEE Transactions on Power Systems,* vol. 29, no. 2, pp. 974-975, 2014.
[123] S. M. Mohseni-Bonab, I. Kamwa, and A. R. Moeini, Abbas;, "Vulnerability Assessment in Power Systems: A Review and Representing Novel Perspectives " presented at the 2020 IEEE Power & Energy Society General Meeting (PESGM), 2020.
[124] A. Soroudi and T. Amraee, "Decision making under uncertainty in energy systems: state of the art," *Renewable and Sustainable Energy Reviews,* vol. 28, pp. 376-384, 2013.
[125] T. Van Cutsem and R. Mailhot, "Validation of a fast voltage stability analysis method on the Hydro-Quebec system," *IEEE Transactions on Power Systems,* vol. 12, no. 1, pp. 282-292, 1997.
[126] J. McCall, "Genetic algorithms for modelling and optimisation," *Journal of Computational and Applied Mathematics,* vol. 184, no. 1, pp. 205-222, 2005.
[127] I. C. Trelea, "The particle swarm optimization algorithm: convergence analysis and parameter selection," *Information processing letters,* vol. 85, no. 6, pp. 317-325, 2003.
[128] E. Atashpaz-Gargari and C. Lucas, "Imperialist competitive algorithm: an algorithm for optimization inspired by imperialistic competition," in *2007 IEEE Congress on Evolutionary Computation*, 2007, pp. 4661-4667: IEEE.
[129] E. Rashedi, H. Nezamabadi-Pour, and S. Saryazdi, "GSA: a gravitational search algorithm," *Information sciences,* vol. 179, no. 13, pp. 2232-2248, 2009.
[130] A. Askarzadeh, "A novel metaheuristic method for solving constrained engineering optimization problems: crow search algorithm," *Computers & Structures,* vol. 169, pp. 1-12, 2016.
[131] [Online]. Available: https://www.gams.com/latest/docs/S_KNITRO.html."
[132] M. de Montigny *et al.*, "Multiagent stochastic simulation of minute-to-minute grid operations and control to integrate wind generation under AC power flow constraints," *IEEE Transactions on Sustainable Energy,* vol. 4, no. 3, pp. 619-629, 2013.